Employment of heterogeneous base catalysts in the depolymerization of lignin and Upgradation of lignin model compounds

Thesis Submitted to AcSIR For the Award of the Degree of

**DOCTOR OF PHILOSOPHY
In CHEMISTRY**

By
Richa Chaudhary
(Enrollment No. 10CC12A26008)

Under the guidance of
Dr. Paresh Laxmikant Dhepe

*Catalysis & Inorganic Chemistry Division
CSIR-National Chemical Laboratory
Pune- 411 008, India
December, 2017*

सीएसआईआर - राष्ट्रीय रासायनिक प्रयोगशाला

(वैज्ञानिक तथा औद्योगिक अनुसंधान परिषद)

डॉ. होमी भाभा मार्ग, पुणे - 411 008. भारत

CSIR - NATIONAL CHEMICAL LABORATORY

(Council of Scientific & Industrial Research)

Dr. Homi Bhabha Road, Pune - 411 008, India

NCL

CERTIFICATE

This is to certify that the work incorporated in this Ph.D. thesis entitled **"Employment of heterogeneous base catalysts in the depolymerization of lignin and Upgradation of lignin model compounds"** submitted by **Mrs. Richa Chaudhary** to Academy of Scientific and Innovative Research (AcSIR) in fulfilment of the requirements for the award of the Degree of **Doctor of Philosophy in Chemistry,** embodies original research work under my supervision/guidance. I further certify that this work has not been submitted to any other University or Institution in part or full for the award of any degree or diploma. Research material obtained from other sources has been duly acknowledged in the thesis. Any text, illustration, table etc., used in the thesis from other sources, have been duly cited and acknowledged.

December, 2017

**Ph.D. Student
Richa Chaudhary**

**Supervisor
Dr. Paresh Laxmikant Dhepe**

Senior Scientist, CSIR-NCL, Pune, India

Assistant Professor, AcSIR, New Delhi, India

<u>Declaration by the candidate</u>

I hereby declare that the thesis entitled *"Employment of heterogeneous base catalysts in the depolymerization of lignin and Upgradation of lignin model compounds"* submitted for the award of the Degree of **Doctor of Philosophy in Chemistry** to the **Academy of Scientific & Innovative Research (AcSIR)**, New Delhi, has been carried out by me at Catalysis & Inorganic Chemistry Division, CSIR-National Chemical Laboratory, Pune-411 008, India, under the supervision of Dr. Paresh L. Dhepe. The work is original and has not been submitted as a part or full by me for any degree or diploma to this or any other university.

December, 2017

Richa Chaudhary

(Enrollment No. 10CC12A26008)

Dedicated to............

Guru Dev,

My Brother,

Parents, Husband

&

my sweet son

Shivendra

ACKNOWLEDGEMENTS

CONTENTS

Chapter 1: General Introduction and Literature Review

Chapter 2: Lignin and Catalyst Characterization

Chapter 2A: Lignin Characterization

Chapter 2B: Catalyst Synthesis and Characterization

Chapter 3: Depolymerization of Lignin using various Solid Base Catalysts

Chapter 4: Coconut Coir: Lignin Isolation, Characterization and Depolymerization of Isolated Lignin and Coir

Chapter 5: Upgradation of Lignin Derived Monomers: Exploring the Effect of Basic Supported Metal Catalyst on Phenol, Guaiacol and Eugenol

Chapter 6: Summary and Conclusions

Appendix

List of Schemes

List of Figures

Chapter 4

Chapter 5

Chapter 6

List of Tables

List of Abbreviations

1D	One dimensional
3D	Three dimensional
ATR	Attenuated Total Reflection
BCD	Base catalysed depolymerization
BB	Brønsted basic sites
BET	Braunauer-Emmett-Teller
BHT	Butylated hydroxyl toluene
CC	Coconut Coir
CC-KL	Klason lignin
CC-ORGL	Organosolv lignin
CC-SL	Soda lignin
CHNS	Carbon, Hydrogen, Nitrogen, Sulfur
DBE	Double bond equivalence
DEE	Diethyl ether
EDAX	Energy Dispersive X-Ray Analysis
EtOAc	Ethyl acetate
FAU	Faujasite
FID	Flame ionization detector
FTIR	Fourier Transform Infrared
GC	Gas Chromatography
GC-MS	Gas Chromatography Mass Spectrometry
HAP	Hydroxyapatite
HHV	Higher heating value
HSP	Hansen solubility parameter
HPLC	High Performance Liquid Chromatography
HT	Hydrotalcite
H-ZSM	Zeolite Socony Mobil (H-form)
HDO	Hydrodeoxygenation
ICP-OES	Inductively Coupled Plasma-Optical Emission Spectrometry

LB	Lewis basic sites
LC-MS	Liquid Chromatography Mass Spectrometry
L-Na	Lignosulfonate sodium salt Lignin
L-Ca	Lignosulfonate calcium salt Lignin
LTA	Linde type A zeolite
LTL	Linde type L zeolite
MALDI-TOF	Matrix Assisted Laser Desorption Ionization Time of Flight
Mn	Number Average Molecular Weight
MPa	Mega Pascal
MT	Metric Ton
MMT	Million Metric Ton
Mw	Weight Average Molecular Weight
MMF	Monomer molecular formula
NMR	Nuclear Magnetic Resonance
RT	Room Temperature
TGA-DTA	Thermo Gravimetric Analysis-Differential Thermal Analysis
UV-Vis	UV-Visible
XRD	X-Ray Diffraction

ABSTRACT OF THESIS

INTRODUCTION

As the demand for non-renewable fossil resources increases, the reserves of fossil resources throughout the world have diminishing dramatically. As a renewable energy and environment-friendly resource, biomass has drawn extensive attention and preparing the fuels and chemicals from biomass resources instead of fossil resources has become a primary subject. Lignocellulosic biomass offers many possibilities as feedstock for the chemical industry due to its chemical composition, abundant availability and relative low costs when the conversion to products can be carried out in an economic and sustainable manner. Furthermore, sustainability criteria and fixation of atmospheric CO_2 are important drivers in using biomass resources.

Lignocellulosic biomass consists of cellulose (40–50%), hemicelluloses (15–30%) and lignin (10–25%) and a variety of extractives such as nutrients, protein and wax (1–10%).[1, 2] Lignin represents about 20 % of terrestrial biomass and is therefore the most abundant organic material. It is predominantly utilized as secondary fuel, but has the potential to partly replace fossil carbon resources, as basis of chemical industry, due to its unique structure, comprised of the three phenyl propane units, trans-p-coumaryl alcohol, coniferyl alcohol and sinapyl alcohol. Hence, the depolymerization of lignin into low molecular weight aromatic products using various solid base catalysts (Scheme 1), isolation of lignin from coconut coir followed by its characterization & depolymerization and upgradation of lignin model compounds was undertaken as my Ph.D. work.
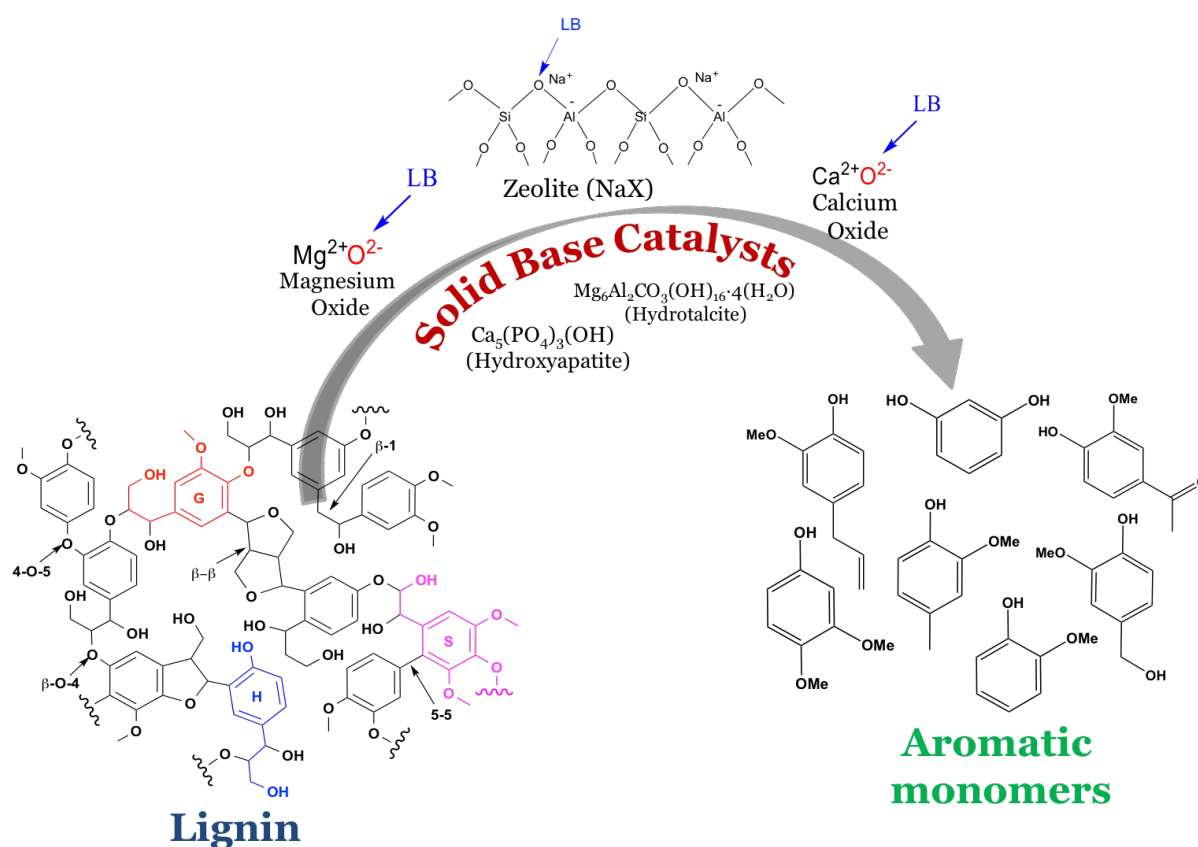
Scheme 1. Lignin depolymerization into aromatic monomers using solid base catalyst.

Excluding introduction chapter my thesis is divided into 5 chapters which discuss the synthesis of various solid base catalysts and characterizations, lignin characterizations, catalytic details, reaction results for lignin depolymerization, isolation of lignin from coconut coir followed by its detailed characterization and depolymerization, upgradation of lignin model compounds, overall summary and novelty of work.

Statement of Problem

Several literature reports suggest that depolymerization of lignin is possible using solid acids,[3-5] homogeneous acids,[6, 7] ionic liquids,[8, 9] supported metal catalysts,[10-12] supercritical fluids[13, 14] etc. to yield low molecular weight aromatic products. However, there are several issues with the current available reports. Those are mentioned below:

- ❖ Use of homogeneous acid catalyst: face serious drawbacks such as difficulty in recovering the catalyst, environmental issues, toxicity, corrosiveness etc.
- ❖ Use of model compounds instead of lignin
- ❖ Difficulties in effective recycling of catalyst
- ❖ Use of multiple reactors for biomass processing; need additional set-up.9,10
- ❖ Low yields with lignin substrates (*Mn* = 890–1700 Da, *Mw* = 4900–8600 Da) and selectivity for desired products.
- ❖ Reactions operation at either higher temperature (≥ 250 °C) or pressures (> 3 MPa) or both.

Based on the above-mentioned drawbacks, it is indispensable to develop a solid base catalyzed methodology for the efficient depolymerization of actual high molecular weight lignin into low molecular weight aromatic products under milder reaction conditions (T ≤ 250 °C) in a one-pot process. Moreover, it is essential to develop a catalyst which can be used for the conversion of direct biomass (coconut coir) into aromatic products, with good recyclability and exploitable at wide range of reaction conditions.

Methodology Used
- ❖ Synthesis of basic zeolites by hydrothermal method and hydrotalcite was done.
- ❖ Supported metal catalysts were synthesized by wet-impregnation method using various metals (Pt, Pd, Ru) and basic supports (NaX, calcined-hydrotalcite (C-HT), CaO).
- ❖ Detail characterizations of all the catalysts using XRD, NMR, TPD-CO2, N2 sorption, ICP-OES, TEM.
- ❖ Detail composition analysis of collected coconut coir (CC) and isolated lignin (Organosolv, Soda and Klason lignin).
- ❖ Use the solid base catalysts as supports along with metals for the upgradation of lignin model compounds.
- ❖ Reactions were carried out in batch mode Parr autoclave and analysis of products obtained was done using GC, GC-MS, HPLC, LC-MS, Microanalysis, NMR and FT-IR.

Sample Results

Solid base catalysts were evaluated for the depolymerization of lignin. Among all the catalysts screened, NaX (Si/Al = 1.2) catalyst showed best activity for the lignin depolymerization into low molecular weight products.

Depolymerization of lignin using solid base catalysts: For the exploration of an efficient catalytic system to depolymerize lignin, various types of solid base catalysts were evaluated at 250 °C for 1 h. As can be seen from Figure 1, zeolites (NaX, NaY, NaP, KLTL), anionic clay (Hydrotalcite (HT)), single metal oxides (MgO, CaO) and hydroxyapatite (HAP) were active for the depolymerization of lignin with varying yields (10–51%) of diethyl ether (DEE) and ethyl acetate (EtOAc) soluble low molecular weight products. Among all the catalysts, the best active catalyst NaX (Si/Al = 1.2) depolymerize lignin into low molecular weight aromatic products with high yield (51 %).[15] Influence of the pH and basic sites in reaction system is shown where due to high pH (> 9.5) shows the strong adsorption of products. Adsorption study was undertaken with mixture of five aromatic monomers (phenol, p-cresol, guaiacol, eugenol and vanillin) which resemble products identified in the depolymerization reactions of lignin and the results imply that the adsorption of formed products is even possible under ambient conditions with strong bases like CaO. Further, Confirmation of aromatic products was done by GC, GC-MS, HPLC, LC-MS, Microanalysis, NMR and FT-IR. Various physico-chemical characterizations for both fresh and spent catalyst was done.
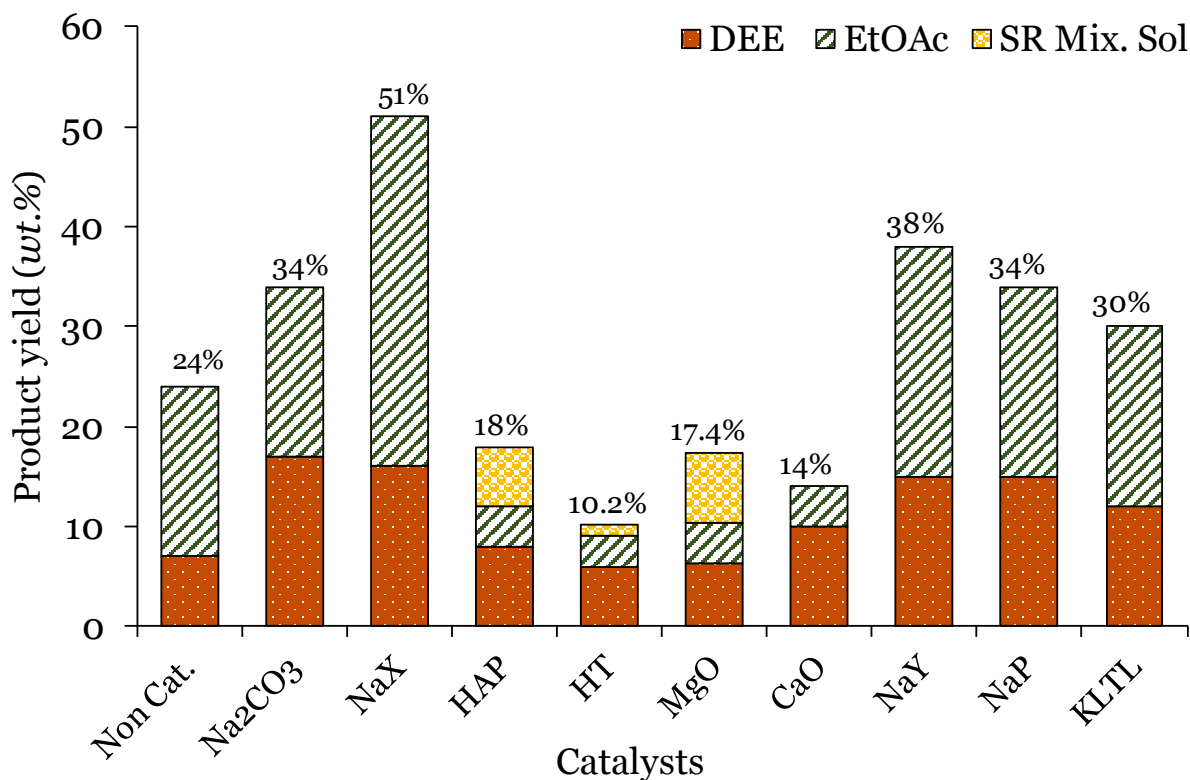
Figure 1. Depolymerization of lignin using solid base catalysts.

Isolation of lignin from coconut coir (CC), its characterization and depolymerization:

Isolation of lignin from coconut coir was accomplished by three different process i.e. organosolv, soda and klason. The 100 % lignin can be isolated from coconut coir using klason method. A detailed characterization of coconut coir and isolated lignin's was done using various techniques like XRD, ^{1}H, ^{13}C NMR, HPLC, LC-MS, microanalysis, EDAX, TGA-DTA, UV visible techniques, etc. After successful implementation of solid bases for the depolymerization of commercially available lignin, it was explored for the depolymerization of isolated lignin (Organosolv, Soda and Klason) and the direct hydrolysis of coconut coir. A maximum product yield of 29% with NaX catalyst (250 ^{o}C, 1h) was achieved for the depolymerization of soda lignin. Analysis of the aromatic products was done using GC and GC-MS. Moreover, 65 % of product yield was achieved for the direct hydrolysis of coir with NaX (Figure 2).
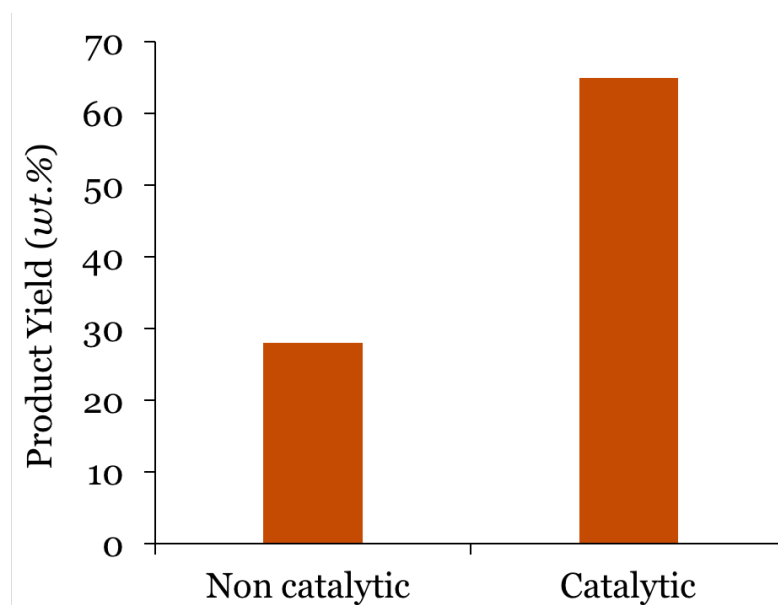
Figure 2. Direct hydrolysis of coir using NaX

Reaction Condition: Coir (0.5 g), NaX (0.5 g), EtOH: H2O (1: 2 *v/v*) 30 mL, 200 °C, 1 h

Upgradation of lignin model compounds:

Higher oxygen contents of lignin derived aromatic monomers reduces the efficiency of fuels. These aromatic monomers can be upgraded via hydrogenation reactions. Lignin derived aromatic monomers like phenol, guaiacol and eugenol was used to study upgradation reactions since similar compounds can be obtained upon lignin depolymerization. Various combination of metals (Pt, Pd, Ru) and supports was chosen [NaX, C-Hydrotalcite (C-HT), CaO]. Since, the basic supports are known to reduce the coke formation on the catalysts and thus increase the catalyst life. Hence we choose solid bases as support. Upgradation of phenol, guaiacol and eugenol was studied in batch mode parr reactor at 250 °C for 1-5 h in 30 mL of hexadecane. 3.0 MPa of H_2 pressure was used for the reaction. Various metal (Pt Pd, Ru) in the combination of basic supports were studied (Figure 3). It can be concluded from the study that selectively ring hydrogenated products can be obtained from basic supports. Effect of various supported metal catalyst were studied and it was observed that 1 *wt.%* Pt/NaX is a good catalyst for the conversion of 55% phenol conversion with 49% yield of cyclohexanol when the S/M ratio changed from 2000 to 200(Figure 4).
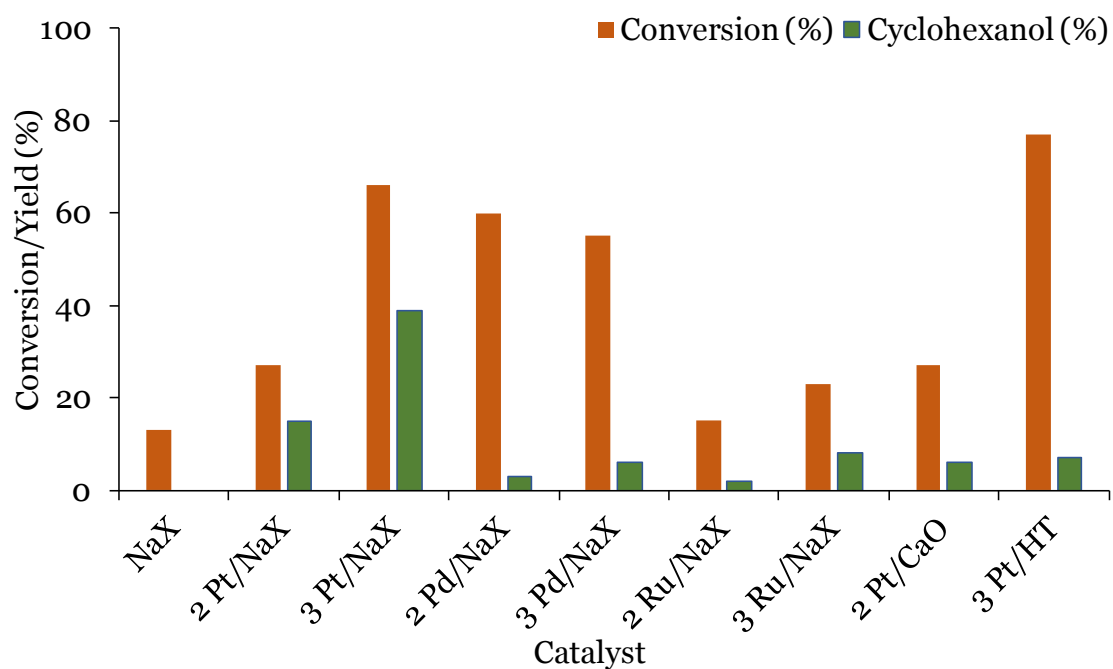
Figure 3. Effect of various supported metal catalysts on the phenol upgradation. Reaction condition: Phenol (2 mmol), Catalyst (S/M = 2000 mol/mol), Hexadecane (30 mL), 250 °C, 3.0 MPa H$_2$ at RT, 5 h.
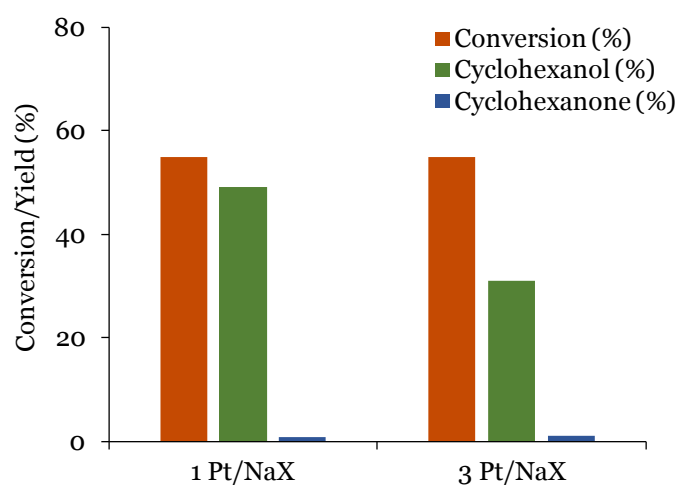
Figure 4. Upgradation of phenol using Pt/NaX (1 *wt.%* and 3 *wt.%*) Reaction condition: Phenol (2 mmol), Catalyst (S/M = 200 mol/mol), Hexadecane (30 mL), 250 °C, 1 h, 3.0 MPa H$_2$ at RT.

References

1. J. Luo, M. Cai and T. Gu, in *Green biomass pretreatment for biofuels production*, Springer, 2013, pp. 127-153.

2. P. i. Mäki-Arvela, T. Salmi, B. Holmbom, S. Willför and D. Y. Murzin, *Chemical reviews*, 2011, 111, 5638-5666.

3. A. K. Deepa and P. L. Dhepe, *RSC Advances*, 2014, 4, 12625.

4. A. K. Deepa and P. L. Dhepe, *ACS Catalysis*, 2015, 5, 365-379.

5. R. K. S. a. N. N. Bakhshi', *Energy & Fuels*, 1992.

6. M. M. H. a. R. W. Thring, *J. Chem. Eng.*, 2000.

7. J. A. Onwudili and P. T. Williams, *Green Chem.*, 2014, 16, 4740-4748.

8. S. K. Singh and P. L. Dhepe, *Green Chem.*, 2016, DOI: 10.1039/c6gc00771f.

9. K. Stark, N. Taccardi, A. Bosmann and P. Wasserscheid, *ChemSusChem*, 2010, 3, 719-723.

10. W. Xu, S. J. Miller, P. K. Agrawal and C. W. Jones, *ChemSusChem*, 2012, 5, 667-675.

11. N. Yan, C. Zhao, P. J. Dyson, C. Wang, L. T. Liu and Y. Kou, *ChemSusChem*, 2008, 1, 626-629.

12. Q. Song, F. Wang, J. Cai, Y. Wang, J. Zhang, W. Yu and J. Xu, *Energy & Environmental Science*, 2013, 6, 994.

13. Wahyudiono, T. Kanetake, M. Sasaki and M. Goto, *Chemical Engineering & Technology*, 2007, 30, 1113-1122.

14. T. Furusawa, T. Sato, M. Saito, Y. Ishiyama, M. Sato, N. Itoh and N. Suzuki, *Applied Catalysis A: General*, 2007, 327, 300-310.

15. R. Chaudhary and P. L. Dhepe, *Green Chemistry*, 2017, 19, 778-788.

Chapter 1
General Introduction and Literature Review

Currently, the demand for petroleum/fossil resource derived chemicals and materials has been increasing in spite of its dwindling availability. Thus, the incentive to use of renewable resources to replace fossil resources is motivating extensive research on new and alternative fuels and chemicals derived from biomass. The reserves of fossil resources throughout the world have been diminishing dramatically, oil prices are increasing, global warming and recycling of waste is also becoming ever more costly and problematic and thus these problems are forcing researchers to look for some other alternatives.[1] Besides these problems, there are many other reasons to justify the use of renewable resources (wind, sun, water, biomass and internal earth heat) in order to shift the current oil based economy into the new renewables-based economy. Anticipated climate changes presumably caused by greenhouse gasses (CO_2 atmospheric accumulation) which are generated by burning of fossil resources, security of energy supply, high and fluctuating energy prices. Development of the rural economy could be considered as the driving forces for finding alternative energy sources, renewable materials and ways to increase the energy efficiency for the production of heat, electricity, transportation fuels, and chemicals.[2, 3]

Countries across the globe have considered increasing the utilization of biomass for meeting their future energy demands in order to meet carbon dioxide reduction targets as specified in the Kyoto Protocol and COP-21 as well as to decrease reliance and dependence on the supply of fossil resources.[4-6] Compared to fossil resources, biomass appears to be a promising renewable resource, which is abundantly available and comparatively cleaner raw material to produce chemicals and fuels.[7] Significant achievements have already been made in the production of ethanol fuel from biomass, primarily from starch and sugar rich components. However, research on second-generation non-edible biomass resource, lignocellulosic biomass for bioethanol production is gaining lot of importance because of its abundant availability,[8, 9] and relatively cheaper than food material feedstock, starch and sugar rich resouces.[10-12]

1.1. Introduction to the Biomass

Biomass can be defined as "biological organic matter derived from living or recently-living organism." Biomass is an extremely important renewable source, that can be used for the power and heat generation and available nearly everywhere. Moreover,

it is a good source of carbon, so it can be used for the production of fuels and chemicals. Biomass feedstocks encompasses a large variety of materials, including wood from various sources, agricultural crops and residues, forestry crops and residues, municipal waste, sewage waste, etc. (Figure 1.1)
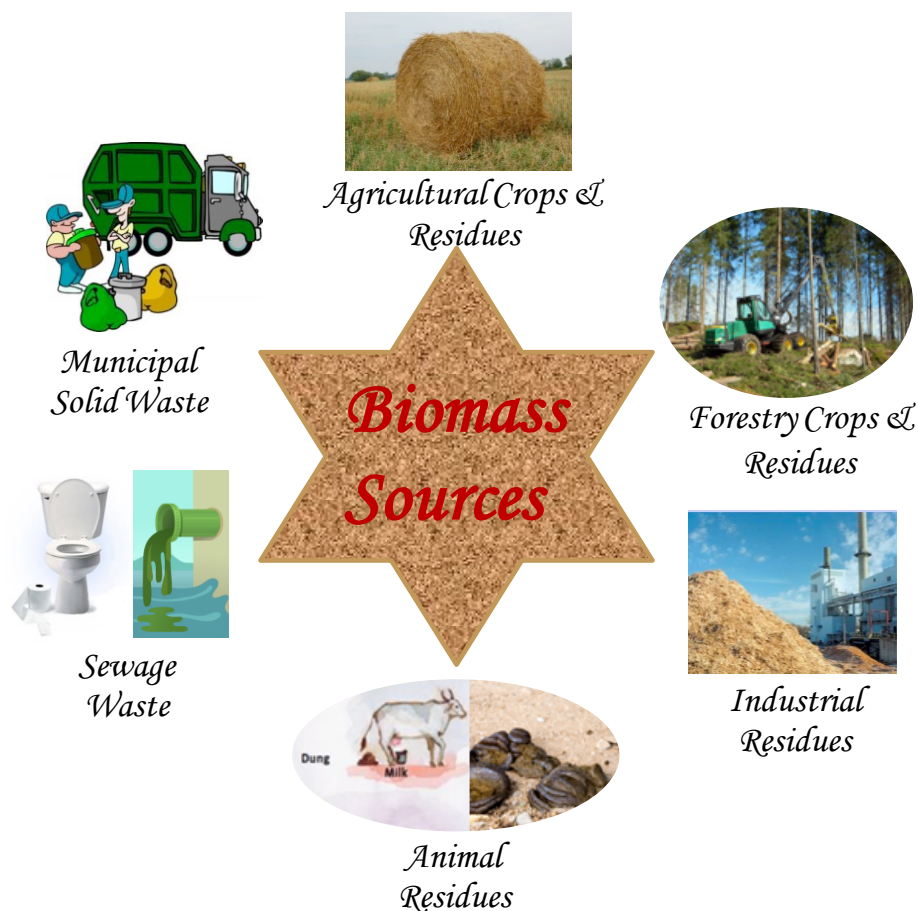
Figure 1.1. Major resources of Biomass.

Biomass can be of plant derived or animal derived. Chitin is the most abundant animal derived biomass while the plant derived biomass includes edible (e.g. starch, sugars) and non-edible biomass. Non-edible plant derived biomass is generally called as lignocellulosic biomass which consists of cellulose, hemicellulose and lignin as main components. In the lignocellulose matrix, these components are bound to each other via various covalent and non-covalent linkages.[13] Biomass has several advantages over conventional fossil resources which can be pointed out as,

- Abundant, inexpensive and locally available renewable resource
- Can lowered the demand for diminishing crude oil supplies
- Sustainability

- Recycling of CO_2
- Improves rural economy

1.2. Lignocellulosic Biomass

The plant derived (non-edible biomass) biomass is normally called as lignocellulosic biomass. The lignocellulosic biomass is mainly made up of 40-50% of cellulose (polysaccharide of glucose units), 25-35% of hemicellulose (heteropolymer of C5 and C6 sugars), and 10-25% of lignin (aromatic polymer) with some minor components such as micro and macro nutrients (micro: boron, copper, iron, chloride, manganese, molybdenum and zinc; macro: nitrogen, phosphorous, potassium, calcium, magnesium and sulfur), proteins and wax (Figure 1.2).[14, 15] Depending on the type of lignocellulosic biomass, these polymers are organized into complex non-uniform three-dimensional structures to different degrees and varying relative composition. Lignocellulose has evolved to resist degradation and this robustness or resistance of lignocellulose stems from the crystallinity of cellulose, hydrophobicity of lignin, and encapsulation of cellulose by the lignin-hemicellulose matrix.[16-18]
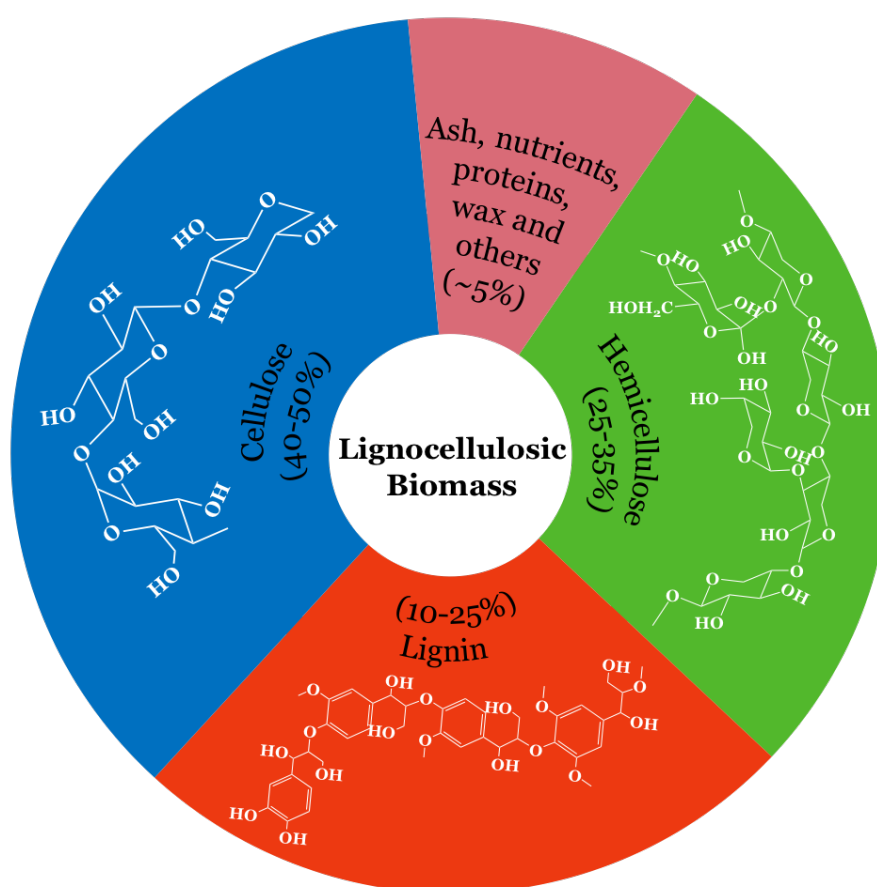
Figure 1.2. Composition and structure of lignocellulosic biomass.

Cellulose is the major component of lignocellulosic biomass and comprises ca. 40-50% of it. Cellulose is a homo-polysaccharide made up of linearly arranged D-glucose units linked together by β-(1→4) glycosidic linkages (Figure 1.2). Its structure consists of strong intramolecular and intermolecular hydrogen bonding. Since about half of the organic carbon in the biosphere is present in the form of cellulose, the conversion of cellulose into fuels and valuable chemicals is extremely important.[19-21]

Hemicellulose is the second most abundant polymer and comprises of ca. 25-35% of lignocellulosic biomass. Unlike cellulose, hemicellulose can be homo- and hetero-polysaccharide made-up of C5 and C6 sugars. Hemicelluloses composition differ from plant to plant; hardwood hemicelluloses contain mostly xylans, whereas softwood hemicelluloses contain mostly glucomannans. According to the composition, hemicellulose can also be called as glucuronoxylan, arabinoxylan, glucomannan and xyloglucan. Hemicelluloses are fixed in the plant cell walls to form a complex network of bonds which provides the structural strength by linking cellulose fibres into micro fibrils and cross-linked with lignin.[22, 23]

Finally, lignin is a three-dimensional polymer of phenylpropanoid units. It functions as the cellular glue which provides the compressive strength to the plant tissue and the individual fibres, stiffness to the cell wall and resistance against insects and pathogens.[24, 25] The structure of lignin formed via the oxidative coupling reactions of three different phenylpropane building blocks: monolignols: p-coumaryl alcohol, coniferyl alcohol, and sinapyl alcohol. The corresponding phenyl propanoid monomeric units in the lignin polymer are p-coumaryl alcohol, coniferal alcohol, sinapyl alcohol (Figure 1.3) and they are generally known as monolignols.

| *p*-Coumaryl alcohol | Coniferal alcohol | Sinapyl alcohol |
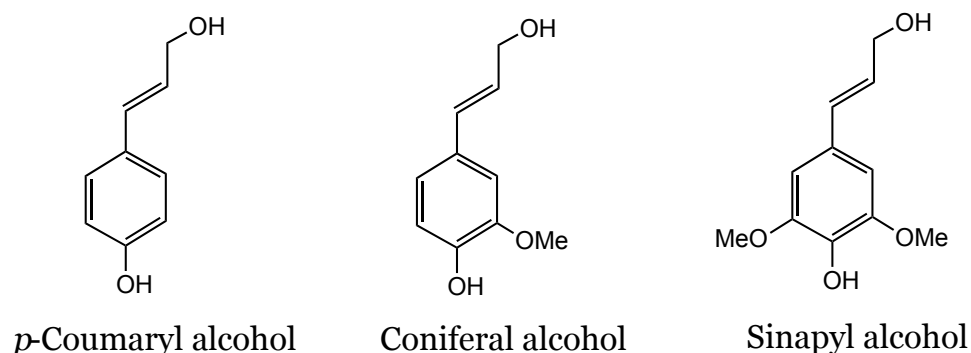
Figure 1.3. Lignin monomer units (monolignols).

1.3. Biorefinery concept

The concept of a biorefinery that integrates processes and technologies for biomass conversion demands efficient utilization of all three components.[26] Presently in the petrochemical industry, crude oil is fractionated and refined to produce various grades of liquid transportation fuels and hydrocarbon feedstocks are functionalized to produce intermediates and specialty chemicals.
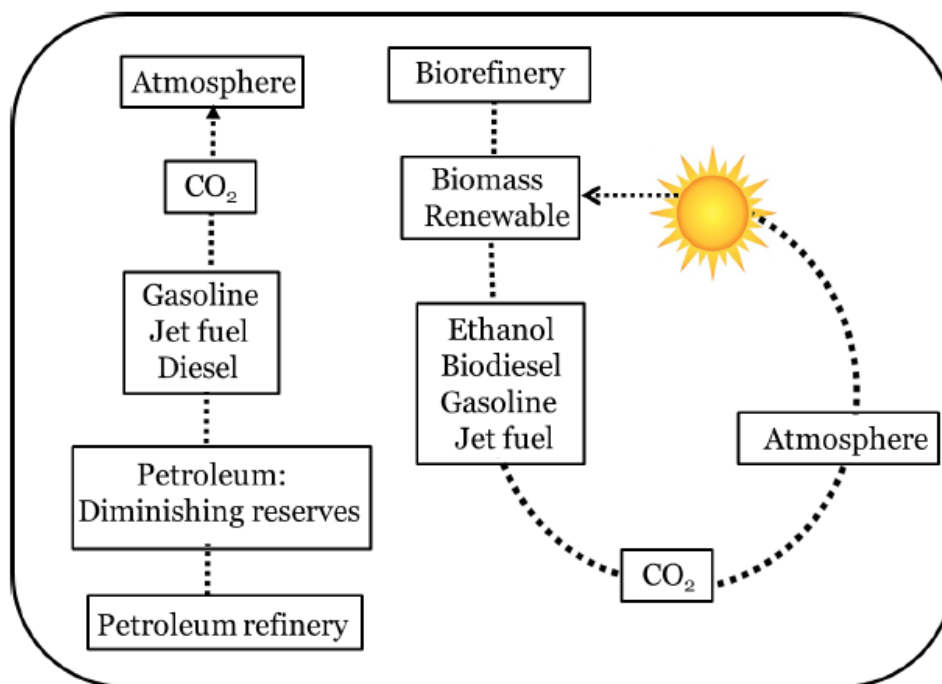
Figure 1.4. Comparison between Biorefinery and petrorefinery.

The analogous concept of biorefining would be similar in scope, with the key difference being that biomass rather than fossil/petroleum would be utilized as a renewable source of carbon[27, 28] that can be transformed into fuels and valuable chemicals within a single facility. Moreover, the quantity and rate of CO_2 emissions from fossil/petroleum feedstocks is far greater than the rate at which it can be recaptured by plants and soils, leading to an increased rate of global warming and many other environmental problems while in the utilization of biomass derivatives reduces the release of greenhouse gas emissions through cycles of regrowth and combustion[29, 30] as illustrated in Figure 1.4. Most of the biorefinery schemes, however, are focused on utilizing easily convertible fractions (cellulose and hemicellulose) while lignin remains relatively underutilized to its potential.[26] Presently, lignin is majorly being utilized only as a low-grade boiler fuel to provide

heat and power.[29, 31] Pulp and paper refineries also generate huge amounts of lignin as waste. Moreover, lignocellulosic to ethanol process makes also the use of cellulose and hemicelluloses while leaving lignin as waste.

1.4. Understanding Lignin

Lignin is the only largest aromatic polymer having 3-dimmensional amorphous aromatic network structure. Depending on the wood species, the content of lignin and ratios of the monolignols (Figure 1.3) differ on the basis of plant. The abundance of lignin in lignocellulosic biomass is in the order: softwood > hardwood > grasses. Typically, Grasses contain all three monomers, while softwood lignins mainly contains coniferyl alcohol and hardwood lignins contain both coniferyl and sinapyl alcohol (Table 1.1).[32] With differing monomer contents, the bonds formed during the polymerization of these monomers also varies as softwood contains more carbon-carbon bonds than hardwood.[33] The diversity in the monomer contents and chemical bonds makes the structure of lignin is extremely complex.

Table 1.1 Composition of monolignols in different plants[34].

Plant	G (%)	S (%)	H (%)
Softwood (gymnosperm)	>95	None or trace	<5
Hardwood (angiosperm)	25-50	46-75	0-8
Grasses (graminaceous)	33-80	20-54	5-33

In general, most lignin linkages are formed by oligomer-oligomer or oligomer-monomer couplings, while fewer are formed from monomer-monomer coupling reactions.[35] The most common linkage, a β-O-4 ether linkage, typically accounts for 50% of bonds formed during the polymerization reaction[36, 37] and is the key target of most degradation studies. Other major linkages include β-5, β-1, β-β, 5-5, and 4-O-5 (Table 1.2 and Figure 1.5) which are significantly more complicated to degrade and often become increasingly difficult to degrade during traditional processing methods

because of significant radical and carbon-carbon bond formations. The structures of several different lignins have been explored through many spectroscopic techniques and chemical methods; however, due to the promiscuous nature of the polymerization, it is doubtful that the full structure of any lignin will ever be fully elucidated.

Table 1.2. Proportion of major linkages in lignin[38].

Linkage type	Softwood (spruce) %	Hardwood (birch) %
(A) β-O-4-Aryl ether	46	60
(B) 5-5-Biphenyl	9.5-11	4.5
(C) α-O-4-Aryl ether	6-8	6-8
(D) β-5-Phenylcoumaran	9-12	6
(E) β-β-(Resinol)	2	3
(F) 4-O-5-Diaryl ether	3.5-4	6.5
(G) β-1-(1,2-Diarylpropane)	7	7
Others	13	5
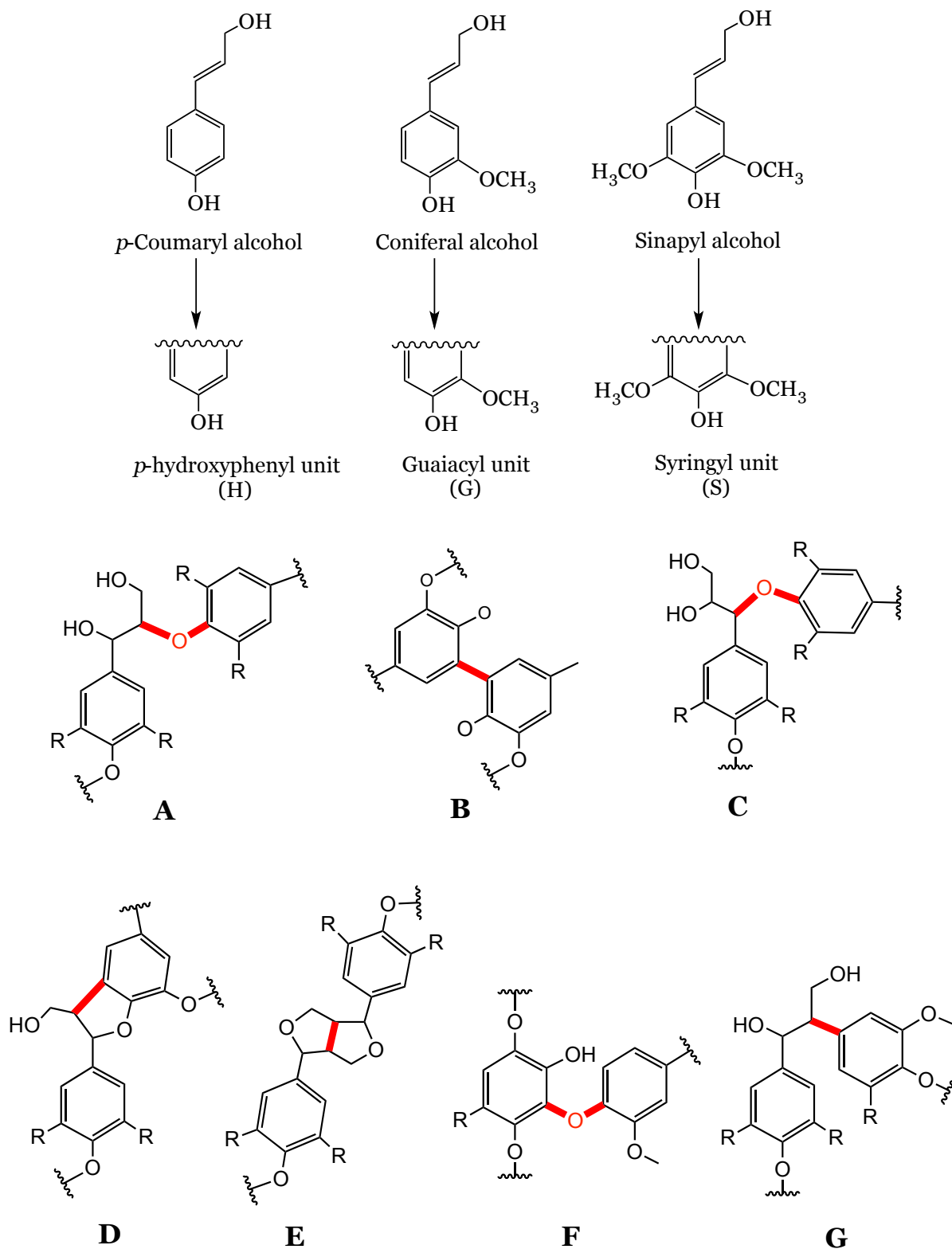
Figure 1.5. Various type of linkages present in lignin
(A) β-O-4, (B) 5-5, (C) α-O-4, (D) β-5, (E) β-β, (F) 4-O-5, and (G) β-1.

1.5. Lignin Isolation Techniques

There are several methods known for the isolation of lignin with the same goal; chemical or physical degradation of the polymeric lignin structure until the resulting fragments become soluble in the pulping media. As per the variation in method used, the properties of the resulting isolated lignin differ. The basic factors in the accomplishment of all process include: the pH of the system, the proficiency of the solvent and/or solute to participate in lignin fragmentation, the proficiency of the solvent and/or solute to prevent lignin recondensation, and the proficiency of the solvent to dissolve lignin fragments.[39] Presently, there are four industrial processes used for the isolation of pure lignin namely; Kraft, Sulfite, Organosolv and Soda. Based on the presence of sulfur in the resulting product it can be divided into two categories namely; sulfur bearing and sulfur free (Table 1.3). Lignins isolated from the Kraft and Sulfite processes contains sulfur, while lignins isolated from the Organosolv and Soda process do not contain sulphur.[40] The sulphur free lignins are considered having more close resemblance to the structure of native lignin. Moreover, based on the isolation procedure resulting products also differ in purity, structure of the resulting fragments and molecular weight of the isolated lignin. Normally, lignins isolated by these methods are denoted as technical lignins.

Table1.3. Commercial production of lignin[40].

Process	Sulfur	Scale (ktpa)	Suppliers
Kraft	Yes	60	Meadwestvaco (U.S.)
Sulfite (Lignosulfonates)	Yes	~ 1000	Borregaard LignoTech (NO, worldwide), TEMBEC (FR, U.S.), Domjo Frabiker (SE), La Rochette Venizel (FR), NipponPaper Chemicals (JNP)
LignoBoost (Kraft)	Yes	27	Domtar (U.S.)
Organosolv	No	~ 3	CIMV (FR), Lignol Innovations (CAN), DECHEMA/Frauhoffer (DE), Dedini (BR)
Soda	No	5–10	Greenvalue (CH, IND)

1.5.1. Sulfite process

The Sulphite process is by far the largest process used commercially to produce lignin, producing approximately 1000 tonnes per year. Sulfite pulping is a process that uses a heated aqueous solution of a sulphite or bisulfite salt with counter cations such as sodium, ammonium, magnesium and calcium.[41] Depending on the identity of the cation and its solubility in aqueous solutions, the resulting pH of the solution varies between 1 to 13.5 and can be a criterion for choice of both cation and anion. The important reaction in delignification by the Sulfite process is the sulfonation of the lignin aliphatic chain, which occurs in different locations depending on the pH of the pulping solution. After reacting, the resulting Lignosulfonate is now water-soluble, making it different from other technical lignins and can be dissolved in the aqueous pulping liquor along with hemicellulose. As carbohydrates are not removed selectively, further purified lignins are obtained by removing the carbohydrate impurities by other techniques such as fermentation, chemical destruction of sugars, ultrafiltration or precipitation.[42]

1.5.2. Soda process

The soda process is typically reserved for non-wood based biomass sources, for example, sugar cane or flax. The Soda lignin process uses sodium hydroxide to dissolve the lignin from lignocellulosic biomass.[43] During this process, the lignocellulosic biomass is added to an aqueous solution of sodium hydroxide and is heated upto 160 °C. Lignin depolymerization primarily occurs with the cleavage of ether bonds (α and β) resulting the free phenolic groups. The resulting lignin fragments are now water-soluble and can simply be isolated from the pulping liquor by precipitation and filtration. Lignin isolated in this method is sulfur free and has a greater purity than that obtained by the Sulfite process but is much lower in molecular weight. The simplified structure of Soda lignin is given in Figure 1.6.

1.5.3. Kraft process

The kraft process also produce sulfated lignin. Normally in this process, the lignocellulosic biomass is added to a mixture of sodium hydroxide and sodium sulfide and heated between 150 and 180 °C for about two hours. Lignin is depolymerized mainly via similar mechanism as the soda process; cleavage of

α and β ether bonds. The majority of the lignin is sulfate-free allowing isolation of the lignin through acidification and precipitation. Although, a small portion of the resultant lignin is sulfated through the presence of hydrosulfide anions.[44] Isolation of lignin from this process has been boosted through LignoBoost technology.[45] This process employs CO_2 as an acid for lignin precipitation from black liquor, after filtration re-dissolved in H_2SO_4 to maximize the quantity and purity of isolated lignin.[46] Domtar has successfully commercialized this process and introduced to the market, producing 27,000 tonnes of kraft lignin in 2013.[47]

1.5.4. Organosolv process

This method utilizes an aqueous-organic solvent mixture, such as ethanol, methanol, acetone, or organic acids (sulphuric, acetic or formic acid) and heated to approximately 180 °C.[48] This method also seen as environmentally friendly as lacks the sulfur, high temperature and pressure. Although the organosolv process has yet to lead the market in production. It is possible that this method will replace kraft lignin over the time, as it is capable of yielding high purity lignin. In addition to the four methods discussed above, there are several other methods like mechano-processes (ball-milling, milling with a catalyst), steam explosion,[49] pyrolysis and processing with ionic liquids[50] employed in the lab or in pilot plant reactors. The simplified general structure of all the lignin is mentioned in Figure 1.6.
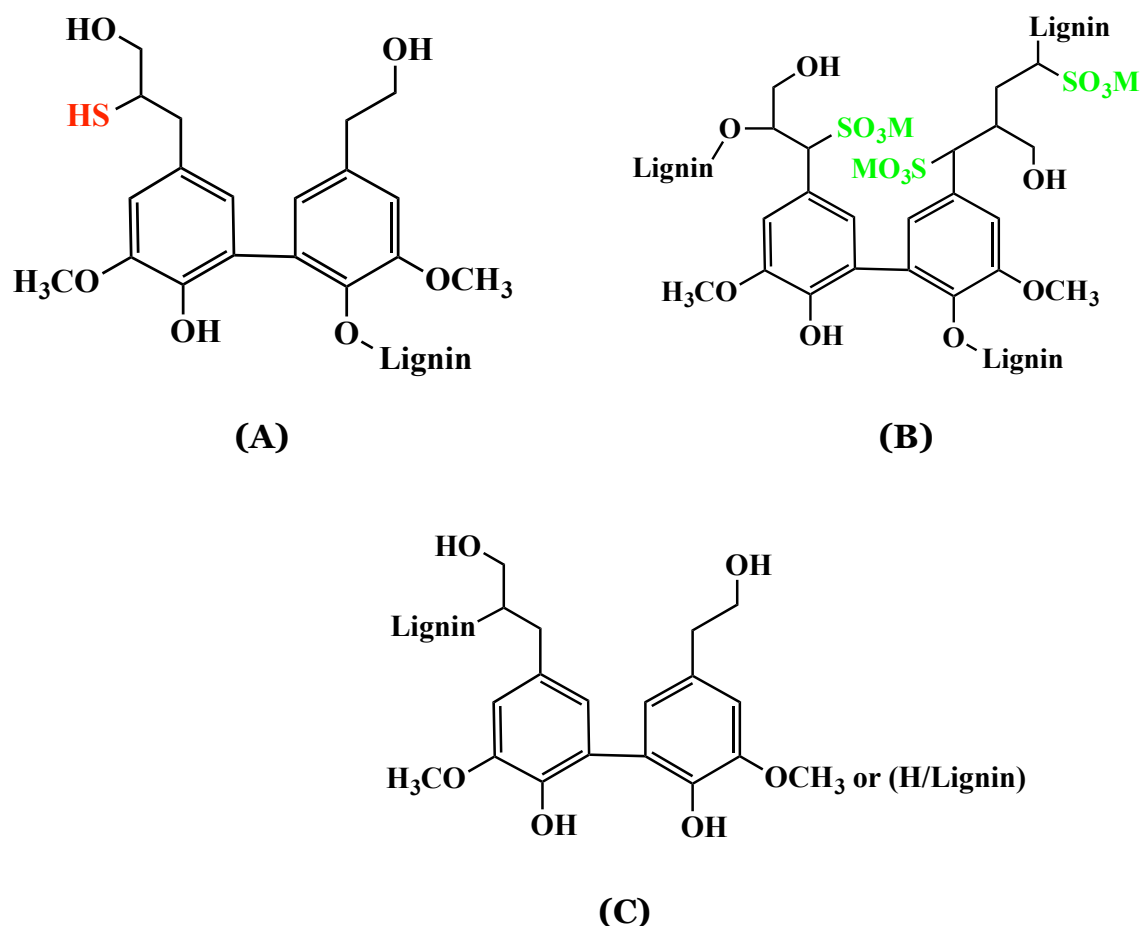
Figure 1.6. Simplified structures of (A) Kraft lignin with introduced thiol group (-SH), (B) Lignosulfonate with introduced sulfonate group and counter ion (-SO₃M), (C) Organosolv and Soda lignin.

1.6. Applications of Lignin

Lignin is a versatile raw material for many applications due to the presence of various functional groups in its structure. As a feedstock, lignin offers great potential for the manufacturing of high value products. The opportunities and challenges for biorefinery lignins are described in an extensive study.[51] This section demonstrates the versatility of lignin for multiple applications. Potential uses of lignin are classified in different groups as listed here after:

1. power-fuel-syngas

2. macromolecules

3. aromatics (phenols, hydrocarbons and oxidized products)

These groups can also be distinguished according to the time-to-market with group 1 as current or near-term applications, group 2 for medium-term applications and

group 3 for the longer-term applications for the production of phenols, hydrocarbons and oxidized products. The potential applications of lignin are shown in Figure 1.7.

- Phenols
- Substituted phenols
- Catechols
- Cresols
- Resorcinols
- Guaiacols
- Syringols
- Coniferols
- Eugenols

Carbon fibers •
Polymer extenders •
Thermoset resins •
Substituted lignins •
Composites •
Adhesives •
Binders •
Preservatives •
Pharmaceuticals •
Polyols •

Phenols

Macro-molecules

Lignin

Hydro-carbons

Syngas products

Oxidized products

- Benzene
- Toluenes
- Xylene
- Cyclohexanes
- Styrene
- Biphenyls

Methanol •
Ethanol •
DME •
Mixed alcohols •
Fisher-Tropsch liquids •
C1-C5 gases •

- Vanillin
- Vanillic acid
- Aromatic acids
- Aliphatic acids
- Aldehydes
- Syringaldehydes
- Cyclohexanols
- Quinones
- DMSO
- β-keto adipate

Figure 1.7. Potential applications of lignin.

In the first group, lignin is used as a carbon source for energy production or is converted in energy carriers such as syngas. The second group make use of lignin's macromolecular nature and will be used in high molecular mass applications like wood adhesives (binders), carbon fibres, and for polymers like polyurethane foams.[52, 53] The third group uses technologies to cleave the lignin structure into monomers without sacrificing the aromatic rings for production of polymer building blocks, aromatic monomers such as benzene, toluene and xylene (BTX), phenol, vanillin, etc.

1.7. Recent Developments on Lignin Depolymerization

In contrast to the earlier discussions, this section will be dedicated to thermal and chemical processes necessary to convert lignin into useful chemical products.

Recently, researchers have shifted their interest to produce aromatic chemicals from lignin without the use of fossil/petroleum-based feedstocks (Figure 1.8). Numerous reviews[54-57] and perspectives[58, 59] have been recently published on lignin valorization. Herein, the methods used to upgrade lignin in to chemicals will be discussed.
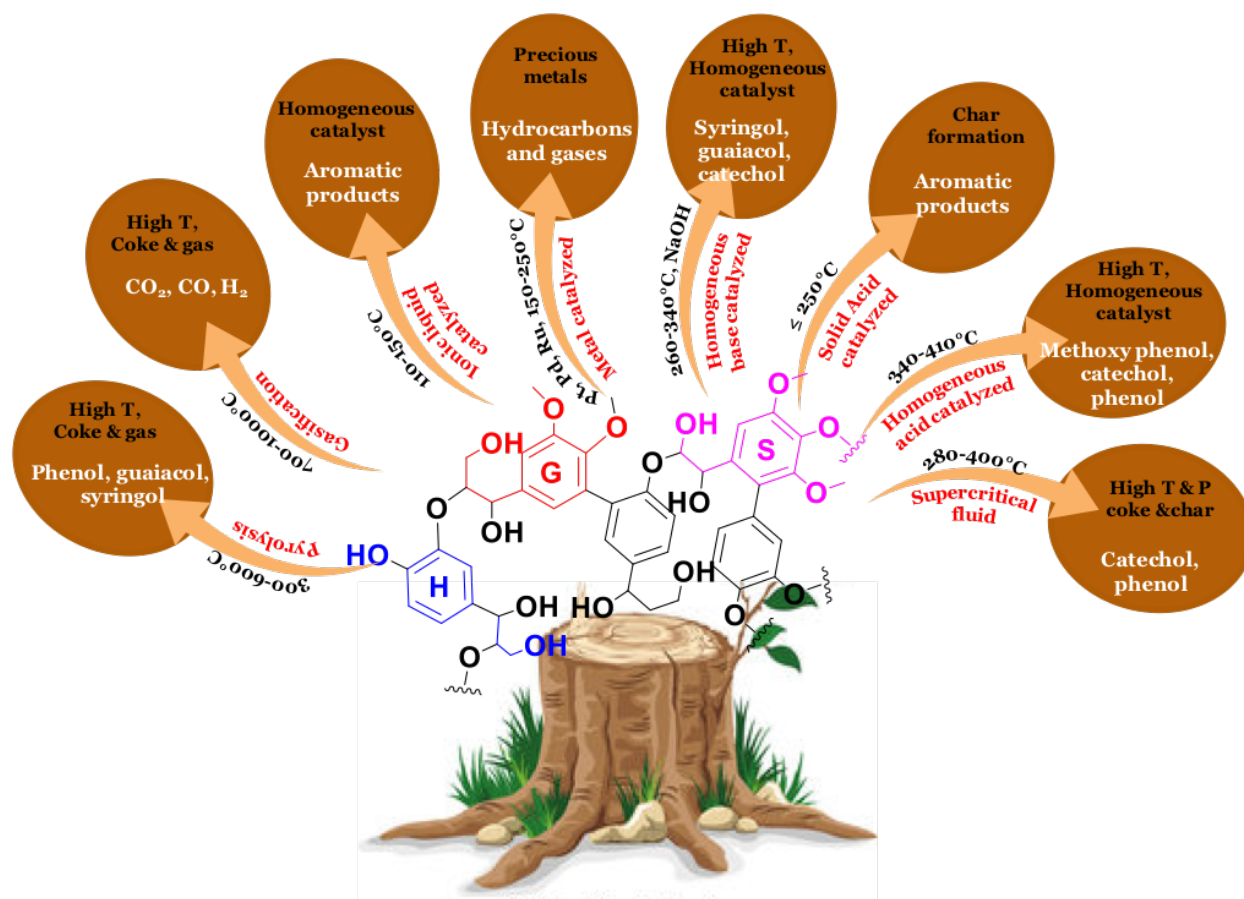
Figure 1.8. Lignin valorization tree.

1.7.1. Thermal Depolymerization

Generally thermal depolymerization covers the pyrolysis and gasification of lignin.

1.7.1.1. Pyrolysis

Pyrolysis involves anaerobic thermal decomposition of lignin into mixtures of small molecules, which can be used to form chemicals and fuels. This is the commercialized process and several pyrolysis plants recently developed in Wisconsin, US (50 tons of biomass/day); in Vancouver, Canada (10-100 tons of biomass/day) and in Finland (12 tons of biomass/day).[60] At the high temperatures of pyrolysis (370-550 °C), vapor-phase products react and condense to form mixture of liquid products. Lignin pyrolysis reactions produce oxygen-containing compounds

including phenol, guaiacol and syringol. Generally, pyrolysis of softwood lignin mostly produces guaiacol derivatives, whereas pyrolysis of hardwood lignin yields both guaiacol and syringyl derivatives.[61-67]

1.7.1.2. Gasification

Gasification of lignin yields syngas (synthesis gas) as product which is a mixture of CO and H_2.[68, 69] This syngas can be further converted into liquid fuels by two different commercial processes: Fischer-Tropsch synthesis[70] and methanol/dimethyl ether synthesis.[71] Supercritical water (374 °C, 218 atm.) was used extensively for gasification of lignin.[69, 72] In terms of thermal efficiency, this process offers the advantage of reducing the need to dry the biomass, which is especially important for lignin with high moisture content. By the optimized reaction conditions and the catalysts, numerous products, ranging from synthetic natural gas, olefins and alcohols to various transportation fuels (gasoline, jet fuel and diesel) can be synthesized through gasification.[73] Although syngas routes for the production of chemicals are well established for coal and natural gas conversion.[51] Biomass gasifiers are still in the developing stage for producing synthetic gas. Few attempts are reported for the lignin gasification at the pilot scale. To evaluate the performance of a pilot plant for the auto thermal gasification of lignin-rich fermentation residues was carried out by Zimbardi[74] and colleagues. They used the feeding rate of 20-30 kg/h. The average production of raw syngas was 1.94 kg of dry residue, of which hydrogen and carbon mono-oxide were 27.2 g and 696 g, respectively.

1.7.2. Chemical Depolymerization

1.7.2.1. Acid Catalyzed

Previously, acid pulping was mainly used for the isolation of lignin from the lignocellulose matrix, rather than in designing the depolymerization of lignin into value-added aromatic monomers.[75] Recently, different types of mineral acids,[76, 77] lewis acids,[78, 79] zeolites,[80-83] acidic ionic liquids,[84, 85] as well as organic acids[86, 87] have been examined for the hydrolysis of lignin and the related model compounds. In acid-catalyzed delignification of wood and lignocellulosic biomass, the hydrolytic cleavages of α and β aryl ether linkages also play a dominant role[88] because aryl-aryl ether bonds, the phenolic C-O bond and C-C bonds between aromatic lignin units are more stable.[89] Lewis acid catalysts such as $FeCl_3$, $ZnCl_2$, BF_3, and $AlCl_3$ have been

used to depolymerize lignin, with the result that low yields of phenols were produced.[90] This was proposed to be a thermodynamically favourable process, since the performance highly depends on the reaction temperature.[91] Bio-oil obtained from the pyrolysis of lignin was studied at a temperature range of 340-410 °C and atmospheric pressure using acidic zeolite (HZSM-5) as a catalyst.[57] The objective is to maximize the concentration of hydrocarbon (83 *wt. %)* in the expected organic distillate product.

1.7.2.2. Base Catalyzed

Most lignin depolymerization processes are conducted at temperatures of 250-650 °C, with or without catalysts. As a result, a complex phenolic mixture of alkylated and poly hydroxylated phenol compounds as well as volatile components and char are formed, which presents challenges for downstream processing to separate phenolic-like compounds or upgrading to more homogeneous mixtures. Base catalyzed hydrolysis of lignin is one exceptional route for the production of simple aromatic chemicals under mild conditions. The catalytic reagents are cheap and commercially available bases such as LiOH, NaOH, and KOH. As aryl-alkyl ether bonds, including β-O-4 bonds, are the weakest bonds in lignin structure,[92] cleavage of ether linkages is a dominant reaction in alkaline delignification processes.[93, 94] An ideal base catalyzed depolymerization would be a reaction affording high yields of monomers aromatics while also allowing their easy separation from the reaction mixture. In the base-catalyzed lignin hydrolysis reaction, the selectivity and yield of the products are particularly dependent on pressure, temperature, time, concentration of the base, and lignin/solvent ratio.[95-97] Equally important, the oil yield and products composition vary strongly depending on the nature of the base. Usually, stronger base gives higher conversion since the polarization of the base governs the kinetics and the mechanism of the depolymerization reaction.[98, 99] The kinetics of reactions is faster in phenols[95] or alcohols[99] than in water due to the ether linkages solvolysis effect. A higher temperature and longer reaction time favour monomers generation. The formation of a solid residue increases due to the condensation/repolymerization reactions of the degradation of intermediates or products. Indeed, repolymerization reactions are believed to be one of the main problems in the production of monomers. Therefore, decreasing the rate of repolymerization and oligomerization reactions during base-catalyzed lignin

depolymerization is the key issue to enhance the yields of the products. Repolymerization of products was tried to resolve by involving the use of capping agent to capture the reactive species. Lercher.[96, 100, 101] They added boric acid, phenol, 2-naphthol, and *p*-cresol in water to capture reactive fragments, such as phenolic compounds and formaldehyde, and cover the active sites. In these methods, complete conversion of lignin without char formation was realized. The use of hydrogen donating solvents, such as formic acid (HCOOH),[102] has been shown to suppress char formation. Other approaches that should be considered to tune the reaction selectivity for base-catalyzed lignin depolymerization include the development of more active catalysts that allow for more milder conditions It should be noted that, in base-catalyzed reactions, acidic molecules are produced during depolymerization reactions, which, over time, can induce the deactivation of the catalyst via acid/base neutralization.

1.7.2.3. Metal Catalyzed

Metallic catalysts were studied to increase the selectivity of lignin depolymerization. It was reported that the treatment of alcell derived lignin was carried out in presence of $NiCl_2$ or $FeCl_3$ by Hepditch and Thring. But only 2.5 *wt.%* yield of catechol was obtained at 305 °C. More recently, several other attempts showed higher efficiency and selectivity.[103-106] A two-step process was carried out by Yoshikawa et al. in the treatment of kraft lignin. Kraft lignin was treated by Si-Al catalyst in H_2O/butanol medium first, followed by reaction on ZrO_2-Al_2O_3-FeOx catalyst to increase the total recovery of phenols. The phenols yield was 6.5 to 8.6%, and the conversion of lignin to methoxyphenols was 92-94%. In order to increase the yield of low-molecular weight fraction, 20 *wt.%* of Pt/C catalyst was used with formic acid and ethanol by Xu et al. in the treatment of organosolv switchgrass lignin.[104] An obvious increase of the guaiacol derivatives yield was observed in presence of metallic enhancer. Another attempt of optimizing the formic acid catalyzed system was carried out by Liguori and Bar.[107] Pd catalyst and Nafion SAC-13 were used in treatment of both lignin model compounds and spruce dry lignin pretreated by different methods in water medium at 300 °C. Guaiacol, pyrocatechol and resorcinol were isolated, but the yields were all lower than 5 *wt.%*. The slight difference of the yield of guaiacol, pyrocatechol and resorcinol is probably because of the different lignin pretreatment methods. Although depolymerization at lower temperature was carried out in

presence of Pt and Pd metallic enhancers compared to simple acid-catalyzed depolymerization, no decrease in the activation energy has been reported. Future research needs to be conducted to clarify the mechanism and function of metallic enhancer in acid-catalyzed lignin depolymerization. Research from Song et al. exhibited a method of nickel compound catalyzed depolymerization of lignosulfonate into guaiacols.[105] The nickel catalyst provided a high conversion of above 60% and a high selectivity of 75 to 95% to guaiacols. More importantly, the reaction temperature was decreased to 200 °C from around 380 °C compared with the pyrolysis process only in presence of acid or base.

1.7.2.4. Supercritical Fluid Assisted

Supercritical fluids are well known to dissolve and depolymerize the lignin. The property of supercritical fluids shows low viscosity which is helpful in the developing a fast, homogeneous and efficient reaction system. There are numerous examples for supercritical fluids, includes carbon dioxide, water, acetone, methanol and ethanol. Depolymerization of lignin model compounds and actual lignin substrates are reported in supercritical alcohols like methanol or ethanol at temperature and pressure above 239 °C and 8 MPa, respectively. Addition of homogeneous base was studied with this system and increase in the depolymerization of lignin was observed.[108, 109] During this process, solvolysis of C-O-C linkages in lignin structure occurs while the C-C linkages remain stable. Depolymerization of organosolv lignin in supercritical water is reported. Effect of the phenol addition was explored with organosolv lignin for completely depolymerization at temperatures between 400-600 °C. The presence of phenol avoid the repolymerization and char formation at high pressures up to 10 MPa.[110] Yield of low molecular weight fraction was increased in supercritical water at 350-400 °C and 25-40 MPa with long reaction time. The water soluble fraction contains catechol, phenol, m-cresol, *p*-cresol and o-cresol suggesting the cleavage of both ether and carbon-carbon bonds.[111] Additives like phenol and *p*-cresol suppress the cross linking reactions by the entrapment of reactive fragments like formaldehyde and capping of active sites in the lignin structure. Gosselink *et al.* used carbon dioxide/acetone/water supercritical fluid to treat organosolv hardwood lignin and wheat straw lignin at temperature around 300-370 °C at 10 MPa pressure to obtain syringol and guaiacol as product.[112] From the earlier reports it was understood that supercritical fluid assisted depolymerization of lignin has

advantages like good solubility for organic compounds, high selectivity towards depolymerized products and can be easily separated by solvent extraction method. But they also have disadvantages like the use of high temperature and pressure for the reactions which increases the capital cost of the process.

1.7.2.5. Ionic Liquid Catalyzed

Ionic liquid (IL) solvents are advantageous for lignin conversion because they readily dissolve lignin[113-115] and favour carbocation-forming reactions.[116, 117] When Lewis acid catalysts such as metal chlorides are applied in ionic liquids, they are more effective in cleaving the β-O-4 bond of lignin and model compounds.[118] In this process, the real catalytic species is the hydrochloric acid, which is formed in situ by the hydrolysis of the metal chlorides. Using acidic ionic liquid as catalyst and solvent (both) for the hydrolysis of lignin model compounds has also been tested. Ekerdt[119] and colleagues employed 1-H-3-methylimidazolium chloride [(Hmim)Cl] for the treatment of lignin model compounds. These two model compounds underwent catalytic hydrolysis to produce guaiacol as the main product with yields higher than 70% at 150 °C. The reactivity and mechanism of the model compounds in the ionic liquid depends not only on the acidity, but also on the nature of cations and anions, and their interaction with the substrate.[120, 121] The ability of ionic liquids to swell or dissolve lignocellulose makes it possible to obtain the direct conversion of raw biomass under mild conditions without pretreatment.[122] Argyropoulos[123] and co-workers showed that the acidic pretreatment of the raw biomass (wood) species in ionic liquid (Amim)Cl resulted in not only the complete hydrolysis of cellulose and hemicellulose but also lignin depolymerization to obtain phenols.

1.7.2.6. Oxidation

Oxidation is another technique utilized to isolate aromatic products from lignin. The products generated from this process typically possess increased complexity and functionalization, in comparison to products from hydrogenation. Industrially, lignin is most commonly oxidized with nitrobenzene, hydrogen peroxide, or metal oxides. Other methods involve utilizing both an oxidant (typically gaseous oxygen) and a catalyst. While a catalyst is not required for the oxidative degradation of lignin with oxygen, reactions without a catalyst are less selective.[124-126] As the oxidation of lignin is decreased without adding a catalyst and industrial methods have not seen recent

modification, we will instead focus on new catalytic oxidative methods found in the literature. The catalytic oxidation of lignin can be divided into two categories (depending on the state or origin of the catalyst): heterogeneous and homogeneous. With ease of catalyst recovery, heterogeneous catalysts are usually preferred industrially and have proven to be advantageous in lignin oxidation.[127]

1.8. Applications of Lignin Depolymerization Products

Previously, lignin has been a burden on the pulp and paper industry with large quantities of excess lignin produced each year. Lignin has to date mainly been used for internal energy supply in the pulp and paper mills. However, the chemical structure of lignin allows its use in a wide range of applications in chemical industry. Current lignin products offer options lignin to bring in higher value-added chemicals than burning for combined heat and power. Application of few of them are discussed below:

Vanillin

Vanillin is widely used as fragrance in food industry. It is used as flavor enhancer in chocolate, candies, biscuits, instant noodles, bread, ice-cream and beverages to improve flavour. It is widely used as intermediate in pharmaceutical for the manufacturing of medicine. Vanillin is also used as fragrance in cosmetics and commercial perfume to endue milk flavor.
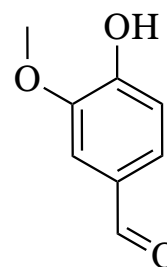
Vanillin

Resorcinol

Resorcinol is a critical raw material for reinforced rubber product adhesion systems, including natural and synthetic rubber to steel, nylon, polyester, aramid, glass and rayon fibers employed in tires. Moreover, it is used in the areas of pharmaceuticals, rubber compounds (tires, hoses, belts),

Resorcinol

polymers, polymer additives (UV absorbers, flame retardants) and composites (polymers and wood). Resorcinol is an essential raw material for the synthesis of many specialty chemicals including ultraviolet light absorbers, fire retardants, polycarbonates, urethane elastomers, etc.
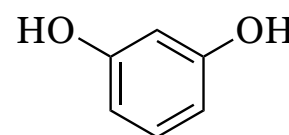
Catechol

Catechol is used in the production of pesticides and as a precursor to fine chemicals such as perfumes and pharmaceuticals. It is a common building block in organic synthesis. Numerous industrially significant fragrances and flavors are prepared from catechol. The catechol unit has been recently developed as a powerful building block for the preparation of a large range of polymeric materials with fascinating structures and interesting properties.
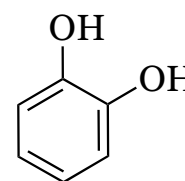
Catechol

Guaiacol

Guaiacol is used as an intermediate for the chemical synthesis of active pharmaceuticals. It is also used as food flavourings and perfumery products. Its derivatives are used for medical purpose as an expectorant, antiseptic and local anesthesia effect.
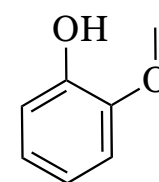
Guaiacol

Eugenol

Eugenol is used in perfumes, flavorings, and essential oils. Eugenol is a major constituent of clove oil and has been widely used for its analgesic and anesthetic effect in dentistry. It possesses significant antioxidant, anti-inflammatory and cardiovascular properties. Eugenol is a very promising candidate for resourceful applications and the design of new drugs based.
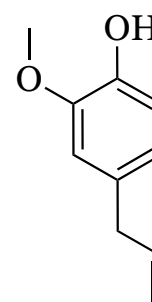
Eugenol

1.9. Catalyst and Catalysis

A catalyst is a substance/mixture of substances, which alters the rate of a chemical reaction by providing a complementary, faster reaction path, without changing the thermodynamic factors. In general, the catalyst remains unaltered at the end of the catalytic process. The properties of a catalyst which can determine its high-quality are mentioned below:

1) The activity of the catalyst which can be expressed in terms of rate of reaction (moles of product/volume of catalyst per hour), turnover number (mole of product/mole of catalyst or active site) and conversion (mole of reactant converted/mole of reactant charged). Moreover, catalyst activity can be conveyed as

the higher the activity of catalyst, higher the productivity of products, and/or lower the volume of the reactor and milder the reaction conditions that can be used.

2) The chemical, stereo or regio selectivity (expressed as mole of desired product/ mole of converted reactant) towards the reaction. The higher the selectivity, the lower the costs of separation or purification and waste treatments.

3) The simplicity of regeneration of spent catalysts (in order to increase the catalyst lifetime and to reduce the problems related to separation of spent catalyst).

4) The toxicity, handling (easily and safely) and the disposal of spent catalysts.

5) The cost of catalyst should be economically favourable.

The process in which a catalyst changes or speeds-up the rate of chemical reaction without being consumed or altered in the process is called as catalysis. Catalysis can be classified into two types according to the phases involved in the process i.e. homogeneous and heterogeneous catalysis.

1.9.1 Homogeneous Catalysis

As the name also indicates, the reactant, product and catalysts are present in the same phase (usually liquid phase). Homogeneous catalysts involve soluble acids, bases, salts and organometallic compounds. It has several advantages and disadvantages too which are summarized below:

Advantages:

- The utilization of almost all the molecules of the catalyst during the catalytic reaction.
- Higher selectivity obtained especially in the synthesis of optically active compounds.
- Temperature for highly exothermic reactions can be controlled easily.

Disadvantages:

- Separation and recovery procedures are very expensive.
- Serious problems of corrosion when acid catalysts/ solvents are engaged.
- Costly treatment for the toxic liquid waste obtained after the separation, regeneration and recycling of the catalysts.
- Possibility of contamination of desired products by catalysts.

1.9.2. Heterogeneous Catalysis

The reactants, products and catalysts are present in the different phase. Generally, the reactant and products are present in liquid or vapour phase while catalyst is in solid phase. Heterogeneous catalysts involve inorganic solids such as metal oxides, zeolites, clays, resins, supported metals, etc. The advantages and disadvantages associated with this is as follows:

Advantages:

• Separation of catalyst from the reactants or products is easier.

• Elimination of corrosion problems and liquid waste treatments.

• Recovery and regeneration of catalysts are very simple.

Disadvantages:

• Difficulty in the temperature control for highly exothermic reactions.

Out of the several types (solid acids, solid bases, supported metals, etc.) of heterogeneous catalyst. Here, I am giving brief introduction of solid base catalysts since those are used in the present thesis for the depolymerization of lignin.

1.10. Solid Base Catalysts

Solid acids and solid bases are the significant catalysts for the replacement of homogeneous systems. Solid acid catalyzed process are well stabilized for lignin depolymerization. For bases, homogeneous base catalyzed for the depolymerization (BCD) of lignin process are broadly studied in the literature. But these methods possess several drawbacks such as difficulty in recovery of the catalyst, environmental issues, toxicity, corrosiveness, etc. So, in order to overcome the drawbacks associated with homogeneous system, solid base catalysts were studied for the depolymerization lignin.

In particular, base-catalyzed reactions have been studied to a lesser extent as compared to acid-catalyzed reactions in heterogeneous systems. The first study of heterogeneous base catalyst, that sodium metal dispersed on alumina acted as an effective catalyst for double bond migration of alkenes.[128] Considering the strong tendency of sodium to donate the electrons, it looks natural that sodium dispersed on alumina acts as a heterogeneous base catalyst. In the same period, Hattori et al. reported that calcium oxide and magnesium oxide exhibited high activities for 1-butene isomerization after the pretreatment of catalysts under proper conditions

such as high temperature and high vacuum.[129] A number of materials have been reported in the literature to act as heterogeneous base catalysts. The types of various heterogeneous base catalysts are listed in Table 1.4. Excluding the non-oxide catalysts, the basic sites are believed to be surface oxygen atoms. Oxygen atoms existing on any materials can be act as basic sites because the oxygen atoms would be able to interact nicely with a proton.

Table 1.4. Type of solid base catalysts.

S.No.	Type	Example
1	Metal oxides	CaO, MgO, Al_2O_3, ZrO_2, SiO-CaO, SiO-MgO, Al_2O_3-MgO (calcined hydrotalcite)
2	Alkali compounds supported on alumina	KF/Al_2O_3, K_2CO_3/Al_2O_3, $NaOH/Al_2O_3$, KOH/Al_2O_3.
3	Supported alkali metal	Na/Al_2O_3, K/Al_2O_3, K/MgO, $Na/zeolite$, MgO/SiO_2, $CsO_2/zeolites$
4	Anion exchangers	Anion exchange resins (Tulsion A-27)
5	Zeolites	K, Rb, Cs-exchanged X-zeolite
6	Clay	Sepiolite
7	Phosphates	Natural phosphates, hydroxyapatite

The materials listed in Table 1.4 act as a heterogeneous base toward most of the reactions and therefore are called as heterogeneous basic catalysts or solid base catalysts. The four reasons for recognizing certain materials as heterogeneous basic catalysts are well documented in the literature are as follows.

(1) Characterization of the surfaces indicates the existence of basic sites: Characterizations of the surfaces by various methods such as color change of the acid-base indicators adsorbed, surface reactions, adsorption of acidic molecules and spectroscopies (W, IR, XPS, ESR, etc.) indicate that basic sites exist on the surfaces.

(2) There is a parallel relation between catalytic activity and the amount and/or strength of the basic sites: The catalytic activities correlate well with the amount of basic sites. Also, the active sites are poisoned by acidic molecules such as HCl, H_2O and CO_2.

(3) The material has similar activities to those of homogeneous basic catalysts for "base-catalyzed reactions" well-known in homogeneous systems: There are numeral reactions known as base-catalyzed reactions in homogeneous systems. Certain solid materials also catalyze these reactions to give the same products. The reaction mechanisms occurring on the surfaces of catalysts are suggested to be basically the same as those observed in homogeneous basic solutions.

(4) There are indications of anionic intermediates participating in the reactions: Mechanistic studies of the reactions, product distributions and spectroscopic observations of the species adsorbed on certain materials indicate that anionic intermediates are involved in the reactions. The more details on the solid base catalysts, basic sites present and various characterization are described in Chapter 2B.

1.11. Closest Available Literature for the Present Work

A hydrotalcite supported Ni catalyst (Ni/HTC) was reported to cleave the β-O-4 aryl-ether bond present in the lignin model compound, 2-phenoxy-1-phenethanol (PE) at 270 °C to yield phenol and acetophenone as products.[130] The same catalyst was also used for the depolymerization of organosolv and ball milled lignin to yield a mixture of alkyl-aromatic products.[130] The employment of a porous metal oxide (PMO) supported copper catalyst (Cu-PMO) for the depolymerization of organosolv lignin into derivatives of catechol and some oligomers under 3-6 MPa H_2 pressure at 140-220 °C is also reported.[131] The Cu doped PMO catalyst was again studied for the conversion of the lignin model compound dihydrobenzofuran (DHBF) under supercritical conditions to achieve ether hydrogenolysis and aromatic ring hydrogenation at 300 °C.[132] Recently, at 250 °C the depolymerization of pine lignin with MgO as a catalyst was reported to yield ca. 13% of phenolic monomers at >90% conversion level.[133] However, the use of low molecular weight lignin (*Mn.* = 892 Da & *Mw.* = 1360 Da) and the formation of solids of high molecular weight (*Mn.* = 540-600 Da and *Mw.* = 790-900 Da) are drawbacks of this method. Recently, over a nitrate-intercalated hydrotalcite catalyst, cleavage of the β-O-4 linkage in the lignin

model compound 2-phenoxyl-1-phenethanol (PE) to phenol, acetophenone and 1-phenethanol was shown to be possible.[134] Furthermore, the same catalyst was evaluated for the depolymerization of lignin-enriched substrates at 275 °C and ca. 8% yield for monomers was achieved.[134] The use of high temperature, difficulties in effective recycling of catalyst and low yields with lignin substrates (*Mn.* = 890–1700 Da, *Mw.* = 4900–8600 Da) are the few shortcomings of this study.

Table 1.5. Available literature for the use of solid bases.

Lignin/Model compound	Catalyst	Reaction Condition T / P	Major product yield (%)
Model compound: 2-phenoxy-1-phenethanol (PE) Lignin: Organosolv & ball-milled lignin	Ni/HTC	270 °C/ -	Phenol (21%), Acetophenone (17%), Alkyl-aromatic products
Lignin: Organosolv lignin	Cu-PMO	140-220 °C/ 30-60 bar H_2	Catechol derivatives (63%) and some oligomers
Model compound: Phenethyl Ph ether	Na-ZrO_2	400 °C/ 100 -200 bar H_2	Styrene & Phenol
Model compound: 2,3-dihydrobenzofuran (DHBF)	Cu-doped PMO	300 °C/ -	2-ethylcyclohexanol (67%) Ethyl cyclohexane (1.2%)
Lignin: Extracted lignin (*Mw.* = 1600-2800 Da)	MgO	250 °C/ -	Phenolics (13%)
Model compound: 2-phenoxyl-1-phenethanol (PE)	nitrate-intercalated HT	275 °C/ -	phenol, acetophenone and 1-phenethanol 8% monomers

1.12. Upgradation of Lignin Derived Compounds

Depolymerization of lignin is known to yield a mixture of aromatic compounds which can be used as platform chemicals, fuel additives and octane enhancers. But the high oxygen content of these aromatic compounds will reduce the efficiency to be used as fuels. Therefore, they have to be upgraded before using them as fuels. Upgradation of lignin derived aromatic compounds can be done via hydrodeoxygenation, hydrogenation and deoxygenation process. Hydrogenation is a chemical reaction in which a pair of hydrogen atoms is involved to reduce or saturate the organic compounds. The double or triple carbon-carbon bonds, as well as C=O bonds, are saturated during hydrogenation reactions and this results in the increase of hydrogen percentage in the final products. The selectivity for hydrogenation toward aromatic C=C, olefin C=C, C=O, C≡C, etc. varies significantly due to the different nature of catalysts[135, 136] and is governable via fine manipulation of the catalytic system and reaction conditions. Generally, hydrogenation reactions occur with hydrogenolysis, or is included in the process of hydrodeoxygenation. Recently, the different metals (Al, Fe, Mg and Zn) were reported to be active for the hydrogenation of the carbonyl groups present in the bio-oil (complex mixture of oxygenated hydrocarbons) at ambient temperature and pressure to increase the chemical stability of the obtained products.[137] As a pseudo precious metal catalyst, Mo_2C/C prepared via a facile microwave irradiation was found to be highly active in the selective hydrogenation of naphthalene into tetralin with the selectivity of 100%.[138] Notwithstanding this progress, precious metals are still considered more promising hydrogenation catalysts in spite of their higher costs.[139, 140] Based on the fundamental activities of different precious metal catalysts and manipulation of reaction engineering pyrolysis oils was converted into industrial chemical feedstock [141]. In this system, Ru/C and Pt/C were employed for the hydrogenation of pyrolysis oil to produce polyols and alcohols. The hydrogenated products were then converted into light olefins and aromatic hydrocarbons over zeolite. For the hydrogenation of lignin and model compounds catalyzed with supported metal catalysts, the nature of support, metal dispersion, the choice of solvent, as well as the alkenyl substituent of the substrate are all crucial in determining the hydrogenation selectivity.[142, 143]

It was understood from the literature that the major role of metals is to hydrogenate the aromatic rings while support is to stabilize the active catalytic

species in a dispersed form. Various type of acidic supports are extensively reported in the literature to carry out these reactions but use of very few basic supports are known for this reaction. A major disadvantage with the use of acidic support is the high yields of coke that is associated with the acidic surface sites. Weak Lewis acid sites present in the catalyst supposed to lead to coke formation during upgradation reactions. In order to avoid the coke formation basic supports can be helpful. Recent investigations have focused on developing new supports system/solvent system for decreasing the hydrogen consumption and minimizing coke formation.

1.13. Motivation of Work

Since lignin is abundantly available and can be used as a renewable carbon source. The aromatic nature of lignin is one of the driven force for its value-addition. Depolymerization of lignin is known to produce aromatic monomers/low molecular weight products, which can be used as fuel additives or octane enhancers. But the complex nature of lignin makes the process complicated. Previously, several attempts were made for the valorization of lignin, but most of them are associated with several drawbacks (Figure 1.8). In earlier reports, homogeneous acids or bases were used which may cause corrosion of the reactor systems, needs an additional step of neutralization and furthermore it increases the capital cost of the process. Solid acid catalyzed process for the depolymerization of lignin was studied but the char formation was problematic. Metal catalyzed depolymerization of lignin showed that compared to other heterogeneous catalysts relatively milder reaction conditions were used in these processes. But still possess a drawback of employing the precious metal catalysts with excess of hydrogen which is not cost-effective and also face a problem of catalyst deactivation during the reaction. Furthermore, the major drawbacks for depolymerization of lignin was that most of the studies are done using lignin model compounds like dimers and trimers instead of using actual lignin substrates with high molecular weight. Considering the drawbacks associated with the known methods it is decided to develop a new method to convert actual lignin substrates into aromatic monomers under milder reaction conditions (T ≤ 250 °C) using heterogeneous base catalysts. Since the lignin depolymerisation is well known with the homogeneous base catalysts so it was assumed that similar type of reaction can be carried out using solid bases.

1.14. Objectives and Scope of the Thesis

By considering the above discussions regarding lignin depolymerization, importance of the utilization of lignocellulosic biomass and the importance of aromatic products, following are the objectives of my work:

- *To develop an efficient and one pot method for the depolymerization of lignin into low molecular weight aromatic monomers using heterogeneous bases.*

  1) To achieve this objective, it was decided to use the actual lignin substrate instead of using model compounds like dimers, trimers etc. for the lignin depolymerization reactions.

  2) Easy recovery and reusability of the catalysts.

  3) Explore the effects of various solid bases and optimization of reaction conditions in order to achieve the maximum low molecular weight aromatic products.

  4) Suppress the degradation products and gas formation by using milder reaction conditions (T ≤ 250 °C) with solid base catalysts.

  5) Avoid the repolymerization of products.
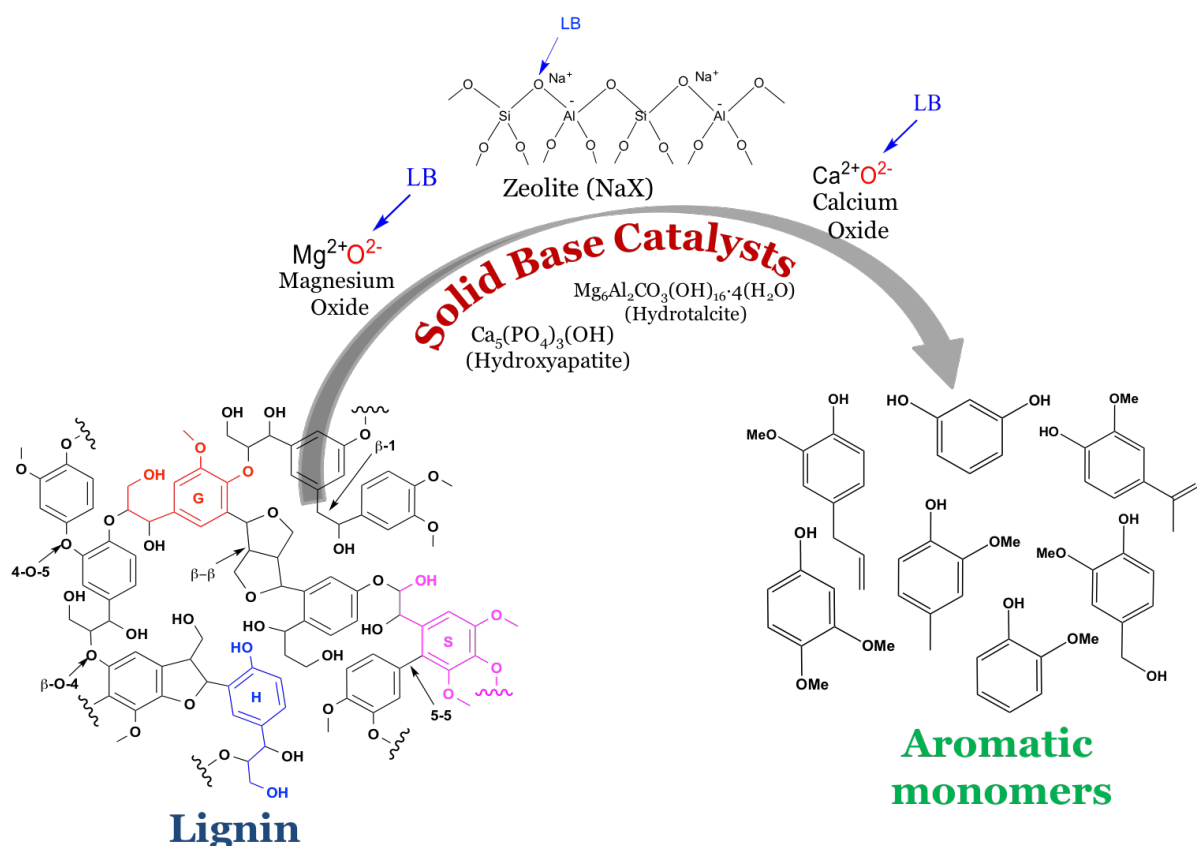
Scheme 1.1. Lignin depolymerization into aromatic monomers using solid base catalysts.

- *Correlation of structural and functional properties of lignin substrates before employed in the depolymerization reactions to obtain low molecular weight aromatic monomers.*

  As discussed in the introduction that the structure and linkages present in lignin depends on the plant species and the isolation techniques used for the isolation of lignin from lignocellulosic matrix. Therefore, before employing the lignin for depolymerization reactions, five different samples are well characterized using various techniques like NMR and FTIR/ATR analysis to identify the presence of functional groups; CHNS and ICP-OES for elemental analysis; XRD analysis to confirm the amorphous nature of lignin and TGA-DTA analysis to study the thermal degradation behaviour of lignin substrates.

- *To replace the homogeneous base catalyzed lignin depolymerization via solid base catalysts depolymerization of lignin into low molecular weight aromatic monomers.*

  Solid base catalysts having different physico-chemical properties like crystalline or amorphous nature, basic amount, surface area, pore size and pore volume, pH, etc. Properties of solid base catalysts has to studied using techniques like XRD to determine its morphology, CO_2-TPD analysis to determine the basic amount (weak, medium and strong), N_2 sorption analysis to determine the surface area, pore volume and pore diameter, ICP-OES to determine the elemental composition.

- *Isolation of lignin from coconut coir (raw biomass), characterization and depolymerization.*

  In order to develop a sustainable future technology use of abundant and inexpensive lignocellulose material (coconut coir) directly for the synthesis of value-added aromatic chemicals is performed. Klason, Organosolv and Kraft process used for the lignin isolation. Coconut coir is directly use for the synthesis of value-added chemicals. Correlation of coconut coir, isolated lignin and products is performed using various techniques like XRD, ICP-OES, ATR, NMR, etc.

- *To perform the upgradation of lignin derived monomers via hydrogenation reactions*

  To explore the effect of basic supported metal catalyst on the upgradation of phenol, guaiacol and eugenol was studied. Physical mixture of model compounds were also studied since these are the representative of bio-oil. Drawbacks associated with conventional Mo based catalyst can be overcome by the use of solid base supported noble metal catalysts. Noble metals are preferred because they are found to be highly active for hydrogenation reactions. Supported metal catalysts are synthesized by impregnation method. To study the physico-chemical properties of supported metal catalysts, various characterizations were performed like XRD, N_2 sorption, ICP-OES and HRTEM analysis. Optimization of reaction conditions (temperature, time, etc.) for the upgradation of lignin derived aromatic monomers will be performed to obtain maximum yield.

1.15. Outline of the Thesis

Thesis is divided into six chapters. In the present chapter, brief introduction on biomass and its components is discussed. Further details on the lignin isolation and depolymerization methods along with the importance of lignin derived products are described. Brief introduction of the solid base catalysts and upgradation of lignin derived products are also given. Lastly, motivation of the work followed by the scope and objective of the thesis is discussed.

In the second chapter, synthesis and characterization of various solid base catalysts and lignin is performed. This chapter is divided into two sections. In chapter 2A, detailed characterization of five lignin substrates are described using various techniques. Chapter 2B comprises the introduction to solid base catalysts, the basic sites present in the catalysts followed by its detailed characterization. Moreover, the synthesis of various supported metal catalysts and its characterizations using various techniques like XRD, ICP-OES, CO_2-TPD, TEM, etc. are also discussed.

In the Chapter three, depolymerization studies of lignin using various solid base catalysts is performed. Analysis and conformation for the formation of low molecular aromatic products is discussed with the help of GC, GC-MS, HPLC, ATR, etc. An unique product adsorption study of lignin model compounds is also explored.

In the fourth Chapter, coconut coir is used for the lignin isolation by three different methods (Klason, Organosolv and Soda). Detailed characterization and correlation of isolated lignin samples with the coir and products is discussed using different analysis ATR, NMR, XRD, etc. Furthermore, direct hydrolysis of coconut coir is also performed and the formation of aromatic products was confirmed by GC, GC-MS, HPLC, etc.

In the fifth chapter, upgradation studies for the lignin derived monomers are performed using supported metal catalysts. Effect of metal, metal loading and support are discussed.

In the sixth chapter, main results and novelty of the work are summarized in the form of conclusion.

1.16. References

1. S. Octave and D. Thomas, *Biochimie*, 91, 659-664.

2. J. Sanders, E. Scott, R. Weusthuis and H. Mooibroek, *Macromolecular Bioscience*, 2007, 7, 105-117.

3. Y.H.P. Zhang, *Journal of Industrial Microbiology & Biotechnology*, 2008, 35, 367-375.

4. N. Sarkar, S. K. Ghosh, S. Bannerjee and K. Aikat, *Renewable Energy*, 37, 19-27.

5. H. Yang, R. Yan, H. Chen, D. H. Lee and C. Zheng, 2007, 12-13, 1781-1788.

6. E. A. B. d. Silva, M. Zabkova, J. D. Araujo, C. A. Cateto, M. F. Barreiro, M. N. Belgacem and A. E. Rodrigues, *Chemical Engineering Research and Design*, 2009, 87, 1276-1292.

7. H. Yang, R. Yan, H. Chen, D.H. Lee and C. Zheng, *Fuel*, 2007, 12-13, 1781-1788.

8. P. A. M. Claassen, J. B. V. Lier, A. M. L. Contreras, E. W. J. V. Niel, L. Sijtsma, A. J. M. Stams, S. S. D. Vries and R. A. Weusthuis, *Applied microbiology and biotechnology*, 1999, 52, 741-755.

9. S. Zhang, F. Marechal, M. Gassner, Z. Perin-Levasseur, W. Q. Z. Ren, Y. Yan and D. Favrat, *Energy & Fuels*, 2009, 23, 1759-1765.

10. J. Lee, *Journal of biotechnology*, 1997, 1, 1-24.

11.   B. Kamm and M. Kamm, *White Biotechnology. Springer Berlin Heidelberg*, 2007, 175-204.

12.   B. E. Dale and S. Kim, *Ullmann's Encyclopedia of Industrial Chemistry*, 2007, 41-66.

13.   J. Pérez, J. Muñoz-Dorado, T. d. l. Rubia and J. Martínez, *International Microbiology*, 2002, 53-63.

14.   H. Kobayashi and A. Fukuoka, *Green Chem.*, 2013, 15, 1740.

15.   Maki-ArvelaP, T. Salmi, B. Holmbom, S. Willfor and D. Y. Murzin, *Chem. Rev.*, 2011, 5638.

16.   A. Barakat, H. d. Vries and X. Rouau, *Bioresour. Technol*, 2013, 362-373.

17.   V. B. Agbor, N. Cicek, R. Sparling, A. Berlin and D. B. Levin, *Biotechnol. Adv.*, 2011, 29, 675–685.

18.   S. Morais, E. Morag, Y. Barak, D. Goldman, Y. Hadar, R. Lamed, Y. Shoham, D. B. Wilson and E. A. Bayer, *mBio*, 2012.

19.   C. H. Zhou, X. Xia, C. X. Lin, D. S. Tong and J. Beltramini, *Chem. Soc. Rev.*, 2011, 5588–5617.

20.   C. Somerville, H. Youngs, C. Taylor, S. C. Davis and S. P. Long, *Science*, 2010, 790–792.

21.   E. Taarning, C. M. Osmundsen, X. Yang, B. Voss, S. I. Andersen and C. H. Christensen, *Energy Environ. Sci.*, 2011, 793.

22.   V. B. Agbor, N. Cicek, R. Sparling, A. Berlin and D. B. Levin, *Biotechnol. Adv.*, 2011, 675–685.

23.   H. V. Scheller and P. Ulvskov, *Annu. Rev. Plant Biol.*, 2010, 263-289.

24.   E. M. Rubin, *Nature*, 2008, 841-845.

25.   A. M. Abdel-Hamid, J. O. Solbiati and I. K. Cann, *Adv. Appl. Microbiol.*, 2013, 1–28.

26.   M. Kleinert and T. Barth, *Energy & fuels*, 2008, 22, 1371-1379.

27.   S. Cheng and S. Zhu, *BioResources*, 2009, 4, 456-457.

28.   F. Carvalheiro, L. C. Duarte and F. M. Girio, *Journal of Scientific & Industrial Research*, 2008, 849-864.

29.   G. W. Huber, S. Iborra and A. Corma, *Chemical reviews*, 2006, 106, 4044-4098.

30.   A. Hendriks and G. Zeeman, *Bioresource technology*, 2009, 1, 10-18.

31.   G. W. I. Huber, S.; Corma, A., *Chemical Reviews*, 2006, 4044-4098.

32. E. Dorrestijn, L. J. J. Laarhoven, I. W. C. E. Arends and P. Mulder, *J. Anal. Appl. Pyrolysis*, 2000, 153-192.

33. T. Nguyen, E. Zavarin and E. M. Barral, *J. Macromol. Sci., Polym. Rev.* , 1981, 1–65.

34. G. Henriksson, M. Ek and G. Gellerstedt, *Wood Chemistry and Wood Biotechn.*, 2005.

35. J. Ralph, K. Lundquist, G. Brunow, F. Lu, H. Kim, P. Schatz, J. M. Marita, R. D. Hatfield, S. A. Ralph and J. H. e. a. Christensen, *Phytochem. Rev.* , 2004, 29-60.

36. R. Whetten and R. Sederoff, *Plant Cell*, 1995, 1001–1013.

37. A. M. Boudet, C. Lapierre and Grima-Pettenati, *New Phytol.* , 1995, 203–236.

38. W. Boerjan, J. Ralph and M. Baucher, *Annual Review of Plant Biology*, 2003, 519-546.

39. T. J. McDonough, *Tappi*, 1993, 186–193.

40. Z. Strassberger, S. Tanase and G. Rothenberg, *RSC Adv.* , 2014, 25310–25318.

41. J. Lora, M. N. Belgacem and A. Gandini, *Eds. Elsevier: New York*, 2008, 225-241.

42. J. Lora, *Elsevier, Oxford, UK*, 2008.

43. A. Abacherli and F. Doppenberg, *U.S. Patent No. 6239198, 2001.* .

44. J. Gierer, 1980, 4, 241-266.

45. F. Oehman, H. Theliander, P. Tomani and P. Axegard, *Chem. Abstr.* , 2009, 268770.

46. A. G. Maldonado and G. Rothenberg, *Chemical Engineering Progress*, 2009, 105, 26-32.

47. A.V. Gaikwad, P. Verschuren, T. van der Loop and G. Rothenberg, *E. Eiser, Soft matter*, 2009, **5**, 1994-1999.

48. P. Kumar, D. M. Barrett, M. J. Delwiche and P. Stroeve, *Ind. Eng. Chem. Res.*, 2009, 3713–3729.

49. B. K. Avellar and W. G. Glasser, *Biomass Bioenergy* 1998, 205–218.

50. A. Brandt, J. Gräsvik, J. P. Hallett and Welton, *Green Chem.*, 2013, 550–583.

51. J.E. Holladay, J.J. Bozell, J.F. White and D. Johnson, *Pacific Northwest National Laboratory and the National Renewable Energy Laboratory.*, 2007.

52. A. Abe, K. Dusek, S. Kobayashi, H. Hatakeyama and T. Hatakeyama, *Biopolymers. Springer Berlin Heidelberg*, 2010, 1-63.

53. A. Toledano, L. Serrano, A. Pineda, A.A. Romero, R. Luque and J. Labidi, *Applied Catalysis B: Environmental*, 2014, 43-55.

54. J. S. Luterbacher, D. M. Alonso and J. A. Dumesic, *Green Chem.*, 2014, 4816–4838.

55. B. P. Zakzeski J, Jongerius AL, Weckhuysen BM., *Chem Rev* 2010, 110, 3552–3599.

56. S. D. Heiko Lange, Claudia Crestini *European Polymer Journal*, 2013, 49, 1151-1173.

57. M. P. Pandey and C. S. Kim, *Chem. Eng.Technol.* , 2011, 29-41.

58. Z. Strassberger, S. Tanase and G. Rothenberg, *RSC Adv.*, 2014, 25310–25318.

59. A. J. Ragaukas, G. T. Beckham, M. J. Biddy, R. Chandra, F. Chen, M. F. Davis, B. H. Davison, R. A. Dixon, P. Gilna, Keller and M. e. al., *Science*, 2014, 709–719.

60. S. Czernik and A. V. Bridgwater, *Energy Fuels* 2004, 590-598.

61. A. Gutierrez, R. K. Kaila, M. L. Honkela, R. Siloor and A. O. I. Krause, *Catal. Today,* , 2009, 239-246.

62. D. Y. Hong, S. J. Miller, P. K. Agrawal and C. W. Jones, *Chem. Commun.*, 2010, 1038–1040.

63. C. Zhao, Y. Kou, A. A. Lemonidou, X. B. Li and J. A. Lercher, *Angew. Chem. Int. Ed.*, 2009, 3987–3990.

64. R. C. Runnebaum, T. Nimmanwudipong, D. E. Block and B. C. Gates, *Catal. Lett.,* 2011, 817–820.

65. T. Nimmanwudipong, R. C. Runnebaum, S. E. Ebeler, D. E. Block and B. C. Gates, *Catal. Lett.,* , 2012.

66. M. A. Gonzalez-Borja and D. E. Resasco, *Energy Fuels*, 2011, 4155–4162.

67. E. Dorrestijn, L. J. J. Laarhoven, I. W. C. E. Arends and P. Mulder, *J. Anal. Appl. Pyrolysis*, 2000, 153–192.

68. A. Farzaneh, T. Richards, E. Sklavounos and A. A. van Heiningen, *BioResources* 2014, 3052–3063.

69. A. Yamaguchi, N. Hiyoshi, O. Sato and M. Shirai, *Top. Catal.* , 2012,, 889–896.

70. G. P. van der Laan and A. Beenackers, *Catal. Rev.: Sci. Eng.* , 1999, 255-318.

71. P. J. A. Tijm, F. J. Waller and D. M. Brown, *Appl. Catal., A* 2001, 275-282.

72. F. L. P. Resende, S. A. Fraley, M. J. Berger and P. E. Savage, *Energy Fuels*, 2008, , 1328–1334.

73. Y. C. Lin and G. W. Huber, *Energy Environ. Sci.*, 2009, 68-80.

74. N. Cerone, F. Zimbardi, L. Contuzzi, E. Alvino, M. O. Carnevale and V. Valerio, *Energy Fuels*, 2014, 3948–3956.

75. P. J. Deuss, M. Scott, F. Tran, N. J. Westwood, J. G. d. Vries and K. Barta, *J. Am. Chem. Soc. Rev.*, 2015, 7456–7467.

76. J. Papadopoulos, C. L. Chen and I. S. Goldstein, *Holzforschung* 1981, 283–286.

77. T. H. Kim, *Korean J. Chem. Eng.* , 2011, 2156–2162.

78. M. M. Hepditch and R. W. Thring, *Can. J. Chem. Eng.*, 2000, 226–231.

79. S. Constant, C. Basset, C. Dumas, F. Di Renzo, Robitzer, A. M.; Barakat and F. Quignard, *Ind. Crops Prod.* , 2015,, 180–189.

80. R. W. Thring, S. P. R. Katikaneni and N. N. Bakhshi, *Fuel Process. Technol.* , 2000,, 17–30.

81. A. K. Deepa and P. L. Dhepe, *RSC Advances*, 2014, **4**, 12625.

82. A. K. Deepa and P. L. Dhepe, *ACS Catalysis*, 2015, **5**, 365-379.

83. H. X. Ben and A. J. Ragauskas, *RSC Adv.* , 2012, 12892–12898.

84. S. K. Singh and P. L. Dhepe, *Green Chem.*, 2016, DOI: 10.1039/c6gc00771f.

85. B. J. Cox and J. G. Ekerdt, *Bioresour.Technol.* , 2012, 584–588.

86. U. Wongsiriwan, Y. Noda, C. S. Song, P. Prasassarakich and Y. Yeboah, *Energy Fuels*, 2012, 3232–3238.

87. P. J. Deuss, M. Scott, F. Tran, N. J. Westwood, J. G. d. Vries and K. Barta, *J. Am. Chem. Soc. Rev.*, 2015, 7456–7467.

88. M. Meshgini and K. V. Sarkanen, *Holzforschung* 1989, 239–243.

89. V. M. Roberts, R. T. Knapp, X. Li and J. A. Lercher, *ChemCatChem* 2010, 1407–1410.

90. S. Constant, C. Basset, C. Dumas, F. Di Renzo, Robitzer, A. M.; Barakat and F. Quignard, *Ind. Crops Prod.*, 2015, 180–189.

91. T. R. Varga, Z. Fazekas, Y. Ikeda and H. Tomiyasu, *J. Supercrit. Fluids* 2002, 163–167.

92. V. M. Roberts, S. Fendt, A. Lemonidou, X. Li and J. A. Lercher, *Appl. Catal., B* 2010, 71–77.

93.   Z. S. Yuan, S. N. Cheng, M. Leitch and C. B. Xu, *Bioresour. Technol.* , 2010, 101, 9308–9313., 9308-9313.

94.   J.-M. Lavoie, W. Baré and M. Bilodeau, *Bioresour. Technol.*, 2011, 4917–4920.

95.   Z. Yuan, S. Cheng, M. Leitch and C. C. Xu, *Bioresour Technol*, 2010, **101**, 9308-9313.

96.   V. M. Roberts, V. Stein, T. Reiner, A. Lemonidou, X. Li and J. A. Lercher, *Chemistry*, 2011, **17**, 5939-5948.

97.   N. Mahmood, Z. Yuan, J. Schmidt and C. C. Xu, *Bioresour. Technol.* , 2013, 13–20.

98.   A. Toledano, L. Serrano and J. Labidi, *Journal of Chemical Technology & Biotechnology*, 2012, 87, 1593-1599.

99.   J. E. Miller, L. Evans, A. Littlewolf and D. E. Trudell, *Fuel* 1999, , 1363–1366.

100.   A. Toledano, L. Serrano and J. Labidi, *Fuel*, 2014, 617–624.

101.   J. B. Li, G. Henriksson and G. Gellerstedt, *Bioresour. Technol.* , 2007, 3061-3068.

102.   R. J. A. Gosselink, W. Teunissen, J. E. G. van Dam, E. de Jong, G. Gellerstedt, E. L. Scott and J. P. M. Sanders, *Bioresour. Technol.*, 2012, 173–177.

103.   T. Yoshikawa, T. Yagi, S. Shinohara, T. Fukunaga, Y. Nakasaka, T. Tago and T. Masuda, *Fuel Processing Technology*, 2013, 69-75.

104.   W. Xu, S.J. Miller, P.K. Agrawal and C.W. Jones, *ChemSusChem* 2012, **5**, 667-675.

105.   Q. Song, F. Wang, J. Cai, Y. Wang, J. Zhang, W. Yu and J. Xu, *Energy & Environmental Science,*, 2013, 6, 994-1007.

106.   M. R. Sturgeon, M. H. O'Brien, P. N. Ciesielski, R. Katahira, J. S. Kruger, S. C. Chmely, J. Hamlin, K. Lawrence, G. B. Hunsinger, T. B. Foust, R. M. Baldwin, M. J. B. & and G. T. Beckham, *Green Chem.,* , 2014, 824-835.

107.   L. Liguori and T. Barth, *Journal of Analytical and Applied Pyrolysis,*, 2011, 2, 477-484.

108.   J. E. E. Miller, L.; , A. Littlewolf and D. E. Trudell, *Fuel* 1999, 1363-1366.

109.   E. Minami, H. Kawamoto and S. Saka, *J. Wood Sci.* , 2003, 158-165.

110.   Z. Fang, T. Sato, R. L. Smith Jr, H. Inomata, K. Arai and J. A. Kozinski, *Bioresour. Technol.*, 2008, 3424-3430.

111. Wahyudiono;, M. Sasaki and M. Goto, *Chem. Eng. Process.: Process Intensification* 2008, 1609-1619.

112. R. J. A. Gosselink, W. r. Teunissen, J. E. G. van Dam, E. de Jong, G. Gellerstedt, E. L. Scott and J. P. M. Sanders, *Bioresour. Technol.* , 2012, 173-177.

113. N. Sun, M. Rahman, Y. Qin, M. L. Maxim, H. Rodríguez and R. D. Rogers, *Green Chem.*, 2009, 646–655.

114. Y. Q. Pu, N. Jiang and A. J. Ragauskas, *J. Wood Chem. Technol.*, 2007, 23-33.

115. W. Ji, Z. Ding, J. Liu, Q. Song, X. Xia, H. Gao, H. Wang and W. Gu, *Energy Fuels*, 2012, 6393–6403.

116. X. Creary, E. D. Willis and M. Gagnon, *J. Am. Chem. Soc. Rev.*, 2005, 18114–18120.

117. D. Zhao, M. Wu, Y. Kou and E. Min, *Catal. Today* 2002, 157–189.

118. S. Y. Jia, B. J. Cox, X. W. Guo, Z. C. Zhang and J. G. Ekerdt, *Ind. Eng. Chem. Res.*. 2011, , 849–855.

119. S. Jia, B. J. Cox, X. Guo, Z. C. Zhang and J. G. Ekerdt, *ChemSusChem*, 2010, 1078-1084.

120. B. J. Cox, S. Jia, Z. C. Zhang and J. G. Ekerdt, *Polym. Degrad. Stab.*, 2011, 426-431.

121. S. K. Singh and Paresh L. Dhepe, *Green Chemistry.*, 2016, 18, 4098-4108.

122. C. Z. Li, Q. Wang and Z. K. Zhao, *Green Chem.* , 2008, 177-182.

123. B. F. Li, I.; and D. S. Argyropoulos, *Ind. Eng. Chem. Res.* , 2010, 3126-3136.

124. V. E. Tarabanko, N. V. Koropatchinskaya, A. V. Kudryashev and B. N. Kuznetsov, *Russ. Chem. Bull.*, 1995, 367–371.

125. J. C. Villar, A. Caperos and F. Garcia-Ochoa, *Wood Sci. Technol.* , 2001, 245–255.

126. P. C. Rodrigues, E. A. Borges da Silva and A. E. Rodriguez, *Ind. Eng. Chem. Res.*, 2011, 741-748.

127. L. K. Das, P.; and R. Sharma-Shivappa, *Biofuels* 2012, 155-166.

128. H. (Pines, J. A. Veseley and V. N. Ipatieff, *J. Am. Chem. Soc. Rev.*, 1955, 6314.

129. H. Hattori, N. Yoshii and K. Tanabe, *Proceedings of the 5th International Congress on Catalysis, Miami Beach, FL.*, 1972, 233.

130. M. R. Sturgeon, M. H. O'Brien, P. N. Ciesielski, R. Katahira, J. S. Kruger, S. C. Chmely, J. Hamlin, K. Lawrence, G. B. Hunsinger, T. D. Foust, R. M. Baldwin, M. J. Biddy and G. T. Beckham, *Green Chem.*, 2014, 16, 824-835.

131. K. Barta, G. R. Warner, E. S. Beach and P. T. Anastas, *Green Chem.*, 2014, 191-196.

132. G. S. Macala, T. D. Matson, C. L. Johnson, R. S. Lewis, A. V. Iretskii and P. C. Ford, *ChemSusChem*, 2009, 2, 215-217.

133. J. Long, Q. Zhang, T. Wang, X. Zhang, Y. Xu and L. Ma, *Bioresour Technol*, 2014, 154, 10-17.

134. J. S. Kruger, N. S. Cleveland, S. Zhang, R. Katahira, B. A. Black, G. M. Chupka, T. Lammens, P. G. Hamilton, M. J. Biddy and G. T. Beckham, *ACS Catalysis*, 2016, 6, 1316-1328.

135. P. Gallezot and D. Richard, *Catal. Rev.: Sci. Eng.*, 1998, 81–126.

136. H. Cai, C. Li, A. Wang and T. Zhang, *Catal. Today* 2014, 59-65.

137. W.-J. Liu, X.-S. Zhang, Y.-C. Qv, H. Jiang and H.-Q. Yu, *Green Chem.*, 2012, 2226-2233.

138. M. Pang, C. Liu, W. Xia, M. Muhler and C. Liang, *Green Chem.*, 2012, 1272-1276.

139. T. Nimmanwudipong, R. C. Runnebaum, S. E. Ebeler, Block, D. E.; and B. C. Gates, *Catal. Lett.*, 2012, 151–160.

140. H. Ben, W. Mu, Y. Deng and A. J. Ragauskas, *Fuel*, 2013, 1148-1153.

141. T. P. Vispute, H. Zhang, A. Sanna and R. H. Xiao, G. W., *Science*, 2010, 1222-1227.

142. T. Nimmanwudipong, R. C. Runnebaum, S. E. Ebeler, Block, D. E.; and B. C. Gates, *Catal. Lett.*, 2012, 151-160.

143. J. A. Anderson, A. Athawale, F. E. Imrie, F. M. McKenna, A. McCue, D. Molyneux, K. Power, M. Shand and R. P. K. Wells, *J. Catal.*, 2010, 9-15.

Chapter 2
Lignin and Catalyst Characterization

Chapter 2A
Lignin Characterization

2A.1. Introduction

Lignin is a three dimensional heteropolymer built up of hydroxylated and methoxylated phenyl propane units. Lignin molecules are extremely complicated due to their natural variability. Lignin accounts 10-25% of lignocellulosic biomass and produced by the oxidative polymerization of coniferyl alcohol catalyzed by laccase.[1] Lignin is up till now the only renewable resource, potentially available in enough quantities, for the industrial production of aromatics. Efficient production of high volume aromatics from a material as structurally complex and diverse as lignin is a big challenge but seems to be a viable long-term opportunity. Aromatic chemical building blocks include benzene, toluene and xylene (BTX) obtained from fossil resources in a global production volume of about 36, 10 and 35 Mt/annum, respectively.[2] Potentially, these aromatics can be obtained from lignin. As about 60% of all aromatics are produced starting from BTX, the conversion of biomass and lignin to these chemicals seems to be most interesting.[3]

According to the sources of raw biomass lignin can be categorized into softwood and hardwood. Depending on the fractionation methods, lignin are known as Steam explosion, Kraft, Organosolv, Soda, Klason, Alkaline oxidation, Pyrolysis lignins, and so forth.[4] The most easily hydrolyzable bonds in lignin are the ester and ether bonds compared to carbon-carbon bonds. Generally, softwood has 45-48 *wt.%* and hardwood has 60 *wt.%* of β-O-4 aryl glycerol ether bonds, determined by 2D-NMR techniques. Softwood has about 5 *wt.%* and hardwood has 0-2 *wt.%* of dibenzodioxocin 5-5′-α, β-O-4′ bonds. In addition, softwood has 3.5-8 *wt.%* and hardwood has 6-9 *wt.%* of diphenyl ether 5-O-4 linkages determined by thioacidolysis-hydrogenolysis.[4, 5] Moreover, the amounts of some C-C linkages are also varying, such as 5-5 linkage (softwood 19-22 *wt.%* and hardwood 3-9 *wt.%*).[5] Although the proportion of these linkages varies according to the type of wood. Major linkages include β-5, 4-O-5, β-1, α-O-4 and β-β linkages, as shown in Chapter 1, Figure 1.5.

Since the source and extraction methods are different, bonding present in lignin is varying, so it is obvious that each lignin will differ in their properties. It is well documented in the literature that the composition, molecular weight and linkages present in lignin differ from plant to plant.[6-8] Therefore, it is very important to systematically characterize the various lignin substrates.

2A.2. Materials

The details of the various substrates purchased for lignin depolymerization are summarized in Table 2A.1. All the substrates (lignins) were used as received without any further pretreatment.

Table 2A.1. Summary on substrates used for lignin depolymerization.

S.No.	Chemicals	*Mw.* (Da)	Supplier	Product Code
1.	Alkaline Lignin	60,000[9]	TCI Chemicals	L0082
2.	Dealkaline Lignin	60,000[10]	TCI Chemicals	L0045
3.	Alkali Lignin	28,000[11]	Sigma Aldrich	370959
4.	Lignosulfonate sodium salt Lignin	52,000[12]	Sigma Aldrich	471038
5.	Lignosulfonate calcium salt Lignin	18,000[13]	Sigma Aldrich	471054

It was assumed that the source and extraction methods of lignin are different as lignins are procured from different suppliers and having different molecular weights. Hence, it was expected that lignin will be differing in their properties. Therefore, all the procured lignins were completely characterized using various physico-chemical techniques.

2A.3. Lignin Characterization Methods

Before starting the catalytic runs, various lignin substrates were thoroughly characterized using various techniques like XRD, elemental analysis (CHNS), ICP-OES analysis, SEM-EDAX analysis, ATR, NMR, etc.

2A.3.1. Elemental Analysis

Elemental analysis was done using Thermo Finnigan, Italy; model EA1112 Series Flash Elemental Analyzer. 2-3 mg of oven dried sample was taken for the analysis. The amount of C, H, N and S present in the samples were analyzed by rapid combustion of the sample in pure O_2 (Dumas or flash combustion method).

Since lignin is a phenolic polymer and is made up of phenolic aromatics, it was predicted to have elements like C, H and O. So, CHNS elemental analysis of different types of lignin (alkaline, dealkaline, alkali, lignosulfonate sodium salt and lignosulfonate calcium salt) was performed to determine its elemental composition. CHNS elemental analysis revealed that different lignins are composed of 39-63% C and 5-8% H and having sulphur contamination of 1-3.7%. Possibility of sulphur contamination can be explained on the basis of isolation process used. Alkaline, dealkaline and alkali lignin might have been isolated using Kraft method in which NaOH and Na_2S are used as reagents.[8, 14, 15] In lignosulfonate sodium and calcium salt lignin Na and Ca are observed. Likewise, as their name suggests that those are produced from sulphite pulping process (since in these methods sulphite or bisulfite salts with counter cations such as sodium, ammonium, magnesium, or calcium are used).[16] Based on these results, a general monomer molecular formulae for lignins are derived and are summarized in Table 2A.2. The general formula for all the lignin can be expressed as, $C_xH_yO_z$ (x = 6.5-10.8; y =9.1-13.88; z = 3.36-6.6) which correlates well with the available literature.[6, 17]

Table 2A.2. Elemental analysis of various lignins.

Lignin	C %	H %	S %	O %	MMF*
Alkaline	52	5	2.05	40.95	$C_{8.7}H_{9.1}O_{5.1}S_{0.13}$
Dealkaline	65	7	1	27	$C_{10.8}H_{13.88}O_{3.36}S_{0.06}$
Alkali	63	6	1	70	$C_{10.48}H_{12}O_{3.75}S_{0.06}$
Lignosulfonate sodium salt	42	5	3.7	49.3	$C_7H_{9.1}O_{6.2}S_{0.24}$
Lignosulfonate calcium salt	39	5.4	3.4	52.2	$C_{6.5}H_{9.8}O_{6.6}S_{0.22}$

*MMF: Monomer molecular formula

2A.3.2. Inductively Coupled Plasma-Optical Emission Spectroscopy (ICP-OES) and Scanning Electron Microscopy-Energy Dispersive X-Ray Analysis (SEM-EDAX)

ICP-OES analysis for all the lignin samples were performed using SPECTRO ARCOS Germany, FHS 12 instrument. First lignin samples were burned in air at 650 °C for 6 h under air with a ramp rate of 10 °C/min. It was expected that C, H and O will burn off in the form of CO, CO_2, CH_4, etc. and unburned residue will remain as it is in the crucible. The obtained residue was dissolved to a known volume with Millipore water. The resultant solution was filtered using 0.22 micron filter paper and filtered solution was analyzed by ICP-OES. The ICP-OES analysis confirmed the presence of Na in lignin while from elemental analysis, sulphur presence was also confirmed. So, it can be stated that these lignins were isolated using Kraft and Lignosulfonate pulping process.

The SEM micrographs of the samples were obtained on a Leo Leica Cambridge UK Model Stereoscan 440 scanning electron microscope, with an electron beam of 5-50 *eV*. The elemental composition of the sample was determined using the EDAX attached with the SEM instrument and shown in Figure 2A.1. Results are summarized in Table 2A.3.

Table 2A.3. ICP-OES and SEM-EDAX analysis of lignin.

Lignin	ICP-OES (mg/g)	SEM-EDAX
Alkaline	Na: 69	C, O, Na, S
Dealkaline	Na: 29	C, O, Na, S
Alkali	Na: 70	C, O, Na, S
Lignosulfonate sodium salt	Na: 48	C, O, Na, S
Lignosulfonate calcium salt	Ca: 37	C, O, Ca, S
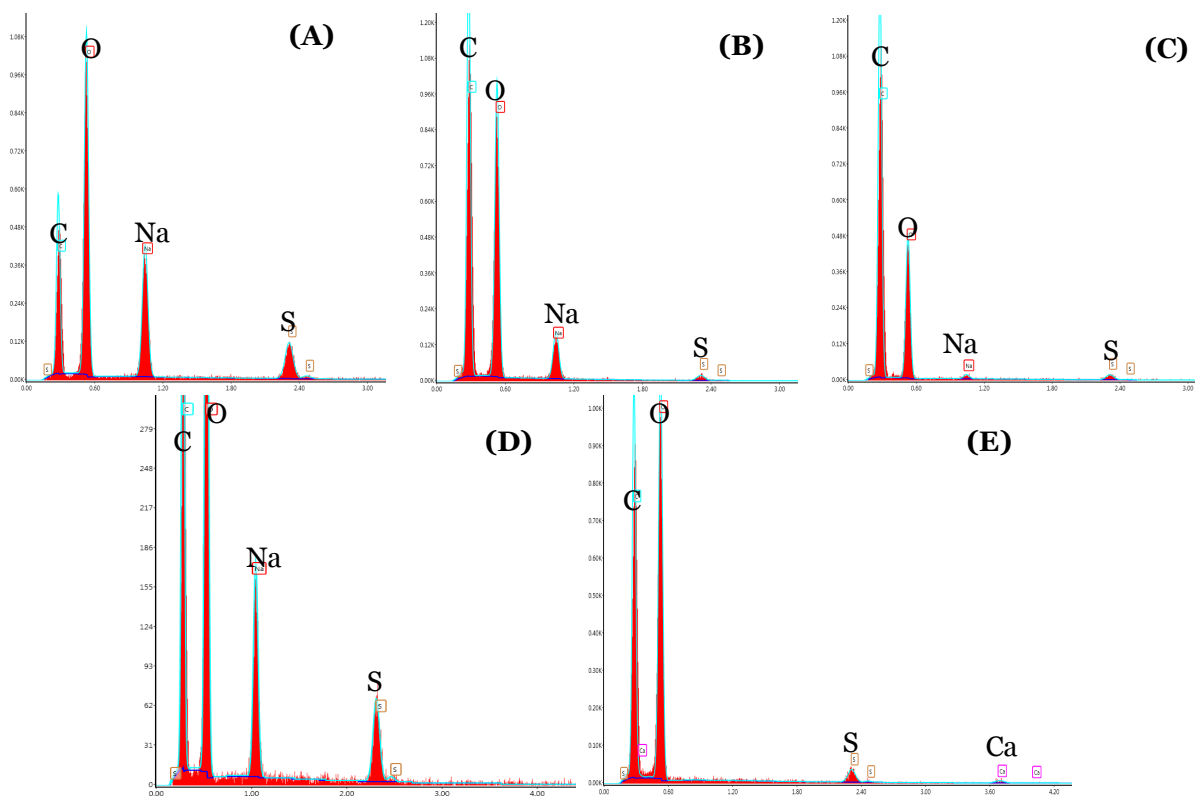
Figure 2A.1. EDAX pattern of various lignin (A) Alkaline lignin, (B) Dealkaline lignin, (C) Alkali lignin, (D) Lignosulfonate sodium salt lignin, (E) Lignosulfonate calcium salt lignin.

2A.3.3. Attenuated Total Reflection (ATR) Spectroscopy

Functional groups present in lignin were analysed using ATR technique. Analysis was done on Bruker Optics ALPHA-E spectrometer, USA; in the range of 600-4000 cm^{-1} or using an alpha-T Bruker ATR, eco ZnSe spectrophotometer. Prior to the analysis, all the samples were dried in vacuum oven (10^{-4} MPa) for 3 h. ATR for all the lignin samples are shown in Figure 2A.2 to Figure 2A.6.
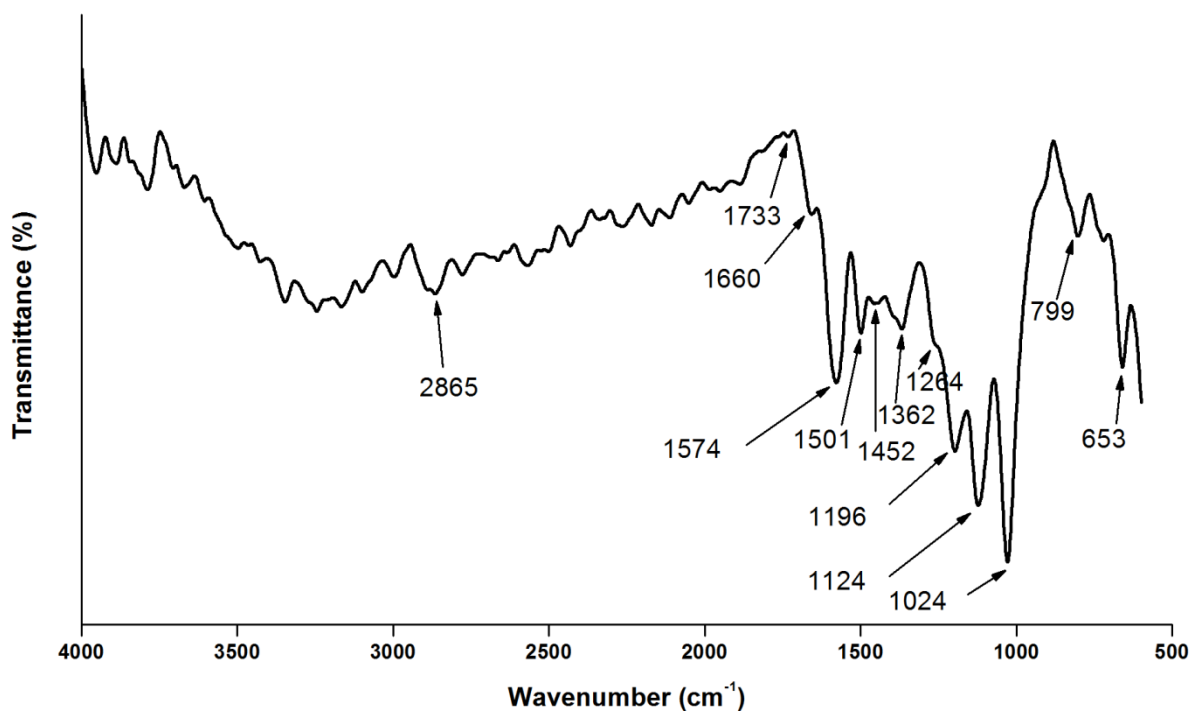
Figure 2A.2. ATR analysis of alkaline lignin.
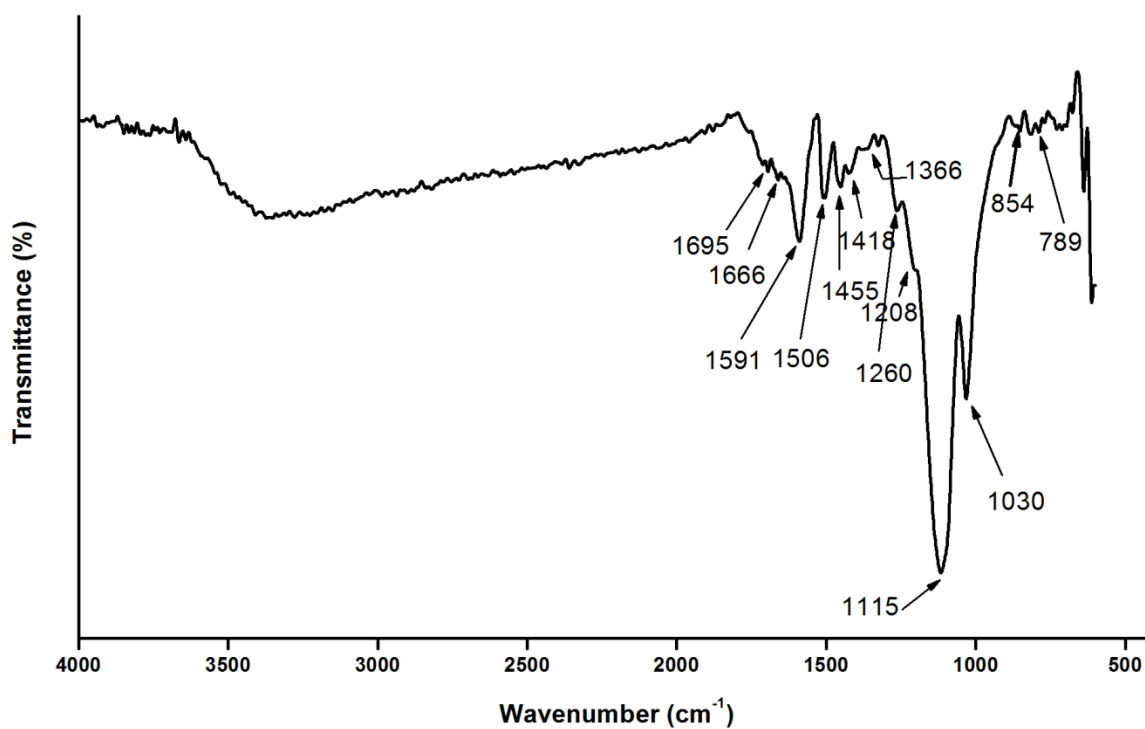
Figure 2A.3. ATR analysis of dealkaline lignin.
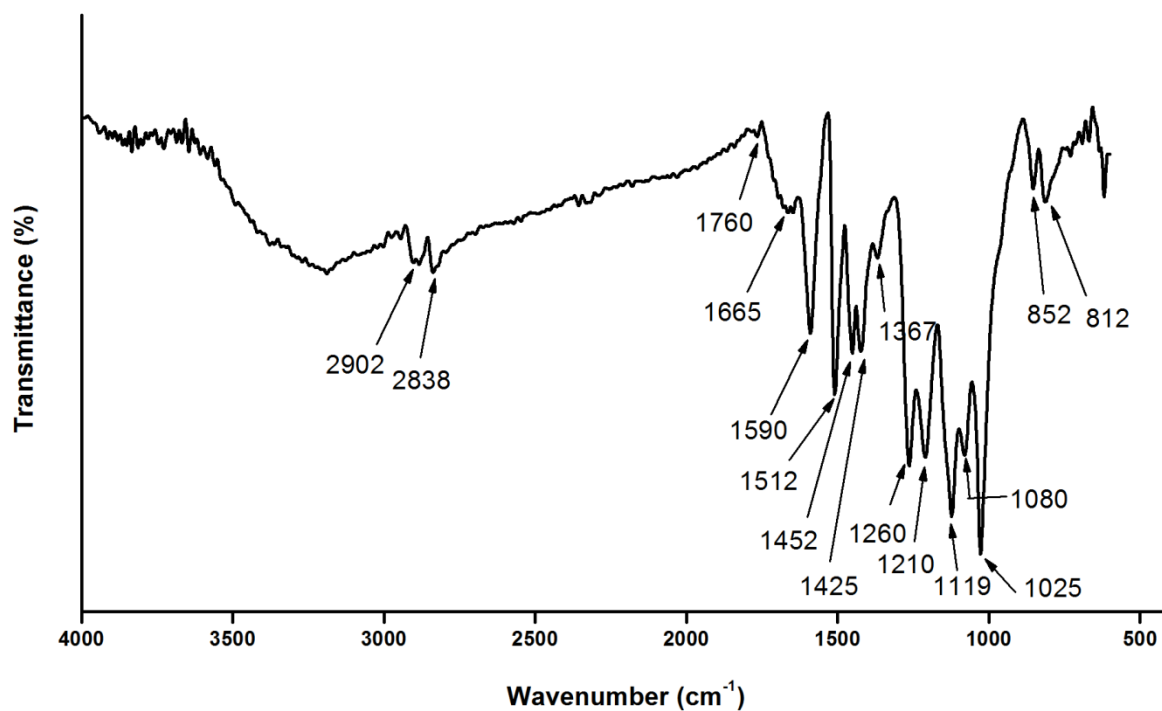
Figure 2A.4. ATR analysis of alkali lignin.
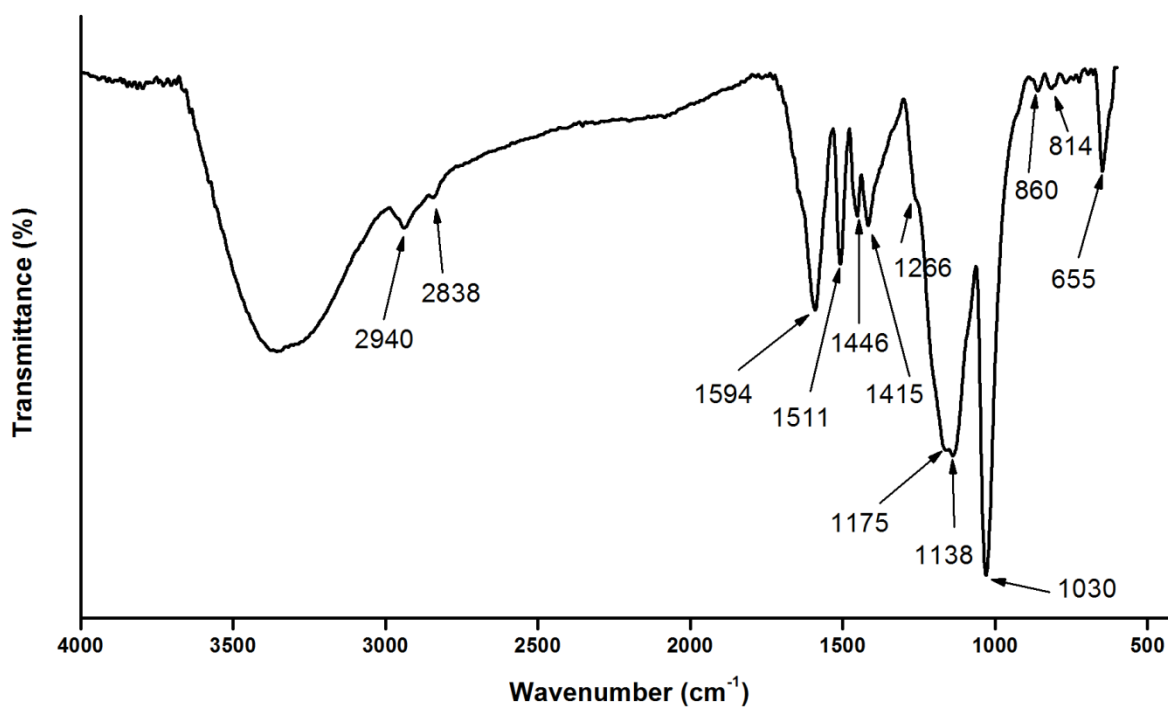
Figure 2A.5. ATR analysis of lignosulfonate sodium salt lignin (L-Na)
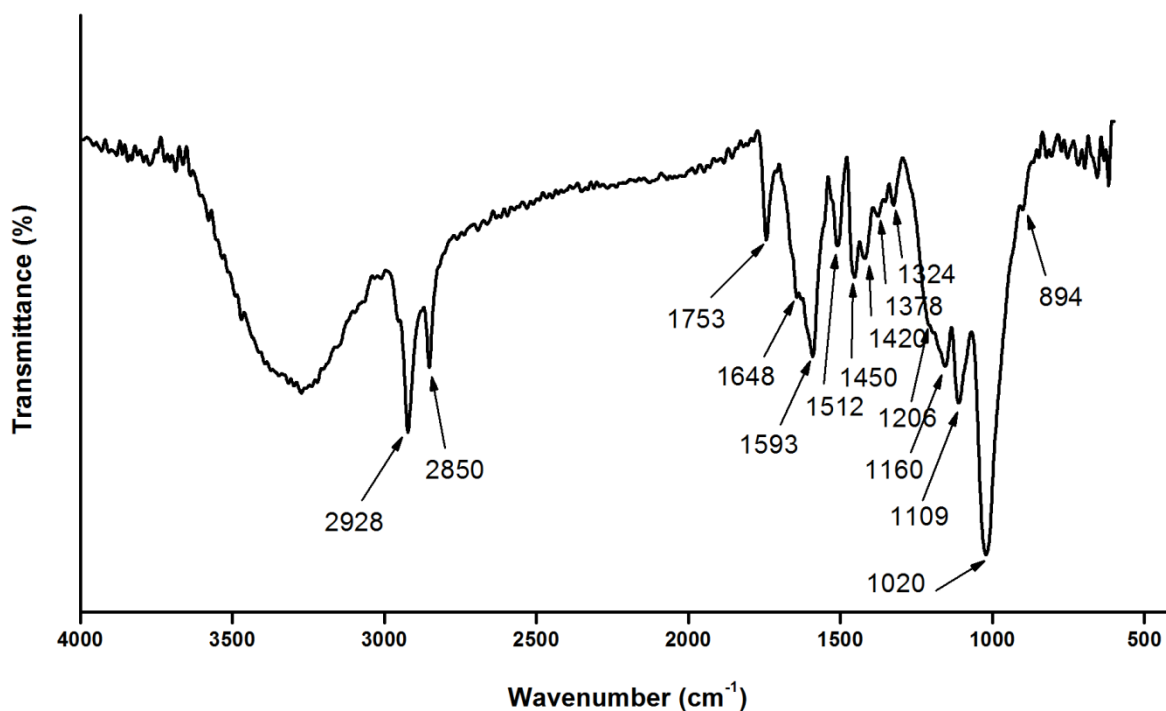
Figure 2A.6. ATR analysis of lignosulfonate calcium salt lignin (L-Ca)

In order to determine the different functional groups present in the lignin, ATR analysis was performed. Band at 3500-3100 cm⁻¹ due to stretching vibrations of alcoholic and phenolic hydroxyl groups (O-H stretching) was observed. C-H stretching vibrations of methoxy and aldehyde groups were present at 2902-2940 cm⁻¹ and 2838-2850 cm⁻¹. The band observed at 1760-1660 cm⁻¹ was attributed to the presence of C=O stretching in α,β-unsaturated aldehydes or ketones. This band can also be assigned to the presence of −C=C− in alkanes. In the range of 1610-1580 cm⁻¹, 1500-1585 cm⁻¹ and 1460-1415 cm⁻¹ bands due to aromatic ring vibrations (C−C stretch (in ring)) and C=O stretch in guaiacyl and syringyl rings are expected. The adsorption band at 1362 cm⁻¹ is characteristic of bend/rock vibration in alkanes. In lignin chemistry, this wavelength is also assigned to the syringyl ring breathing mode with C-O stretching. The bands at 1124-1109 cm⁻¹ and 1196-1140 cm⁻¹ can be assigned to deformation vibrations of C-H bonds in syringyl rings and secondary alcohol or else can be typically assigned to the C-O stretch in alcohols or ethers. Again, a strong band appearing at 1035-1020 cm⁻¹ is attributed to the C-O stretch in C-O (alcohol, ether) or the in-plane deformation vibrations of C-H bonds in aromatic rings. The observance of a peak at 799 cm⁻¹ is due to deformation vibrations of C-H (oop) bonds associated to aromatic rings.

All the lignin shows the presence of similar functional groups with different intensities of the bands. This variation can be possible due to the source of lignin and the isolation method used. Below, the summary of various bands observed in lignins are presented in Table 2A.4.

Table 2A.4. Summary on ATR bands present in various lignin.

Band (cm⁻¹)	Type of vibration	Wavenumber (cm⁻¹)				
		Alkaline	**Dealkaline**	**Alkali**	**L-Na**	**L-Ca**
3500-3100	Alcoholic & phenolic O-H stretching (free and involved in hydrogen bonding)	3351 (b)	3369 (b)	3190 (b)	3371 (b)	3286 (b)
2970-2830	C-H asymmetric stretching in methyl and methylene group	2865 (m)	-	2902 (m) 2838 (m)	2940 (s) 2838 (m)	2928 (s) 2850 (s)
1770-1680	C=O stretching in unconjugated ketone, carbonyl and ester groups	1733 (w)	1695 (w)	1760 (w)	-	1753 (s)
1670-1620	C=O stretching in conjugated substituted aryl group	1660 (m)	1666 (m)	1665 (w)	-	1648 (w)
1615-1590	C=O stretching with aromatic skeleton vibrations	1574 (s)	1591 (s)	1590 (s)	1594 (s)	1593 (s)
1520-1500	Aromatic skeleton vibrations	1501 (s)	1506 (s)	1512 (s)	1511 (s)	1512 (s)
1470-1410	Deformation vibrations of C-H bond	1452 (w)	1455 (m) 1418 (w)	1452 (s) 1425 (s)	1446 (s) 1415 (s)	1450 (s) 1420 (m)

1370-1350	Aliphatic C-H stretching in methyl and phenolic OH	1362 (m)	1366 (w)	1367 (m)	-	1378 (w) 1324 (w)
1300-1200	C-C, C-O, C=O stretching in guaiacyl units	1264 (w)	1260 (m) 1208 (w)	1260 (s) 1210 (s)	1266 (w)	1206 (w)
1195-1124	Deformation vibrations of C-H bonds in syringyl rings	1196 (s)	-	-	1175 (m) 1138 (m)	1160 (m)
1120-1105	Deformation vibrations of C-H bonds in aromatic rings	1124 (s)	1115 (s)	1119 (s)	-	1109 (s)
1030-1010	C-O stretching in alcohol, ether/ in-plane deformation vibrations of C–H bonds in aromatic rings.	1024 (s)	1030 (s)	1025 (s) 1080 (m)	1030 (s)	1020 (s)
875-700	Substitution on aromatic ring or substituted phenolics	799 (s) 653 (s)	854 (w) 789 (w)	852 (m) 812 (m)	860(w) 814 (w) 655 (s)	894 (w)

Note: (b) broad, (s) strong, (m) medium, (w) weak band intensities

2A.3.4. Solid State ^{13}C NMR

The aromatic skeleton of lignin was explored using ^{13}C NMR. ^{13}C NMR was done in Bruker AV300, Germany; at 10 kHz with a pulse program Cp, av and no. of scans was 8192. Vacuum dried samples were used for the analysis. It is very well known from the literature that presence of aromatic rings, carbonyl groups, methoxy and alkoxy

groups in lignin can be explored by NMR.[18] Similar to ATR analysis all the lignin shows the presence of similar type of functional group.

To confirm the presence of aromatic backbone and various functional group in lignin,^{13}C NMR was performed and presented in Figures 2A.7 to 2A.11 and Table 2A.5. Chemical shift at 185-210 ppm was observed for the presence of carbonyl groups (R-CHO). Presence of ester groups (R-CO-R) was confirmed in the range of 160-180 ppm. Intense peak for the presence of sp^2 carbon (-C=C-) in aromatic and alkenes was observed at 110-150 ppm. An intense peak at 55-56 ppm is common in all the lignin confirms the presence of methoxy group (R-OCH$_3$) attached to the aromatic rings. Chemical shift at 55-90 ppm was assigned to sp^3 carbon appearing next to oxygen atom (R-CH$_2$-O, R$_2$-CHO, R$_3$-C-O, in which R corresponds to aryl or alkyl group). At 20-50 ppm presence of alkoxy species (CH$_3$-CO) and alkyl species (R$_3$-CH) was observed.
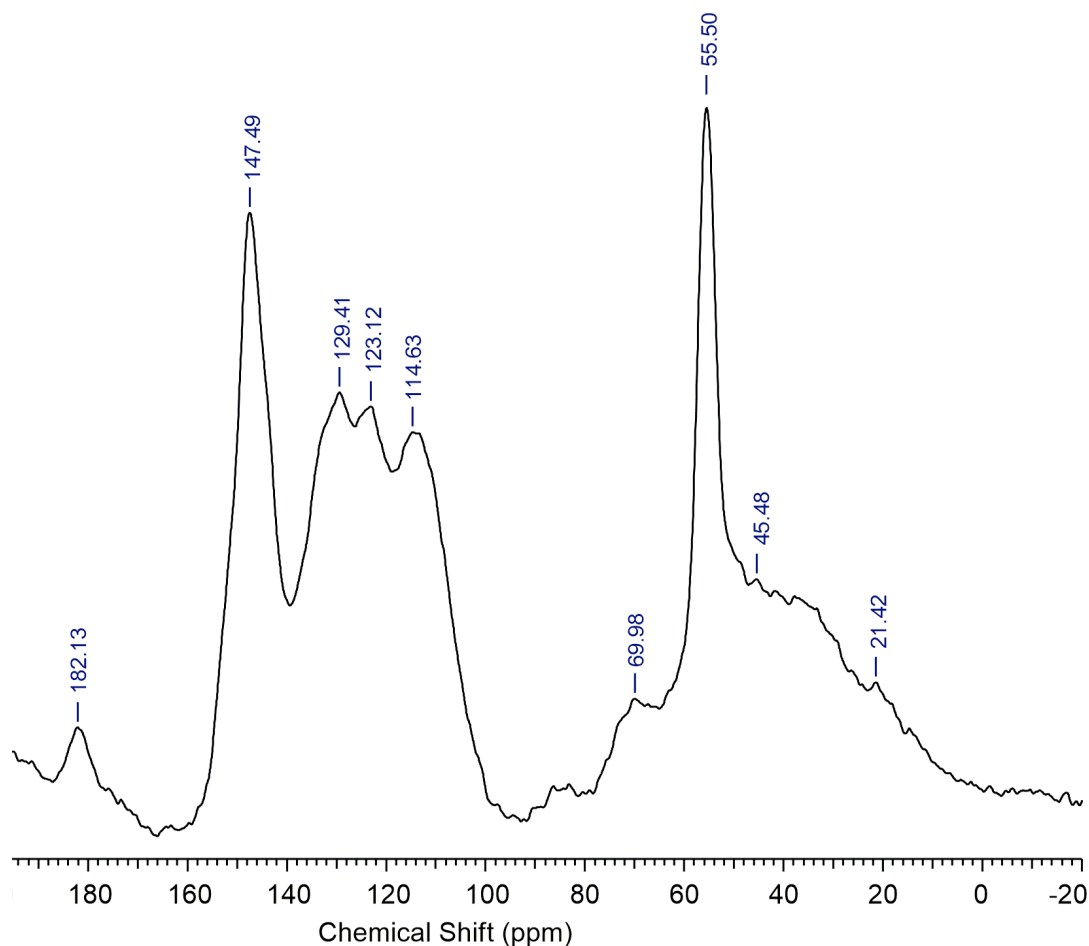
Figure 2A.7. Solid state ^{13}C NMR spectra of alkaline lignin.
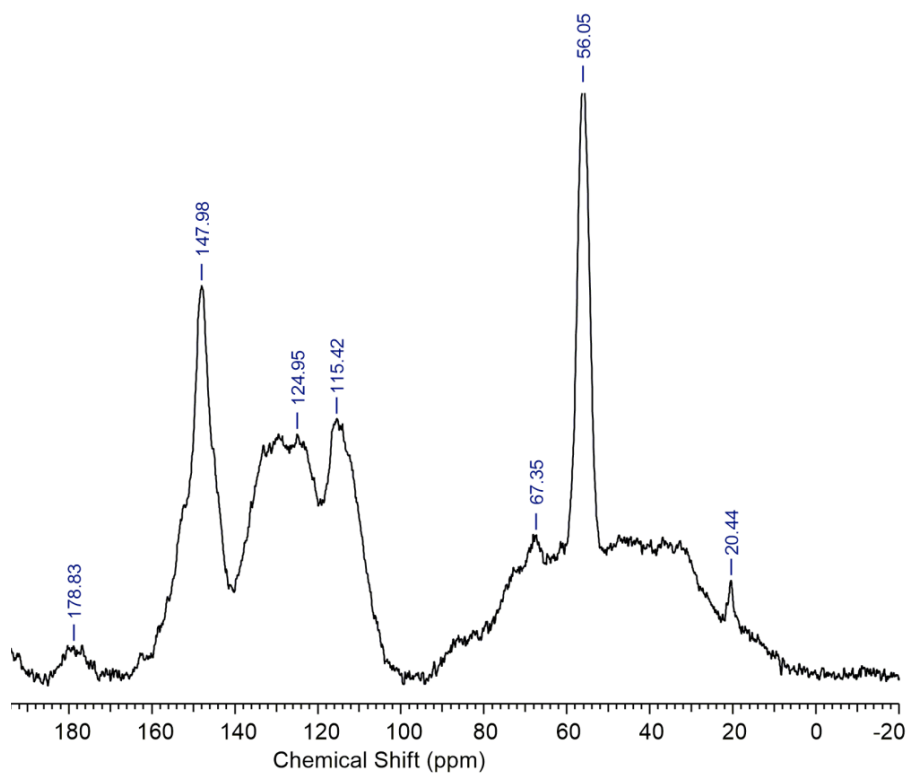
Figure 2A.8. Solid state ¹³C NMR spectra of dealkaline lignin.
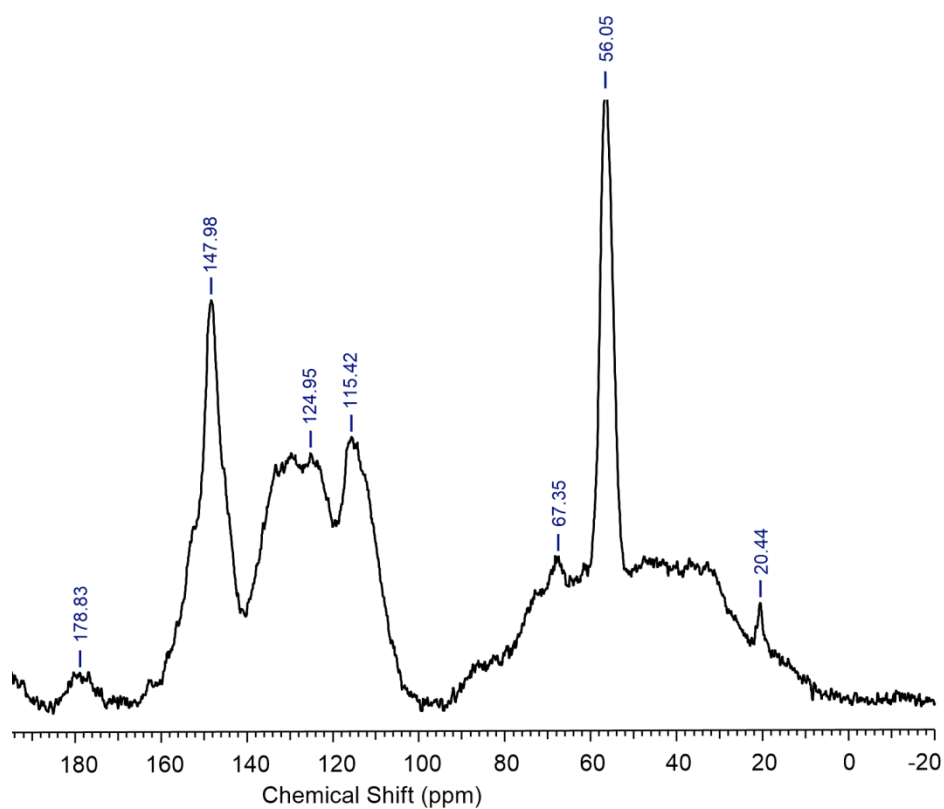
Figure 2A.9. Solid state ¹³C NMR spectra of alkali lignin.
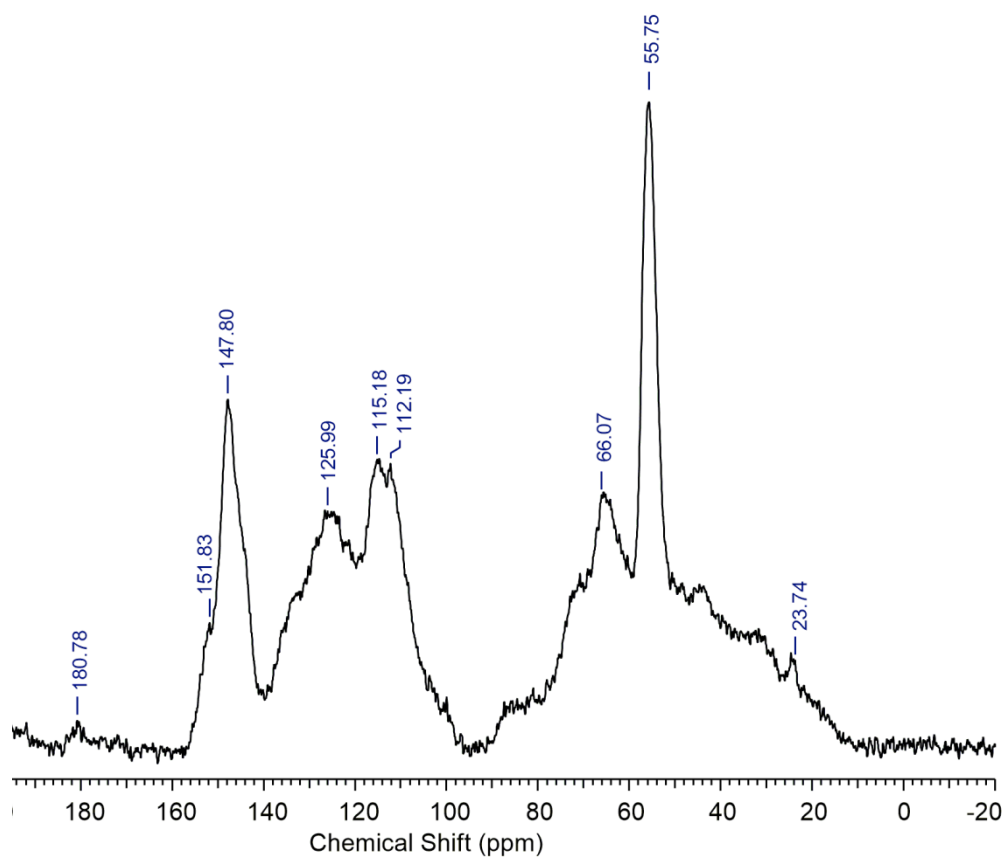
Figure 2A.10. Solid state ¹³C NMR spectra of lignosulfonate sodium salt lignin(L-Na).
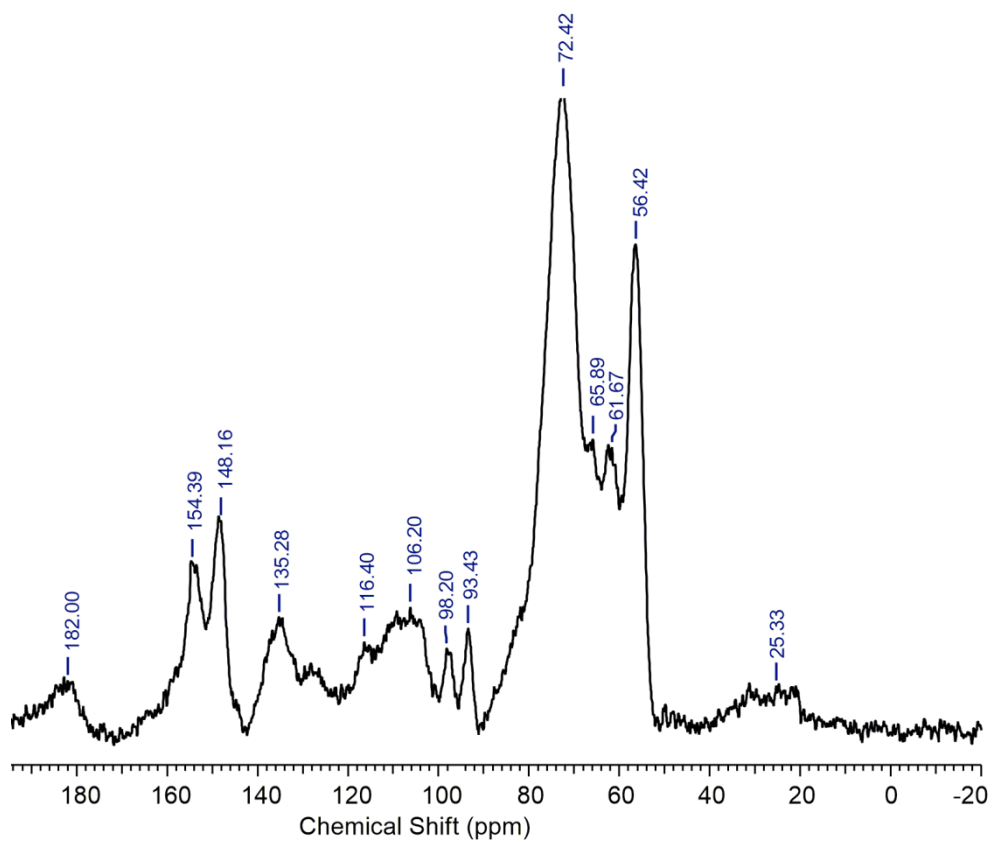
Figure 2A.11. Solid state ¹³C NMR spectra of lignosulfonate calcium salt lignin (L-Ca).

Table 2A.5. Summary on chemical shifts (ppm) of various lignin from ^{13}C NMR.

Functional group	Chemical Shift (ppm)				
	Alkaline	**Dealkaline**	**Alkali**	**L-Na**	**L-Ca**
C=O group in ketone	182.13	178.83	178.83	180.78	182.00
C in β-O-4 substructures linked with C=O	-	-	-	151.83	154.39
C_3 and C_4 in etherified guaiacyl unit	147.49	147.98	147.98	147.80	148.16
-	-	-	-	-	135.28
$C_{2,6}$ in *p*-hydroxyphenyl units	129.41 123.12	124.95	124.95	125.99	-
$C_{3,5}$ in *p*-hydroxyphenyl units	114.63	115.42	115.42	115.18	116.40 116.20
C_2 in guaiacyl units	-	-	-	112.19	
-	-	-	-	-	98.20
C_8 in tricin	-	-	-	-	93.43
Cα in β-O-4 substructures	-	-	-	-	72.42
Cγ in β-O-4 substructures	69.98	67.35	67.35	66.07	65.89 61.67
C-H in methoxyl group	55.50	56.05	56.05	55.75	56.42
α carbon CH$_2$with aliphatic substituted group	45.48	-	-	-	-
-CH$_2$ alkyl group	-	-	-	-	25.33
-	21.42	20.44	20.44	23.74	-

On the basis of NMR signals peaks can be assigned to lignin monomer moieties (guaiacyl alcohol, syringyl alcohol, *p*-hydroxyphenyl alcohol). Peak at 115.4 and 115.18 ppm (in dealkaline, alkali and lignosulfonate sodium salt lignin) can be assigned to guaiacyl unit which is present. However, peaks at 125.9 ppm in lignosulfonate sodium salt lignin and 114.6 in alkaline lignin corresponds to *p*-hydroxyl phenyl moieties

present in lignin. Presence of syringyl unit can be assigned at 106.2 ppm in lignosulfonate calcium salt lignin.

2A.3.5. Thermo Gravimetric Analysis - Differential Thermal Analysis (TGA-DTA)

TGA-DTA analysis was carried out using METTLER TOLEDO TGA /SDTA851 series, USA; instrument. To study the thermal decomposition of lignin TGA-DTA was performed with a temperature range from 30 °C to 1000 °C with heating rate of 10 °C/min. Thermal degradation of lignin was studied in N_2 and air atmosphere. TGA-DTA analysis for all the lignin samples in N_2 and air atmosphere are shown from Figure 2A.12 to Figure 2A.21.
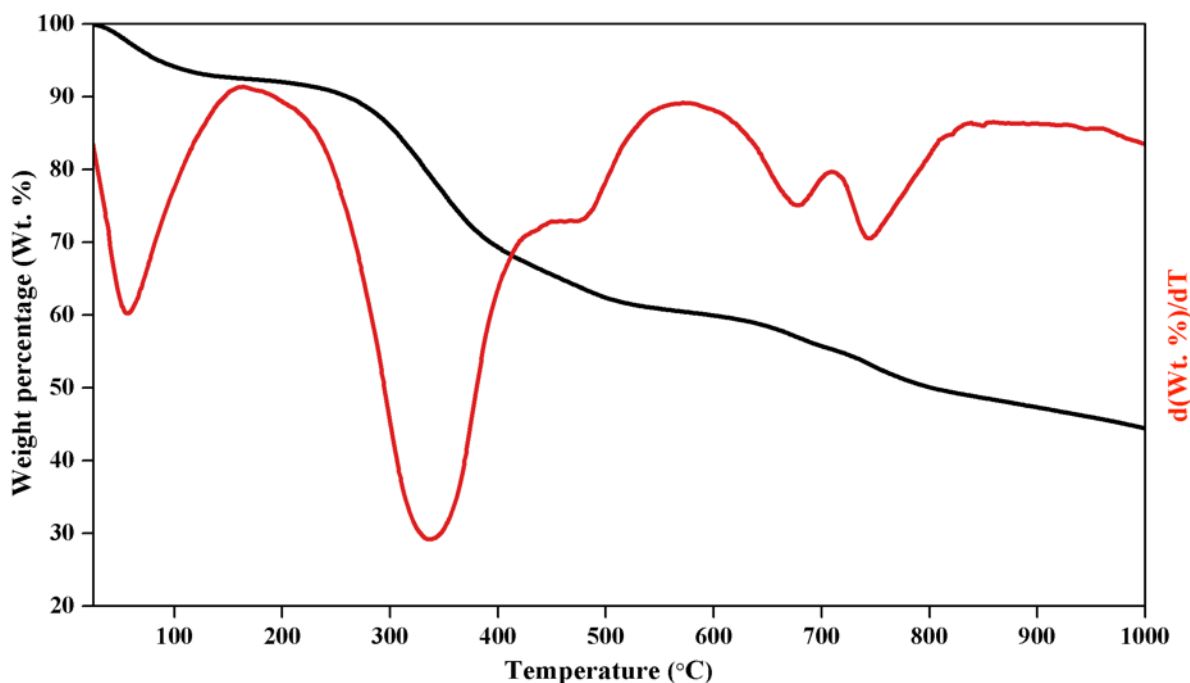
Figure 2A.12. TGA-DTA analysis of alkaline lignin (N_2).
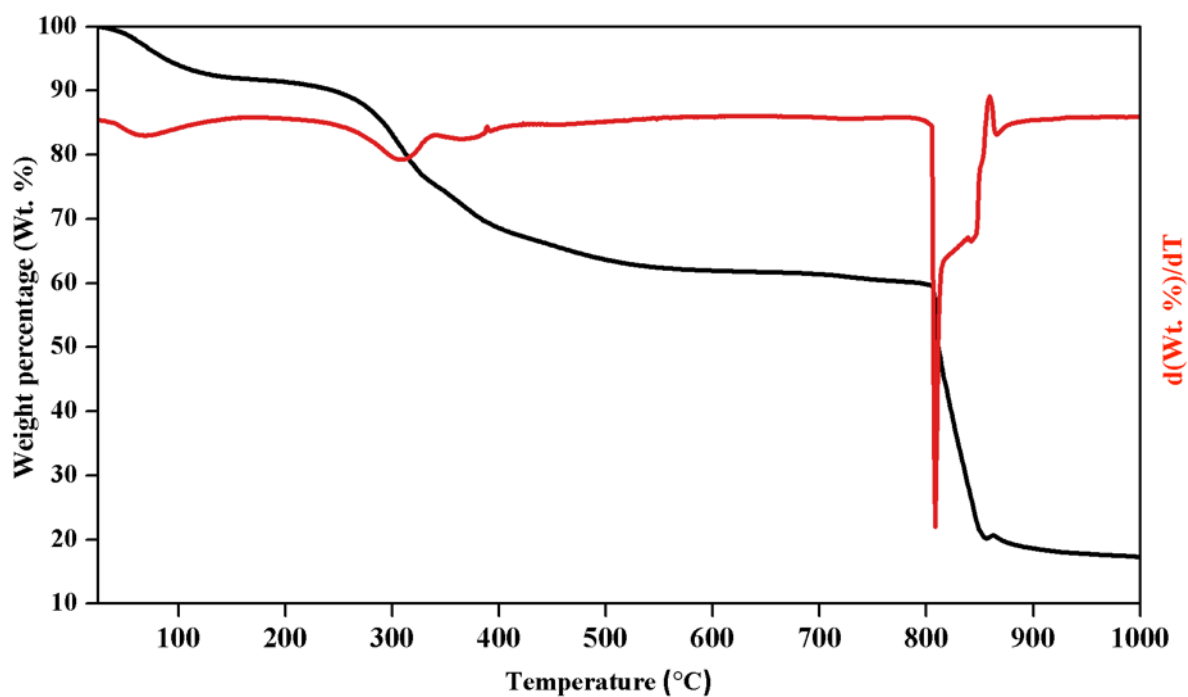
Figure 2A.13. TGA-DTA analysis of alkaline lignin (air).
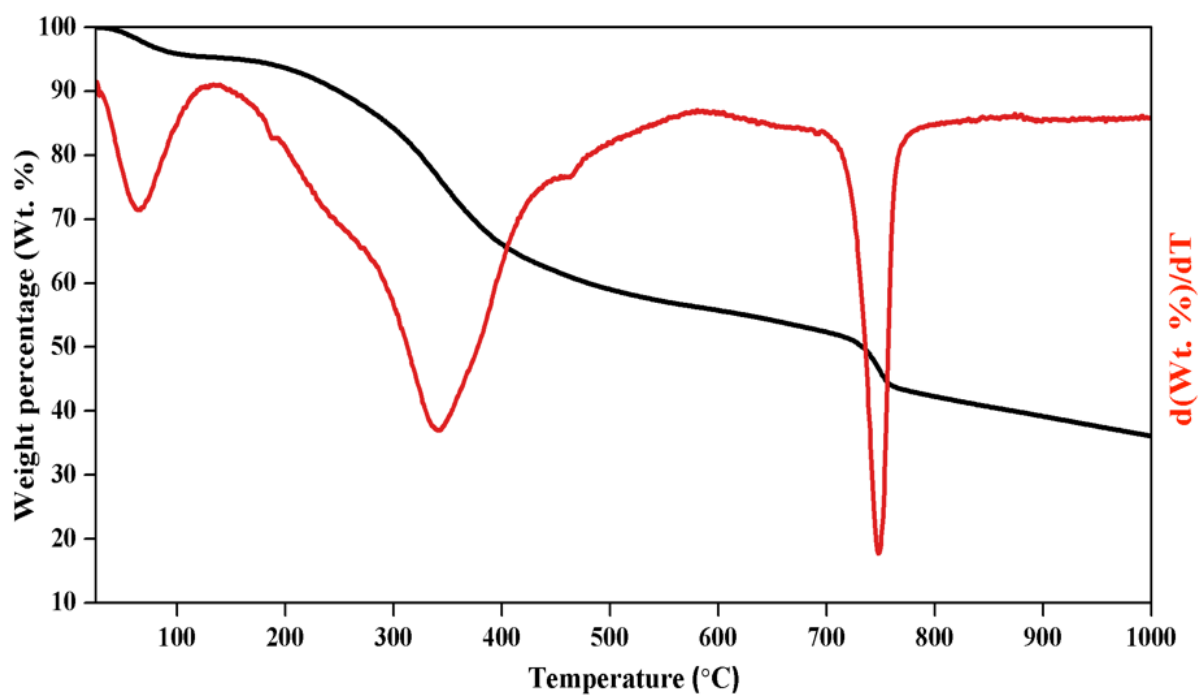
Figure 2A.14. TGA-DTA analysis of dealkaline lignin (N₂).
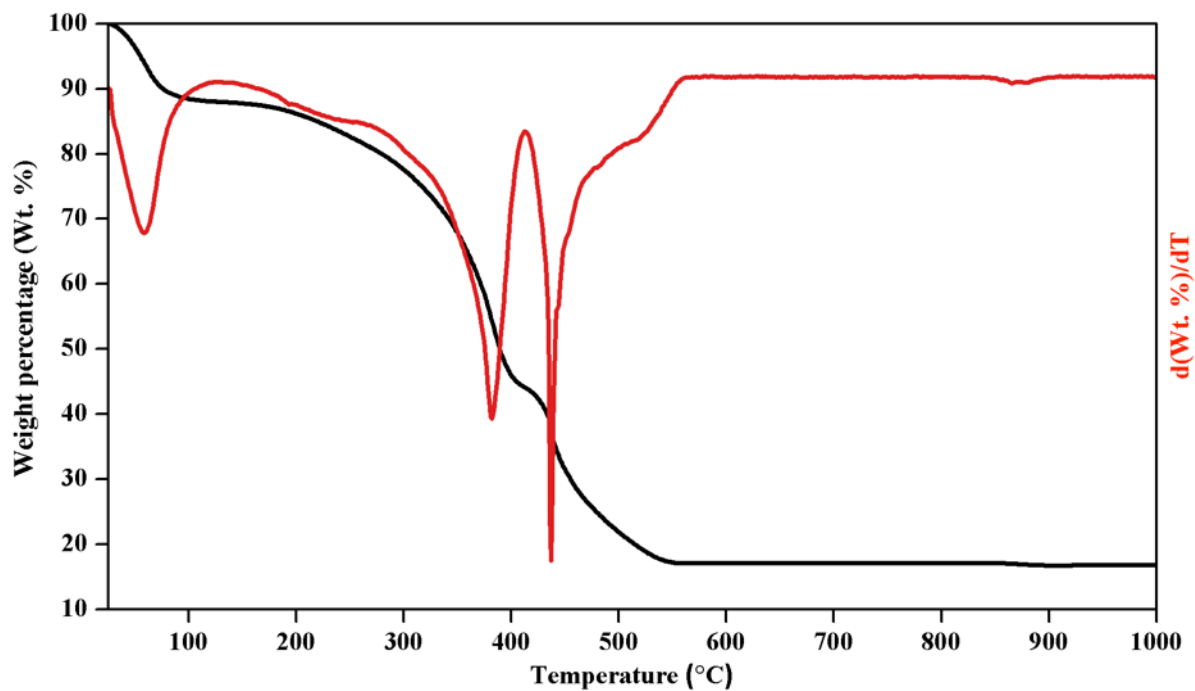
Figure 2A.15. TGA-DTA analysis of dealkaline lignin (air).
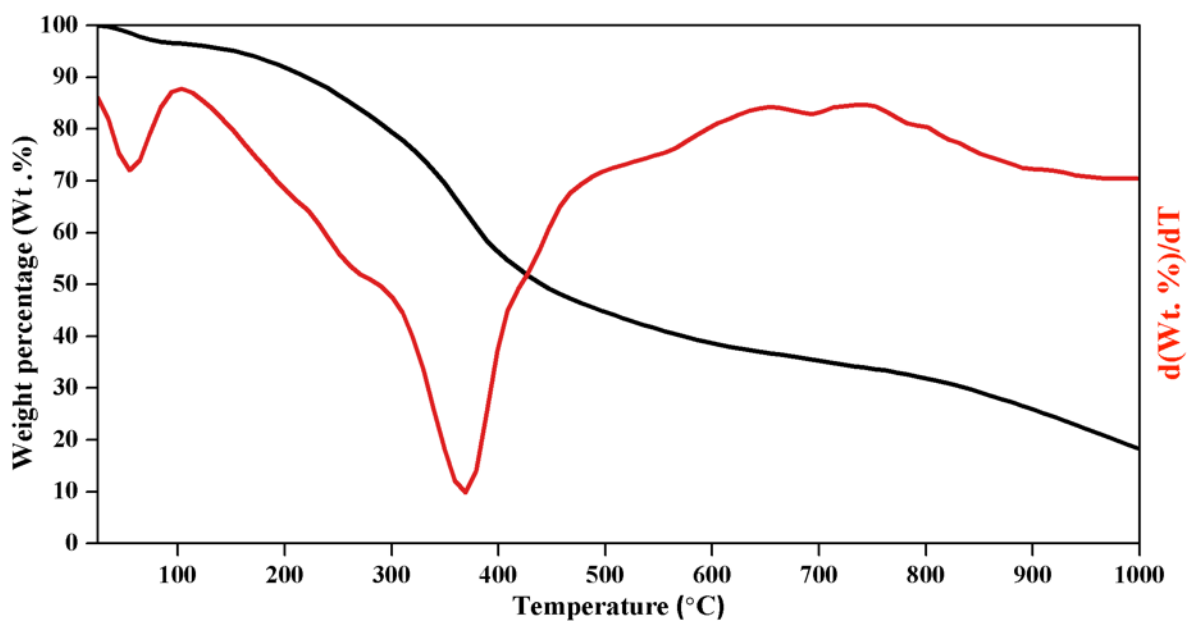
Figure 2A.16. TGA-DTA analysis of alkali lignin (N_2).
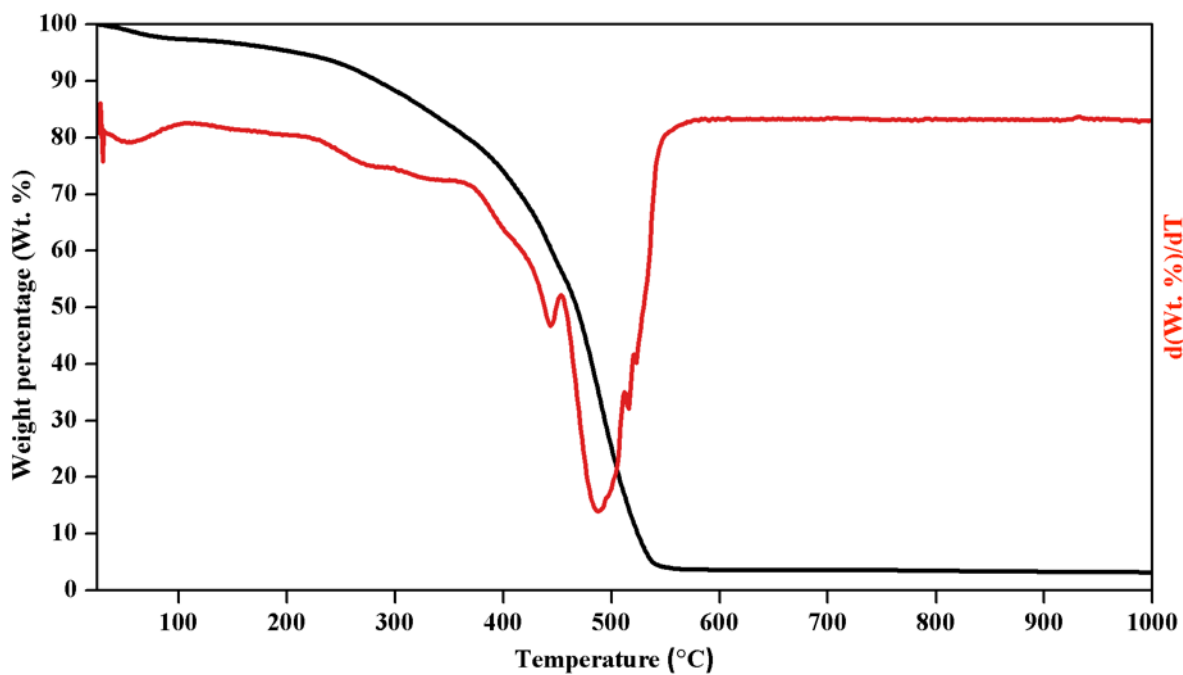
Figure 2A.17. TGA-DTA analysis of alkali lignin (air).
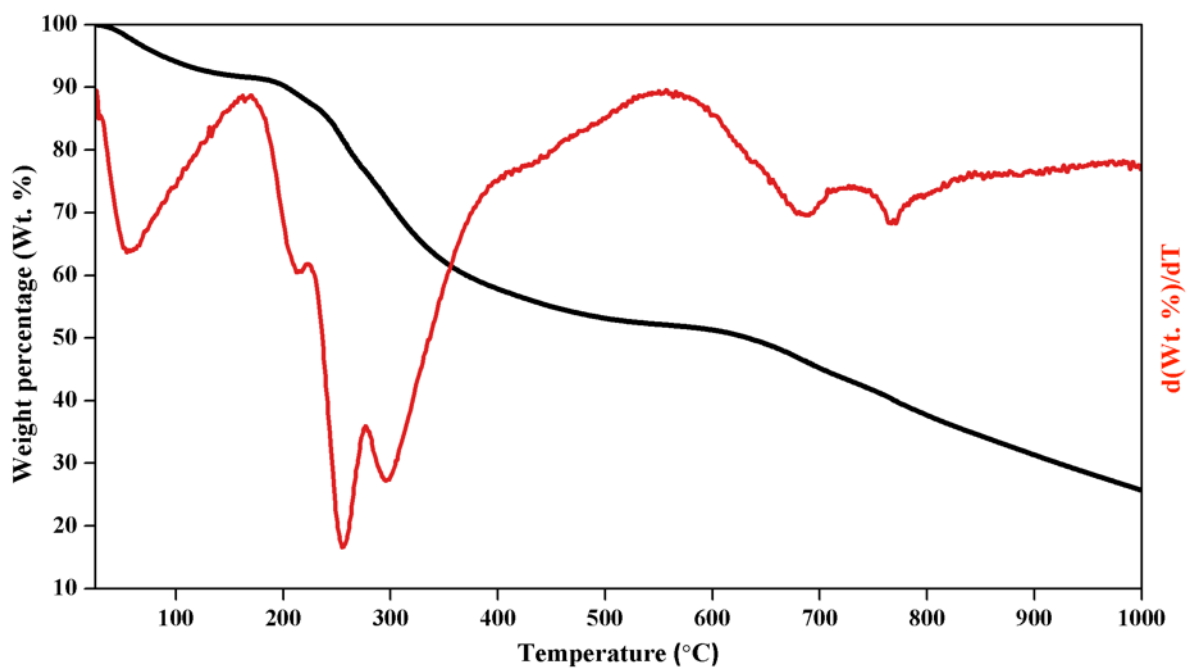
Figure 2A.18. TGA-DTA analysis of lignosulfonate sodium salt lignin (L-Na) (N$_2$).
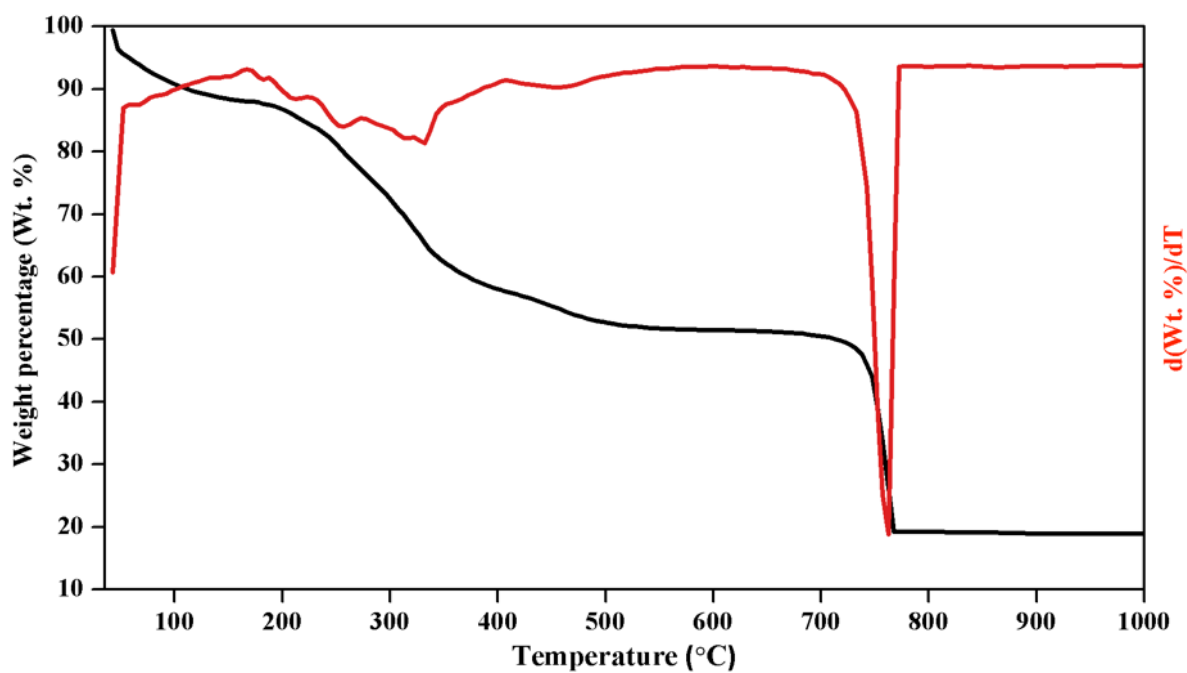
Figure 2A.19. TGA-DTA analysis of lignosulfonate sodium salt lignin (L-Na) (air).
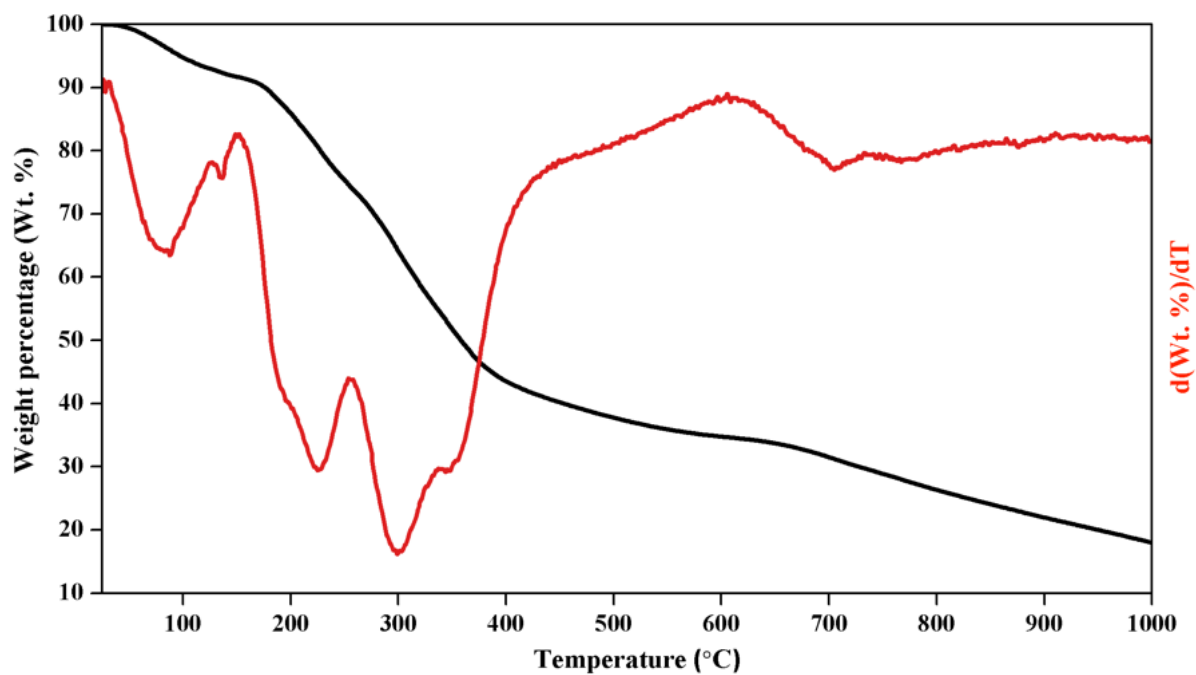
Figure 2A.20. TGA-DTA analysis of lignosulfonate calcium salt lignin (L-Ca) (N_2).
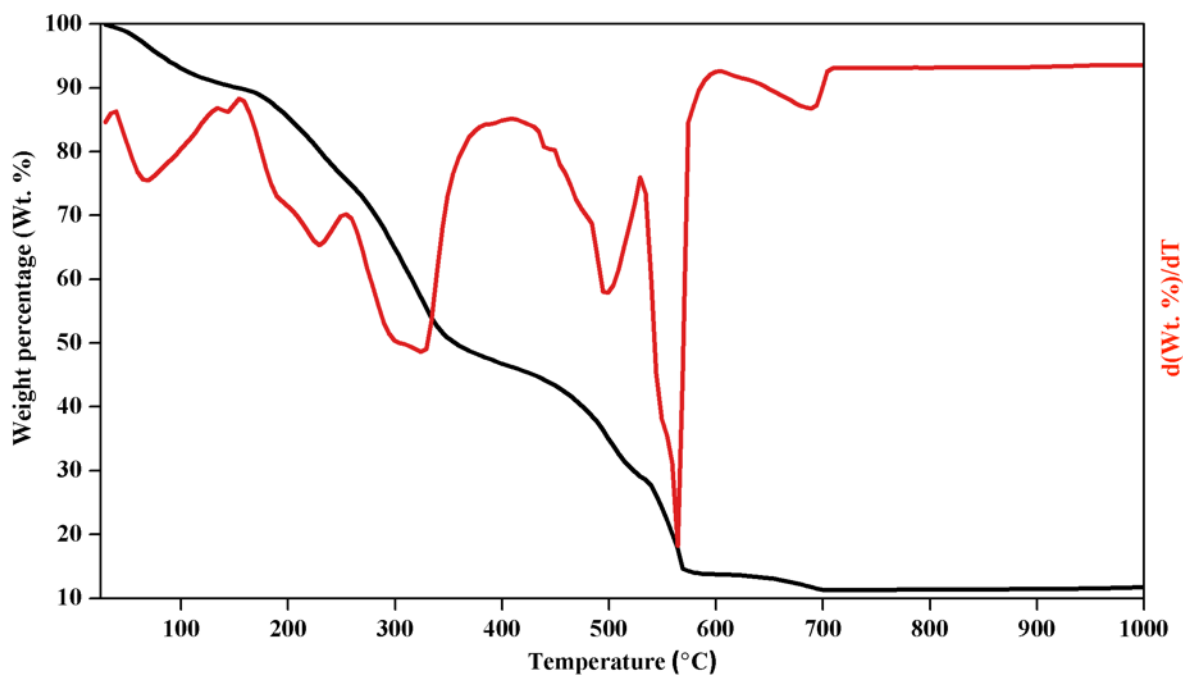
Figure 2A.21. TGA-DTA analysis of lignosulfonate calcium salt lignin (L-Ca) (air).

It was observed that all the samples show a peak below 100 °C which is corresponds to the removal of moisture. Thereafter sample starts degrading from 150 °C to 400 °C which might be due to the cleavage of aryl-ether linkages. Removal of aliphatic side chain was observed around 300 °C. Temperature range from 370 °C to 400 °C was observed for the cleavage of C-C bond present in lignin. Decomposition of aromatic rings was observed around 400-650 °C. The observed thermal degradation steps of various lignins are confirmed with the available literature.[19-22] Change in thermal energy as a function of temperature was studied from DTA analysis and it was observed that all the lignin shows sharp endothermic peak pattern in nitrogen atmosphere around 100 °C, 300 °C (250-350 °C) and 700 °C. However, in the presence of oxygen atmosphere the shape of curve remained almost same but the endothermic effect was changed. Like, in air atmosphere, the endothermic effect in alkaline lignin around 100 and 300 °C was reduced. Moreover, DTA of L-Ca lignin in nitrogen and air atmosphere showed that decomposition took place via three endothermic processes (major peaks) while in the presence of oxygen, the curve showed six endothermic peaks, indicating that combustion reaction of the lignin is quite complicated. Furthermore, the presence of oxygen altered the temperature of peaks also. This perhaps could be due to the difference in the nature of the products formed at the end of endothermic reaction.

A careful observation of TGA-DTA analysis of lignin under nitrogen atmosphere shows some unburnt residue (15-44%) present in it. This could be explained on the basis of carbon, hydrogen and oxygen present in the lignin. In the presence of inert (nitrogen) atmosphere carbon will burn in the form of CO and CH_4 as per the amount of oxygen and hydrogen present in lignin. After complete use of oxygen and hydrogen present in the lignin, some carbon still remains unburnt as some inorganic material. Like in case of alkaline lignin 44% residue is obtained in N_2 while from the molecular formula of $C_{8.9}H_{9.1}O_{5.1}$, if 5 CO and 2 CH_4 will go then 1-2 C will remain which will give 11-22% residue. While this residue is matched well with TGA analysis in air atmosphere (25% residue). The same calculation was done for dealkaline lignin and observed the almost same percentage of residue in N_2 atmosphere gives 28% residue and from the calculation using monomer molecular formula residue is 30-40%. Furthermore, it was observed from the microanalysis that alkaline lignin is having less carbon percentage (52%) compare to dealkaline lignin (65%) and more contamination of Na (69 mg/g) and S (2.05%) compare to dealkaline lignin (Na: 29 mg/g, S: 1%). Possibly the presence of high contamination of sodium and sulphur in the alkaline lignin gives higher residue (inorganic).

2A.3.6. X-Ray Diffraction (XRD) analysis

The morphology of lignin was studied using Powder XRD, PAN analytical X'pert Pro, Netherlands; with duel goniometer diffractor. The source of X-ray was Cu Kα (1.5418 Å) radiation with Ni filter. Prior to analysis all the samples were grinded and dried in vacuum over (10^{-4} MPa). Further, scanning was done from a 2θ value of 5 to 90 ° at the scanning rate of 4.3 °/min.
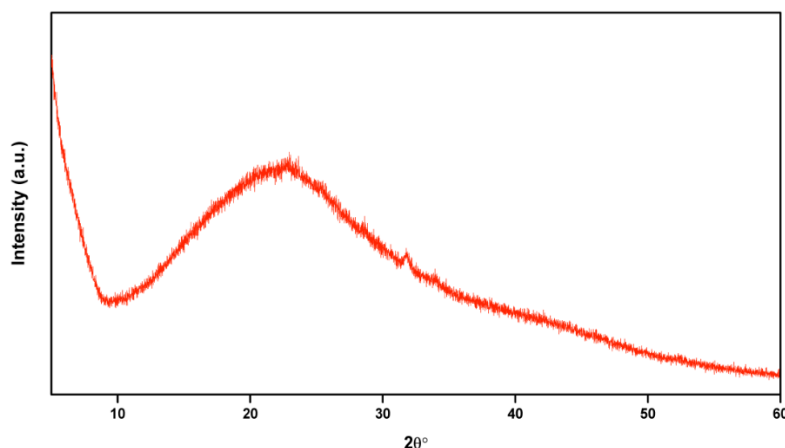
Figure 2A.22. XRD of alkaline lignin.
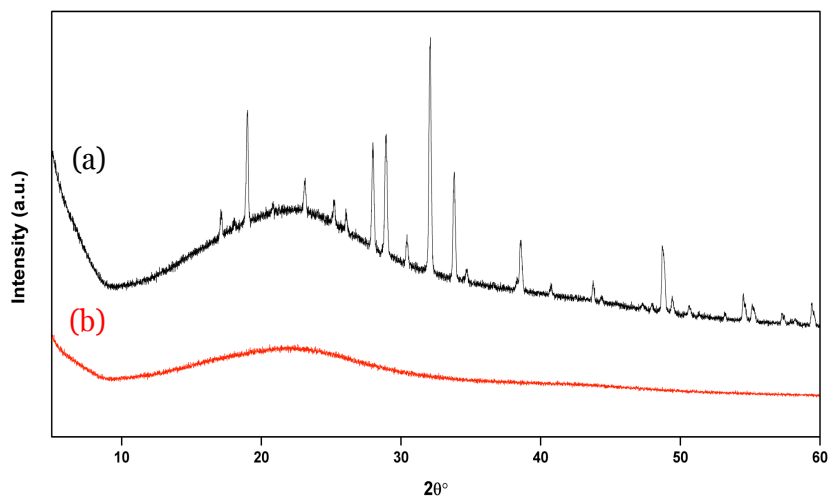
Figure 2A.23. XRD of dealkaline lignin (a) before water washing, (b) after water washing.
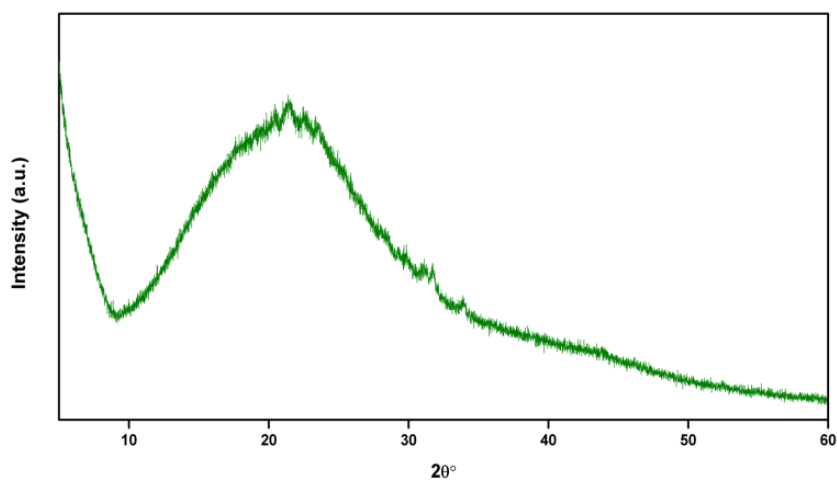
Figure 2A.24. XRD of alkali lignin.
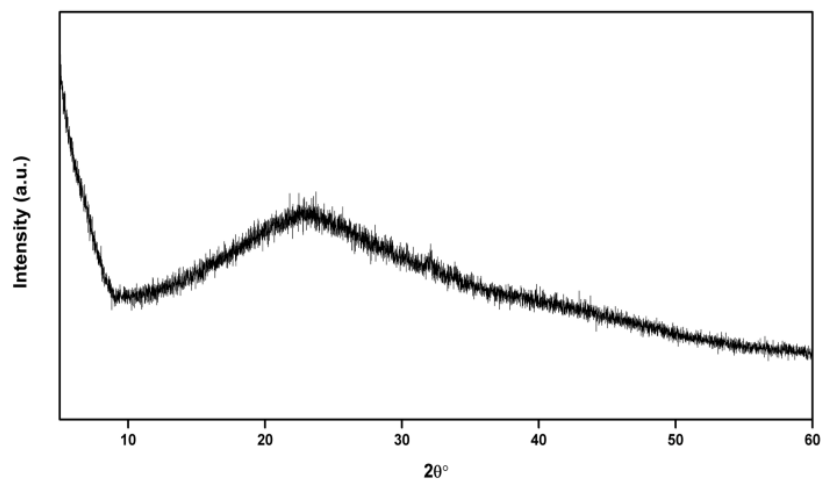
Figure 2A.25. XRD of lignosulfonate sodium salt lignin (L-Na).
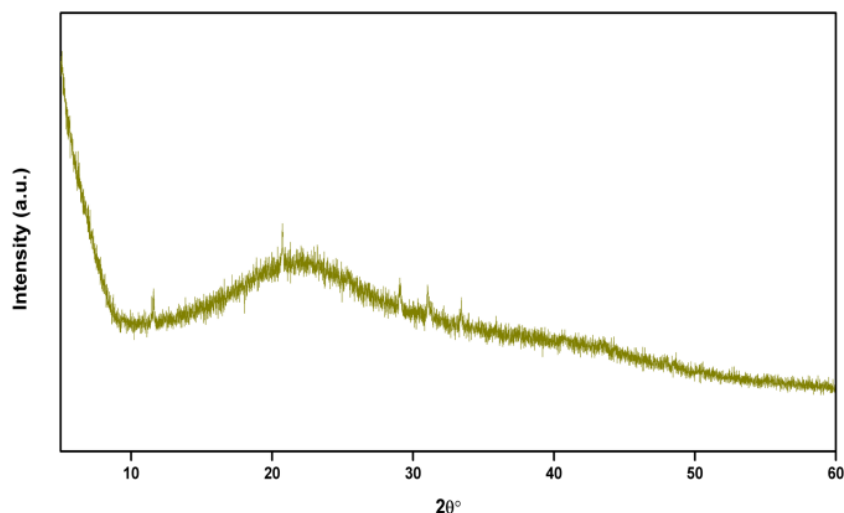
Figure 2A.26. XRD of lignosulfonate calcium salt lignin (L-Ca).

As mentioned in the Chapter 1, lignin can be isolated using various methods in which different reagents and conditions are used. During the isolation of lignin from lignocellulosic biomass, it is possible to get some cellulose impurity. However, it is well known in the literature that lignin is amorphous in nature while cellulose shows the peak for crystalline and amorphous nature at 22.5^o and $17.7-18.5^o$, respectively. XRD patterns for all the lignin are given in Figure 2A.22 to Figure 2A.26. For all the samples, broad peak for the amorphous nature of lignin was observed in the range of $10-30^o$. While in the case of dealkaline lignin some crystalline peaks were also observed. XRD pattern is well matched with Na_2SO_4 XRD pattern (JCPDS File. No. 36-0397). Peaks for sulphur and sodium were observed at 23°, 27.9^o, 28.7^o (S, JCPDS File No. 74-1465) and 32°, 48.5^o (Na, JCPDS File No. 09-0188), respectively. Presence of these peaks conclude that lignin may be isolated using Kraft process in which Na_2S and NaOH are typically used as reagent. When dealkaline lignin was washed with water it does not show any impurity peaks for Na and S also. It might be because that after lignin isolation complete washing was not done. Moreover, dealkaline lignin is 40% soluble in water so after water washing those impurities comes along with water and left over lignin shows completely amorphous peak pattern.

2A.3.7. Ultraviolet-Visible (UV-Vis) Spectroscopy

Color of wood derives from certain structures of lignin. A compound is colored due to the presence of chromophores. The chromophores present in the lignin were identified by UV-Vis absorption measurements of the sample by Perkin Elmer

spectrophotometer (Model-Lambda 650). Lignin was dissolved in mixture of ethanol and water (1:2 *v/v*) and was analyzed in the range of λ = 200-800 nm.

Absorption band in the range of at λ = 278-315 nm can be assigned to lignin building blocks i.e. guaiacyl, sinapyl and p-hydroxyl phenyl. A common peak for all the lignin samples was observed at λ = 280 nm which corresponds to the presence of π-π* electronic transition in aromatic ring of unconjugated phenolic units (Figure 2A.27). A shoulder peak at λ = 230 nm can be assigned to mono and di-substituted aromatic rings. Adsorption band at λ = 200-220 nm was observed due to the presence of π-π* electronic transitions of aromatic rings. Another absorption band was observed at λ = 312 nm having a shoulder at 340 nm with a gradual decrease towards visible region. λ at 312 nm relates to n-π* transition in lignin units with C=C linkages conjugated to the aromatic rings.
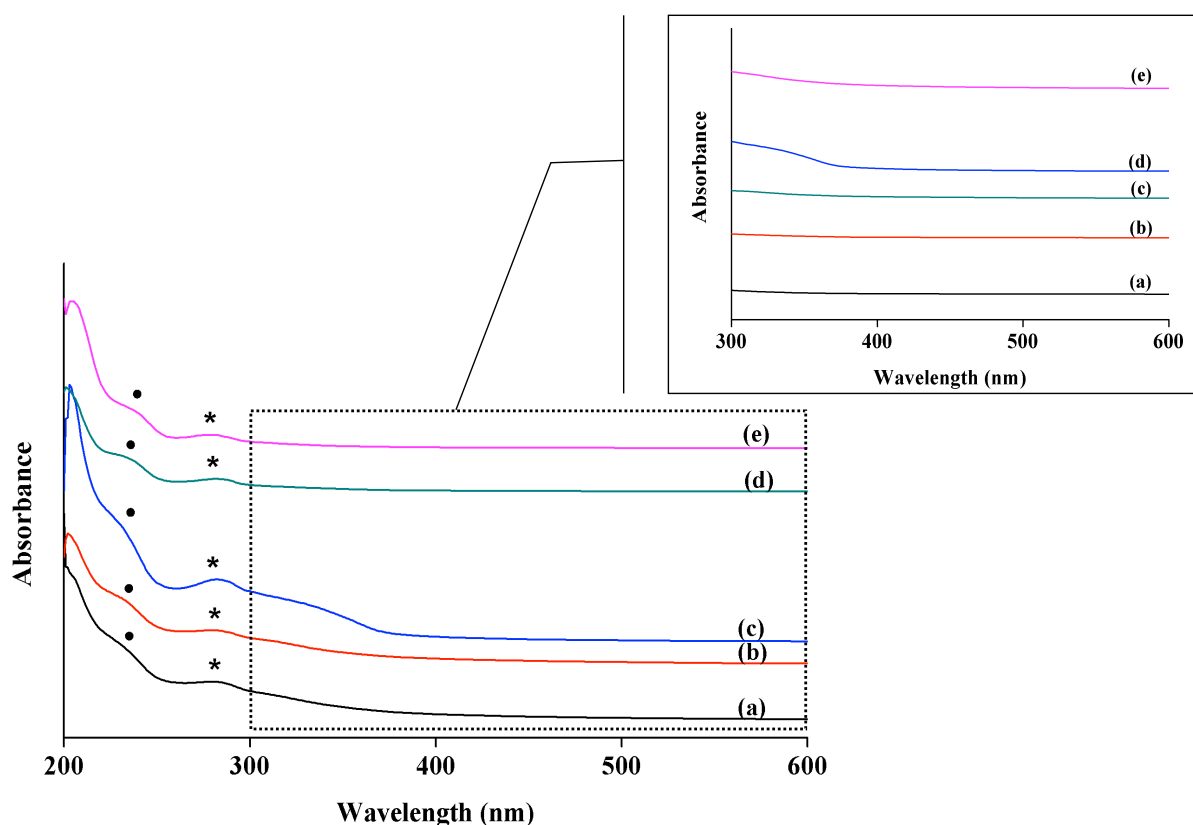
Figure 2A.27. UV-Visible analysis (a) alkaline lignin, (b) dealkaline lignin, (c) alkali lignin, (d) lignosulfonate sodium salt lignin (L-Na), (e) lignosulfonate calcium salt lignin (L-Ca).

2A.3.8. Solubility of lignin

Before proceeding to the catalytic runs, solubility of lignins was determined in a series of organic solvents and the results are tabulated in Table 2A.5. The main reason behind this study was (1) selection of suitable reaction medium to carry out the lignin depolymerization reactions, in which lignin will be completely soluble and (2) selection of solvent in which depolymerized products can be isolated from the reaction mixture. So that unconverted lignin will not come out with the products. Moreover, Hansen solubility parameter (HSP) for lignin, aromatic monomers and solvents was also studied through literature (Table 2A.7). HSP of lignin[23] is 24.51MPa$^{1/2}$ while for solvents, the HSP values was observed higher or closer to the lignin e.g. water (48.0 MPa$^{1/2}$), ethanol (26.2 MPa$^{1/2}$) and methanol (29.7 MPa$^{1/2}$). Alkaline lignin is found to be least soluble in diethyl ether (DEE), ethyl acetate (EtOAc), tetrahydrofuran (THF), etc. and HSP values of these solvents are also close to the aromatic monomers. Hence, these solvents are used for the extraction of aromatic products from lignin depolymerization reaction mixture.

Out of the several solvents checked for lignin solubility (Table 2A.6), water was found to be good solvent for alkaline lignin, lignosulfonate sodium and calcium salt lignin as these became completely soluble in water. These observations suggest the hydrophilic nature of these lignin while alkali and dealkaline lignin found to be hydrophobic in nature. From this study, ethanol:water (1:2 *v/v*) was selected as the reaction medium as lignin is completely soluble in this solvent system. Solvents like diethyl ether and ethyl acetate was selected for the isolation of products as lignin is insoluble in these solvents.

Table 2A.6. Solubility of various lignin in different solvents.

Solvent (Polarity Index)	Lignin Solubility (%)*				
	Alkaline	**Dealkaline**	**Alkali**	**L-Na**	**L-Ca**
Water (9.0)	100	40	1.6	100	100
Ethanol (5.2)	4.1	Insol.	15.45	Insol.	Insol.
Methanol (5.1)	11.8	60	9	30	18
Acetone (5.1)	1.3	Insol.	21	1	2

Ethyl acetate (4.4)	1.0	Insol.	0.58	Insol.	Insol.
Chloroform (4.1)	1.7	Insol.	0.62	Insol.	Insol.
Tetrahydrofuran (4.0)	2.4	Insol.	12.5	2	3.5
Dichloromethane (3.1)	2.7	Insol.	3.45	nd	nd
Diethyl ether (2.8)	0.3	Insol.	0.52	Insol.	Insol.
Toluene (2.4)	nd	Insol.	Insol.	Insol.	Insol.
Hexane (0.0)	nd	Insol.	Insol.	nd	nd
Methanol:water (5:1 *v/v*)	85.5	100	85	100	100
Ethanol:water (1:2 *v/v*)	100	70	55	100	100
*0.08 g lignin dissolved in 5 mL of solvent.					

Table 2A.7. Hansen solubility parameter of various solvents and aromatic monomers.

Solvent	Hansen solubility parameter (HSP) (δ; MPa$^{1/2}$)[24,25,26]	Aromatic compounds	Hansen solubility parameter (HSP) (δ; MPa$^{1/2}$)
Water	48.0	Phenol	24.1
Ethanol	26.2	Vanillin	25.2
Methanol	29.7	Eugenol	22.8
Acetone	19.7	Resorcinol	29.0
Ethyl acetate	18.2	*p*-cresol	22.7
Chloroform	18.7	Benzene	18.7
Tetrahydrofuran	18.5	Toluene	18.3
Dichloromethane	20.8	Xylene	18.2

Diethyl ether	15.4	Acetophenone	19.6
Toluene	18.3	Benzaldehyde	22.5
Hexane	14.9	Benzyl alcohol	25.2

2A.4. Conclusions

Various physio-chemical characterizations were performed for the commercially procured lignins. Structural and functional properties of lignin depend on the origin, type and age of plant from which lignin is isolated. Moreover, the properties of lignin also depend on the method used for the isolation of lignin. Hence, complete characterization of five different lignin samples (alkaline, dealkaline, alkali, lignosulfonate sodium salt and lignosulfonate calcium salt lignin) was performed using various techniques like XRD, CHNS, TGA-DTA, etc. and used in the current work. CHNS elemental analysis was performed which revealed that lignin is composed of 39-63% C and 5-8% H along with sulphur contamination of 1-3.7%. ICP-OES and SEM-EDAX analysis showed the presence of Na and S contamination in lignin which is possible from the isolation process used (Kraft or Sulphite pulping). ATR and ^{13}C NMR analysis was performed for the functional group analysis and aromatic backbone of the lignin. All the lignins studied here showed similar type of functional groups with different intensities. Thermal degradation behaviour of lignin was studied using TGA-DTA analysis and it showed the presence of 18-44% of residue in nitrogen atmosphere. Morphology of lignin was studied using XRD analysis and revels that lignin is completely amorphous in nature while dealkaline lignin shows the presence of few crystalline peaks which corresponds to Na and S contamination which can be removed by water washing. UV-Vis analysis was performed which further confirms the aromatic nature of lignin. Further, solubility of lignin was checked in various solvents and ethanol:water in the ratio of 1:2 *v/v* was chosen as the solvent system for lignin depolymerization reactions. Moreover, diethyl ether (DEE) and ethyl acetate (EtOAc) were selected for the isolation of products as lignin is insoluble (least soluble) in these solvents.

2A.5. References

1.   A. M. Mayer and R. C. Staples, *Phytochemistry*, 2002, 60, 551-565.

2.   F. Cherubini and H. Stromman. Anders, *Biofuels, Bioproducts and Biorefining*, 2011, 5, 548-561.

3.   Jacco van Haveren, L. S. Elinor and J. Sanders, *Biofuels, Bioproducts and Biorefining,* 2008, 1, 41-57.

4.   J. Zakzeski, P.C.A. Bruijnincx, A.L. Jongerius and B. M. Weckhuysen, *Chemical reviews*, 2010, 6, 3552-3599.

5.   W. Boerjan, J. Ralph and M. Baucher, *Annual Review of Plant Biology*, 2003, 519-546.

6.   Zakzeski J, Bruijnincx PCA, Jongerius AL and W. BM., *Chem Rev* 2010, 110, 3552–3599.

7.   Y. H. P. Zhang, S. Y. Ding, J. R. Mielenz, J. B. Cui, R. T. Elander, M. Laser, M. E. Himmel, J. R. McMillan and L. R. Lynd, *Biotechnol. Bioeng.*, 2007, 214-223.

8.   T. H. Kim, J. S. Kim, C. Sunwoo and Y. Y. Lee, *Bioresour. Technol*, 2003, 39-47.

9.   Z. Yuan, S. Cheng, M. Leitch and C. C. Xu, *Bioresour Technol*, 2010, 101, 9308-9313.

10.   A. K. Deepa and P. L. Dhepe, *RSC Advances*, 2014, 4, 12625.

11.   A. K. Deepa and P. L. Dhepe, *ACS Catalysis*, 2015, 5, 365-379.

12.   https://www.sigmaaldrich.com/catalog/product/aldrich/471038?lang=en&region=IN,

13.   https://www.sigmaaldrich.com/catalog/product/aldrich/471054?lang=en&region=IN.

14.   A. S. Jönsson, A. K. Nordin and O. Wallberg, *Chem. Eng. Res. Des.*, 2008, 1271-1280.

15.   L. Stigsson and C. Lindstrom, *U.S. Patent 8,252,141 B2,* 2012.

16.   J. Lora, M. N. Belgacem and A. Gandini, *Eds.Elsevier: New York*, 2008, 225-241.

17.   M. D. A. Aresta and F. Dumeignil, *Walter de Gruyter GmbH &Co KG: Berlin/Boston,* 2012, 446.

18.   E. A. Capanema, M. Y. Balakshin and J. F. Kadla, *J. Agric. Food Chem.*, 2004, 1850-1860.

19.   K. Wang, F. Xu and R. Sun, *Int. J. Mol. Sci.*, 2010, 2988-3001.

20.   D. J. Gardner, T. P. Schultz and G. D. McGinnis, 1985, 85-110.

21.   M. Balat, *Energ. Resour. Part A*, 1981, 620-635.

22.   M. J. Oren, M. M. Nassar, G. D. M. Mackay and Can., *J. Spectrosc.*, 1984, 10-12.

23.   Ni Haiyue, Shixue Ren, Guizhen Fang and Y. Ma, *BioResour.,* 2016, 2, 4353-4368.

24.   M. Belmares, M. Blanco, W. A. Goddard, R. B. Ross, G. Caldwell, S-H. Chou, J. Pham, P. M. Olofson and C. Thomas., *Journal of computational chemistry*, 2004, 15, 1814-1826.

25. G. C. Vebber, Patricia Pranke and C. N. Pereira., *Journal of Applied Polymer Science*, 2014, 1, 131.

26. C. M. Hansen, *CRC press, 2007.*

Chapter 2B
Catalyst Synthesis and Characterization

2B.1. Introduction

As discussed in Chapter 1, solid base catalysts have been actively studied for many decades and this interest is still persistent. Solid bases are well known to catalyze a variety of organic reactions. Particularly, solid base catalysts offer appropriate and environmentally friendly routes for the organic synthesis. A major objective in the modern chemical industry is to avoid the production of toxic and environmentally undesirable wastes.[1-3] Certainly, the replacement of liquid acid catalysts with solid acid catalysts has led to more than 100 industrial processes currently operated in the world.[4] However, to date less success has been achieved with solid base catalysts and only a few processes are in operation using solid base catalysts.[4]

Several solid bases have been proposed for the industrial synthesis of chemicals such as alkali ion-exchanged zeolites,[5, 6] sepiolites,[7] alkaline oxides supported on microporous[8] and mesoporous solids,[9] sodium metal clusters in zeolites,[10] metals supported on alumina,[11, 12] alkaline earth solids such as magnesium[13-15] and barium oxide[16] aluminium magnesium mixed oxides derived from hydrotalcites[17-19] and nitrides.[20, 21] Alkali ion-exchanged zeolites and sepiolites possess only mild basic strength, while alkali metals and alkaline oxides loaded on supports are considered as super bases that can catalyze a wide range of reactions.[22]

In this thesis attempts have been made to use solid base catalysts for the depolymerization of lignin and in this chapter particularly the synthesis and characterization of various solid base catalysts used for the lignin depolymerization has been discussed. Additionally, the synthesis and characterization of various supported metal catalysts used for the upgradation of lignin derived aromatic monomers are also reviewed.

2B.1.1. Solid Base Catalysts

Replacement of liquid bases with solid base catalysts would allow for easier separation from the product(s) as well as possible regeneration and reuse. Hence, in order to avoid the drawbacks associated with the homogeneous base catalysts, solid bases were used for the depolymerization of lignin into aromatic monomers.[23]

Solids bases have Brønsted or Lewis base sites which will be helpful in the cleavage of ether and carbon-carbon linkages present in lignin. For this, a range of solid base catalysts having variation in different properties like basic sites present, pore size, pore volume, surface area, etc. was studied. A wide range of materials are

known having basic character. From those, zeolites (X and Y saturated with alkaline cations of low electronegativity), hydrotalcite-type anionic clays, hydroxyapatite materials and selected single-metal oxides (MgO, CaO) was used.

Zeolites are microporous, aluminosilicate minerals consist of a network of TO_4 tetrahedral (T = Si or Al) linked by one oxygen. This creates a three-dimensional framework (with cages and channels) of interconnected tetrahedra, comprising of aluminium, silicon and oxygen atoms. They consist of a crystalline structure built from $[AlO_4]^{5-}$ and $[SiO_4]^{4-}$, bonded together in such a way that all four oxygen atoms located at corners of each tetrahedron are shared with adjacent tetrahedral crystals. The common oxygen atom between $[SiO_4]^{4-}$ and $[AlO_4]^{5-}$ tetrahedra, remains oriented in such a way that the framework develops voids/pores in the form of cages and channels between the tetrahedra. The structural formula of the zeolite based on its crystal unit cell (assuming both the SiO_2 and AlO_2 as variables) can be represented by $M_{a/n}(AlO_2)_a(SiO_2)_b.wH_2O$, where, w is the number of water molecules per unit cell, and a and b are total numbers of tetrahedra of Al and Si, respectively per unit cell. The b/a ratio usually varies from 1 to 5. Exceptionally, some zeolites are having b/a varying from 10-100 or even higher than 100 for ZSM-5 type zeolites.[24, 25]

The replacement in a zeolite framework atom by another one with a lower valency (for instance Si^{4+} by Al^{3+}) creates a negative charge on the framework which has to be neutralized by a proton or a metal cation. The appearance of the positive and negative charge generates the acidic/basic character of the zeolites. When the framework negative charge is compensated by cations with a low electronegativity, the charge on the oxygen may be high enough to create basic properties. It will be described further that increasing the Al content strengthens the basic character[26] and that replacing Al and/or Si by other atoms (Ga and Ge, P) having different electro negativities or sizes may also modify the basicity.[27] The properties of the zeolite used for the lignin depolymerization are tabulated below (Table 2B.1).

LB
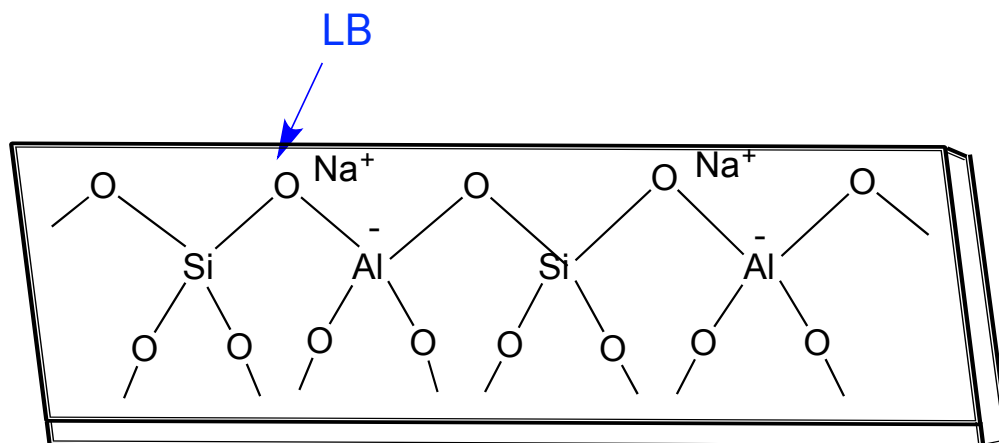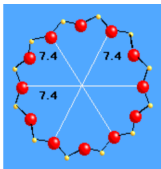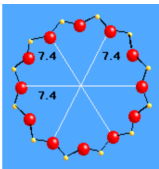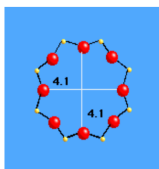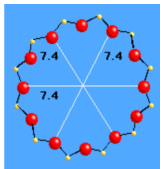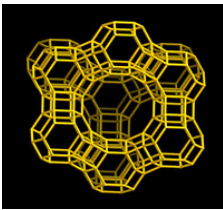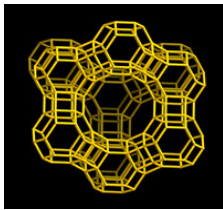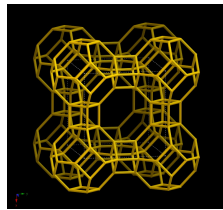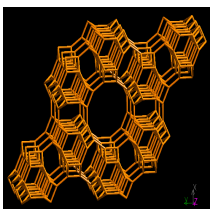
Figure 2B.1. Lewis basic (LB) sites in zeolites.

Table 2B.1. Structural properties of basic zeolites used for lignin depolymerization (Source: IZA).

	NaX (FAU)	NaY (FAU)	NaP (LTA)	KLTL (LTL)
Chemical Composition	$(Na^+{}_2)_2(H_2O)_{240}(Al_5Si_{134}O_{384})$	$(Na^+{}_2)_{29}(H_2O)_{240}(Al_{58}Si_{134}O_{384})$	$(Na^+{}_{12}(H_2O)_{27})_8(Al_{12}Si_{12}O_{48})_8$	$K^+{}_6Na^+{}_3(H_2O)_{21}(Al_9Si_{27}O_{72})$
Ring	12 6 4	12 6 4	8 6 4	12 8 6 4
Pore dimension	7.35 x 7.35 x 7.35 Å	7.35 x 7.35 x 7.35 Å	4.1 x 4.1 Å	7.1 x 7.1 Å
Channel	3D	3D	3D	1D
Structure				

Hydrotalcites (HT) are layered double hydroxide materials made up of positively charged two-dimensional layers of mixed hydroxides with water molecule and exchangeable charge-compensating anions.[28, 29] Hydrotalcite can be prepared with a combination of bivalent (Mg, Ni, Cu, Zn) and trivalent (Al, Fe, Cr) cations.

Reactivity of as-synthesized HT is directed by the intercalated anion and amount of water present.[30] In my studies, I have used Mg-Al hydrotalcite having Mg/Al ratio of 3 [$Mg_6Al_2CO_3(OH)_{16} \cdot 4(H_2O)$]. It shows a brucite like structure of [$Mg(OH)_2$] in which some bivalent metal cations (Mg^{+2}) are replaced by trivalent metal cations (Al^{+3}). The two brucite layers are arranged in a way that they placed one above other and held by weak hydrogen bonding. Replacement of M^{+2} cation by M^{+3} cation creates excess positive charge which is compensated by intercalating anion. Intercalating compensating anions and water molecules are present in the interlayer space between two brucite layers. It is very well documented in the literature that as-synthesized hydrotalcite does not have activity or high activity for some base catalyzed reactions.[31, 32] As the adsorbed water molecules hinder the access of basic sites. So, it is required to calcine these materials at high temperature around 400-600 °C for 8-12 or 24 h.[33, 34] The main role of the calcination is to decompose the intercalating carbonate anions and water molecules so that brucite layers gets converted into [Mg(Al)O] mixed oxide with higher surface area and porosity.[35] As the basicity plays an important role for achieving good catalytic activity, this can be tuned by changing M^{+3}/M^{+2} ratio or change in the intercalating anions. Moreover, Basicity of hydrotalcite can be increased by altering its calcination temperatures.[36, 37] Since the hydrotalcite is a porous material, the surface area and pore volume of calcined hydrotalcite will increase gradually as the calcination temperature increases.

Structure of HT showing the Brønsted basic sites with two brucite like layers can be represented as Figure 2B.2.
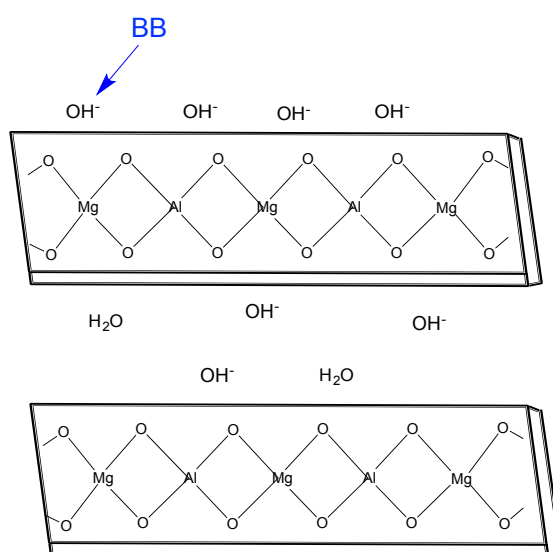
Figure 2B.2. Brønsted Basic sites (BB) in hydrotalcite.

Hydroxyapatite (HAP) and HAP-like materials have attracted considerable interest as bone substitutes for biomedical applications[38, 39] It is well-known that HAP is the dominant inorganic component of vertebrate hard tissues. HAP crystals in the biological system contain various trace elements such as F, Mg, Si and Zn. The flexible structure of HAP can accommodate a wide variety of anionic and cationic substitutions.[40, 41] Stoichiometric HAP has the formula $Ca_{10}(PO_4)_6(OH)_2$ (Ca/P = 1.66) in which external ions are suggested to substitute Ca^{2+}, $(PO_4)^{3-}$ and $(OH)^-$ by Zn^{2+}, $(CO_3)^{2-}$, F^-.[42-44] Not only the crystallization process would be affected by the substitutions of external ions[45, 46] but the physicochemical properties can also be modified.[47, 48] Basic sites present in hydroxyapatite are shown in Figure 2B.3.
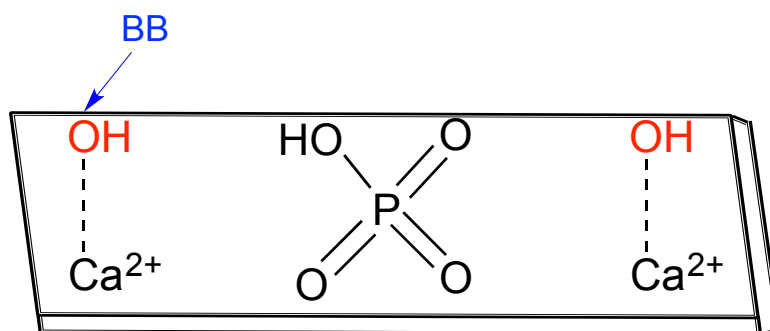
Figure 2B.3. Brønsted Basic site (BB) in hydroxyapatite.

Alkaline-earth metal oxides such as SrO and CaO have been extensively studied as solid superbase catalysts. One of the features of alkaline-earth oxides is their high ability to abstract H^+ of allylic position as revealed in double-bond migration of olefinic compounds. For instance, butene undergoes double bond migration over alkaline-earth metal oxides even at low temperature (50 °C).[49] The super basic materials were generally prepared by heating the metal hydroxides or carbonates at high temperatures under vacuum. The super basic sites that correlate with ion pairs of low coordination numbers are located at corners, edges, or surfaces of planes with high Miller indices. It is known that the ion pairs show strong adsorption of CO_2 and tend to rearrange eagerly at high temperatures.[49] However, the relationship between the ion pairs of low coordination numbers and the sites which are catalytically active remains uncertain.
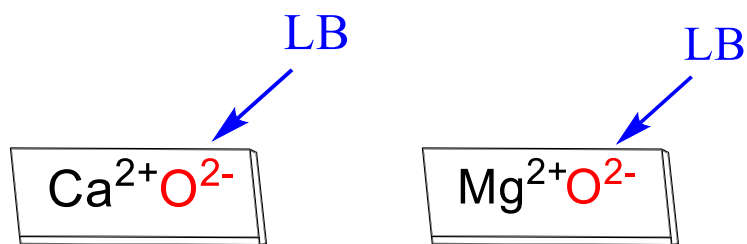
Figure 2B.4. Lewis Basic sites (LB) in CaO and MgO.

Alkaline earth oxides are generally used as solid base catalysts. Among them, catalysis with CaO and MgO is the most widely carried out. MgO has been extensively studied as a promising catalyst,[49-51] modifier or promoter[52, 53] and catalyst support[54, 55] in heterogeneous catalysis. Moreover, they have been demonstrated on a wide range of organic reactions; the isomerization of alkenes, hydrogenation of alkenes, addition of amines to dienes, and the aldol condensation of acetone.[49, 56] The catalytic activities of MgO and CaO prepared from $Ca(OH)_2$ and $Mg(OH)_2$ were also studied and shows that the pretreatment time and calcination temperature can influence the properties of the resulting catalysts, and consequently decide the catalytic behaviour. It was also understood from the literature that high temperature is required to remove the adsorbed water and carbon dioxide.[49, 57] Therefore, the factors to be considered for MgO and CaO as an efficient catalyst depends on the strength of the basic sites. Because of the importance of MgO and CaO as solid base catalyst, it was further studied for lignin depolymerization reactions.

2B.1.2. Supported Metal Catalyst

Supported metal catalysts are a kind of heterogeneous catalysts synthesized by supporting metal(s) on the proper (desired) support. Generally, the catalytic properties of supported metal catalysts are influenced by two main factors (1) the selection of metal (2) the selection of support.[58-60] The main role of support is to help in the better dispersion of metal particles. A massive data is available on the synthesis of supported metal catalysts via various methods like wet-impregnation, co-precipitation, chemical-vapour deposition, etc. followed by its application in several reactions e.g. hydrogenation of sugar/sugar alcohols, lignin hydrodeoxygenation, hydrogenation of furfural, etc.[61, 62] Here various types of supported metal catalysts were prepared in order to develop a good catalytic system

for the upgradation reactions of lignin derived monomers. A part from this, effect of different metal, metal loading and support were also studied. All the supported metal catalysts used in my work were synthesized using established wet-impregnation method. Noble metals like Pt, Pd and Ru were loaded over basic supports like Hydrotalcite and NaX. Noble metals were chosen to synthesize supported metal catalysts since they are known to have better activity for hydrodeoxygenation/hydrogenation reactions.[63-67] Overall supported metal catalysts were prepared in order to upgrade the lignin derived product via hydrogenation reactions. All the synthesized supported metal catalysts were well characterized using various techniques like XRD, TEM, CO_2-TPD, etc.

2B.2. Chemicals and Materials

NaX (Si/Al = 1.2; mol ratio), NaY (Si/Al = 3.6; mol ratio) and NaP (Si/Al = 1.69; mol ratio) zeolite were procured from Zeolyst international, USA. Metal oxides such as calcium oxide (99.99%) and magnesium oxide (98%) were purchased from Sigma Aldrich. Hydrotalcite (Mg/Al = 3; mol ratio) and hydroxyapatite (Ca/P = 1.66; mol ratio) were purchased from Sigma Aldrich. Magnesium nitrate hexahydrate ($Mg(NO_3)_2.6H_2O$) (99%) was purchased from Merck, aluminium nitrate nonahydrate ($Al(NO_3)_3.9H_2O$) was purchased from Thomas Baker, sodium carbonate (Na_2CO_3) (99.5%) and sodium hydroxide (NaOH) (98%) were purchased from Loba Chemie. Noble metals like Pt, Pd and Ru were procured in metal salt form like Tetraamine platinum nitrate [$Pt(NH_3)_4(NO_3)_2$, 99.99%] was purchased from Alfa Aesar, Ruthenium chloride ($RuCl_3$, 45-55 %), and Palladium chloride ($PdCl_2$, ≥ 99.9%) were purchased from Sigma Aldrich. All the metal precursors were used as received without any further modification.

2B.3. Synthesis of Solid Base Catalyst
2B.3.1. Synthesis of Hydrotalcite

Hydrotalcite (Mg/Al = 3; mol ratio) was synthesized by co-precipitation method.[68] Sodium hydroxide (NaOH) was used to maintain the pH, while sodium carbonate (Na_2CO_3) was used as a carbonate source. Catalyst (10 g) was synthesized followed by the preparation of two solutions (Solution A and Solution B). Solution 'A' an aqueous solution (37.5 mL) of $Mg(NO_3).6H_2O$ (0.279 mol/71.5 g) and $Al(NO_3)_3.9H_2O$

(0.093 mol/34.8 g) was slowly added (as this step is an exothermic reaction) into an aqueous solution 'B' (37.5 mL) of NaOH (0.4375 mol/17.5 g) and Na_2CO_3 (0.1125 mol/11.9 g) under vigorous stirring for 2 h. pH of the resultant solution was maintained between 8 and 10 by the addition of NaOH and Na_2CO_3 solution. After the complete mixing of solutions 'A' and 'B' it was vigorously stirred for 1 h at room temperature. Next this solution was kept in an autoclave at 80 °C for 16 h under static condition. This results in the white precipitate solution. Obtained precipitate was then washed with deionised water until pH became neutral. Resultant solid was kept for drying in oven at 55 °C for 18 h. Further it was dried at 80 °C for 16 h under vacuum (10^{-4} MPa) and named as as-synthesized HT (10 g). The obtained as-synthesized material was calcined in muffle furnace at 550 °C under air atmosphere for 8 h with a ramp rate of 2 °C/min. The after calcined material was taken (9.5 g) and named as calcined hydrotalcite (C-HT) (Mg/Al = 3). The calcination program used is depicted in Figure 2B.5.
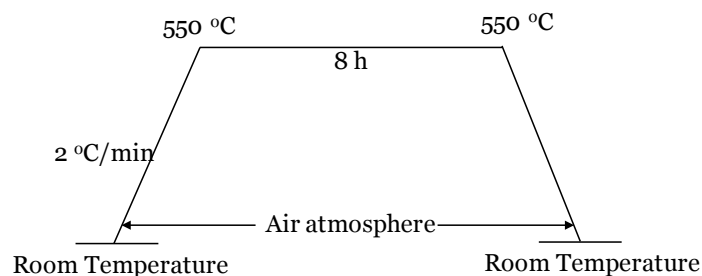
Figure 2B.5. Calcination program for hydrotalcite.

2B.4. Synthesis of Supported Metal Catalyst

Supported metal catalysts were prepared by wet-impregnation method. Prior to the catalyst synthesis, first supports were activated in oven at 55 °C for 16 h followed by vacuum drying (10^{-4} MPa) at 150 °C for 6 h. For the synthesis of 1 *wt.%* Pt/NaX, 1 g of NaX was taken in 10 mL water and stirred for 30 min. at room temperature. After that, 0.83 mL aqueous solution of metal precursor, $Pt(NH_3)_4(NO_3)_2$ solution (12 mg/mL Pt) was added drop wise to the suspension of support and allowed to stir for 16 h at room temperature. Water was removed by rotary evaporator and the obtained material was dried in oven at 55 °C for 16 h. Further it was dried under vacuum (10^{-4} MPa) at 150 °C for 6 h and finally subjected for the calcination in a tubular furnace under O_2 flow (20 mL/min) and then reduced under H_2 flow (20 mL/min) at 400 °C for 2 h each. The same synthesis procedure and

calcination-reduction program was used for the all supported metal catalysts (Table 2B.2). The detailed calcination-reduction program is shown is Figure 2B.6.
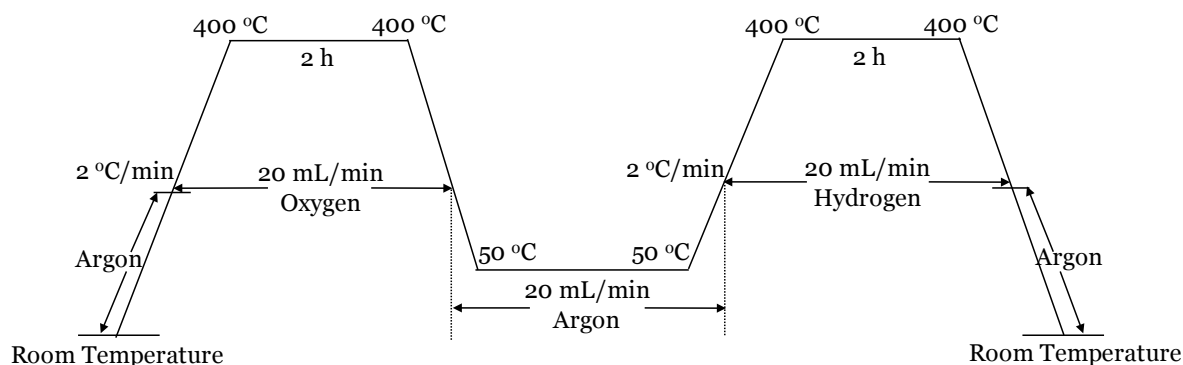
Figure 2B.6. Calcination-reduction program used for supported metal catalysts.

Table 2B.2. List of supported metal catalysts synthesized in current work.

Sr. No.	Catalyst	Metal loading (*wt.%*)
1	Pt/NaX	1, 2 and 3
2	Pt/HT	3
3	Pt/CaO	2
4	Ru/NaX	2 and 3
5	Pd/NaX	2 and 3

Before employing these solid base catalysts for the lignin depolymerization and aromatic monomers upgradation, all the catalysts were activated at 150 °C for 2 h in vacuum (10^{-4} MPa). Prior to the catalytic runs their properties were also studied using various physicochemical techniques. XRD was used to determine the morphology of the catalysts on bulk level. To determine the surface area, pore volume and pore diameter N_2 sorption analysis was performed and CO_2-TPD analysis was used to determine the basic sites (strong and weak) present in the catalyst. ICP-OES analysis was used to determine the Si and Al content in zeolites catalysts and to check the actual and theoretical loading of metal in supported metal catalysts.

2B.5. Catalyst Characterizations

All the catalysts were characterized using various characterization techniques such as ICP-OES, XRD, TEM, N_2 sorption and CO_2-TPD. The details of characterization techniques (instruments used and operating conditions, etc.) and results for characterizations are discussed in this section.

2B.5.1. Solid Base Catalysts

Before employing the solid base catalysts for the lignin depolymerization reactions, those were thoroughly characterized using various techniques like, XRD for the morphology of the catalyst, ICP-OES analysis was performed for determining the Si/Al ratio, CO_2-TPD was used to know the basicity of the catalyst, etc.

2B.5.1.1. X-Ray Diffraction (XRD) Analysis

X-ray diffraction analysis of solid base catalysts like zeolites NaX (Si/Al = 1.2, mol/mol), NaY (Si/Al = 3.6 mol/mol), NaP (Si/Al = 1.69 mol/mol) and KLTL (Si/Al = 2.7 mol/mol), alkali metal oxides (calcium oxide and magnesium oxide), clays (hydrotalcite) and hydroxyapatite was performed in a 2θ range of 5-90 ° at a scan rate of 4.3 °/min (Figures 2B.7 to Figure 2B.10). In the case of zeolites and metal oxides, sharp peaks were observed in the XRD pattern, which confirmed the crystalline nature of these materials. But in the case of hydrotalcite broad hump for the amorphous nature was also observed which corresponds to the mixed oxide phase i.e. periclase phase of the material in the range of 15-28 °.
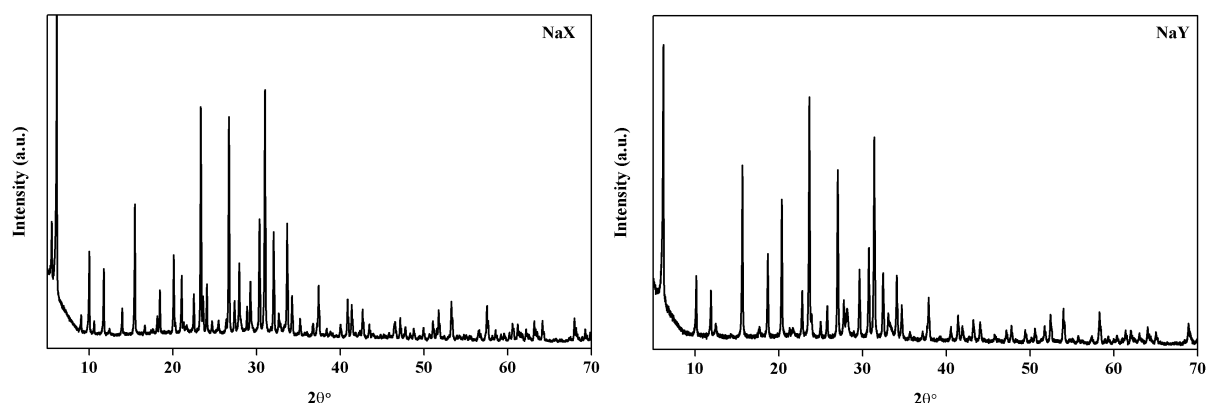
Figure 2B.7. XRD patterns of NaX[69] (left) and NaY[70] (right).
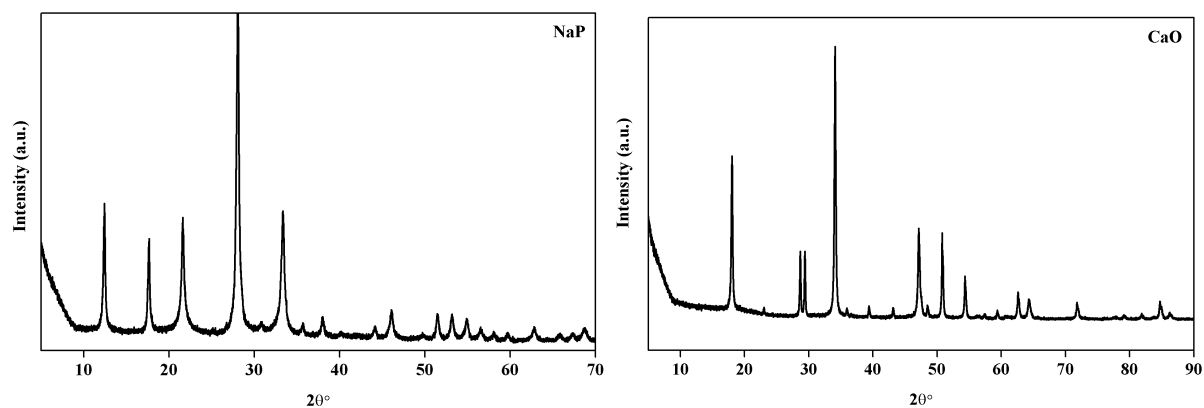
Figure 2B.8. XRD patterns of NaP (left) and CaO(right).
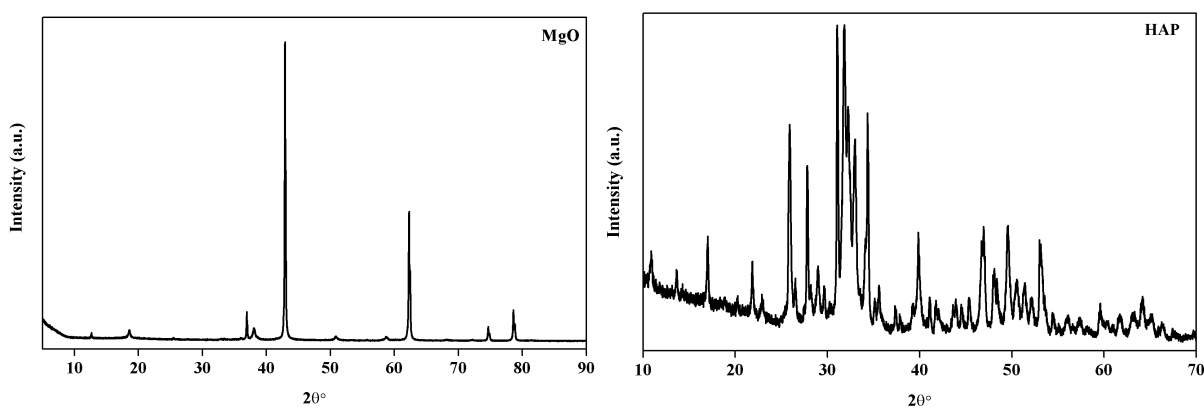
Figure 2B.9. XRD patterns of MgO (left) and Hydroxyapatite (right).
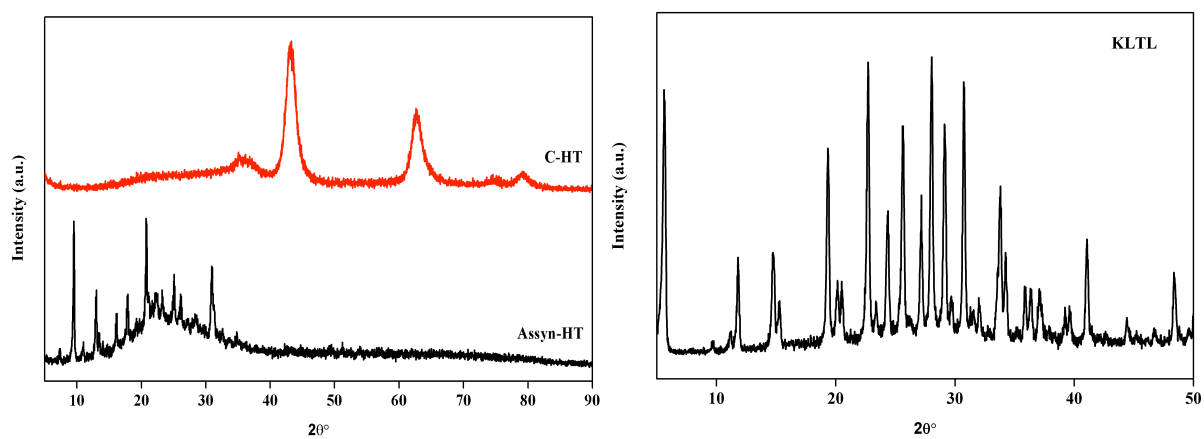
Figure 2B.10. XRD patterns of as-synthesized and calcined hydrotalcite
(Assyn-HT and C-HT) (left) and KLTL (right).

2B.5.1.2. Inductively Coupled Plasma-Optical Emission Spectrometry (ICP-OES) Analysis

ICP-OES analysis was performed to determine the Si/Al ratio of zeolites. Samples were analyzed in SPECTRO ARCOS Germany, FHS 12 instrument. 0.1 g of sample was weighed in the polypropylene bottle followed by the addition of 2-3 mL of HF. The mixture was heated at 80 °C to remove the excess HF. This process removes the silica from the sample.

$$SiO_2 + 4HF \longrightarrow SiF_4\,(g) + 2H_2O$$

$$SiO_2 + 6HF \longrightarrow H_2SiF_6 + 2H_2O$$

$$H_2SiF_6 \longrightarrow SiF_4\,(g) + 2HF$$
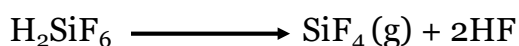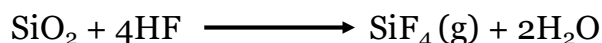
Further, solid residue obtained after HF treatment was dissolved in 3 mL of freshly prepared aquaregia (mixture of nitric acid and hydrochloric acid, in a molar ratio of 1:3) and diluted with 7 mL of deionized water. This solution was filtered with 0.22 micron filter before the analysis and the results obtained are summarized in Table 2B.3. Si/Al molar ratios obtained were found be similar to the ratio given by the supplier (Zeolyst International).

Table 2B.3. Summary on ICP-OES analysis of solid base catalysts.

Catalyst	Si/Al ratio (Theoretical)	Si/Al ratio (Actual)
NaX	1.2	1.19
NaY	3.6	3.4
NaP	1.69	1.7
K-LTL	2.7	2.7

2B.5.1.3. Temperature Programmed Desorption (CO_2-TPD) Analysis:

CO_2-TPD analysis was performed to quantify the total basicity present in the solid base catalysts. Micromeritics AutoChem 2910 instrument was used for the analysis. In this technique, CO_2 was used as acidic probe molecule which is adsorbed on the basic sites of the catalyst. There are at least two ways suggested in the literature (processes I and II) for the migration of adsorbed carbonate species over the surface for solid base catalysts (e.g. MgO).[71] In the process I, carbon dioxide moves over the surface in such a way that the free oxygen atom in the bidentate carbonate (CO_3^{2-}) approaches the adjacent Mg atom on the surface. In process II, the carbon atom approaches the adjacent O atom on the surface. The repetition of both process (I and II) results in the exchange of one oxygen atom. It is proposed that the bidentate carbonate formed at the room temperature and adsorption of CO_2 migrates over the surface as the temperature is raised in the TPD run. Moreover, the basic sites are not fixed on the surface but are able to move over the surface when carbon dioxide is adsorbing and desorbing. The position of the basic site (surface O atom) changes as CO_2 migrate over the basic site. The proposed mechanism for the migration of the surface bidentate carbonate are shown in Figure 2B.11.[71]
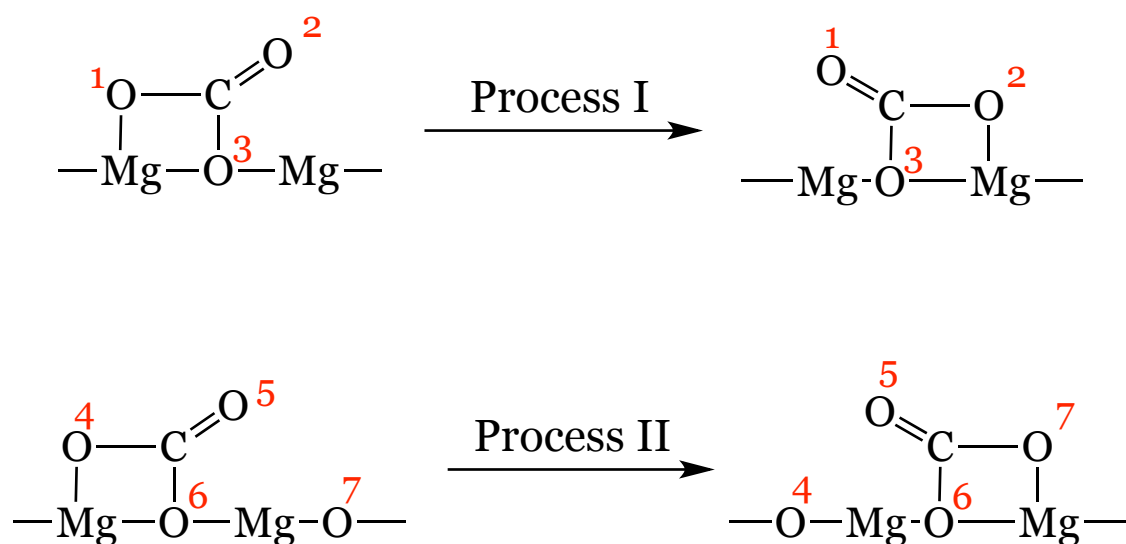
Figure 2B.11. Proposed mechanism for the migration of surface bidentate carbonate.[71]
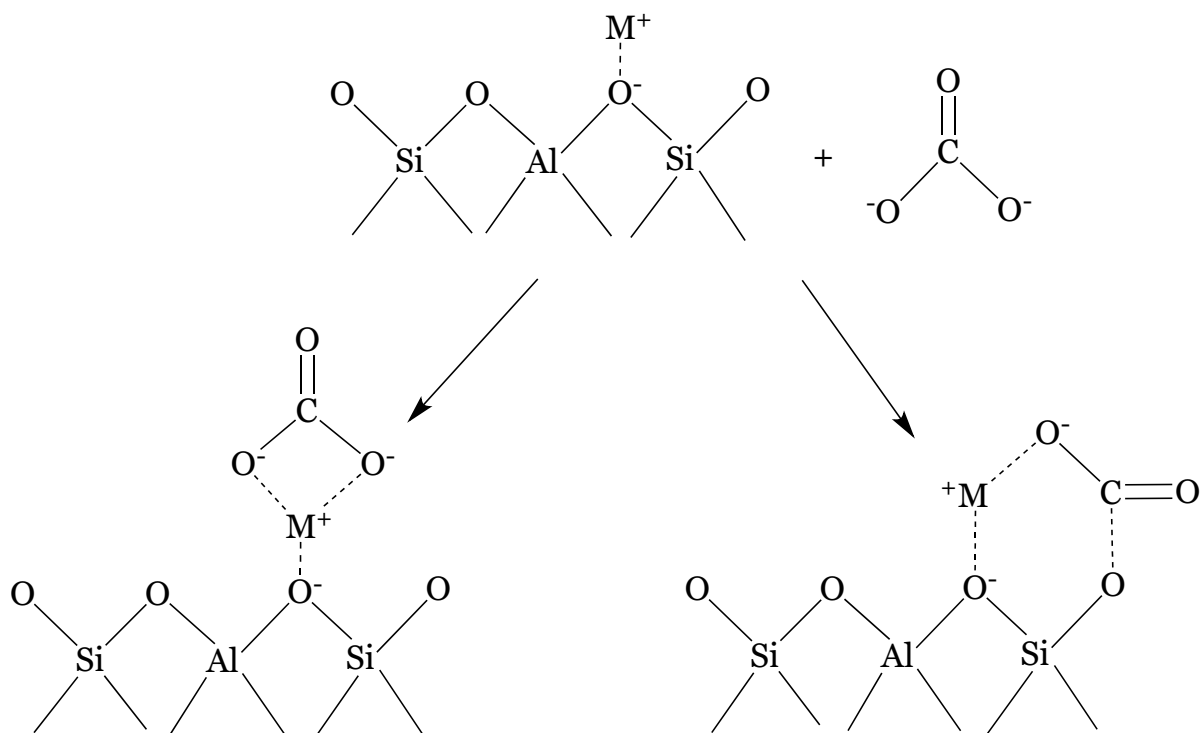
Figure 2B.12. Possible mode for the adsorption of CO_2 on the basic zeolite.

For analysis, prior to measurement, samples were activated at 350 °C for 15 min in helium flow (30 mL/min). Next temperature was allowed to decrease to 50 °C. The adsorption of CO_2 was done at 50 °C and then the sample was kept at 100 °C for 30 min. under helium gas flow (30 mL/min). Later, at the rate of 10 °C/min. temperature was increased from 100 °C to 700 °C in helium flow (30 mL/min) and TPD profile was recorded. For better understanding, CO_2-TPD program is represented in Figure 2B.12. The amount of CO_2 molecules desorbed corresponds to the amount of basic sites present in the catalyst.
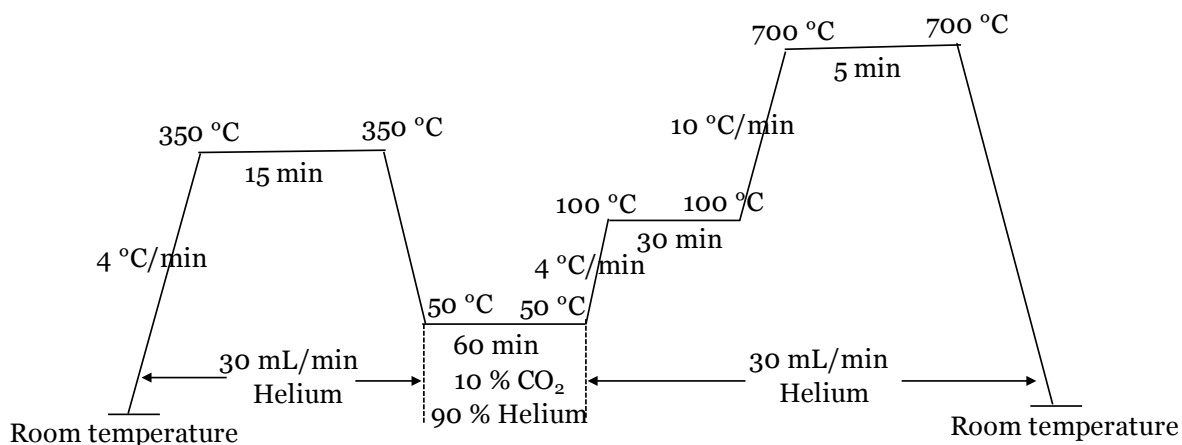
Figure 2B.13. CO_2-TPD programme used for solid base catalysts.
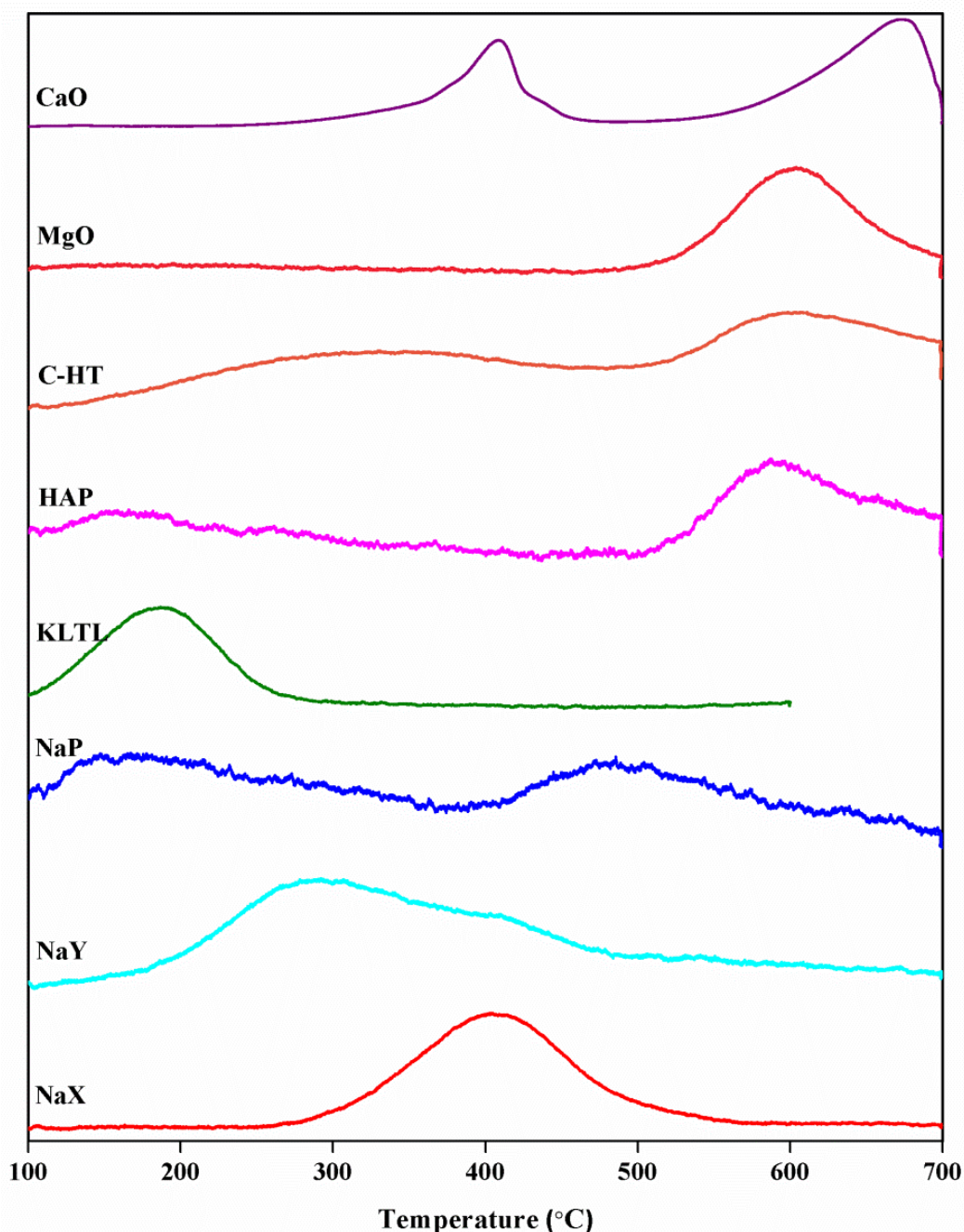
Figure 2B.14. CO_2-TPD profile of various solid base catalysts.

From the CO_2-TPD analysis the total amount of basic sites and their distribution as strong, moderate and weak basic sites present in the solid base catalysts was measured (Figure 2B.13 and Table 2B.4). It was observed that all the catalysts having different basic sites like zeolites shows weak or either moderate basic sites while CaO and MgO shows the presence of moderate and strong basic sites. Hydrotalcite and hydroxyapatite having weak and strong basic sites. The CO_2-TPD plots of CO2

desorbed from the MgO and CaO are compared (Figure 2B.14). The number of basic sites per unit weight that can retain the CO_2 under adsorption condition in more for CaO (CaO > MgO). Hence, the strength of the basic sites was observed more for CaO than MgO. Similar observations were made for the zeolites, hydrotalcite and hydroxyapatite also. Higher the basic strength of NaX was found compare to NaY, NaP and K-LTL. Si/Al ratio for NaX is 1.2 mol/mol while for NaY, NaP and K-LTL is 3.6, 1.69 and 2.7 mol/mol, respectively. As the Al content increases in the zeolite decrease in the Si/Al ratio can obtained. Among the mentioned four zeolites, NaX is having lower Si/Al ratio of 1.2 mol/mol (higher Al) which results in the higher basicity of the catalyst. Likely, the basicity for hydrotalcite and hydroxyapatite can be correlated. Hence, from CO_2-TPD analysis data it was understood that the solid bases selected for lignin depolymerization had various amounts of strong, moderate and weak basic sites which may govern the different activity in the depolymerization of lignin into aromatic monomers.

Table 2B.4. Summary on CO_2-TPD analysis.

Catalysts	Basicity (mmol/g)			Peak maxima (℃)
	Weak (w) (150-300 ℃)	Medium (m) (300-450 ℃)	Strong (s) 450-700 ℃)	
NaX (Si/Al = 1.2)	-	0.42	-	404 (m)
NaY (Si/Al = 3.6)	0.34	-	-	292 (w)
NaP (Si/Al = 1.69)	0.04	0.05	-	171 (w) & 486 (m)
K-LTL (Si/Al = 2.7)	0.14	-	-	188 (w)
C-HT (Mg/Al = 3)	0.17	-	0.23	294 (w) & 603 (s)
HAP (Ca/P = 1.66)	0.03	-	0.09	166 (w) & 587 (s)
CaO	-	0.49	1.47	408 (m) & 673 (s)
MgO	-	-	0.24	604 (s)

Note: w: weak, m: medium, s: strong basic sites in the given temperature range

2B.5.1.4. N$_2$ Sorption Analysis

Surface area, pore size and pore volume can be determined using nitrogen sorption analysis. Analysis was done in Autosorb 1C Quantachrome, instrument, USA. Prior to the analysis, samples were activated in vacuum at 200 °C for 3 h. The specific surface area was determined using BET method, pore size data was obtained using BJH & HK method and pore volume using t-plot method. Results are summarized in Table 2B.5.

Table 2B.5. Summary of N$_2$ sorption analysis.

Catalyst	N$_2$ sorption		
	BET Surface area* (m^2/g)	Pore volume (cm^3/g)	Pore diameter (nm)
NaX (Si/Al = 1.2)	586	0.32	1.10
NaY (Si/Al = 3.6)	575	0.33	1.15
NaP (Si/Al = 1.69)	14	0.10	1.8
KLTL (Si/Al = 2.7)	220	0.13	nd
C-HT (Mg/Al = 3)	207	0.95	9.2
HAP (Ca/P = 1.66)	39	0.18	9.08
CaO	12	0.05	8.2
MgO	9.2	0.02	4.8

*Brunauer-Emmett-Teller (BET), nd-not determined.

From N$_2$ sorption analysis it was observed that among the solid base catalysts, NaX (Si/Al = 1.2) was having the highest surface area of 586 m^2/g. Zeolites showed a pore diameter of < 2 nm which confirmed its microporous nature and is in good correlation with the literature. It was expected that catalyst having higher surface area might show better catalytic activity compared to others as more active sites are accessible.

2B.5.1.5. pH measurement

Before subjecting these solid base catalysts for lignin depolymerization reactions, pH was also checked in water and the reaction mixture chosen. To measure the pH of all the solid base catalysts, same quantity as similar to reaction mixture was taken. Solution was stirred for 10-15 minutes. After this pH was measured with the help of pH meter and following order was observed:

a) In water (Catalyst = 0.5 g, H_2O = 30 mL, RT)

CaO (pH ≥ 13.4) > NaX (pH 11.7) > MgO (pH 11.2) > KLTL (pH 10.9) > HT (pH 10.6) > NaP (pH 9.9) > NaY (pH 9.4) > HAP (pH 6.5)

b) In reaction mixture (Lignin (0.5 g) : Catalyst (0.5 g) = 1:1 *wt./wt.*, EtOH:H_2O (1:2 *v/v*) 30 mL, RT

CaO (pH ≥ 13.4) > HT (pH 12.5) > MgO (pH 10.5) > KLTL (pH 9.4) > NaX (pH 9.2) > NaY = NaP (pH 8.7) ≈ HAP (pH 8.5)

Overall, several solid base catalysts were characterized using various techniques like XRD, ICP-OES, CO_2-TPD, etc. It was observed from the XRD analysis that all the procured samples are stable under the pretreatment given for the activation of the catalyst. ICP-OES analysis was performed in order to check that Si/Al ratio of the zeolites and found to be similar as the acquired samples. Finally, to choose an appropriate catalyst, pH of all the catalysts was checked in water and reaction system chosen for the lignin depolymerization.

2B.5.2. Supported Metal Catalysts

All the synthesized supported metal catalysts were characterized using various techniques like XRD, ICP-OES, N2 sorption, etc. The details of characterization techniques and obtained results are discussed in this section.

2B.5.2.1. X-Ray Diffraction (XRD)Analysis

X-ray diffraction analysis was performed for supports as well as supported metal catalysts. All the samples were scanned in a 2θ range of 5-90 ° with a scan rate of 4.3 °/min. Figure 2B.15 represents the XRD pattern for 1, 2 and 3 *wt.%* Pt/NaX. For all the three catalysts Pt showed a diffraction pattern for the characteristic peaks at 2θ

values 39.8 °, 46 °, 67 ° and 81.3 °. These peaks are assigned to planes (111), (200), (220) and (311), respectively (JCPDS file no. 01-088-2343). Figure 2B.16. shows the XRD pattern for different metal (Pd, Ru) and support (NaX, CaO, C-HT). Pd showed diffraction patterns at 2θ values 40 ° (111), 46 ° (200) and 68 ° (220) (JCPDS File No. 87-0638). XRD pattern of Ru catalysts shows peaks at 2θ of 40 °, 42.5°, 47.4 °, 68.08° and 78.68° which are attributed to the (100), (101), (102), (110) and (103) crystalline planes, respectively (JCPDS File No. 06-0663). Peaks for Pt at at 2θ values 39.8 ° (111), 46 ° (200), 67 ° (220) in 2 *wt.%* Pt/CaO (JCPDS File No. 87-0640) and 39.8 ° (111), 46 ° (200) in 3 *wt.%* Pt/C-HT could also be clearly seen (JCPDS File No. 01-1235). XRD patterns for the CaO and C-HT is shown in Figure 2B.17.
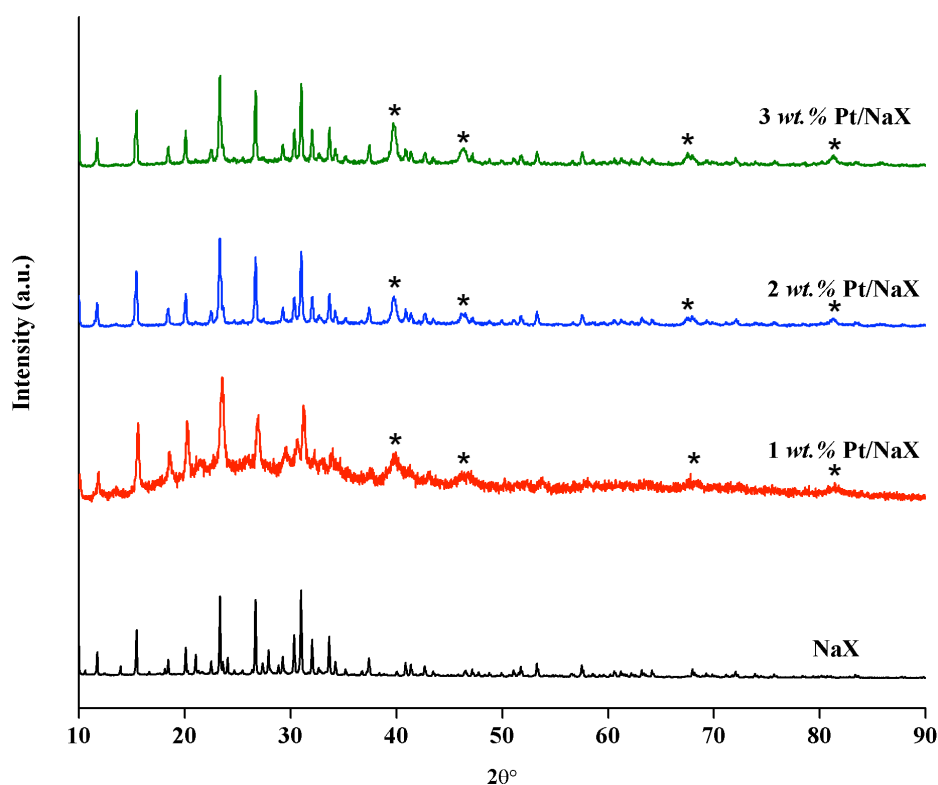
Figure 2B.15. XRD patterns for 1, 2 and 3 *wt.%* Pt/NaX. (* indicates the presence of metal peak).
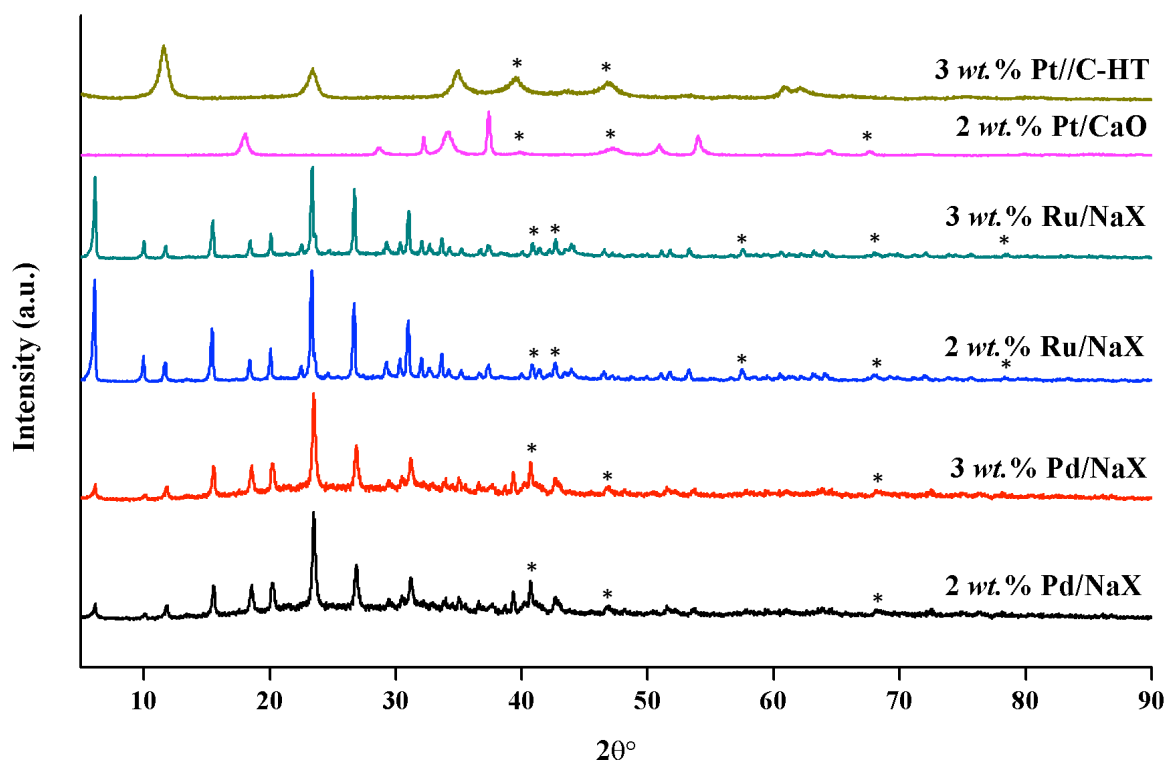
Figure 2B.16. XRD patterns for different catalysts. (* indicates the presence of metal peak).
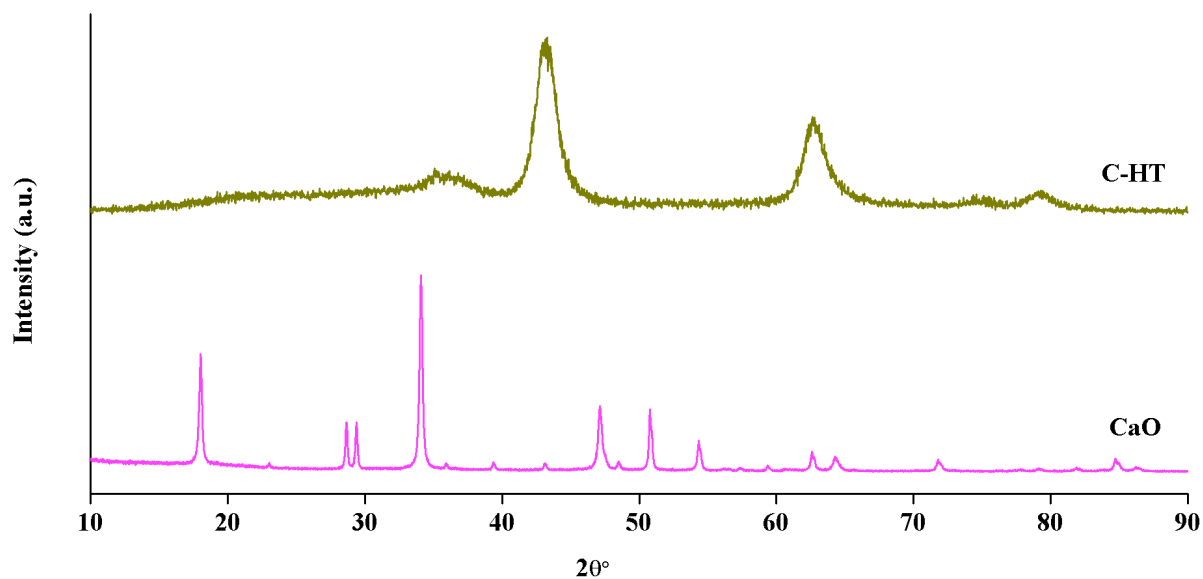
Figure 2B.17. XRD pattern of CaO and C-HT supports.

2B.5.2.2. Inductively Coupled Plasma-Optical Emission Spectroscopy (ICP-OES) Analysis

Since the supported metal catalysts were prepared by impregnation method. So, in order to check the theoretical and actual metal loading on supports, ICP-OES

analysis was performed by taken 0.05 g weight of sample (Table 2B.6). The detailed procedure for the sample preparation is mentioned in section 2B.5.1.2. It was confirmed from ICP-OES analysis that loading of Pt, Pd and Ru metal on NaX, CaO and C-HT was found to be almost similar as theoretical loading. Results are summarized in Table 2B.6.

Table 2B.6. ICP-OES analysis of supported metal catalysts.

Catalyst	Theoretical loading (*wt.%*)	Actual loading (*wt.%*)
Pt/NaX	1.0	0.9
Pt/NaX	2.0	1.8
Pt/NaX	3.0	3.0
Pd/NaX	2.0	1.8
Pd/NaX	3.0	2.9
Ru/NaX	2.0	1.9
Ru/NaX	3.0	2.8
Pt/CaO	2.0	2.0
Pt/C-HT	3.0	2.8

2B.5.2.3. N$_2$ Sorption Analysis

BET surface area of supported metal catalysts and supports was determined using N2 sorption analysis. For the better dispersion of metal nanoparticles higher surface area of the support is preferable. It was observed that after metal loading, the surface area of support was found to be decreased as the surface is covered by the metal particles. The obtained results are summarized in Table 2B.7.

Table 2B.7. Summary on N_2 sorption analysis of supported metal catalysts.

Catalyst	N₂ sorption		
	BET Surface area (m²/g)	Pore volume (cm³/g)	Average Pore size (nm)
NaX	586	0.32	1.10
CaO	12	0.05	8.2
C-HT	207	0.95	9.2
1 *wt.%* Pt/NaX	528	0.09	1.35
2 *wt.%* Pt/NaX	521	0.30	1.17
3 *wt.%* Pt/NaX	515	0.29	1.03
2 *wt.%* Pd/NaX	413	0.11	2.04
3 *wt.%* Pd/NaX	405	0.20	2.0
2 *wt.%* Ru/NaX	423	0.24	1.15
3 *wt.%* Ru/NaX	410	0.20	1.09
2 *wt.%* Pt/CaO	15.4	0.02	2.59
3 *wt.%* Pt/C-HT	168	0.2	2.39

2B.5.2.4. Temperature Programmed Desorption of CO₂ (CO₂-TPD) Analysis

CO_2-TPD technique was used for the determination of basicity of the synthesized catalysts. Basicity of NaX was found to be 0.42 mmol/g, while after loading of 1, 2 and 3 *wt.%* of Pt slight decrease in the basicity and peak shift towards the lower temperature was observed. As moved from 1 to 3 *wt.%* of Pt loading basicity decreases due to the less availability of basic sites. Similar phenomenon for the drop-in basicity and peak shifting was observed with 2 *wt.%* Pd/NaX and 2 *wt.%* Ru/NaX from 0.42 mmol/g to 0.29 and 0.30 mmol/g, respectively. Likewise, 3 *wt.%* Pd/NaX and 3 *wt.%* Ru/NaX shows 0.27 and 0.28 mmol/g of basicity. Bare support CaO shows the basicity of 1.96 mmol/g, while with 2 *wt.%* Pt/CaO it decreases to 1.78 mmol/g. It might be possible due to the low surface area to CaO. CO₂-TPD profiles depict that after impregnation of Pt over C-HT, basicity has decreased. Basicity of

calcined hydrotalcite (C-HT) was found to be 0.40 mmol/g, while after impregnation of Pt it decreases to 0.31 mmol/g. Again, this indicates that stronger basic sites are killed after impregnation of metal. Another possible reason could be that because of the interaction between the electron rich surface negative charge present on the zeolite is with the electron deficient metal. Due to the strong interaction between metal and support, basic sites will not be easily available to interact with the CO_2, results decrease in the basicity. Moreover, in the presence of metal CO_2 will not adsorb strongly on the catalyst surface and it starts desorbing at lower temperature compare to bare supports, as observed from the CO_2-TPD profile also. CO_2-TPD data for the various catalysts and supports are summarized in Figure 2B.18 and Table 2B.8.
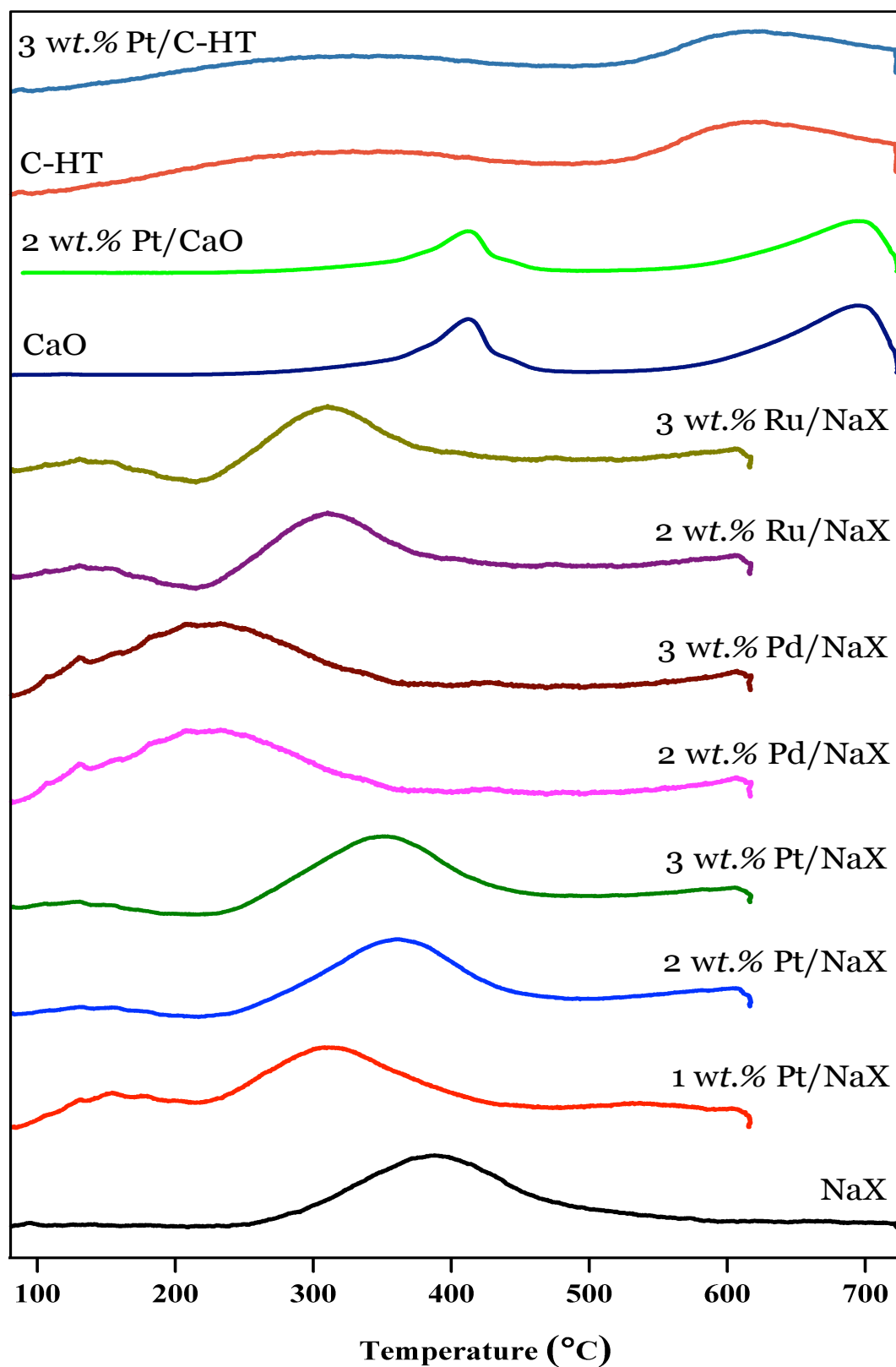
Figure 2B.18. CO_2-TPD profile of various solid base catalysts

Table 2B.8. Basicity of various supported metal catalysts.

Catalyst	Basicity (mmol/g)			Peak maxima (ºC)
	Weak (w) (150-300 ºC)	Medium (m) (300-450 ºC)	Strong (s) 450-700 ºC	
NaX	-	0.42	-	404 (m)
CaO	-	0.49	1.47	408 (m) & 673 (s)
C-HT	0.17	-	0.23	294 (w) & 603 (s)
1 *wt.%* Pt/NaX	-	0.38	-	312 (m)
2 *wt.%* Pt/NaX	-	0.38	-	368 (m)
3 *wt.%* Pt/NaX	-	0.33	-	354 (m)
2 *wt.%* Pd/NaX	-	0.29	-	233 (w)
3 *wt.%* Pd/NaX	-	0.27	-	237 (w)
2 *wt.%* Ru/NaX	-	0.30	-	312 (m)
3 *wt.%* Ru/NaX	-	0.28	-	312 (m)
2 *wt.%* Pt/CaO	-	0.41	1.37	407 (m) & 671 (s)
3 *wt.%* Pt/C-HT	0.12	-	0.19	290 (w) & 593 (s)

Note: w: weak, m: medium and s: strong basic sites.

2B.5.2.5. Transmission Electron Microscopy (TEM) Analysis

TEM analysis was employed to determine the average particle size, morphology and the dispersion of metal nanoparticles on the supports. TEM images of supported metal catalysts were obtained using FEI TECNAI T20 model instrument working at an accelerating voltage of 200 kV. Samples were dispersed in iso-propyl alcohol

(IPA) by sonication and a drop of the solution was deposited on carbon coated copper grid. TEM images of all the supported metal catalysts are shown in Figure 2B.19 to Figure 2B.21. Average particle size and percentage of dispersion of metal nanoparticles was calculated using this technique. Results are summarized in Table 2B.9.

Table 2B.9. Summary on average particle size and dispersion of supported metal catalysts determined by TEM analysis.

Catalyst	Average particle size (nm)	Dispersion (%)
1 *wt.%* Pt/NaX	4.0	28
2 *wt.%* Pt/NaX	8.0	14
3 *wt.%* Pt/NaX	3.5	32
2 *wt.%* Pd/NaX	10	11
3 *wt.%* Pd/NaX	40	3
2 *wt.%* Ru/NaX	35	4
3 *wt.%* Ru/NaX	40	3
2 *wt.%* Pt/CaO	10	11
3 *wt.%* Pt/C-HT	7.0	16

1 *wt.*% Pt/NaX
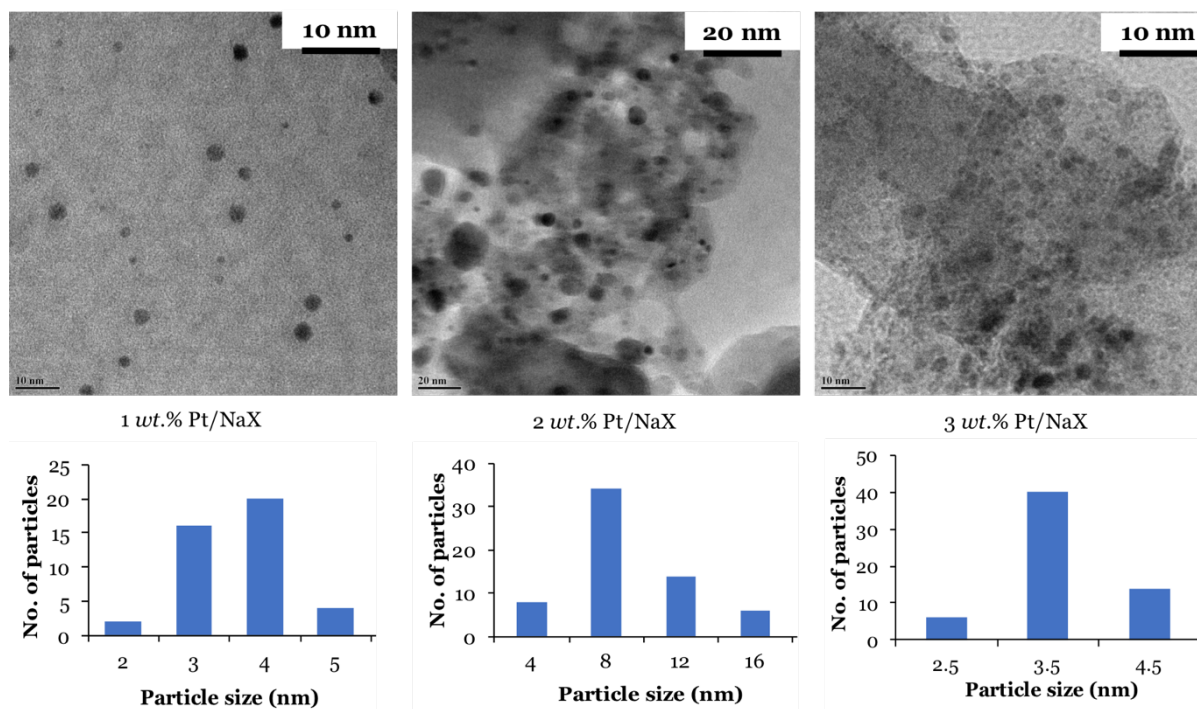
2 *wt.*% Pt/NaX

3 *wt.*% Pt/NaX

Figure 2B.19. TEM images of 1, 2 and 3 *wt.*% Pt/NaX

2 *wt.*% Pd/NaX
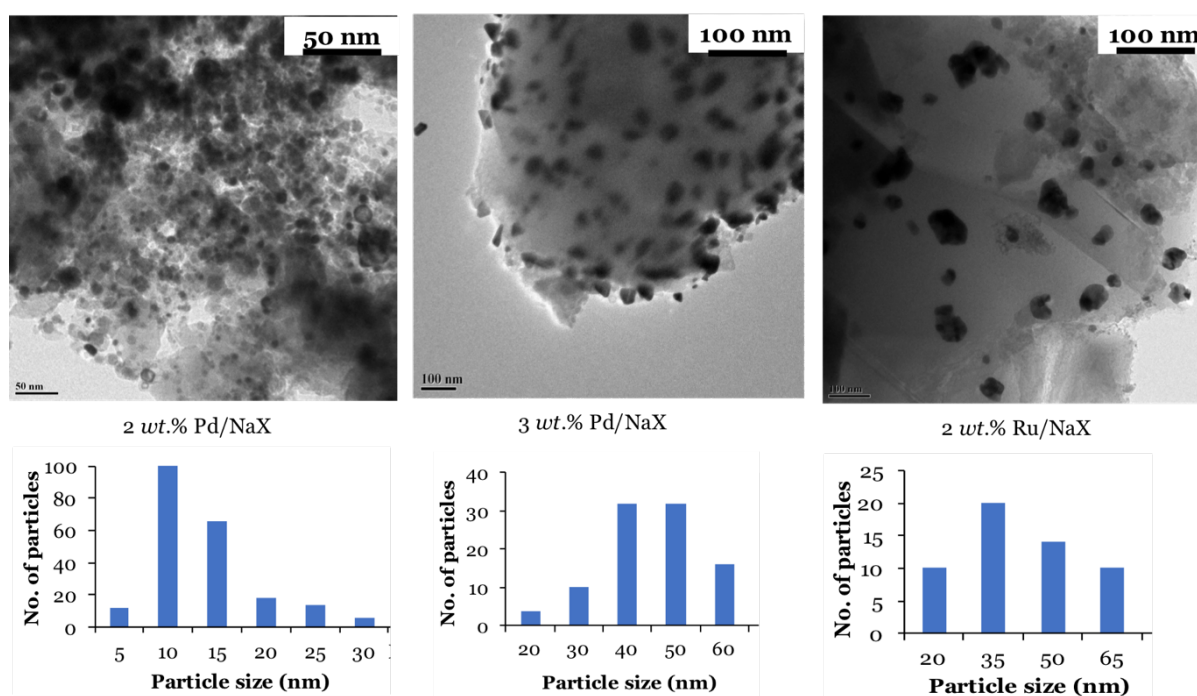
3 *wt.*% Pd/NaX

2 *wt.*% Ru/NaX

Figure 2B.20. TEM images of 2, 3 *wt.*% Pd/NaX and 2 *wt.*% Ru/NaX
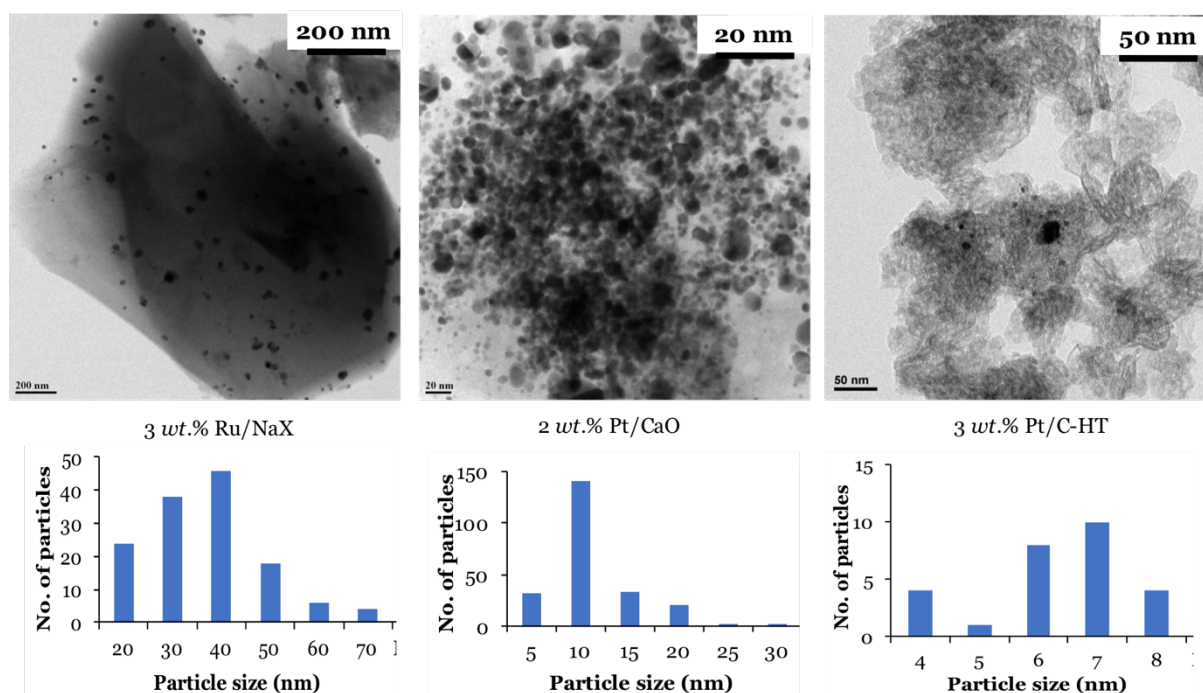
Figure 2B.21. TEM images of 3 *wt.%* Ru/NaX, 2 *wt.%* Pt/CaO and 3 *wt.%* Pt/C-HT catalysts

From TEM analysis the average particle size was calculated and mentioned in Table 2B.9 and Figure 2B.19 to Figure 2B.21. From the TEM images, it was observed that the particle size of metal varies 1) different metal loading, 2) same metal with different support, 3) same support with different metal. The average particle size for Pt in 1, 2 and 3 *wt.%* Pt/NaX catalyst was calculated to 4 nm, 8 nm and 3.5 nm, respectively. Contradictory, in the case of 3 *wt.%* Pt supported on NaX catalyst shows the decrease in the particle size while increasing the metal loading. Furthermore, for 2 *wt.%* Pd/NaX the average particle size was observed 10 nm while increase in the Pd loading to 3 *wt.%* bigger particle size (40 nm) was observed. The percent dispersion for 2 and 3 *wt.%* Pd/NaX was calculated and the lower dispersion for 3 *wt.%* Pd/NaX (3%) was observed. Similar phenomenon was observed from XRD analysis (Figure 2B.14) decrease in the peak intensity was found while increasing the metal loading. The same trend was observed for 2 and 3 *wt.%* Ru/NaX with the particle size of 35 nm and 40 nm, respectively. Moreover, when Pt was impregnated on CaO (2 *wt.%* Pt/CaO) and C-HT (3 *wt.%* Pt/C-HT), particle size of 10 nm and 7 nm was observed, respectively. It is known in the literature that catalytic activity of catalysts depends on the dispersion of metal. So, by looking to the TEM images, it is expected that the

Pt catalyst supported on NaX (14-32% dispersion) and 3 *wt.%* Pt/C-HT (16% dispersion) will give higher activity for the reaction.

2B.6. Conclusions

Various catalysts were studied for the depolymerization of lignin in to aromatic monomers or low molecular weight products. Since lignin depolymerization is well known with homogeneous base catalysts (NaOH, CsOH, etc), so, in order to replace these homogeneous catalysts, various heterogeneous base catalysts from weak (NaY, NaP) to moderate (NaX, C-HT, etc.) and strong (CaO, MgO) were studied. Thoroughly characterization of all the catalysts was done using various techniques. ICP-OES analysis was performed to determine the Si/Al ratio of zeolites and it was found to be similar to the ratio given by the supplier. XRD analysis confirms the crystalline nature of zeolites and metal oxides which C-HT shows the amorphous peak pattern. From the CO_2-TPD, types of basic sites were studied and concluded that NaX is having moderate basic sites while all other catalysts show the presence of either weak basic sites (NaY, KLTL) or the combination of weak-strong (C-HT, HAP) and medium-strong (CaO) or strong basic sites (MgO). N_2 sorption analysis show the highest surface area for NaX zeolite and confirms the microporous nature of all the zeolites. Moreover, pH of the solid base catalysts was checked in water and reaction mixture in order to choose the appropriate reaction system.

In order to study the upgradation of lignin derived products via hydrogenation reactions, various metal and support combinations were studied. To explore the effects of supports and metal; different types of support materials (NaX, CaO, C-HT) and metals (Pt, Pd and Ru) are used. All the supported metal catalysts were synthesized by wet-impregnation method. The detailed characterizations of all the synthesized catalysts were done using various characterization techniques. XRD patterns of synthesized catalysts showed the characteristic peaks of the metals (Pt, Pd and Ru). Variation in the peak intensities was seen from support to support according to the dispersion of metals. ICP-OES analysis proved that the metal loading in all supported metal catalysts is almost similar to the theoretical metal loading. N_2 sorption analysis shown the decrease in the surface area after metal impregnation, which is obvious. From CO_2-TPD analysis, presence of basic sites was studied and slight decrease in the basicity for the supported metal catalysts

compared to bare supports was observed. This could be attributed to the surface covered by the metal particles. From the TEM analysis it was observed that the metal loaded on the NaX support having high surface area (586 m²/g) shows the high percentage of dispersion (28, 14 and 32% for 1, 2 and 3 *wt.%* Pt/NaX). After the complete characterization of catalysts, those are subjected for the lignin depolymerization reactions (please refer Chapter 3 and Chapter 4).

2B.7. References

1.   L. Krumenacker and S. Ratton., *L'Actualité chimique*, 1986, 6, 29-44.

2.   Hölderich, *W. F. Studies in Surface Science and Catalysis*, 1993, 127-163.

3.   J. M. Thomas, Robert Raja, Gopinathan Sankar, Brian FG Johnson and D. W. Lewis., *Chemistry-A European Journal* 2001, 7, 2972-2978.

4.   K. Tanabe and W. F. Hölderich., *Applied Catalysis A: General*, 1999, 181, 399-434.

5.   A. Corma, V. Fornes, R. M. Martin-Aranda, H. Garcia and J. Primo., *Applied Catalysis A: General*, 1990, 1, 237-248.

6.   D. Barthomeuf, G. Coudurier, and J. C. Vedrine., *Materials chemistry and physics* 1988, 18, 553-575.

7.   A. Corma, and R. M. Martin-Aranda., *Applied Catalysis A: General*, 1993, 105, 271-279.

8.   J. C. Kim, Hong-Xin Li, Cong-Yan Chen, and M. E. Davis., *Microporous Materials*, 1994, 2, 413-423.

9.   K. R. Kloetstra, and H. Van Bekkum., *Studies in Surface Science and Catalysis*, 1997, 105, 431-438.

10.   L. R. Martens, Piet J. Grobet, and Peter A. Jacobs., *Nature 315*, 1985, 568-570.

11.   G. Suzukamo, M. Fukao, T. Hibi and K. Tanaka., *In Proc. Int. Symp*, 1989, 405.

12.   V. Vishwanathan, Steven Ndou, Lucky Sikhwivhilu, Neville Plint, K. Vijaya Raghavan and N. J. Coville., *Chemical Communications* 2001, 10, 893-894.

13.   H. Moison, Françoise Texier-Boullet and A. Foucaud., *Tetrahedron 43,,* 1987, 3, 537-542.

14. A. S. Ndou, N. Plint and N. J. Coville., *Applied Catalysis A: General* 2003, 251, 337-345.

15. A. S. Ndou and N. J. Coville, *Applied Catalysis A: General* 2004, 275, 103-110.

16. A. Aguilera, A. R. Alcantara, J. M. Marinas and J. V. Sinisterra., *Canadian journal of chemistry* 1987, 65, 1165-1171.

17. A. Corma, V. Fornes, R. M. Martin-Aranda and F. Rey, *Journal of Catalysis*, 1992, 134, 58-65.

18. A. Guida, Mohammed Hassane Lhouty, Didier Tichit, Francois Figueras and P. Geneste., *Applied Catalysis A: General* 1997, 164, 251-264.

19. A. Corma, S. Iborra, S. Miquel and J. Primo., *Journal of catalysis* 1988, 173, 315-321.

20. P. Grange, Philippe Bastians, Roland Conanec, Roger Marchand and Y. Laurent., *Applied Catalysis A: General*, 1994, 114, 191-196.

21. M. J. Climent, A. Corma, V. Fornes, A. R. G. L. Frau, R. Guil-Lopez, S. Iborra and J. Primo., *Journal of Catalysis* 1996, 163, 392-398.

22. B. F. Sels, Dirk E. De Vos and P. A. Jacobs., *Catalysis Reviews*, 2001, 43, 443-488.

23. V. M. Roberts, V. Stein, T. Reiner, A. Lemonidou, X. Li and J. A. Lercher, *Chemistry*, 2011, 17, 5939-5948.

24. B. Jha, and D. N. Singh., *Journal of Materials Education*, 2011, 33, 65.

25. G. Gottardi, *Pure and Applied Chemistry*, 1986, 58, 1343-1349.

26. D. Barthomeuf, *The Journal of Physical Chemistry*, 1984, 88, 42-45.

27. A. Corma, R. M. Martin-Aranda, and F. Sanchez., *Journal of Catalysis* 1990, 126, 192-198.

28. G. Centi, and Siglinda Perathoner., *Microporous and mesoporous materials*, 2008, 1, 3-15.

29. A. Vaccari, *Catalysis Today* 1998, 1, 53-71.

30. D. Tichit and B. Coq., *Cattech*, 2003, 7, 206-217.

31. James H Clark and C. N. Rhodes, *Royal Society of Chemistry*, 2007, 49-53.

32. Y. Ono, and Hideshi Hattori., *Springer Science & Business Media,*, 2012, 101, 157-169.

33. J. C. A. A. Roelofs, D. J. Lensveld, A. J. Van Dillen and K. P. D. Jong., *Journal of Catalysis*, 2001, 1, 184-191.

34.   Y. Liu, Edgar Lotero, James G. Goodwin and X. Mo., *Applied Catalysis A: General* 2007, 138-148.

35.   Y. Liu, Edgar Lotero, James G. Goodwin and X. Mo., *Applied Catalysis A: General*, 2007, 138-148.

36.   F. Li, Xiaorui Jiang, David G. Evans and X. Duan., *Journal of Porous Materials*, 2005, 1, 55-63.

37.   W. M. Antunes, Cláudia de Oliveira Veloso and C. A. Henriques., *Catalysis Today*, 2008, 548-554.

38.   L.L. Hench, *J. Am. Ceram. Soc*, 1998, 1705-1728.

39.   J.L. Ong and D. C. Chan, *Crit. Rev. Biomed. Eng.* , 2000, 667-707.

40.   T. Tamm and M. Peld, *J. Solid State Chem.*, 2006, 1581-1587.

41.   K. Kawabata and T. Yamamoto, *J. Ceram. Soc. Jpn.* , 2010, 548-549.

42.   T.J. White and D. ZhiLi, *Acta Crystallogr. B*, 2003, 1-16.

43.   R. Murugan and S. Ramakrishna, *Acta Biomater.*, 2006, 201-2016.

44.   D.M. Ibrahim, A.A. Mostafa and S. I. Korowash, *Chem. Cent. J.*, 2011, 74.

45.   A. Yasukawa, T. Yokoyama, K. Kandori and T. Ishikawa, *Colloids Surf. A* 2007, 203-208.

46.   D. Laurencin, N. Almora Barrios, N.H. de Leeuw, C. Gervais, C. Bonhomme, F. Mauri, W. Chrzanowski, J.C. Knowles, R.J. Newport, A. Wong, Z.H. Gan and M.E. Smith, *Biomaterials* 2011, 1826-1837.

47.   K.A. Bhadang, C.A. Holding, H. Thissen, K.M. McLean, D.R. Haynes, J.S. Forsythe and Acta, *Biomater.*, 2010, 1575-1583.

48.   B. Busse, B. Jobke, M. Hahn, M. Priemel, M. Niecke, S. Seitz, J. Zustin, J. Semler, M. Amling and Acta, *Biomater.* , 2010, 4513-4521.

49.   H. Hattori, *Chem. Rev.*, 1995, 537-558.

50.   H. Kabashima, H. Tsuji and H. Hattori, *Appl. Catal. A* 1997, 319-325.

51.   M.A. Aramendia, V. Borau, C. Jiménez, J.M. Marinas, J.R. Ruiz and F. J. Urbano, *Appl. Catal. A* 2003, 207-215.

52.   Y. Wang, J.H. Zhu, J.M. Cao, Y. Chun and Q. H. Xu, *Micropor. Mesopor. Mater*, 1998, 175-184.

53.   D.E. Jiang, G.C. Pan, B.Y. Zhao, G.P. Ran, Y.C. Xie and E. Z. Min, *Appl. Catal. A*, 2001, 169-176.

54. Y. Sakurai, T. Suzaki, K. Nakagawa, N. Ikenaga, H. Aota and T. Suzuki, *J. Catal.*, 2002, 16-24.

55. S. Freni, S. Cavallaro, N. Mondello, L. Spadaio and F. Frusteri, *Catal. Commun.*, 2003, 287-293.

56. H. Hattori, *Stud. Surf. Sci. Catal.*, 1993, 35.

57. K. Tanabe, J. Fraissard and L. Petrakis, *Nato asi. ser.*, 1995, C444, 403.

58. O. Deutschmann, Helmut Knozinger, Karl Kochloefl and T. Turek, *Ullmann's Encyclopedia of Industrial Chemistry*, 2009.

59. J. M. Campelo, Diego Luna, Rafael Luque, José M. Marinas and A. A. Romero, *ChemSusChem*, 2009, 1, 18-45.

60. R. A. Sheldon and Herman Van Bekkum, *John Wiley & Sons*, 2008.

61. G. Ertl, H. Kn¨ozinger and J. Weitkamp, *Handbook of Heterogeneous Catalysis*, Wiley-VCH, Weinheim, 2nd edn., 2007.

62. J. W. Geus, J. R. van Veen, J. A. Moulijn, P.W. N. M. van Leeuwen and R. A. v. Santen, *An Integrated Approach to Homogeneous, Heterogeneous and Industrial Catalysis*, Elsevier, Amsterdam, 1999.

63. X. Li, Guanyi Chen, Caixia Liu, Wenchao Ma, Beibei Yan and J. Zhang, *Renewable and Sustainable Energy Reviews*, 2016, 71, 296-308.

64. A. K. Deepa, and Paresh L. Dhepe *ChemPlusChem* 2014, 11, 1573-1583.

65. H. Lee, Hannah Kim, Mi Jin Yu, Chang Hyun Ko, Jong-Ki Jeon, Jungho Jae, Sung Hoon Park, Sang-Chul Jung and Y.-K. Park., *Scientific reports*, 2016, 6, 28765.

66. H. Kobayashi, Hidetoshi Ohta, and Atsushi Fukuoka, *Catalytic Hydrogenation for Biomass Valorization,* 2014, 13, 52.

67. Z. Si, Xinghua Zhang, Chenguang Wang, Longlong Ma and R. Dong, *Catalysts 7*, 2017, 6.

68. A. Tathod, Tanushree Kane, E. S. Sanil, and Paresh L. Dhepe, *Journal of Molecular Catalysis A: Chemical*, 2014, 388, 90-99.

69. http://www.iza-online.org/synthesis/Recipes/XRD/Linde Type X.jpg).

70. http://www.iza-online.org/synthesis/Recipes/XRD/Linde Type Y.jpg).

71. H. Hattori, *Chemical Reviews*, 1995, 3, 537-558.

Chapter 3
Depolymerization of Lignin using various Solid Base Catalysts

3.1. Introduction

Lignocellulosic material (wood, forest residues, and agricultural residues) has a huge potential to be used as a starting material in place of fossil feedstock for the synthesis of chemicals. This profusely available renewable material is made up of three components namely, cellulose,[1] hemicellulose[2] and lignin. Although under biorefinery concept, cellulose and hemicelluloses have been thoroughly studied for their conversions into bulk and fine chemicals[3-6] but lignin has drawn less attention on this aspect. It is estimated that in the biosphere ca. 3×10^{11} tons of lignin is available and additionally ca. 2×10^{10} tons is generated annually thus making it one of the largest naturally available polymer.[7] Lignin is obtained as a major by-product during bio-ethanol production and is also isolated as black liquor in paper and pulp industries. It is a complex 3-D amorphous polymer present in plant (10-25%) comprising of three basic phenylpropanol alcohol precursors namely, coumaryl alcohol, coniferyl alcohol and sinapyl alcohol, which are collectively called as monolignols. In lignin, numerous aromatic units are linked via ≡C-O-C≡ (60-70%) and ≡C-C≡ bonds.[8] While out of various types of ≡C-O-C≡ linkages present in lignin, the β-O-4 linkage is the most abundant linkage as it comprises around 45-60% of all the linkages found in lignin, other linkages such as, dihydrobenzofuran, β-β, β-5 and 4-O-5 are present in minor quantities.[9, 10] Contrary to well established structures of cellulose and hemicelluloses, lignin does not have a definite structure (Figure 3.1) since it varies depending on local weather, humidity, temperature, plant species, age of plant etc. Nevertheless, as discussed, several building blocks of lignin are randomly distributed and coupled via numerous linkages to produce worlds only naturally occurring aromatic polymer.
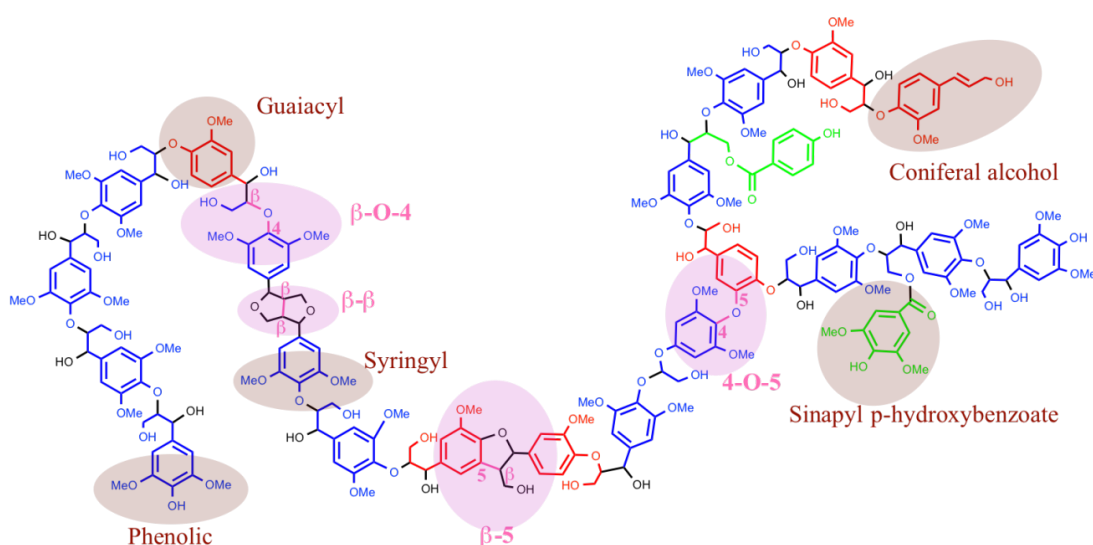
Figure 3.1. Schematic representation of lignin.

Conventionally lignin is employed for the generation of heat and power (cogeneration) but, it is argued in many forums that until valuable chemicals are synthesized from lignin through bio-refinery concept, cellulose to ethanol process will not become economical.[11]

Since, the polyphenolic aromatic structure of lignin is ideally suitable to obtain value added low molecular weight aromatic compounds, which can be used as building blocks or platform chemicals for the subsequent synthesis of several chemicals; in recent times efforts are diverted on the development of catalytic methods for the depolymerization of lignin. Several literature reports suggests that depolymerization of lignin is possible using solid acids (215-275 °C, 30-120 min., alcohol: water as solvent),[12-14] homogeneous acids (100-450 °C, 60-120 min., alcohol: water as solvent), [15, 16] ionic liquids (110-250 °C, 30-120 min., alcohol: water as solvent),[17, 18] supported metal catalysts (150-350 °C, 60-360 min., alcohol: water, tetralin, decalin, etc. as solvent),[19-22] supercritical fluids (250-400 °C, 2-60 min., CO_2, water as solvent)[23, 24] etc. to yield low molecular weight aromatic products. However, most of these methods are associated with quite a few drawbacks such as use of model compounds instead of lignin and also operation at either higher temperatures (≥ 250 °C) or pressures (> 3 MPa) or both.

Considering the drawbacks associated with these reports (either use of low molecular weight lignins or use of model compounds and low yields of desired products), it is indispensable to develop a solid base catalyzed methodology for the efficient depolymerization of actual high molecular weight lignin into low molecular weight aromatic products under milder reaction conditions (T ≤ 250 °C) in a one-pot process. For this purpose, diverse solid base catalysts were evaluated for their depolymerization activities at low temperature (≤ 250 °C) & atmospheric pressure with lignin having molecular weight of ca. 60,000 Da.[25] To carry out the depolymerization study, several types of solid base catalysts could be used for e.g. alkali metal exchanged zeolites, clays, alkali and alkaline earth metal oxides and rare earth metal oxides etc.[2, 26, 27] Particularly, zeolites with lower Si/Al ratio were used in this work because they tend to be more stable under alkaline conditions.

3.2. Experimental Section

3.2.1. Chemicals & Materials

Alkaline lignin and dealkaline lignin used in this study were obtained from TCI chemicals, India.[28] Alkali lignin, lignosulfonate sodium salt lignin and lignosulfonate calcium salt lignin were purchased from Sigma Aldrich. All the obtained lignins were used without any pre-treatment. Basic zeolites, NaX (Si/Al = 1.2) and KLTL (Si/Al = 2.7) was synthesized in the lab by hydrothermal method. NaY (Si/Al = 3.6) and NaP (Si/Al = 1.69) zeolite was procured from Zeolyst International, USA.[29] Metal oxides such as calcium oxide (99.99%) and magnesium oxide (98%) were purchased from Sigma Aldrich. Hydrotalcite (Mg/Al = 3) and hydroxyapatite (Ca/P = 1.66) were purchased from Sigma Aldrich. Various aromatic monomers (Guaiacol, 2-methoxy-4-methylphenol, Pyrocatechol, Resorcinol, 2,6-dimethoxyphenol, 4-hydroxy benzyl alcohol, Homovanillic acid, Hexadecane, Diethylterephthalate, 2,4-ditert-butylphenol, Acetoguaiacone, 4-hydroxy-3-methoxybenzyl alcohol, 1,2,4-trimethoxy-benzene, Vanillin, Eugenol, 3,4-dimethoxyphenol) used for GC calibration were purchased from Sigma Aldrich, Alfa Aesar and TCI chemicals. All the chemicals were used as received. Prior to the catalytic runs all the catalysts were oven dried at 55 °C for 16 h followed by vacuum drying at 150 °C for 2 h (10^{-4} MPa). At last activated at 150 °C for 2 under high vacuum.

Solvents like methanol (MeOH, 99.9%, LOBA Chemie, India), ethanol (EtOH, 99%, Changshu Yangyuan Chemical Co., Ltd, China), diethyl ether (DEE, 99.9%, LOBA Chemie, India), ethyl acetate (EtOAc, 99.9%, LOBA Chemie, India), tetrahydrofuran (THF, 99.8%, LOBA Chemie, India), chloroform (99.8%, LOBA Chemie, India), hexane (99%, LOBA Chemie, India), dichloro methane (99.8%, LOBA Chemie, India), acetone (99%, LOBA Chemie, India) and toluene (99%, LOBA Chemie, India) were purchased and used as received. Sodium hydroxide (NaOH, 98%, Loba Chemie, India), Sodium carbonate (Na_2CO_3, 99.5%, Loba Chemie, India), Hydrochloric acid (HCl, 37%, Merck, India), and Hydrofluoric acid (HF, 48%, Merck, India) were also purchased and used as received. Distilled water was used for all the experiments.

3.2.2. Solid Base Catalyzed Depolymerization of Lignin

Lignin depolymerization reactions were conducted in a batch mode autoclave (Parr, USA). EtOH: H_2O (1:2 *v/v*, 30 mL) was used as reaction media in all the reactions. In a typical reaction, lignin:solvent (ethanol:water) mass ratio was 1:60 and the lignin:catalyst mass ratio was maintained at 1:1. For the depolymerization reaction, 0.5 g of lignin and 0.5 g of catalyst was taken followed by the addition of 30 mL solvent (EtOH:H_2O, 1:2 *v/v*). Initially, reactor was flushed with nitrogen gas at least three times and heating of reactor was started under slow stirring (100 rpm). After attaining the desired reaction temperature (250 °C) stirring was increased to 1000 rpm and this was considered as the starting time of the reaction. At 250 °C, 4.2 MPa pressure was observed. When reaction was done at higher or lower temperature (230 °C, 240 °C and 260 °C) varying final pressures (3.2, 3.7 and 5.0 MPa, respectively) were observed. After the reaction, reactor was cooled to room temperature under air and water flow. Catalyst was separated from reaction mixture by centrifugation and washed thoroughly with EtOH: H_2O in order to remove any adsorbed lignin or products on the catalyst.

3.2.3. Extraction of Products

After separation of solid (catalyst and any other degradation products insoluble in solvent) from solvent (ethanol: water), acidification of the liquid layer was done with 2N HCl solution until pH was reached 1~2. This treatment helped precipitate out high molecular weight products (filter cake). After separation of precipitate from liquid by centrifugation and filtration, following workup procedure was applied (Figure 3.2). The liquid fraction was subjected to a liquid-liquid extraction process subsequently with diethyl ether (DEE) and with ethyl acetate (EtOAc), since lignin is not soluble in these solvents (Chapter 2A, Table 2A.6). The solid (filter cake) was also subjected to DEE and EtOAc treatments consequently for extraction of any products in these solvents. The soluble fraction was filtrated and the undissolved solid (residual lignin or oligomers) was oven-dried at 55 °C. The organic solutions obtained after treating liquid and solid were vacuum evaporated to obtain the oily products. The percentage of organic solvent soluble products was calculated based on the

solid recovered after evaporating the respective solvents. The detailed methodology for the separation of products is presented in Figure 3.2.
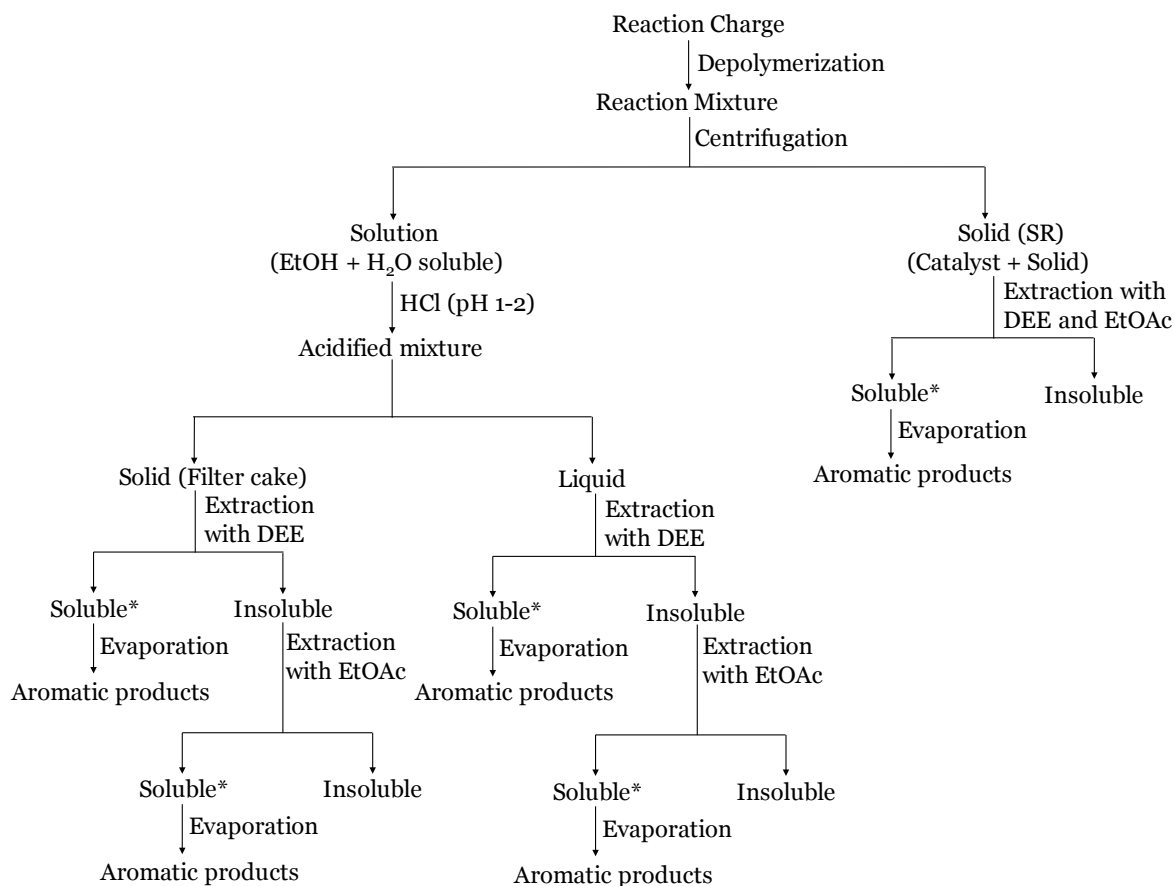
Figure 3.2. Methodology for the separation of products (*Analyzed using GC, GC-MS and HPLC).

3.2.4. Analysis of Products

The organic solvent soluble products were analyzed by gas chromatograph (GC), GC-mass spectroscopy (GC-MS), high performance liquid chromatography (HPLC), liquid chromatography-mass spectroscopy (LC-MS), Nuclear Magnetic Resonance (NMR, ^{1}H and ^{13}C), elemental analysis (CHNS), Matrix Assisted Laser Desorption Ionization Time of Flight (MALDI-TOF) and Inductively Coupled Plasma Optical Emission Spectroscopy (ICP-OES) and Fourier Transform Infrared Spectroscopy (FTIR) techniques for the identification and quantification of products.

3.2.4.1. Gas Chromatography (GC-FID)

Products formed after the depolymerization of lignin were analyzed by GC using Agilent 7890B model GC, with flame ionization detector (FID). It was equipped with HP-5 capillary column (5 % phenyl 95 % dimethyl polysiloxane) (30 m length, 0.25

mm diameter). N_2 (30 mL/min) is used as a carrier gas, H_2 (25 mL/min) is used for flame and air as oxidizer (300 mL/min). Carrier gas flow was 0.6 mL/min.

Injector temp: 275 °C, Detector temp: 280 °C

The Column oven program used was:

Temperature (°C)	Hold time (min.)	Ramping rate (°C/min.)	Total time (min.)
100	4	-	4
275	20	10	42

To confirm the products formed, GC-MS study was also done by using the same program.

3.2.4.2. Gas Chromatography-Mass Spectrometry (GC-MS)

The Varian 3800 GC-MS, (Saturn 2000MS) with the VF-5 capillary column (5% phenyl 95% dimethyl polysiloxane) (30 m x 0.25 mm) and Agilent GC-MS (7890B GC and 5977A MSD) equipped with DB-5MS column (30 m x 0.25 mm) was used to determine the molecular weight of the products identified using GCMS. Helium (0.6 mL/min) is used as a carrier gas; the column oven program used is same as that for GC analysis. From the mass spectrum obtained, m/z value of the compounds and then corresponding M.W is obtained. The GC-MS peaks are matched with the mass spectra in NIST library for compound identification.

3.2.4.3. High Performance Liquid Chromatography (HPLC)

Reaction mixture was analysed using Agilent make High Performance Liquid Chromatograph (HPLC) system equipped with autosampler, C18 column (Length: 250 mm, Internal diameter: 4.6 mm, 40 °C) and refractive index (RI) detector (40 °C). CH_3OH: H_2O (1: 1 *v/v*) was used as a mobile phase with a flow rate of 1 mL/min. The identification of compounds in the reaction mixture was done by injecting standards.

3.2.4.4. Liquid chromatography-Mass Spectrometry (LC-MS)

Reaction mixture was analysed using Thermo Scientific system (Model no. Q Extractive), C18 column (Length: 150 mm, Internal diameter: 4.6 mm) and mass detector (Orbitrap analyzer). Reverse phase system was used with CH_3OH: H_2O

(9: 1 *v/v*) as mobile phase and pumped at a flow rate of 0.35 mL/min. Oven temperature was set at 30 °C and an electron source ionization ion source was used for the analysis.

3.2.4.5. Nuclear Magnetic Resonance (NMR)

^{1}H and ^{13}C NMR spectra of lignin (alkaline, dealkaline, alkali, lignosulfonate sodium salt and lignosulfonate calcium salt) and products were recorded at 500 and 200 MHz, respectively on Bruker Ascend- using D_2O and CD_3OD as solvent with TMS as an internal standard. No. of scans used for ^{1}H, ^{13}C NMR is 16384 and 8192, respectively.

3.2.5. Yield Calculations

In order to separate the aromatic monomers from the mixture, organic solvents diethyl ether (DEE) and ethyl acetate (EtOAc) were used. The percentage of organic solvent soluble products was calculated based on the solid recovered after evaporating the respective solvents.

To remove solvent contribution in the weight of solid, the solid obtained after evaporating the solvents was dried at 55 °C in oven for 16 h. Further the solid was kept at 60 °C under vacuum (10^{-4} MPa) for 2 h. This treatment will completely remove the solvents present in the solid. Then the resulting solid was weighed and used for the yield calculations. Moreover, to check that volatile products have not escaped during the rotary evaporation, the solvents (DEE and EtOAc) were collected in the collection flask after the rotary evaporator and were analyzed by GC-FID. Except solvents (DEE and EtOAc) none of the peak was observed in the GC-FID chromatograph for the products.

Finally, quantification of products was done by calibrating the standards using GC and GC-MS.

To remove the contribution of moisture and residue present in lignin, TGA-DTA analysis of all the lignin samples was performed at 1000 °C in air (Table 3.1), it is very clear from TGA-DTA that alkaline lignin contains 8% of moisture and 17% of unburnt residue (inorganic residue/ash). So, if 0.5 g of the alkaline lignin is taken for the reaction, then it contains 0.04 g (8%) of moisture 0.085 g (17%) is inorganic residue in it. So, the actual weight of alkaline lignin charged is only 0.375 g (0.5 g − (0.04 g+0.085 g)). Similar calculations were done for all the samples.

Subsequently, the final calculation has to be done based on the bases of this information. Similar type of calculations was done for all other lignins employed in this study.

Table 3.1. Summary on TGA-DTA analysis.

Lignin	TGA-DTA (Air)		*Wt.* loss due to moisture (g)*	*Wt.* loss due to residue (g)*$	Actual *wt.* of lignin charged (g)*
	Moisture (%)	Residue$ (%)			
Alkaline	8	17	0.04	0.085	0.375
Dealkaline	11	17	0.055	0.085	0.360
Alkali	2	3	0.010	0.015	0.475
Lignosulfonate sodium salt	8	17	0.04	0.085	0.375
Lignosulfonate calcium salt	10	11	0.05	0.055	0.395

*Calculations are done by considering 0.5 g of lignin taken

$Inorganic residue

$$\% \text{ Yield for DEE soluble products } = \frac{\text{Weight of DEE soluble products (g)}}{\text{Weight of lignin (g)}} \times 100$$

$$\% \text{ Yield for EtOAc soluble products } = \frac{\text{Weight of EtOAc soluble products (g)}}{\text{Weight of lignin (g)}} \times 100$$

Weight of alkaline lignin (g) = *Wt.* of lignin charged (g) − *Wt.* of (moisture + ash) (g)

$$= 0.5 \text{ g} - (0.04 + 0.085) \text{ g}$$

$$= 0.375 \text{ g}$$

3.2.5.1. Mass Balance Calculations

Percent mass balance is calculated by, (Initial mass - Final mass/Initial mass) x 100. Now applying this equation for lignin reaction and mass balance for the lignin depolymerization reaction can be calculated as,

$$\text{Mass Balance (\%)} = \frac{\begin{array}{c}\text{Weight of DEE and EtOAc soluble products (g) +Weight of EtOAc insoluble products (g)} \\ \text{+ Weight of solid deposited on the catalyst (g) (catalyst recovered – catalyst charged)}\end{array}}{\text{Weight of lignin charged (g)}} \times 100$$

Based on the above calculations, the mass balance can be calculated as follows: Reaction conditions: Alkaline lignin (0.5 g), Solid base catalyst (0.5 g), EtOH: H_2O (1:2 *v/v)*, 250 °C, 1 h, 1000 rpm.

Solid charged before the reaction	Solid recovered after the reaction
Alkaline lignin = 0.46 g (0.5 g - 0.04 g of moisture)	Depolymerized lignin (DEE, EtOAc Soluble products + EtOAc insoluble) = 0.42 g
Catalyst amount = 0.50 g	Solid (containing catalyst) recovered= 0.49 g
Total solid charged= (0.46 g +0.50 g) = **0.96 g (including ash)**	Total solid recovered = (0.42 g +0.49 g) = **0.91 g**

Based on the above observations, the mass balance for the charged lignin was calculated as,

Mass balance = (0.42/0.46) x 100 = **91%**

Similar calculation was done for all the reactions and a mass balance of 90±5% is observed for the lignin depolymerization reactions catalyzed by solid bases.

3.2.5.2. Substrate/Catalyst (S/C) Calculations

The average molecular weight of monomeric lignin unit was taken as 180 (based on the monomer molecular formula derived, Refer Chapter 2A, Section 2A.2, Table 2A.1). Molecular weight of 180 is considered for the molecular formula $C_{10}H_{12}O_3$.

Basic sites of NaX (Si/Al=1.2) catalyst = 0.42 mmol/g

This implies that when 0.50 g of catalyst is charged in the reactor actually, 0.21 mmol/0.50 g of basic sites are present in reaction.

Mol of alkaline lignin: From TGA-DTA analysis it was calculated that actual weight of lignin is 0.375 g out of 0.5 g lignin taken (after removing moisture + ash). So, this 0.375 g will be considered for the mol calculation.

0.375 g (alkaline lignin)/180 = 2.08 x 10^{-3} mol (2.08 mmol)

0.5 g (catalyst loading) x 0.42 = 0.21 mmol

S/C (mol basis) = 2.08 /0.21 = **9.90**

Similar calculation for all the catalysts used in the study was done and shown in Table 3.2.

Table 3.2. Lignin: Catalyst mole ratio.

Catalyst	Amount of basic sites (mmol/0.5 g)	Lignin : Catalyst (Mole ratio)
NaX	0.21	9.9:1
NaY	0.17	12.2:1
NaP	0.045	46.2:1
KLTL	0.07	29.7:1
HT	0.2	10.0:1
HAP	0.06	34.7:1
CaO	0.98	2.1:1
MgO	0.12	17.3:1

Note: Weight of alkaline lignin taken for reaction = 0.5 g, Weight of alkaline lignin taken for reaction (after correction of ash & moisture) = 0.375 g, mmol of alkaline lignin actually charged in the reactor (considering monomer molecular weight of 180 mol/g) = 2.08 mmol.

3.3. Results and Discussions

For base catalyzed depolymerization of lignin performed in ethanol: water, a variety of solid base catalysts were used and their physico-chemical properties are discussed in the Chapter 2B. The reactions were performed in a batch mode reactor and after the reaction, low molecular weight products were extracted from the reaction mixture in diethyl ether (DEE) and ethyl acetate (EtOAc) solvents.

3.3.1. Evaluation of Various Solid Base Catalysts for Lignin Depolymerization

For the exploration of an efficient catalytic system to depolymerize lignin, various types of solid base catalysts were evaluated at 250 °C for 1 h. Various solid bases were selected as they possess different basicity, pore size and surface area which will

definitely affect the depolymerization reaction (Please refer Chapter 2B, Section 2B.5.1.3 and Section 2B.5.1.4). From TGA-DTA (Chapter 2, Section 2A.3.5, Figure 2A.12) analysis it was observed that mass loss of lignin starts from 180 °C and a sharp peak between 300-350 °C is observed. Moreover, it is well known from the literature that lignin contains 60-70% of ether linkages which can be broken at milder reaction condition compared to carbon-carbon linkages. Furthermore, lignin depolymerization using solid acids is also known at 250 °C.[12, 13] Considering these factors, I have decided to do reaction at 250 °C. Additionally, all the reactions mentioned here were performed with alkaline lignin, unless specified. The catalytic reactions were done in a batch mode Parr autoclave with varying reaction parameters. After the reaction was over, reactor was cooled under air and water flow. The cooled reaction mixture was centrifuged in order to separate out the catalyst from it. The obtained reaction mixture (free of solid) was acidified with 2N HCl to pH 1-2. This treatment helped to precipitate out high molecular weight products (filter cake). After separation of precipitate from liquid by centrifugation and filtration both the fraction liquid and solid (filter cake) were subsequently extracted with first diethyl ether (DEE) and DEE insoluble fraction was further extracted with ethyl acetate (EtOAc), since all the lignins used in my work are not soluble in these solvents (Chapter 2A, Table 2A.6). The DEE and EtOAc soluble products were vacuum evaporated to obtain the oily products. The percentage of organic solvent soluble products was calculated based on the solid recovered after evaporating the respective solvents. The detailed work up procedure, analysis of reaction mixtures by various techniques like GC-FID, GC-MS, HPLC, LC-MS, NMR, FTIR and calculations of product yield are described in section 3.2.3 to 3.2.5 and Figure 3.2. As can be seen from Figure 3, zeolites (NaX, NaY, NaP, KLTL), anionic clay (Hydrotalcite (HT)), single metal oxides (MgO, CaO) and hydroxyapatite (HAP) were active for the depolymerization of lignin with varying yields (10-51%) of diethyl ether (DEE) and ethyl acetate (EtOAc) soluble low molecular weight products. Among all the catalysts, the Na exchanged X zeolite (NaX) showed the best activity of 51%. All other zeolite catalysts (NaY, NaP and KLTL) also showed better activity (30-38%) compared to the other catalysts. Under similar reaction conditions, without catalyst, 24% yield for low molecular weight products was observed, which illustrates that lignin depolymerization is a catalytic reaction. It was assumed that with HT, MgO and CaO should show high activity towards depolymerization however low yields with these catalysts (HAP, HT, MgO, CaO) was observed (10-18%). There can be three

possible reasons for this behaviour; 1) either reaction is going further with HT, MgO, HAP and CaO catalysts, 2) products formed during the reaction are adsorbing on the catalyst and 3) degradation reactions of the formed products on these catalysts. As no gas formation was observed during the reaction, confirms that most probably the reaction is not going further. Furthermore, to understand these results, the weight of the separated solid (by centrifugation before acidification, Figure 3.2) was checked and it was noticed that with these catalysts, only an increase in the weight of solid (after recovery, the solid was dried in an oven at 55 °C for 16 h) was seen compared to any other catalyst such as NaX, NaY, NaP and KLTL (Table 3.4). This corroborate the fact that products might be adsorbing on these catalysts. For this to check, the product adsorption study was performed (Please refer Section 3.3.4). Further obtained products were identified and quantified using GC and GC-MS and the details are given in Section 3.3.2.
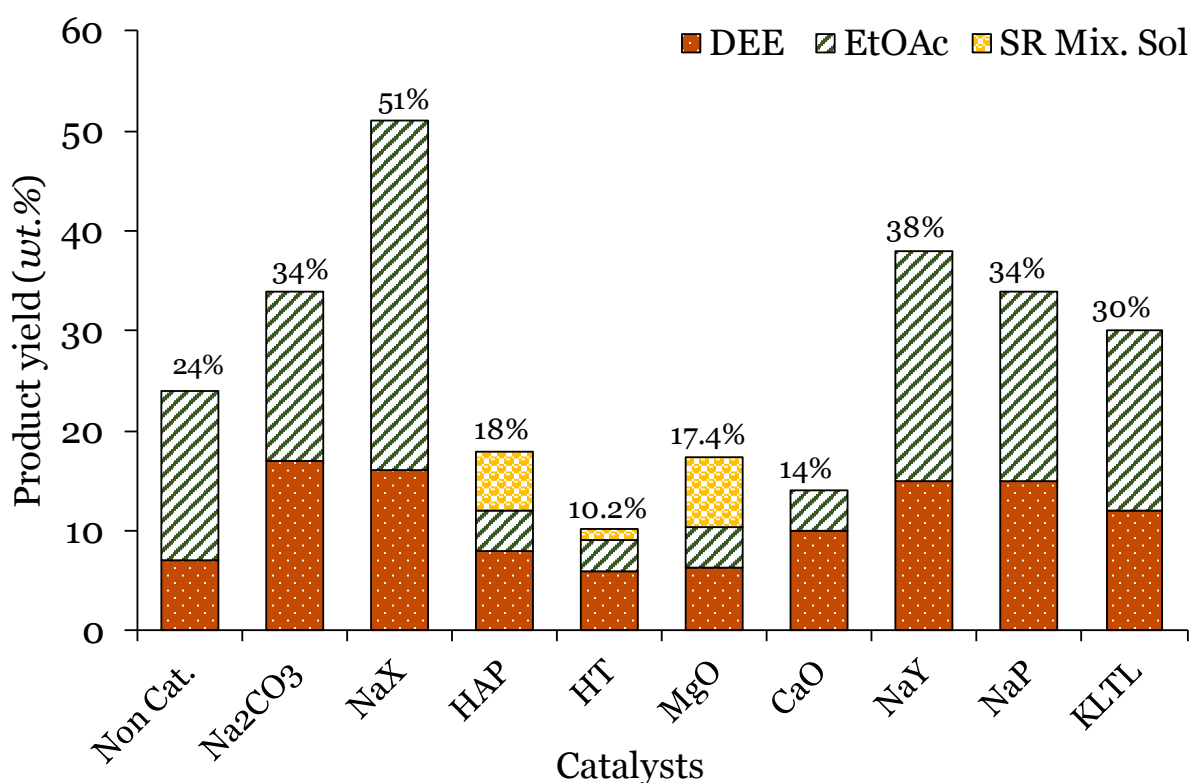
Figure 3.3 Depolymerization of lignin using solid base catalysts.

Reaction conditions: Alkaline lignin (0.5 g): Catalyst = 1: 1 $wt./wt.$, EtOH: H2O (1: 2 v/v) 30 mL, 250 °C, 1 h. DEE: diethyl ether, EtOAc: ethyl acetate, SR Mix. Sol.: products extracted from solid (catalyst + adsorbed products) using a mixture of DEE and EtOAc (1: 1 v/v) presented by yellow colour. Orange and green bar indicates the total products extracted using DEE and EtOAc (liquid + solid fraction). All the experiments were done 3 times and ±3% error in yields was observed. The results presented in this figure are the average of three runs.

To corroborate the fact that lignin depolymerization is a catalytic reaction; NaP catalyst was added to a reaction without catalyst, and a 13% increase in yield (37%) was observed. To do this first, non-catalytic reaction was done with same reaction condition used earlier, After the reaction of 1 h, reactor was cooled to room temperature and in the same reactor without removing the reaction charge, NaP (0.5 g) was added and reaction was started at the same optimized reaction condition (250 °C & 1 h). After the reaction, same work up procedure was followed as mentioned (Figure 3.2) and 13% (37% yield) increase in the product yield was observed compared to non-catalytic reaction (24% yield).

For the comparison of yields obtained with solid base catalysts, homogeneous base (Na_2CO_3) catalyzed depolymerization of lignin was carried out under similar conditions (250 °C, 1 h) (Figure 3.3). However, in literature most of the reports used NaOH and CsOH as base. But here weak base was chosen as strong base may corrode the reactor. The results reveal that with a homogeneous base, 34% yield is obtained, which was comparable with most of the solid base catalysts, yet it was lower than that obtained with the NaX catalyst (51%). Conventionally, homogeneous base catalyzed lignin depolymerization reactions are carried out with strong bases like NaOH or CsOH instead of a weak base like Na_2CO_3. But under these reaction conditions, when the effect of pH on the depolymerization was studied (Section 3.3.5), it is established that a pH of 9 is the optimum to achieve the best catalytic results and with a weak base like Na_2CO_3 employed in this work, a pH of 9.2 under the reaction conditions could be maintained.

3.3.2. Identification of Depolymerized Products

The formation of low molecular weight products was confirmed by GC, GC-MS, HPLC and LC-MS analysis. In the GC-MS profiles (Figure 3.4-3.7) of DEE and EtOAc soluble products obtained in NaX catalyzed reaction of alkaline lignin, majority of the peaks identified were for low molecular weight products (*Mw*. < 350 Da). The identified and quantified products are guaiacol, pyrocatechol, 2-methoxy-4-methylphenol, resorcinol, 4-hydroxy benzyl alcohol, 2,6-dimethoxy phenol, eugenol 1,2,4-trimethoxy benzene, vanillin, 3,4-dimethoxyphenol, 4-hydroxy-3-methoxybenzyl alcohol, acetoguaiacone, 2,4-ditert-butylphenol, hexadecane, homovanillic acid and diethyl-terephthalate.
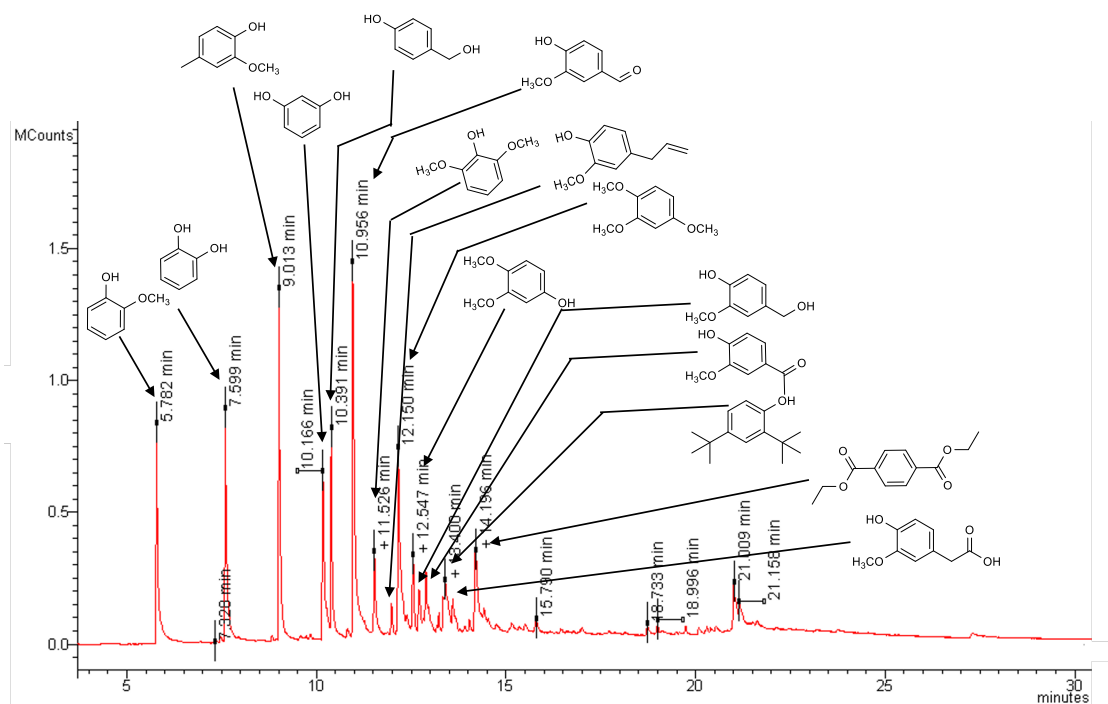
Figure 3.4. GC-MS chromatograph of products extracted in diethyl ether (liquid fraction) from the solid recovered after evaporation of reaction solvent.

Reaction condition: Alkaline lignin:NaX = 1:1 *wt./wt.*, EtOH:H$_2$O (1:2 *v/v*) 30 mL, 250 ^{o}C, 1 h.
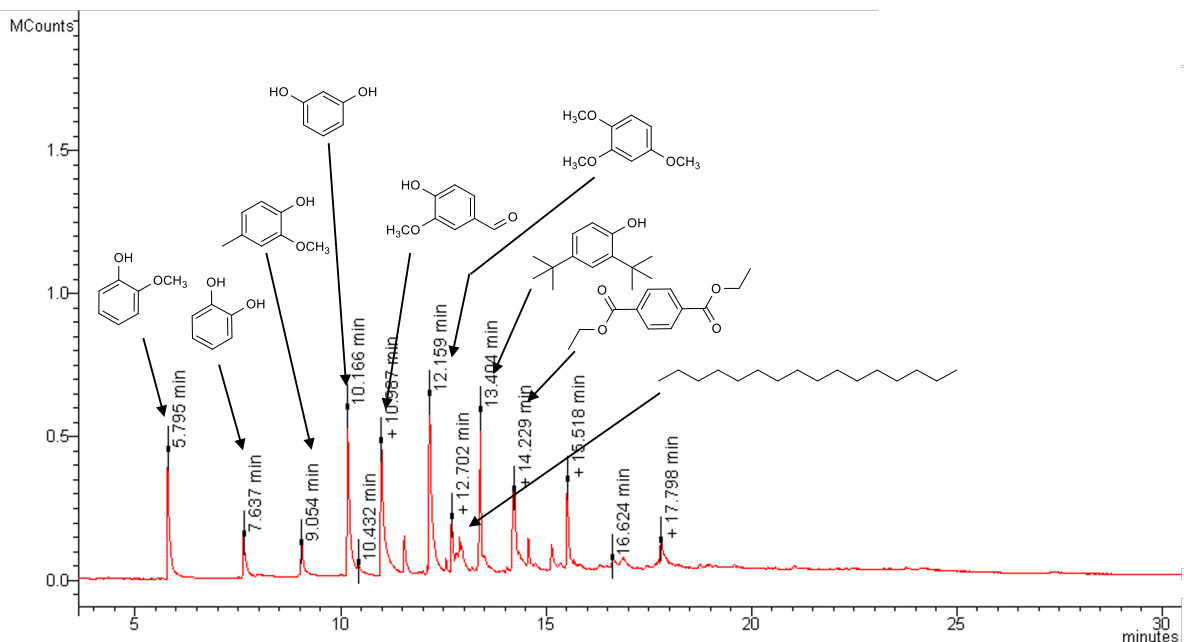
Figure 3.5. GC-MS chromatograph of products extracted in ethyl acetate (liquid fraction) from the solid recovered after evaporation of reaction solvent.

Reaction condition: Alkaline lignin:NaX = 1: 1 *wt./wt.*, EtOH: H$_2$O (1: 2 *v/v*) 30 mL, 250 ^{o}C, 1 h.
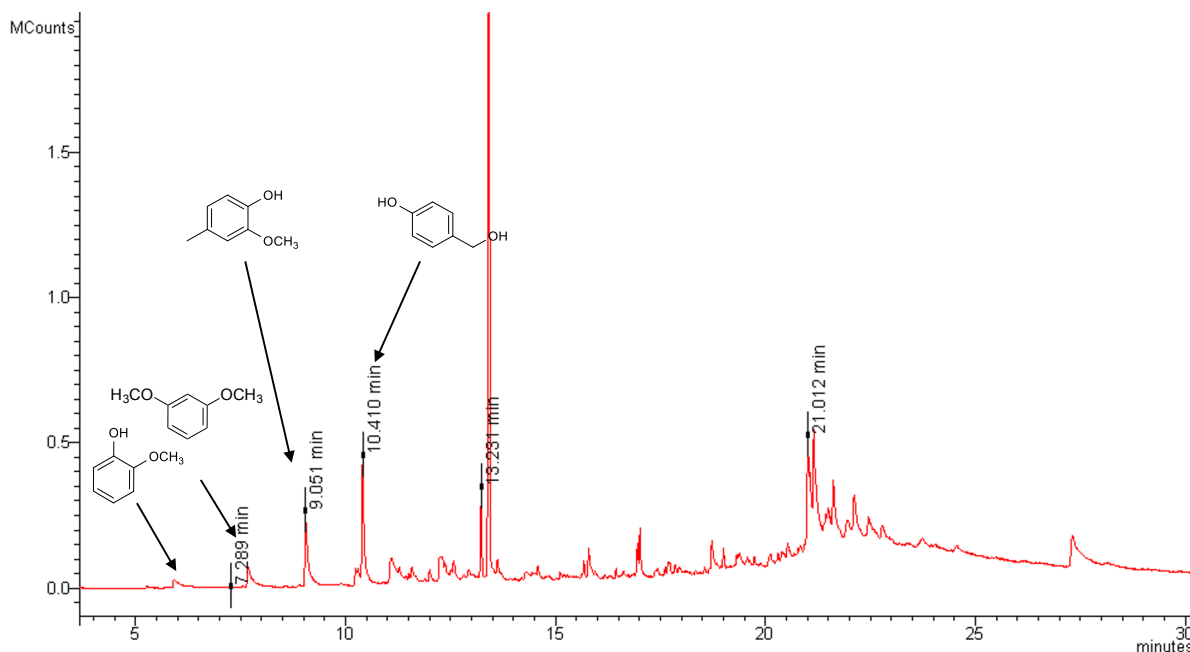
Figure 3.6. GC-MS chromatograph of products extracted in diethyl ether (solid fraction or filter cake) from the solid recovered after evaporation of reaction solvent.

Reaction condition: Alkaline lignin: NaX = 1: 1 *wt./wt.*, EtOH: H₂O (1: 2 *v/v*) 30 mL, 250 °C, 1 h.
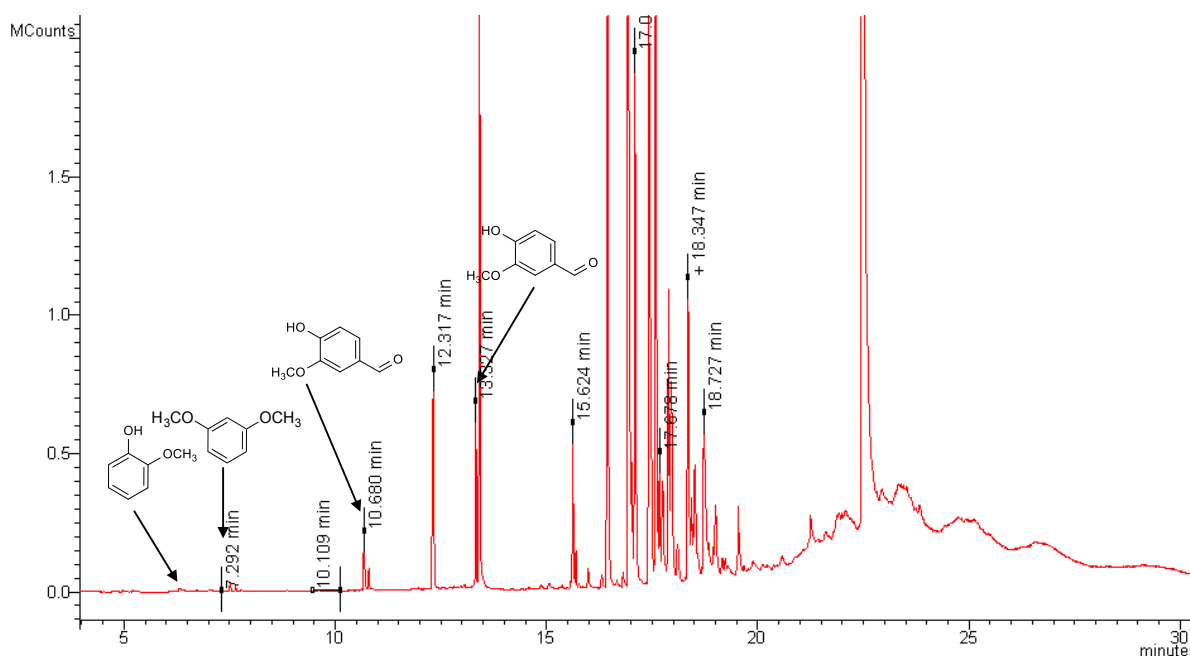
Figure 3.7. GC-MS chromatograph of products extracted in ethyl acetate (solid fraction or filter cake) from the solid recovered after evaporation of reaction solvent.
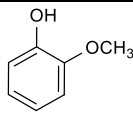
Reaction condition: Alkaline lignin: NaX = 1: 1 *wt./wt.*, EtOH: H₂O (1: 2 *v/v*) 30 mL, 250 °C, 1 h.

A careful look at GC-MS chromatographs of DEE and EtOAc extracted products from liquid reveals that concentration of low molecular weight products extracted in DEE is much higher compared with EtOAc (Figures 3.4 and 3.5). This is understandable since from the liquid, products were first extracted in DEE and then EtOAc was used to extract the products from liquid. However, the weight of the products isolated in EtOAc is higher than extracted in DEE (Figure 3, NaX catalyzed reaction). Considering this, it is expected that in EtOAc solvent, oligomers (dimers, trimers) are extracted (which again are depolymerization products but not complete). This phenomenon is also evident from the fact that higher concentration of products (typically oligomers which are precipitated out during acidification)[30, 31] from filter cake (solid) were extracted in EtOAc (Figure 3.7) than DEE (Figure 3.6). Moreover, the intensity of peaks in the DEE (Figure 3.4) soluble products from liquid is higher than EtOAc (Figure 3.5) soluble products. This is because first products were extracted in DEE and the left-over products were extracted using EtOAc. Furthermore, intensity of peaks is more in case of EtOAc soluble products (Figure 3.7) from solid (filter cake) compare to DEE which concludes the fact that EtOAc soluble products is rich in dimers and trimers.

3.3.3. Quantification of Depolymerized Products

From the GC-MS analysis of organic solvent soluble products, few compounds were identified and based on that those were commercially procured. With the aid of the commercially procured standard compounds, it was feasible to quantify these products (ca. 35% out of 51% products yield) and the details on their structures and yields are summarized in Table 3.3.

Table 3.3. Quantification of identified lignin depolymerisation products. Reaction condition: Alkaline lignin: NaX = 1: 1 $wt./wt.$, EtOH: H_2O (1:2 v/v) 30 mL, 250 ^{o}C, 1 h.

Monomer	Structure	Yield ($wt.\%$)
Guaiacol		1

Pyrocatechol		0.3
2-methoxy-4-methylphenol		3.7
Resorcinol		0.8
4-hydroxy benzyl alcohol		1.4
2,6-dimethoxy phenol		0.03
Eugenol		0.4
1,2,4-trimethoxy benzene		0.03
Vanillin		3.6
3,4-dimethoxyphenol		0.02
4-hydroxy-3-methoxybenzyl alcohol		0.3
Acetoguaiacone		4.1
2,4-ditert-butylphenol		0.5
Hexadecane		0.5
Homovanillic acid		0.3
Diethyl- terephthalate		0.6

From the identified products, it is safe to comment that ethanol, which is used as a reaction solvent does not participate in the reaction as a substrate. This is because in most of the products, $-OCH_3$ (methoxy) groups are attached to the aromatic ring instead of $-OCH_2CH_3$ expected if ethanol is contributing towards product formation. This also reveals that lignin does not undergo alcoholysis reaction but rather is

depolymerized through hydrolysis reaction (by yielding -OH groups on aromatic rings. Presence of -OH groups is also observed in almost all identified products).

3.3.4. Product Adsorption Study

An attentive look at Figure 3 reveals that with MgO, CaO, HT and HAP catalysts contribution by DEE soluble products in overall yield is higher than EtOAc extracted products. This trend is contradictory to the results obtained with NaX, NaY, NaP and KLTL catalysts (Figure 3.3) where products extracted in EtOAc were more than extracted in DEE. But, still total yield for DEE soluble products is higher in NaX, NaY and NaP catalysts than other catalysts. It is astonishing to see (Figure 3.3) that with HAP, HT, MgO and CaO as catalysts, overall yield of products (10-18%) is lower than the non-catalytic reaction (24%). This is probable because of two reasons; one due to adsorption of formed products on these catalysts or second due to further (degradation) reactions of formed products on these catalysts. It is also reasonable to believe that both of these reasons might be responsible for observing this phenomenon. To understand these results further, weight of the separated solid (by centrifugation before acidification, Figure 3.2) was checked and it was noticed that with these catalysts only increase in weight of solid (after recovery solid was dried in oven at 55 °C for 16 h) was seen compared to any other catalyst such as, NaX, NaY, NaP and KLTL (Table 3.4).

Table 3.4. Summary on fresh and recovered catalyst weight.

Catalyst	Fresh catalyst weight (g)	Recovered solid weight (g)	Solid other than catalyst (g) (Recovered - Fresh)	After extraction of adsorbed products weight of solid (g)*
NaX	0.5	0.4900	-	-
NaY	0.5	0.483	-	-
NaP	0.5	0.491	-	-
KLTL	0.5	0.4800	-	-

HT	0.5	0.6349	0.1349	0.6304
HAP	0.5	0.5384	0.0384	0.5145
MgO	0.5	0.7583	0.2583	0.7095
CaO	0.5	0.9178	0.4178	0.8929
MgO	0.03	0.0412	0.0112	0.0378
CaO	0.0055	0.0122	0.0067	0.01

* After extraction of adsorbed products in mixture of DEE and EtOAc (1:1 *v/v*, 30 mL), dried at 55 °C for 16 h.

Since lignin and depolymerized low molecular weight products are soluble in reaction solvent (ethanol:water), the solid recovered after reactions is either only catalyst or catalyst with adsorbed products. To comprehend this possibility, products adsorbed on these catalysts (HAP, HT, MgO and CaO) were attempted for their extraction in the mixture of DEE and EtOAc and as seen in Figure 3.3 and Table 3.4, only 1-7% of products could be extracted from these solids. Still, even after extraction of adsorbed products in mixture of solvents, weight of solid (catalyst + adsorbed products) was higher than the charged catalyst (Table 3.4). This is indicative of the fact that either products or unconverted lignin/ oligomers are strongly adsorbed on the catalyst. Adsorption study with lignin was performed at 30 °C and reaction condition (Table 3.6).

Further to check the adsorption of these products, a set of experiments were done with mixture of five aromatic monomers (phenol, *p*-cresol, guaiacol, eugenol and vanillin) which resemble with products identified in depolymerization reactions of lignin. The reactions were done under optimized reaction condition (250 °C, 1 h) with NaX and CaO as catalysts and it was apparent from the GC chromatographs that while with NaX as a catalyst slight decrease in peak intensities for eugenol (5%) and vanillin (41%) were seen, with
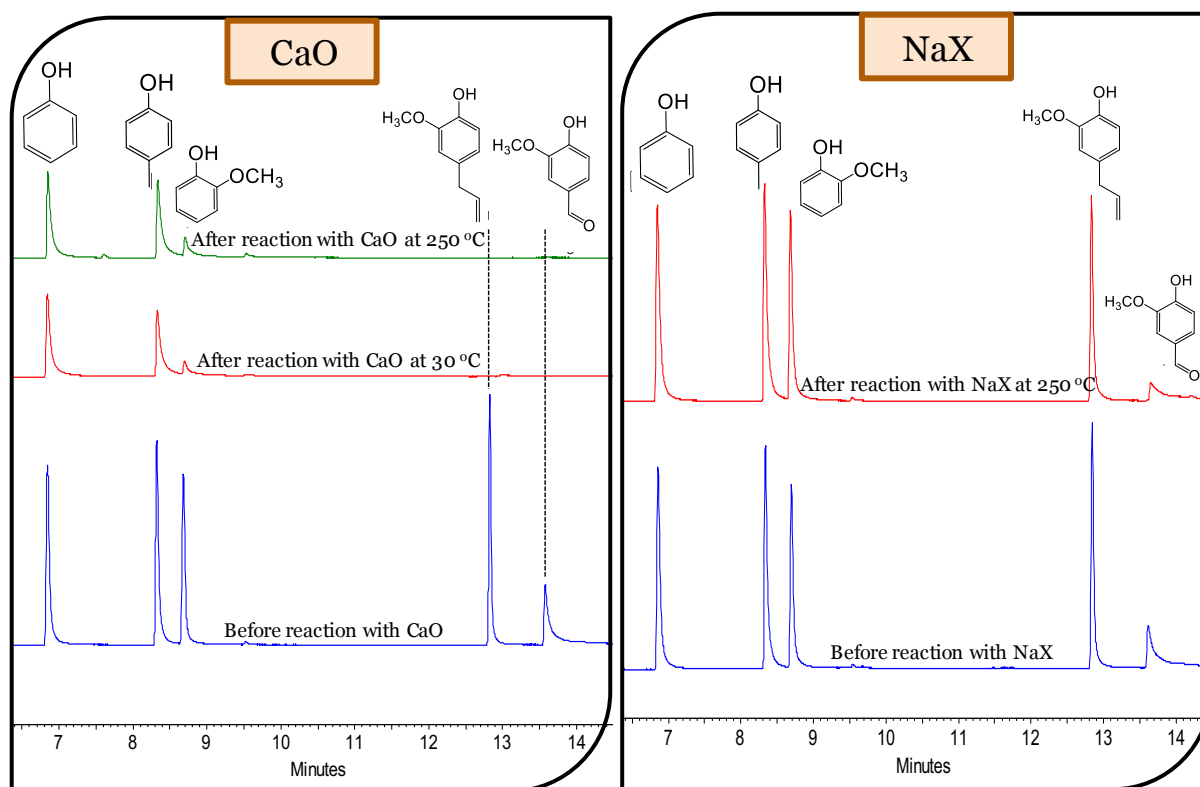
Figure 3.8. GC chromatographs of mixture of Phenol, p-cresol, Guaiacol, Eugenol and Vanillin in EtOH: H_2O (1: 2 v/v) 30 mL. Reaction Condition: Monomers (0.1 g each), Catalyst (0.5 g), 1 h.

CaO as a catalyst, huge decrease in the peak intensities for 3 monomers was observed along with disappearance of peaks for eugenol and vanillin. A careful look from the Figure 3.8 indicates that eugenol having high intense peak compared to others and vaneshes completely after the reaction with CaO. The phenomenon might be possible due to the presence of allylic double bond in eugenol. This double bond can interact strongly through π-π bonding with CaO compared to the aromatic ring. Moreover, recovered CaO catalyst was washed with organic solvents (DEE, EtOAc) and it was observed that the separation of few products was possible from the catalyst (Figure 3.9). It is suggested that since Eugenol and Vanillin are so strongly adsorbed on the catalyst that those are not possible to extract. Moreover, from the identification or quantification of the products using GC-MS (Table 3.3), it was noticed that products obtained contains different functional groups. This could be possible reason for obtaining the higher weight of the solid (after extraction of products from it) in the lignin depolymerization reaction (Table 3.4).
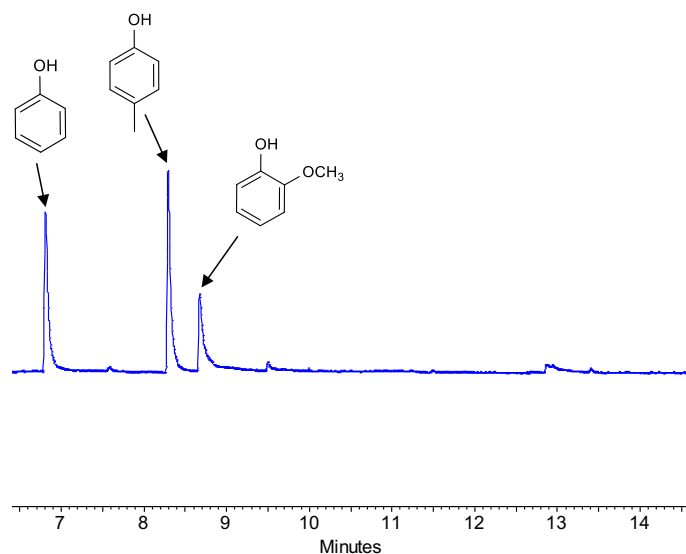
Figure 3.9. GC chromatograph of products extracted from catalyst after reaction with CaO at 250 °C, 1 h.

These results clearly indicate that on CaO large amount of products were adsorbed but on NaX minimal amount of products were adsorbed. Similar experiments were also performed with HAP, HT & MgO and analogues results as that obtained with CaO were seen. Although, it was obvious from above study that products are adsorbed on CaO, but there was likelihood that the products underwent some reaction at reaction conditions employed for adsorption study. Hence to check this, subsequently the adsorption study was done under ambient conditions (30 °C, 1 h, nitrogen flushing) and the results imply that adsorption of formed products is even possible under ambient conditions (Figure 3.8). Similarly, it is also indicative that these products are not degrading under reaction condition (no prominent extra peak was visible in GC chromatographs, Figure 3.8).

Further, adsorption study was performed with single molecules also. Vanillin and Eugenol were chosen for the study as these molecules adsorbed much more compared to others on the catalyst. It was observed from the earlier studies that these products adsorbed on catalyst under ambient condition. So, further experiments were performed at 30 °C for 1 h. It is understood from the study that with single molecules also similar type to adsorption phenomenon was observed (Figure 3.10 and Table 3.5). This also confirms that the presence

of an allylic bond or carbonyl group can interact with catalyst through pi-pi bonding which will results in the strong adsorption of these compounds.
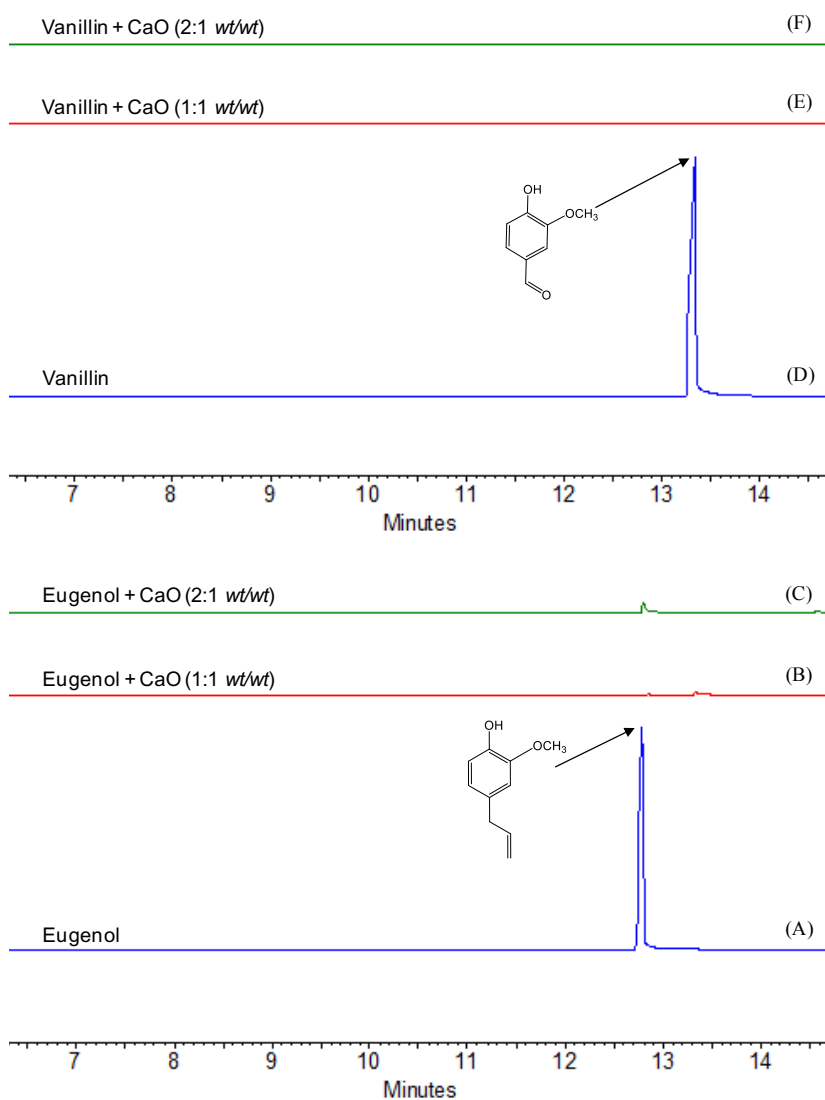
Figure 3.10. GC chromatographs of adsorption study with single molecules performed in EtOH: H_2O (1: 2 v/v) 6 mL at 30 °C. (A) Eugenol, (B) Eugenol: CaO (1: 1 $wt./wt.$), (C) Eugenol: CaO (2: 1 $wt./wt.$), (D) Vanillin, (E) Vanillin: CaO (1: 1 $wt./wt.$), (F) Vanillin: CaO (2: 1 $wt./wt.$)

Table 3.5. Adsorption study with single molecules.

Aromatic monomers	CaO fresh weight (g)	*Wt./Wt.* ratio (monomers/catalyst)	Recovered solid weight (g)
Vanillin (0.1 g)	0.10	1:1	0.1600
Vanillin (0.1 g)	0.05	2:1	0.0730

Eugenol (0.1 g)	0.10	1:1	0.1841
Eugenol (0.1 g)	0.05	2:1	0.1216

Further, the effect of CaO loading to check the adsorption of products was also studied.

	Weight of CaO taken	Percentage of monomers adsorbed
With **0.005 g** CaO at 30 °C	0.005 g	15%
With **0.05 g** CaO at 30 °C	0.05 g	26%
With **0.5 g** CaO at 30 °C	0.5 g	76%
Before addition of CaO at 30 °C	-	-
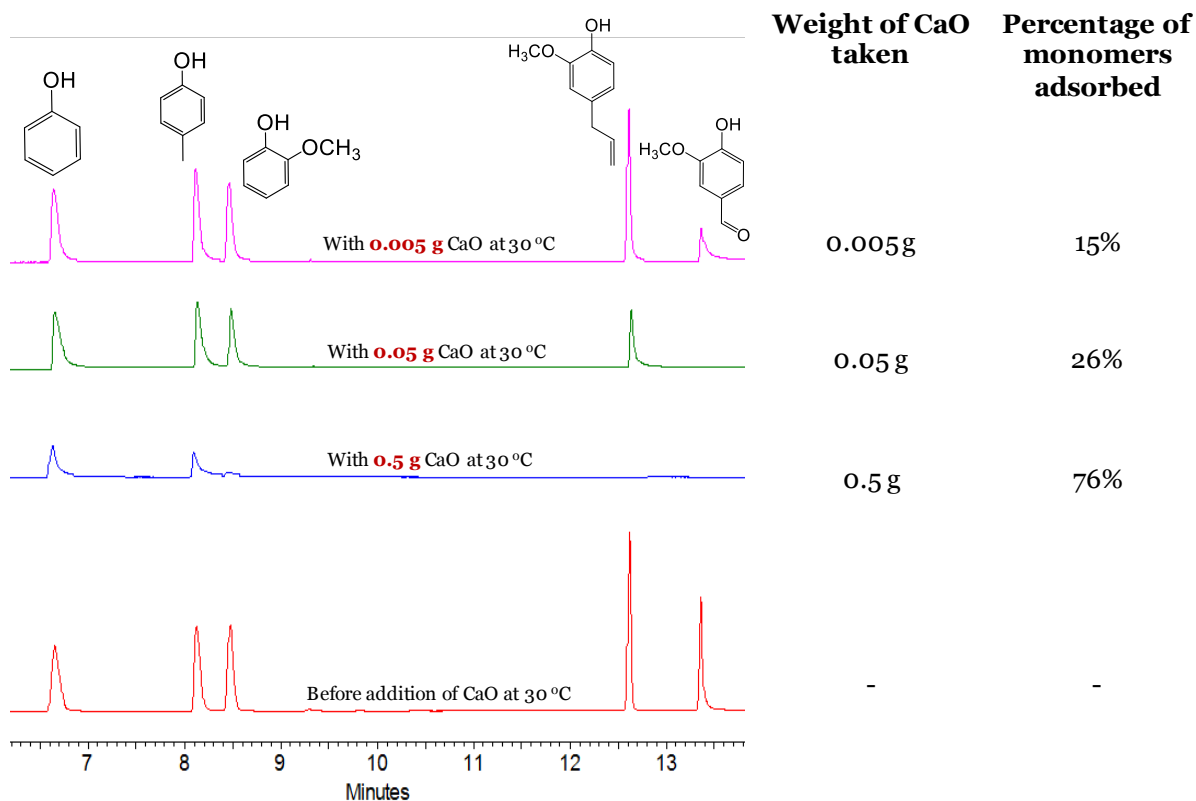
Figure 3.11. Effect of CaO loading on monomer adsorption.

It was very clear from the figure that with a decrease in the amount of CaO loading, percentage of monomer adsorption decreases. This fact (GC chromatograph) is well correlated with the percentage of monomers adsorbed.

3.3.4.1. Correlation of Adsorption Phenomenon with Lignin Depolymerization Reaction

The effect of CaO loading was studied with lignin substrate at 30 °C and at optimized reaction condition (250 °C, 1 h) (Results are shown in Table 3.6). Again, it established the fact that adsorption phenomenon decreases with decrease in the catalyst loading. A careful look suggests that the percentage of

adsorption at 250 °C, 1 h is less compared to 30 °C, 1 h which shows that at reaction condition (250 °C, 1 h) lignin undergoes depolymerisation and due the adsorption-desorption phenomenon of substrate/product on the catalyst, percentage of adsorption decreases.

Table 3.6. Products/Substrate adsorption at 30 °C and reaction condition.

Reaction condition (with 0.5 g lignin in 30 mL EtOH:H_2O)	CaO weight taken (g)	Percentage of substrate/products adsorbed (%)
30 °C, 1h	0.5	96
30 °C, 1h	0.05	40
30 °C, 1h	0.005	35
250 °C, 1h	0.5	84
250 °C, 1h	0.05	10
250 °C, 1h	0.005	1.4

Further, to make sure that there is not a significant effect from series degradation reactions, I have performed the depolymerization reactions by normalizing the reaction time to the mass of catalyst. Details are represented in Figure 3.12. As seen from Figure 3.12(A), when reactions were performed for 1 h, with the decrease in CaO loading, increase in yield was observed. This may be due to pH or product adsorption effect. Later, reactions were performed with varying catalyst loading and accordingly reaction time was changed. For e.g. with 0.5 g CaO catalyst loading, reaction was performed for 1 h however, when 0.1 g of CaO was charged in the reactor, reaction was carried out for 20 min. (i.e. 5 times decrease in both, catalyst and time). Subsequently, reaction was carried out with 0.05 g CaO for 10 min. The results (Figure 3.12(B)) show that though with decrease in time according to decrease in catalyst loading, slight improvement in the yields was seen. However, this increase is marginal considering when reaction was carried out for 1 h with 0.05 catalyst (Figure 3.12(A)). This suggests that pH (9.2) along with time is important to achieve better yields.
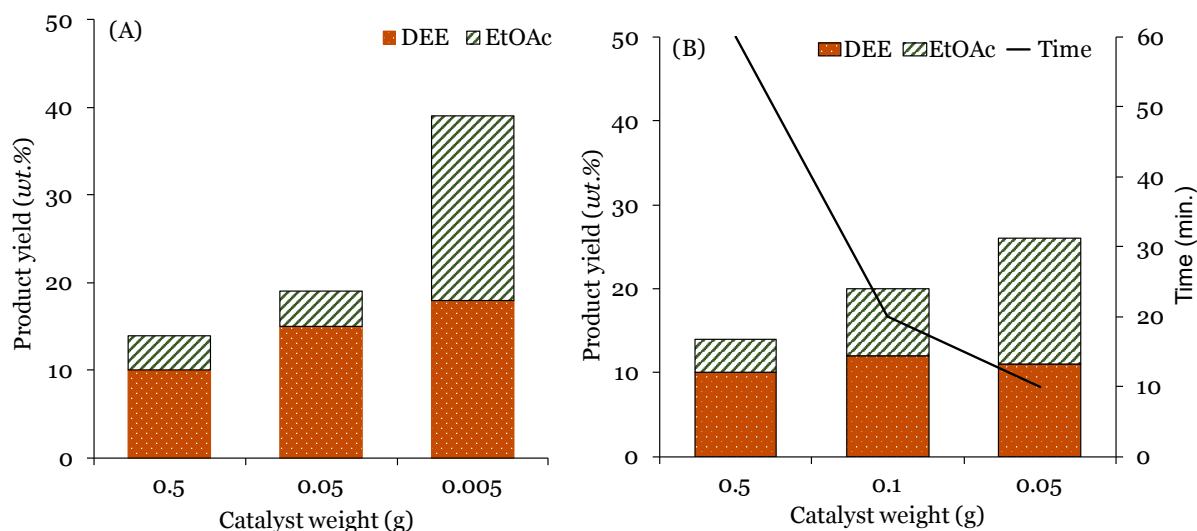
Figure 3.12. Depolymerization of lignin using CaO catalyst.
Reaction condition: (A) Alkaline lignin (0.5 g), EtOH: H_2O (1: 2 v/v) 30 mL, 250 °C, 1 h. (B) Alkaline lignin (0.5 g), EtOH: H_2O (1: 2 v/v) 30 mL, 250 °C.

3.3.5. Effect of pH/Basicity on Lignin Depolymerization

To realize the reason for disparity observed in the activity of various catalysts employed in this work, it was important to correlate the activity with basicity of the catalysts. First, pH of all the catalysts was measured (Alkaline lignin:Catalyst = 1:1 $wt./wt.$, EtOH:H_2O (1:2 v/v) 30 mL, 25 °C) and the following order of decrease in pH was seen,

CaO (pH ≥ 13.4) > HT (pH 12.5) > MgO (pH 10.5) > KLTL (pH 9.4) > NaX (pH 9.2) >NaY (pH 8.7) = NaP (pH 8.7) ≈ HAP (pH 8.5) > Millipore water (pH 6.8)

As seen from Figure 3.13, maximum product yield (51%) was observed at pH 9.2 measured for NaX catalyst. It is anticipated that with an increase in pH, side reactions are possible to be dominant and hence yield for desired products would decrease. Since during the reactions with NaY (38%) and NaP (34%) having pH of 8.7 good activities compared with other catalysts were observed (Figure 3.3), reaction with NaX (by decreasing the loading of catalyst) was carried out at pH 8.7 but decrease in yield (39%) was observed. This highlights the fact that pH 9.2 might be better to achieve higher yields (Figure 3.13).
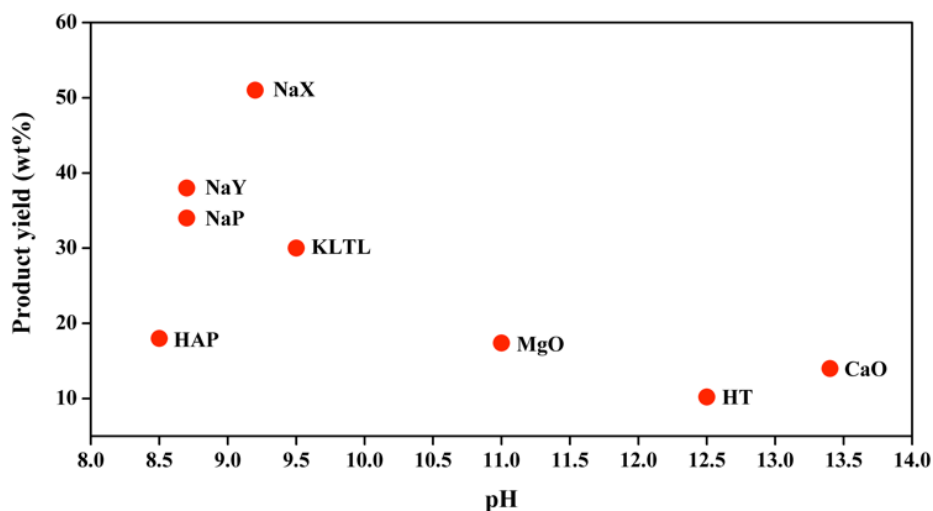
Figure 3.13. Effect of pH on the product yield.

Reaction condition: Alkaline lignin:Catalyst = 1:1 *wt./wt.*, EtOH:H$_2$O (1:2 *v/v*) 30 mL, 250 °C, 1 h.

Subsequently, reactions were done with CaO and MgO by charging appropriate quantities of catalysts to maintain pH of 9.2 (Table 3.7).

Table 3.7. Catalyst charged in the reactor to maintain the particular pH.

Catalyst	Weight of the catalyst (g)	pH
NaX	0.5	9.2
NaX	0.08	8.7
NaY	0.5	8.7
NaP	0.5	8.7
MgO	0.5	10.5
MgO	0.03	9.2
CaO	0.5	≥ 13.4
CaO	0.0055	9.2
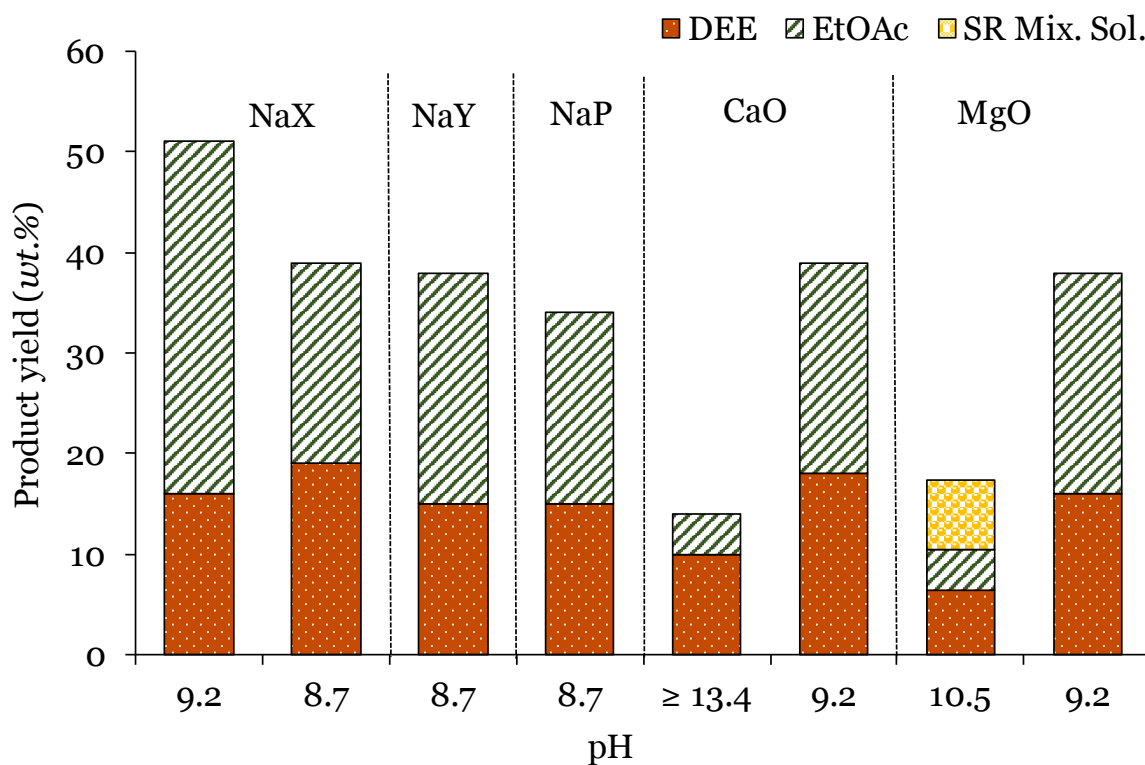
Figure 3.14. Effect of pH on the lignin depolymerization using various solid base catalysts.

Reaction condition: Alkaline lignin (0.5 g), Catalyst, EtOH: H_2O (1: 2 *v/v*) 30 mL, 250 ^oC, 1 h.

As seen from Figure 3.14, when pH was maintained at 9.2, product yield was almost doubled with these catalysts (CaO, 39% yield; MgO, 38% yield) compared to reactions performed at higher pH (Figures 3.3 and 3.13). These results establish the fact that pH is a vital factor in achieving higher yields of products. However, it is also possible that with the decrease in catalyst loading (CaO and MgO, Table 3.7) to maintain the pH at 9.2, the amount of products adsorbed on catalyst may change. This in turn can show higher yields in the reaction. To ascertain this fact, weight of the solid obtained after reaction (catalyst+adsorbed products) was checked (Table 3.4) however, this data cannot conclude the observance of increase in yields and detailed study on the same is necessary.

Though, it is observed that pH plays an important role in governing the activity of a catalyst, it is related with the amount of basic sites available on catalyst. This is particularly important in this work since all the catalytic reactions were performed by charging similar weight of catalyst. Therefore,

CO_2-TPD study was performed to know the concentration of basic sites on each catalyst (Chapter 2B, Section 2B.5.1.3) and following trend of basicity with respect to catalyst was seen,

CaO (1.96 mmol/g) > NaX (0.42 mmol/g) ≈ HT (0.40 mmol/g) >NaY (0.34 mmol/g) > MgO (0.24 mmol/g) > KLTL (0.14 mmol/g) ≈ HAP (0.12 mmol/g) > NaP (0.09 mmol/g)

From this data it was tricky to draw any conclusion since on both NaX and HT catalysts although almost same amount of basic sites are available but those showed very different depolymerization activities (NaX, 51%; HT, 10.2%) (Figure 3.3). Nonetheless, partially this difference in activity can be explained on the basis of dissimilarity between adsorption of products on these catalysts since compared to NaX on HT adsorption of products was very high, as shown in Figure 3.14. Comparable observations of difference in activity even with almost similar basic sites concentrations was also made with NaP (0.09 mmol/g, 34%) and HAP (0.12 mmol/g, 18%) catalysts. So, broadly it is suggested that irrespective of concentration of basic sites on the catalyst, adsorption also plays an important role in governing the activities of catalysts. To extend this further, when pH was maintained at 9.2 with CaO and MgO catalysts, improvements in activities was achieved (Figure 14) even though these catalysts are known to adsorb products (Figure 3.3 and 3.8). To explain this, it is proposed that adsorption of products might be a pH dependent phenomenon, i.e. with increase in pH, possibility of adsorption of products increases. This is evident from the fact that product adsorption study with catalysts like NaX (pH, 9.2) and CaO (pH, 13.4) was done with dissimilar pH. But when reaction with CaO was performed at pH of 9.2, higher activity (39%, Figure 3.14) was seen than the reaction done with same catalyst at pH of 13.4 (Figure 3.3). This is possible may be due to lower amount of products are adsorbed at pH of 9.2. This explanation is practical considering that under reaction condition, 5 model compounds used in adsorption study did not show any degradation (Figure 3.8).

Another interesting information could be extracted from catalytic results and the data on concentration of basic sites on different catalysts is that even if with NaP (34%) and NaY (38%) catalysts similar catalytic activity was achieved (Figure 3), the concentration of basic sites on these catalysts is different (NaY = 0.34 mmol/g; NaP = 0.09 mmol/g). To explain this fact, data on strength of

basic sites was helpful (Chapter 2B, Section 2B.5.1.3). By considering that desorption of CO_2 at lower temperatures (< 500 ^{o}C) represents presence of weak basic sites and desorption of CO_2 at higher temperatures (> 500 ^{o}C) represents presence of strong basic sites, difference in activities is correlated with strength of basic sites in catalysts. From the CO_2-TPD profiles of both NaY and NaP catalysts it is seen that both these catalysts have only weak basic sites and they show similar pH (8.7). Whereas from the CO_2-TPD profiles of other catalysts (HT, MgO, CaO, HAP) which typically showed lower product yield (Figure 3.3) it was observed that they have either along with weak basic sites, strong basic sites or have only strong basic sites (Chapter 2B, Section 2B.5). These observations may suggest that presence of strong basic sites might be responsible for achieving lower yields. This also can be correlated with the fact that due to presence of strong basic sites, pH of these catalysts was higher (pH > 10) even though when total basicity was lower (MgO, 0.24 mmol/g; HAP, 0.12 mmol/g) in these catalysts than best catalyst, NaX (0.42 mmol/g, pH 9.2). The observance of weak basic sites on zeolites is expected since in zeolites basicity arises due to covalently bonded framework oxygen and it is reported that if basic zeolites are prepared by ion-exchange method then those show weak basicity than alkaline earth metal oxide catalysts.

Even though efforts are made to correlate the activity with basicity of the catalysts, discussions on strength of basic sites can not be established only on the basis of CO_2-TPD studies since basic catalysts invariantly gain their basicity after treating those at very high temperatures (> 550 ^{o}C) by removing water and carbon dioxide which have poisoned the catalytically active sites. Nevertheless, since in this work, water is used as one of the solvent, it is possible that basic sites on catalysts may get poisoned and have different morphologies than expected. Moreover, MgO and CaO being almost insoluble in water (reaction solvent) would form hydroxide species ($Mg(OH)_2$ and $Ca(OH)_2$)[32] which would have completely different basic strength under reaction conditions. These hydroxide species are known to be sparingly soluble in water and give turbid solutions (lime water). Particularly, at higher temperatures, many hydroxides again tend to form oxides and thus lose their ability to dissolve in water (solubility of $Ca(OH)_2$ in water: 0.159 g/100 g at 25 ^{o}C to 0.071 g/100 g at 100 ^{o}C; solubility of CaO in water: 0.120 g/100 g at 25 ^{o}C to 0.054 g/100 g at 100 ^{o}C).[33] On the contrary, solubility of $Mg(OH)_2$ in water follows reverse trend and has found

higher solubility in water with increase in temperature (0.0009 g/100 g at 18 °C to 0.004 g/100 g at 100 °C;[34] solubility of MgO in water, 0.086 g/100 g at 30 °C) (Table 3.8).

Table 3.8. Solubility of Catalysts in water at different temperatures.

Catalyst	Solubility in water (g/100 mL)		Solubility (g/30 mL)*
	25 °C	**100 °C**	
CaO	0.120	0.054	
Ca(OH)$_2$	0.159	0.070	0.021
MgO	0.086	-	
Mg(OH)$_2$	0.0009	0.004	0.0012

*Calculated in 30 mL of water (this volume is used in reaction) by considering solubility of hydroxides at 100 °C in 100 mL.

Calculation on percentage (%) catalyst in heterogeneous phase:

$$MgO \xrightarrow{\ H_2O\ } Mg(OH)_2$$

(Mw. = 40 g/mol)   (Mw. = 58 g/mol)

0.5 g of MgO taken $\longrightarrow$ 0.725g of Mg(OH)$_2$ (formation
for reaction   considering 100%
conversion of
MgO into
Mg(OH)$_2$)
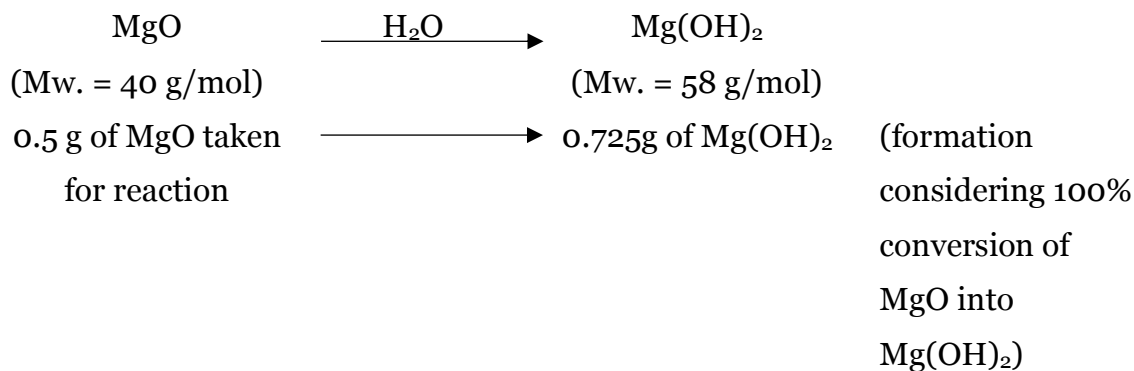
If 0.725g $\longrightarrow$ 100%

0.0012g (solubility $\longrightarrow$ (100 x 0.0012) /
of Mg(OH)$_2$ in 30   0.725
mL water)

= 0.1655 % Mg(OH)$_2$
is only soluble in 30
mL water

Hence, only 0.1655% catalyst is soluble in water considering 100% formation of $Mg(OH)_2$ under reaction conditions from MgO.

Thus, expected heterogeneous form of catalyst = total MgO taken −solution of $Mg(OH)_2$ in H_2O = 0.5 g − 0.0012g

= 0.4988 g which is 99.76% of total catalyst taken.

Thus, 99.76% catalyst remains as heterogeneous.

Similar to MgO, calculations are also done for CaO,

CaO	$\xrightarrow{H_2O}$	$Ca(OH)_2$	
(Mw. = 56 g/mol)		(Mw. = 74 g/mol)	
0.5 g of CaO	$\longrightarrow$	0.6607 g of $Ca(OH)_2$	Considering
taken for reaction			100% conversion
			of CaO into
			$Ca(OH)_2$
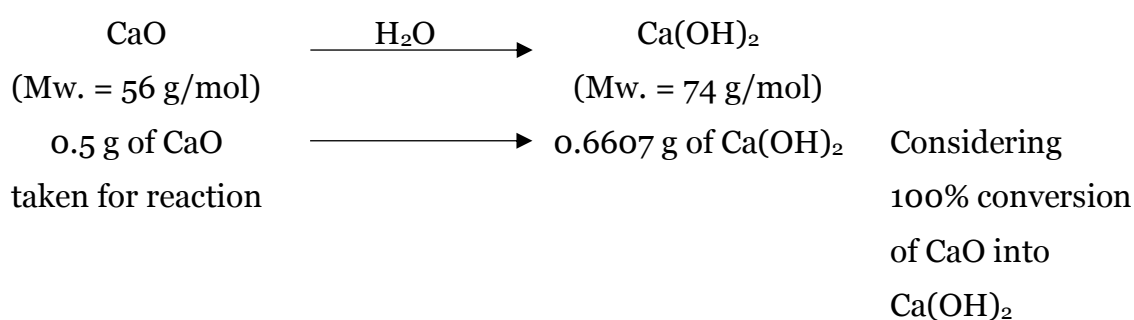
If 0.6607 g	$\longrightarrow$	100%
0.021 g	$\longrightarrow$	(100 x 0.021) / 0.6607
(solubility of		
$Ca(OH)_2$ in 30 mL		
water)		

= 3.17 % of $Ca(OH)_2$ is
soluble in 30 mL water

Hence, only 3.17% catalyst is soluble in 30 mL water considering 100% conversion of CaO into $Ca(OH)_2$.

Expected heterogeneous form of catalyst = total CaO taken −solution of $Mg(OH)_2$ in H_2O

= 0.5 g − 0.021g

= 0.479 g of catalyst remains as heterogeneous (95.80%)

Thus, 95.80% catalyst remains as heterogeneous.

The calculations suggest that > 95% of catalyst still remains in heterogeneous form under reaction conditions. Nonetheless, typically when solubility of M(OH)x is < 0.01 g/100 g of water it is considered as insoluble in water.[35]

Further, to check whether $Ca(OH)_2$ could catalyse this reaction, an experiment with 0.016 g $Ca(OH)_2$ was carried out considering only 3.17% of CaO exists in $Ca(OH)_2$ form (Table 8). The observance of 23% yield of products states that $Ca(OH)_2$ does not contribute to the reaction. This is because without catalyst also we observed 24% yield. This shows that the reaction is mainly catalyzed by solid CaO and MgO.

Additionally, since Na exchanged zeolites showed good activity and from CO_2-TPD and catalytic results it is known that higher basic strength might not be favorable in this reaction, other alkali ions (Cs, K etc. having higher basic strength compared to Na) exchanged zeolites were not used except KLTL in this study. Because of same reason other alkaline earth oxides (BaO, SrO) having higher basic strengths compared to CaO and MgO also were not expected to show enhancement in the yields and thus were not evaluated. Nonetheless, still the scope remains to evaluate catalytic activity of these catalysts having higher basic strength by maintaining ca. 9.2 of pH.

Thus, all the above discussions establish the fact that catalytic activities are dependent on many factors like, pH, concentration of basic sites, type of basic sites, presence of alkali metal, adsorption of products, etc. and all these factors are interconnected with each other. Therefore, it is essential to optimize the catalyst property to achieve higher activity and from this work, it is proposed that to achieve higher yields the most important factor is to maintain the pH of reaction solution around 9.2. Moreover, it is proposed that zeolitic catalysts, if those are stable under reaction conditions and are completely insoluble in water would be better choice than the metal oxides.

3.3.6. Effects of Temperature and Pressure

By now, it is apparent that amongst all the catalysts evaluated, NaX shows the best yield (51%) within 1 h at 250 °C. Nevertheless, to enhance the yield of low molecular weight products, reaction was conducted at 240 °C for 1 h with NaX catalyst as it was expected that by lowering the reaction temperature, degradation of formed products

(if any) would be suppressed. However; with the decrease in temperature decline in the yield (33%) was observed (Figure 3.15(A)).

Further decrease in temperature to 230 °C, again showed lower yields (14%). This decline in yields may be attributed to simple temperature effect or property of ethanol. Since ethanol has *Pc* of 6.06 MPa and *Tc* of 241 °C, it is evident that at reaction temperature (250 °C), ethanol is present in subcritical state (4.2 MPa pressure was observed at 250 °C). Though, at 240 °C also ethanol can be under subcritical state but pressure was only 3.7 MPa. To comprehend the effect of pressure (Figure 3.15(B)), reaction was carried out at 240 °C by charging 0.3 MPa and 0.6 MPa of nitrogen (at room temperature) and total pressure of 4.3 MPa and 4.6 MPa was attained at 240 °C. Under these conditions, 43% and 49% yield was obtained which is 10-16% higher than achieved when reaction was carried out in absence of nitrogen pressure at 240 °C. This suggests that pressure plays an important role in achieving higher yields.
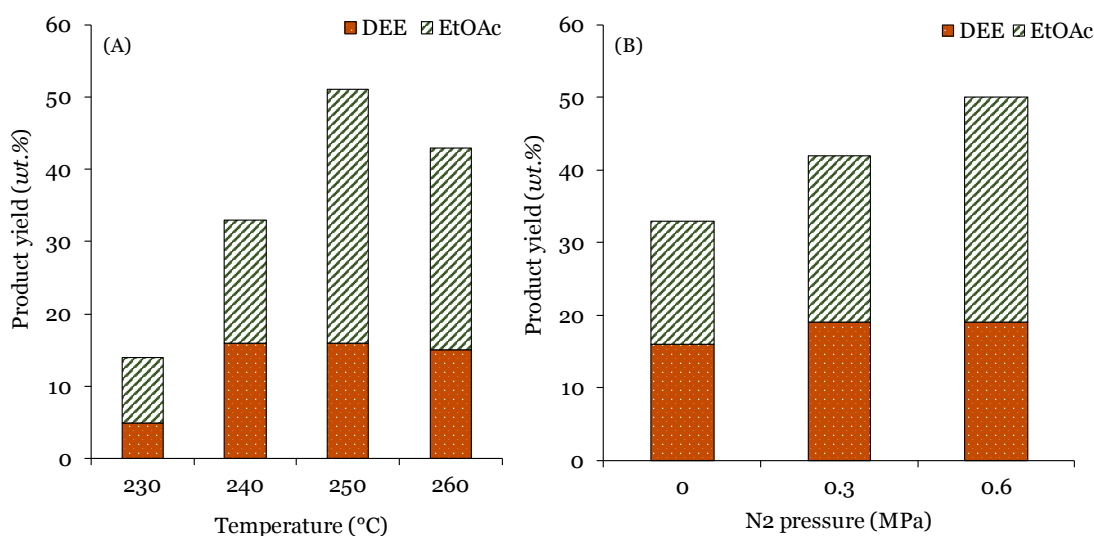
Figure 3.15. Effect of (A) temperature and (B) pressure on depolymerization of lignin.

Reaction condition: Alkaline lignin:Catalyst = 1: 1 *wt./wt.*, EtOH:H₂O (1: 2 *v/v*) 30 mL, 1 h.

In our earlier work on solid acid catalyzed depolymerization, effect of pressure on the reaction was studied in detail and it was established that with an increase in pressure, yield of products increases.[12, 13] Subsequently, reaction was performed at higher temperature (260 °C) believing that higher pressures would benefit the reaction but, again slight decrease in yield (46%) was seen, which

was against expectation. Thus, 250 °C is an optimum temperature to carry out depolymerization of lignin using NaX catalyst. Since on NaX catalyst unlike CaO and other catalysts, only minimal quantity of products were adsorbed under reaction conditions, it is assumed that decrease in yield at higher reaction temperatures is due to degradation and/or repolymerization reactions. Nevertheless, detailed study is required to comment further on this matter.

3.3.7. Effects of Time

The effect of reaction time on the product yield was investigated at 250 °C over NaX as a catalyst in ethanol: water (1: 2 *v/v*) solvent system (Figure 3.16). The products yield was increased up to 51% for a reaction time of 1 h and beyond this time products yield started declining. However, a careful look at the results imply that although overall yield decreased in 2 h, but contribution from DEE soluble products was increased in 2 h reaction. This implies that EtOAc soluble products like oligomers are over the period of time was converted into low molecular weight products.
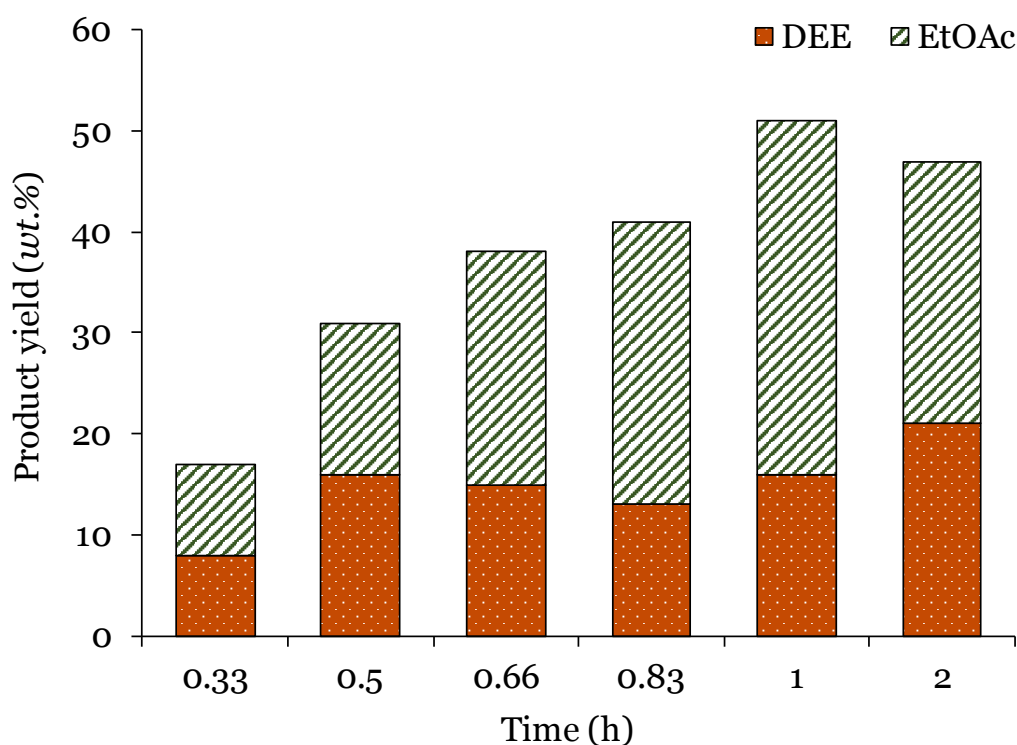
Figure 3.16. Effect of time on depolymerization of lignin.
Reaction condition: Alkaline lignin:NaX = 1:1 *wt./wt.*, EtOH:H$_2$O (1:2 *v/v*) 30 mL, 250 °C.

3.3.8. Effect of Catalyst Quantity

To make the process more economical viable, it is better to use less amount of catalyst quantity for the reactions. For that, depolymerization of lignin was done in ethanol:water (1: 2 *v/v*) solvent system with NaX as catalyst at 250 °C for 1 h (Figure 3.17), as at this reaction condition higher product yield was observed. Catalyst quantity was changed from 0.125 to 0.5 g. It was observed from the results, that with lower loading of catalyst (NaX, 0.25 g) i.e. Alkaline lignin:catalyst = 2: 1 *wt./wt.*, 52% of the product yield could be achieved.
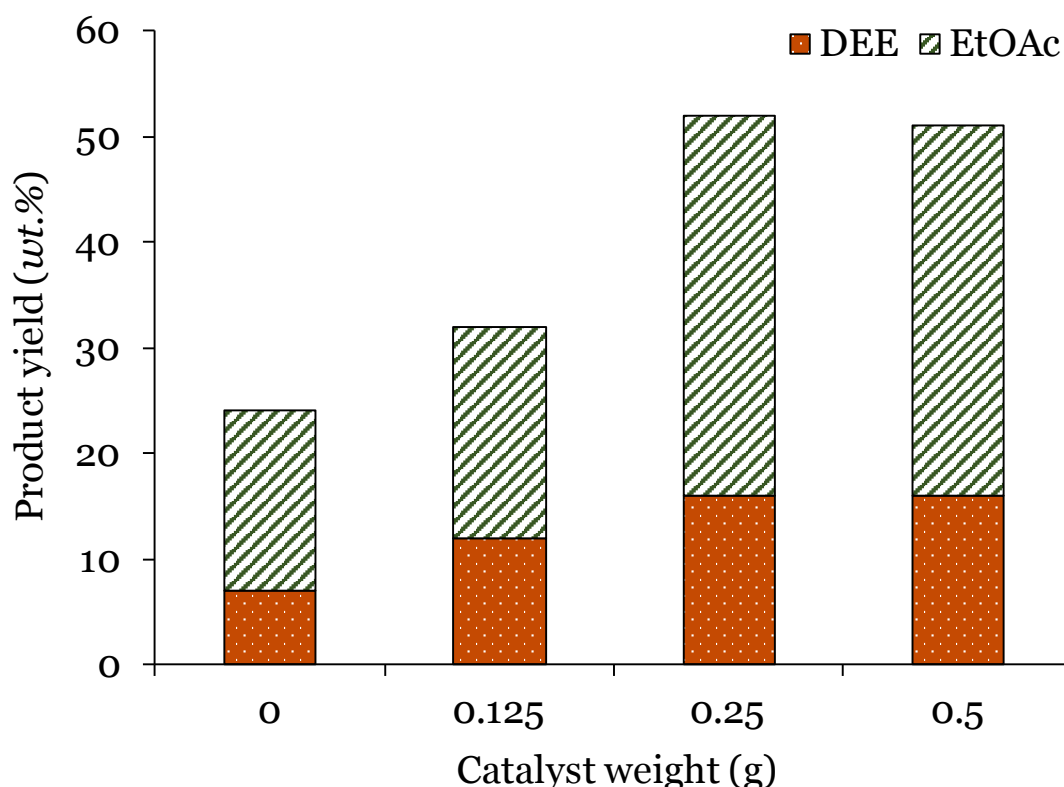
Figure 3.17. Effect of catalyst quantity on depolymerization of lignin. Reaction condition: Alkaline lignin (0.5 g), NaX, EtOH:H$_2$O (1: 2 *v/v*) 30 mL, 250 °C, 1 h.

3.3.9. Effect of Solvent System

Mostly, lignin depolymerization reactions are carried out in alcohol:water mixture for achieving better yields due to solubility of lignin in the solvent system which makes the reaction system homogeneous (when water soluble catalysts are used). Since alkaline lignin used in this study is completely soluble in water (Chapter 2A, Section 2A.3.8, Table 2A.6), reaction was carried out at 250 °C with NaX as a catalyst for 1 h in only water. However, no product formation was seen in this reaction. This result could not be explained on the basis of pressure effect as with water as a solvent at 250

°C, total pressure of 4.0 MPa was observed while when reaction is carried out with ethanol:water (1: 2 v/v) solvent system, 4.2 MPa pressure was monitored yet 51% yield was achieved. So, it can be considered that presence of ethanol in subcritical condition is helpful in forwarding the reaction. Subsequently, reactions were performed by varying the ratio of ethanol-water (2: 1, 1: 1, 1: 5 v/v) and maximum yield was observed in 1: 2 (v/v) solvent system. One of the reasons for reactions to proceed in presence of ethanol might be due to the formation of sodium ethoxide (reaction between Na^+ on catalyst and ethanol), which can act as strong base. This scenario is not possible when only water is used in this reaction. Though, the in-situ formation of sodium ethoxide could not be confirmed under reaction conditions. Yet, it is expected that when reaction is completed Na^+ will compensate the negative charge on zeolites. This is because during spent catalyst characterization studies no loss of Na^+ was observed.

3.3.10. Effect of Various Lignin Substrates

As discussed in the Introduction chapter that structure of lignin varies from plant to plant and the pretreatment method applied for its isolation. Hence, it is very important to develop a process which can be used for different lignin substrates having diverse physical and chemical properties. After the optimization of the reaction conditions for the depolymerization of alkaline lignin (NaX, ethanol:water (1:2 v/v) 30 mL, 250 °C, 1 h, 1000 rpm) various other lignin substrates having different molecular weight like, alkali lignin (*Mw.* = 28,000 Da), dealkaline lignin (*Mw.* = 60,000 Da), lignosulfonate acid sodium salt (L-Na) (*Mw.* =52,000 Da) and lignosulfonate acid calcium salt (L-Ca) (*Mw.* =18,000 Da) were evaluated under similar reaction conditions. Figure 3.18 shows that NaX can depolymerize most of the lignin substrates with different product yields (12-51%). The difference in the product yield can be explained on the basis of pH effect. As discussed earlier 9.2 is the optimum pH for lignin depolymerization while here most of the substrates having less pH (Figure 3.18) which gives less product yield. Another factor is that for low molecular weights lignins, repolymerization of products dominates as the same reaction condition was applied. Finally, it can be stated here that these results clearly prove that using this catalytic system it is able to convert various lignin substrates.

	L-Ca	Alkali	L-Na Lignin	Dealkaline	Alkaline
Mw. (Da)	18,000	28,000	52,000	60,000	60,000
pH of R.M.	7.8	7.5	8.5	6.9	9.2
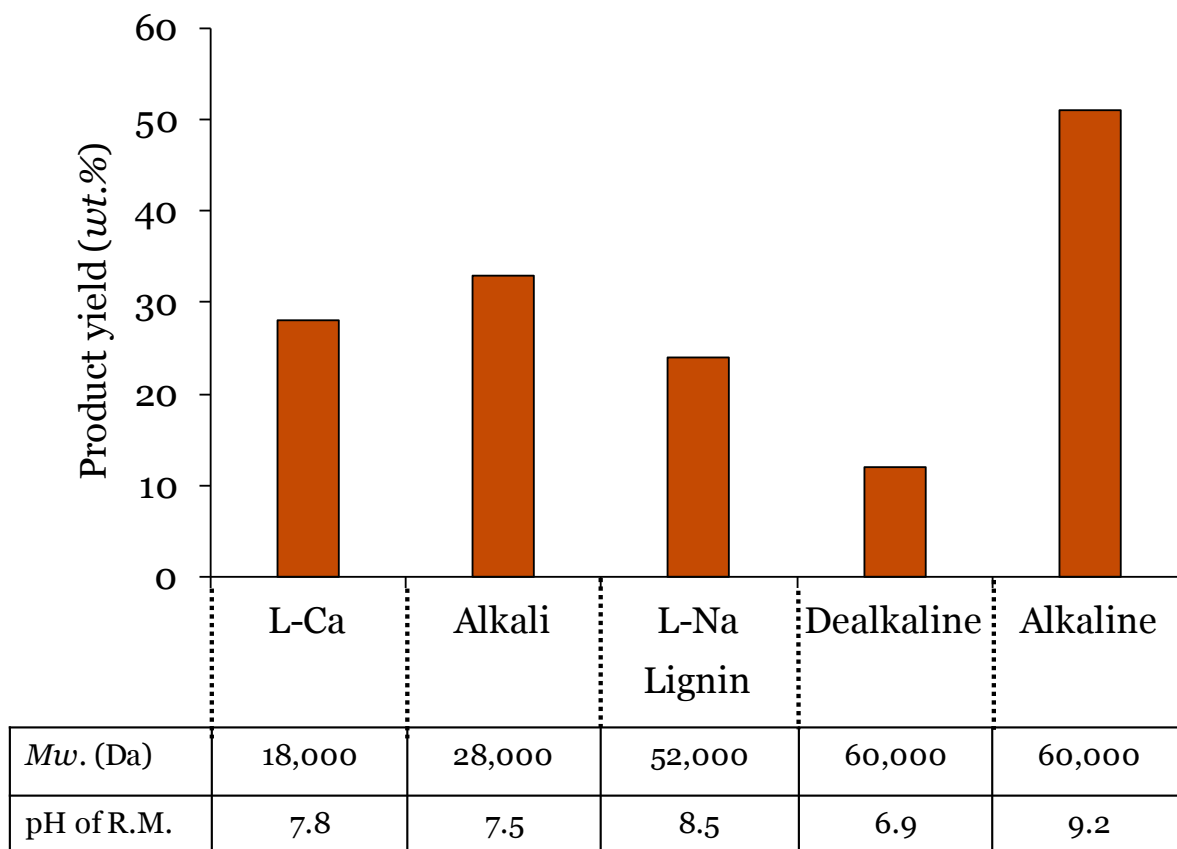
Figure 3.18. Effect of various substrates on depolymerization of lignin.
Reaction condition: Lignin: NaX = 1: 1 $wt./wt.$, EtOH: H_2O (1: 2 v/v) 30 mL, 250 °C, 1 h.
R.M. = Reaction mixture

3.3.11. Confirmation of Aromatic Monomers Formation: GC-FID, GC-MS, HPLC, LC-MS

The primary characterization of organic solvent soluble products (aromatic monomers) was done using GC-FID and GC-MS techniques. But, there might be a possibility of breaking down the organic solvent soluble products (DEE and EtOAc) during GC-FID and GC-MS analysis (as temperatures used for analysis are higher than the reaction temperature (section 3.2.4.1 and 3.2.4.2). To abolish this effect, samples were analyzed by HPLC and LC-MS techniques (section 3.2.4.3 and 3.2.4.4). HPLC profile obtained for reaction mixture is shown in Figure 3.19. The products observed in HPLC analysis are similar to those identified using GC-FID and GC-MS techniques (Figure 3.4-3.7, Table 3.3). Also, from LC-MS analysis it was confirmed that oligomeric products were not formed during the depolymerization reaction of alkaline lignin over solid base catalysts (Figure 3.20-3.23). These results imply that the majority of the products formed under the reaction conditions are aromatic monomers.
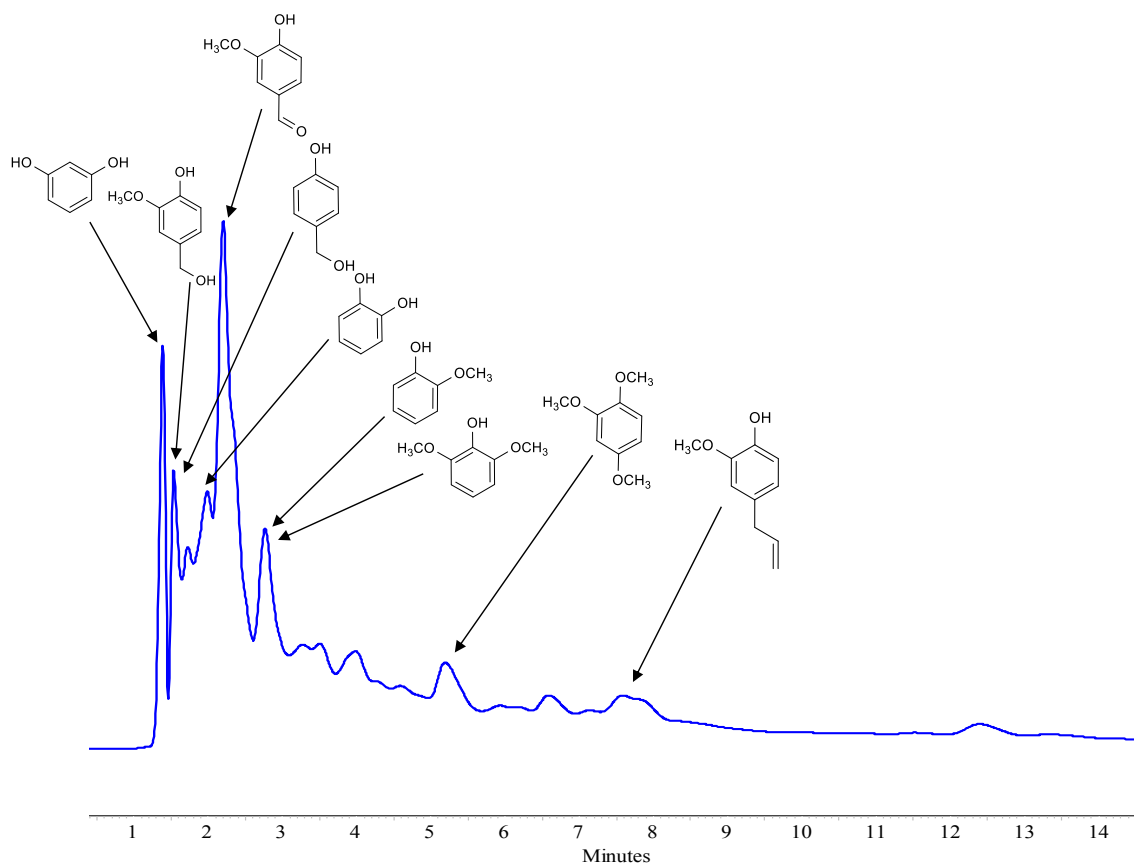
Figure 3.19. HPLC chromatograph of lignin depolymerization products.
Reaction condition: Alkaline lignin: NaX = 1: 1 *wt./wt.*, EtOH: H₂O (1: 2 *v/v*) 30 mL,
250 ºC, 1 h.
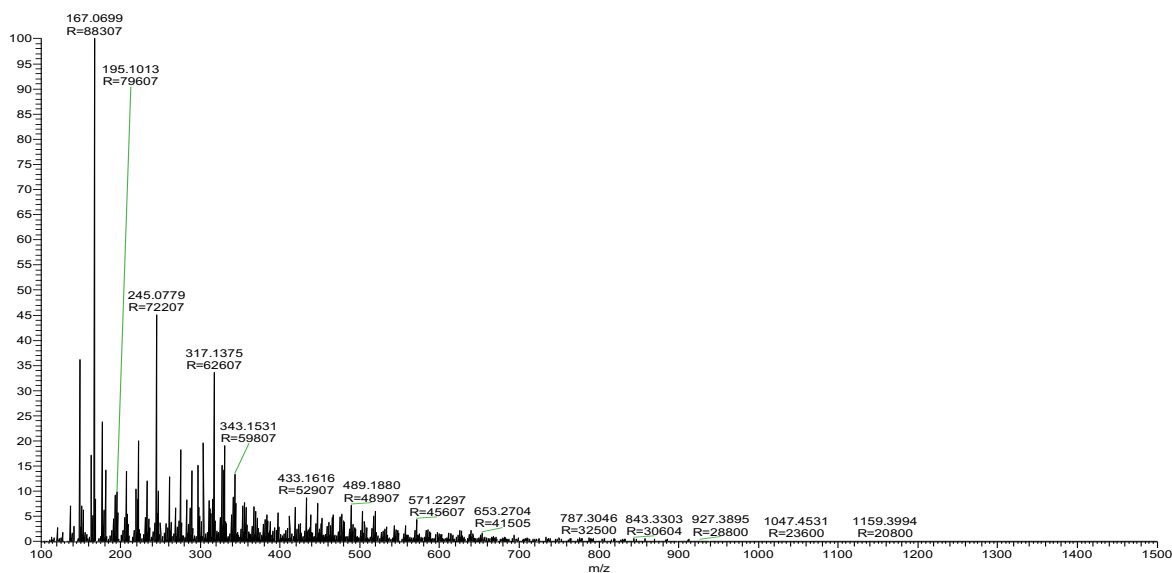
Figure 3.20. LC-MS chromatograph of products extracted in diethyl ether (liquid
fraction) from the solid recovered after evaporation of reaction solvent.
Reaction condition: Alkaline lignin: NaX = 1: 1 *wt./wt.*, EtOH: H₂O (1:2 *v/v*) 30 mL,
250 ºC, 1 h.
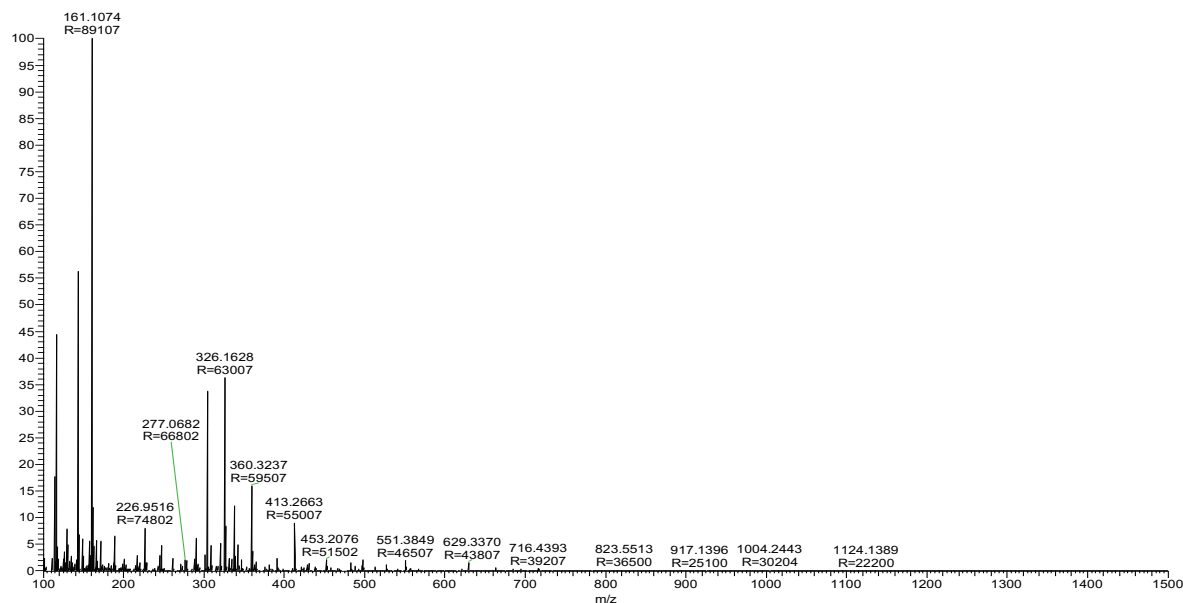
Figure 3.21. LC-MS chromatograph of products extracted in ethyl acetate (liquid fraction) from the solid recovered after evaporation of reaction solvent.

Reaction condition: Alkaline lignin: NaX = 1: 1 *wt./wt.*, EtOH: H_2O (1: 2 *v/v*) 30 mL, 250 °C, 1 h.
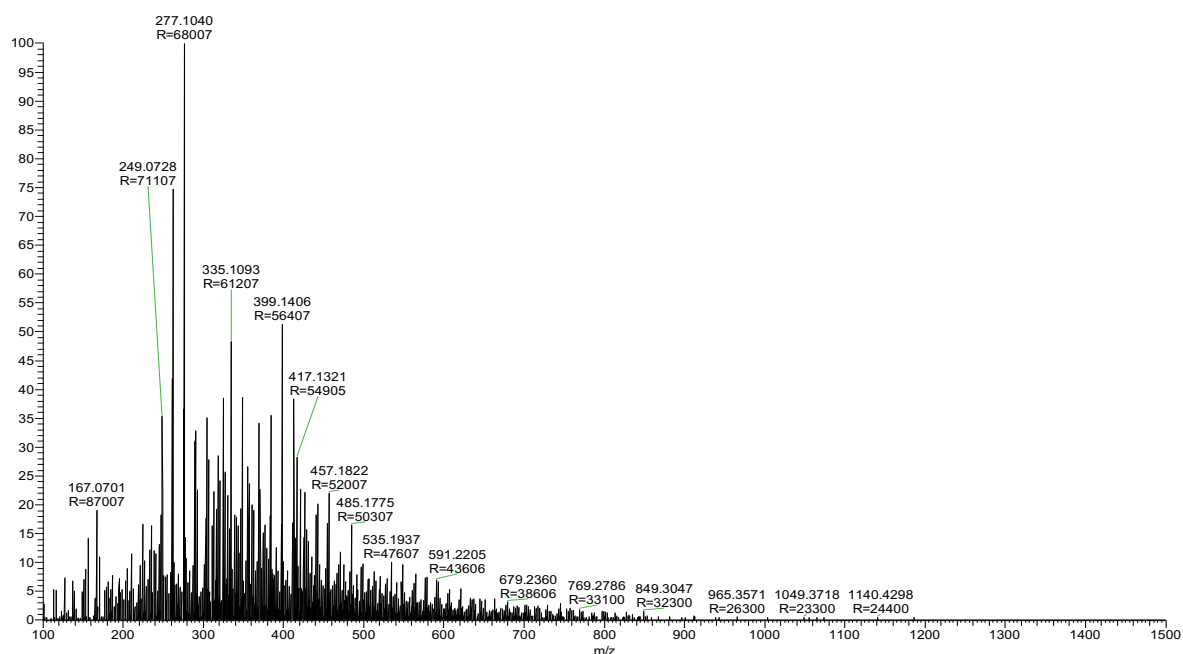
Figure 3.22. LC-MS chromatograph of diethyl products extracted in diethyl ether (solid fraction or filter cake) from the solid recovered after evaporation of reaction solvent.

Reaction condition: Alkaline lignin: NaX = 1: 1 *wt./wt.*, EtOH: H_2O (1: 2 *v/v*) 30 mL, 250 °C, 1 h.
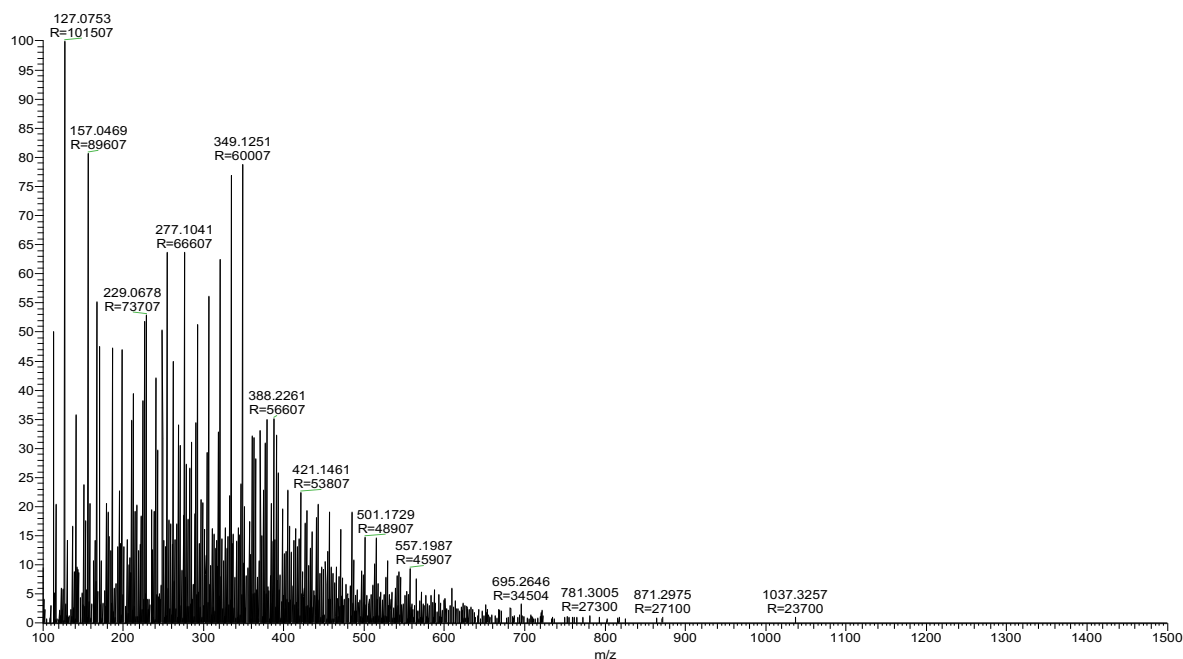
Figure 3.23. LC-MS chromatograph of products extracted in ethyl acetate (solid fraction or filter cake) from the solid recovered after evaporation of reaction solvent. Reaction condition: Alkaline lignin: NaX = 1: 1 *wt./wt.*, EtOH: H_2O (1: 2 *v/v*) 30 mL, 250 °C, 1 h.

3.3.12. Lignin and products characterization

In order to establish a correlation between the structure of the starting material (lignin) and depolymerization products with different functional groups (Table 3.3), FT-IR analysis of alkaline lignin, DEE and EtOAc soluble products was done.
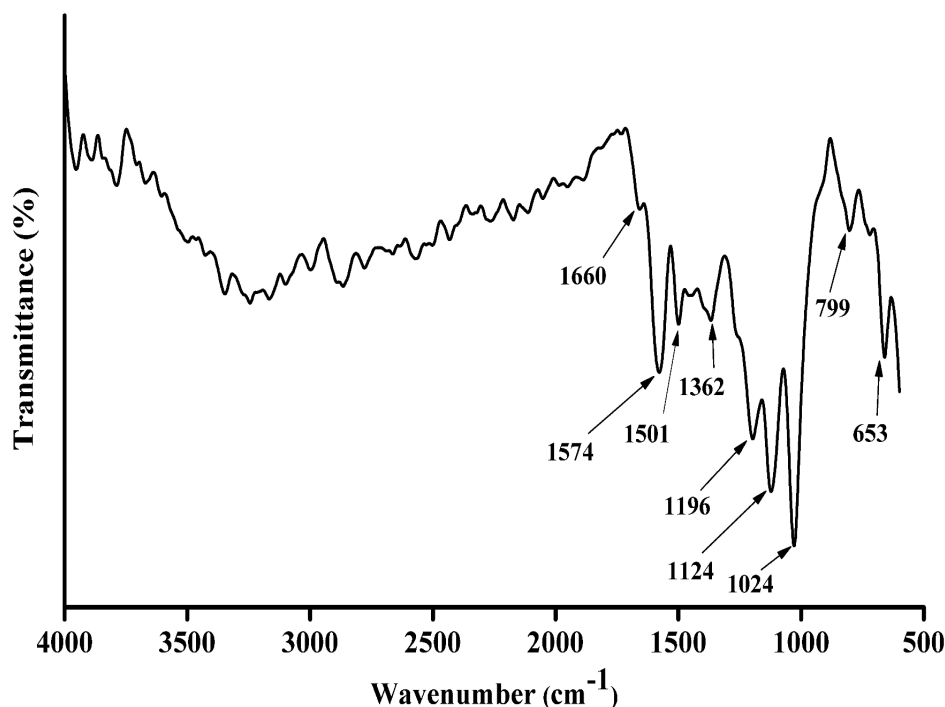
Figure 3.24. FT-IR spectra of alkaline lignin.

As observed from Figure 3.24, alkaline lignin shows a broad peak at 3500-3100 cm⁻¹ for stretching vibrations of alcoholic and phenolic hydroxyl groups (O-H stretching). Peak observed at 1660 cm⁻¹ was attributed to the presence of C=O stretching in α,β-unsaturated aldehyde or ketone. The peak can also be assigned to presence of -C=C- in alkanes. In the range of 1500-1585 cm⁻¹ peaks due to aromatic ring vibrations (C-C stretch (in ring)) are expected. Peak at 1362 cm⁻¹ is characteristic of bend/rock vibration in alkanes. In lignin chemistry this wavelength is also assigned to the syringyl ring breathing with C-O stretching. The peaks at 1124 and 1196 cm⁻¹ can be assigned to deformation vibrations of C-H bonds in syringyl rings or else can be typically assigned to the C-O stretch in alcohols or ethers. Again a strong peak appearing at 1024 cm⁻¹ is attributed to C-O stretch in C-O (alcohol, ether) or the in-plane deformation vibrations of C-H bonds in aromatic rings. The observance of a peak at 799 cm⁻¹ is due to deformation vibrations of C-H (oop) bonds associated to aromatic rings.
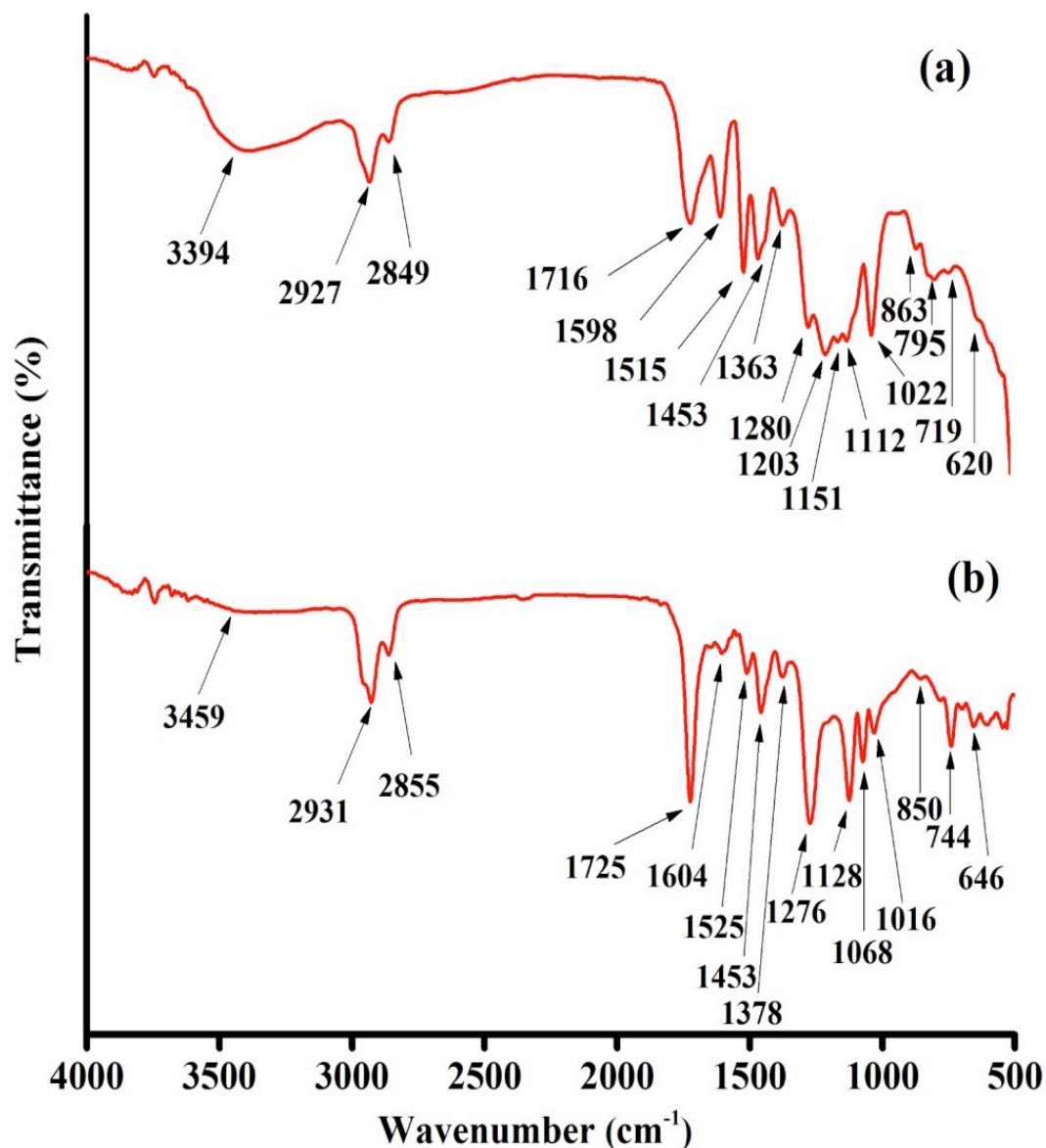
Figure 3.25. FT-IR spectra of DEE (a) and EtOAc (b) soluble products. Reaction condition: Alkaline lignin: Catalyst = 1: 1 *wt./wt.*, EtOH: H_2O (1: 2 *v/v*) 30 mL, 250 °C, 1 h.

An observation of IR spectrum for DEE and EtOAc soluble products (Figure 3.25 a & 3.25 b) shows peaks due to C-H deformation at 620-646 cm⁻¹. Presence of aromatic C-H bending was confirmed with the peak at 700-865 cm⁻¹. A careful look indicates that the intensity of peaks at 1022 and 1068 cm⁻¹ due to alkoxy groups has decreased, indicating that the −C-O-C- bonds are breaking during depolymerization. The retention of the peak at 1112/1128 cm⁻¹, though with lower intensity indicates the presence of vibrations of C-H bonds in syringyl ring. Intense peak seen at 1276 cm⁻¹ is might be due to

asymmetrical ethers formation (Ar-O-CH$_3$). The peak appeared at 1363-1378 cm^{-1} due to bend/rock vibrations in alkanes. The intensities of the peaks from 1450 to 1600 cm^{-1} emphasize that the aromaticity is intact in the products. An intense peak arise at 1716 and 1725 cm^{-1} can be assigned to α,β-unsaturated aldehyde or ketone in depolymerized products. The new peak appearing at 2849 and 2855 cm^{-1} is attributed to the presence of C-H stretching in the aldehyde group. Moreover, another peak at 2927 and 2931 cm^{-1} can be assigned to C-H stretching in alkanes/alkyl groups. A broad peak appearing at 3394 and 3359 cm^{-1} confirm the cleavage of the Ar(C)-O-Ar bond to form the Ar(C)-OH bond. It can be clearly understood that most of the functionalities present in lignin are retained in products. Moreover, appearance and increase in the intensities of peaks of -OCH$_3$, -CHO, and -CH$_3$ groups validate that lignin undergoes depolymerization reaction and gives rise to aromatic monomers which have functional groups as mentioned above. Summary of FT-IR peaks present in lignin and products are consolidated in Table 3.9.

Table 3.9. Summary of FT-IR bands present in lignin and products.

Bands (cm^{-1})	Type of vibration	Wavenumber (cm^{-1})		
		Lignin	Products (DEE)	Products (EtOAc)
3500-3100	Alcoholic & phenolic O-H stretching (free and involved in hydrogen bonding)	3351	3394	3459
2970-2830	C-H asymmetric stretching in methyl and methylene group	2865	2927 2849	2931 2855
1770-1680	C=O stretching in unconjugated ketone, carbonyl and ester groups	1733	1716	1725

1670-1620	C=O stretching in conjugated substituted aryl group	1660	-	-
1615-1590	C=O stretching with aromatic skeleton vibrations	1574	1598	1604
1530-1500	Aromatic skeleton vibrations	1501	1515	1525
1470-1410	Deformation vibrations of C-H bond	1452	1453	1453
1380-1350	Aliphatic C-H stretching in methyl and phenolic OH	1362	1363	1378
1300-1200	C-C, C-O, C=O stretching in guaiacyl units	1264	1280 1203	1276
1195-1124	Deformation vibrations of C-H bonds in syringyl rings	1196	1151	1128
1120-1105	Deformation vibrations of C-H bonds in aromatic rings	1124	1112	-
1030-1010	C-O stretching in alcohol, ether/ in-plane deformation vibrations of C–H bonds in aromatic rings.	1024	1022	1016
875-700	Substitution on aromatic ring or substituted phenolics	799 653	863 795 719	850 744

Elemental analysis of DEE and EtOAc soluble products was done. Presence of 53% C and 4% H was observed, this matches well with the elemental analysis of alkaline lignin (Refer chapter 2A, Section 2A.3.1, Table 2A.2, C = 52% and H = 5%) indicating that almost no loss of any functional groups even after depolymerization reaction. The molecular formula thus calculated for products with the help of CHNS analysis, ($C_{8.8}H_{7.9}O_{5.4}$) almost matches with alkaline lignin ($C_{8.7}H_{9.1}O_{5.1}S_{0.13}$). The absence of 'S' in the products might be due to the insolubility of 'S' containing products in DEE and EtOAc solvents in which products are extracted. Again, it proved from CHNS analysis also that no functional groups are lost during the depolymerization.

To further prove that in this work mainly aromatic monomers are formed as products, UV-Vis spectroscopy analysis of the DEE and EtOAc soluble products was done (Figure 3.26).
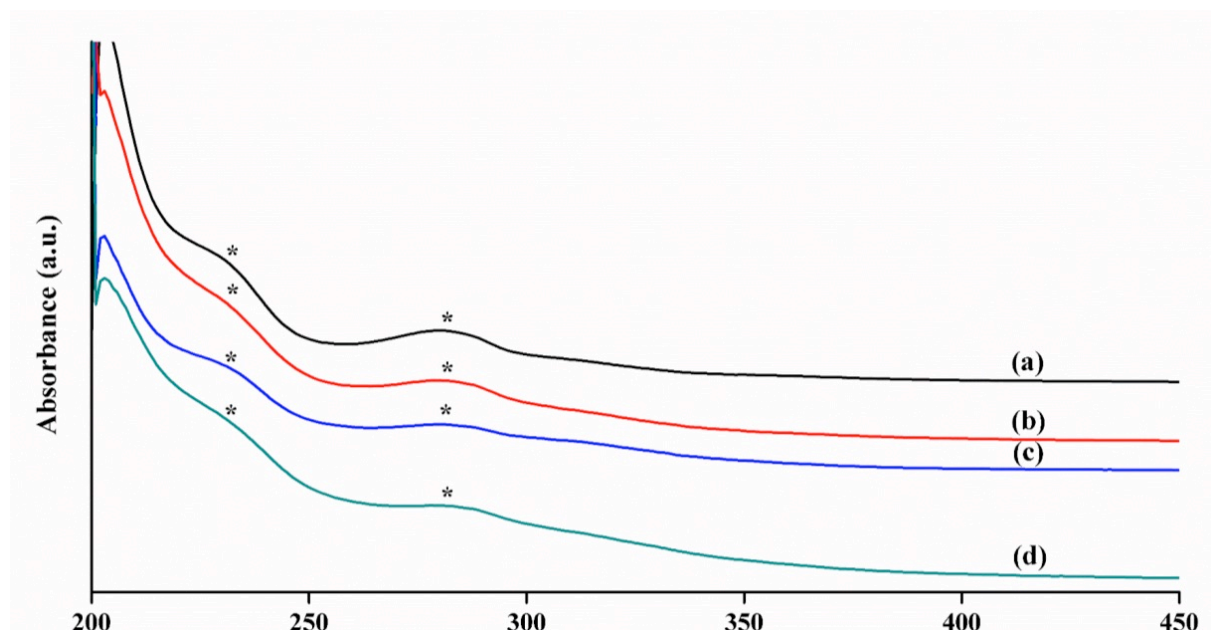
Figure 3.26. UV analysis of products (a) DEE soluble products from liquid, (b) EtOAc soluble products from liquid, (c) DEE soluble products from solid, (d) EtOAc soluble products from solid. Reaction Condition: Lignin: NaX = 1: 1 *wt./wt.*, EtOH: H_2O (1: 2 *v/v*) 30 mL, 250 °C, 1 h (* Characteristics peak for aromatics).

It is known that absorption bands due to aromatics appear between 200 and 350 nm because of π/π* transitions. Figure 3.26 shows the UV-Vis pattern for the products and it matches well with the UV-Vis pattern of alkaline lignin (Chapter 2A, Section 2A.3.7). It is also known that if polycyclic aromatic compounds are formed then absorption bands shifts to longer wavelengths. Since in the products it is not

possible to see absorption bands at such a higher wavelength, hence it was again confirmed that only aromatic monomers are formed.

3.3.13. Catalyst Recyclability

In the catalyst recyclability study, NaX was recovered from the reaction mixture by centrifugation and later was washed with ethanol: water (1: 2 *v/v*). Further catalyst was dried at 55 °C for 16 h and used in the next reaction. With fresh catalyst, 51% yield was observed and later in the 1st recycle run decrease in yield to 34% was seen. In subsequent recycle run almost similar yield was seen (35% in 2nd run, 33% in 3rd run) (Figure 3.27). Nevertheless, it is interesting to note here that though in recycle runs total yield was decreased but formation of DEE soluble products was same, which actually is important in this reaction. The non-catalytic reaction under similar reaction conditions gave 24% yield which is still less than the recycle run.
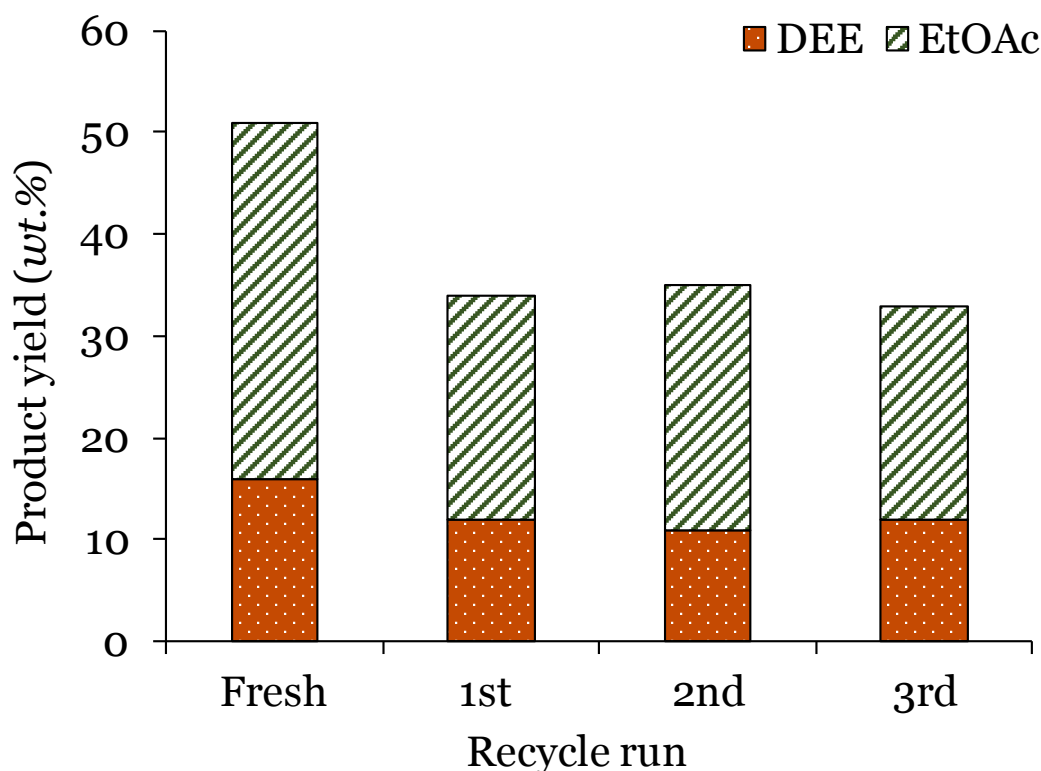
Figure 3.27. Recyclability of catalyst (NaX).
Reaction condition: Alkaline lignin: NaX = 1: 1 *wt./wt.*, EtOH: H_2O (1: 2 *v/v*) 30 mL, 250 °C, 1 h.

3.3.13.1. Catalyst Characterization and Stability

All the catalysts evaluated for their depolymerization activities in this study were characterized by CO_2-TPD, XRD, ICP, and N_2 sorption techniques (Chapter 2B, catalyst characterization) and the details on their properties are summarized in Table 2B.2.1.

Since NaX catalyst has shown best activity and was also used in recycle runs, properties of spent NaX catalyst (250 °C, 1 h) were compared with fresh catalyst. The XRD of fresh and spent NaX catalyst showed similar peak pattern (Figure 3.28) although with decrease in the peak intensities in spent catalyst. This indicates that the catalyst underwent slight structural deformations during the reaction, which might be the reason why catalyst showed decline in activity in recycle runs. However, it was seen that the Si/Al ratio in spent catalyst matched well with the fresh catalyst (ICP, Table 3.9).
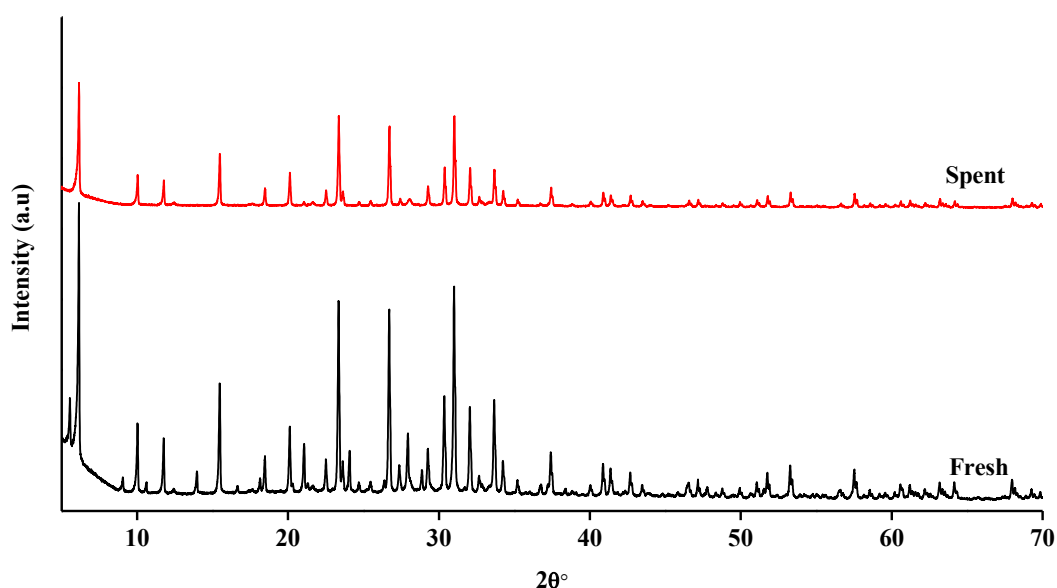
Figure 3.28. XRD of fresh and spent NaX catalyst.

From the CO_2-TPD analysis, total basicity in spent and fresh catalysts was calculated. As seen from Figure 3.29, the TPD profiles for both fresh (0.42 mmol/g) and spent (0.41 mmol/g) catalysts match well and therefore almost similar basicity was calculated. From these characterizations (Table 3.10 and Figure 3.29) it is revealed that the catalyst is mostly stable under reaction conditions. From ICP-OES analysis

(Table 3.9), it is observed that 3.24 mg of additional Na is observed on the spent catalyst as against 17.3 mg Na present on fresh NaX catalyst. The increase of Na may arise from the lignin substrate (Table 3.10 and Chapter 2A, Table 2A.3).

Table 3.10. CO_2-TPD, N_2 sorption and ICP-OES analysis of fresh & spent NaX catalyst.

Catalyst	CO_2-TPD	Nitrogen sorption			ICP-OES		
NaX	Total basicity (mmol/g)	BET surface area (m^2/g)	Pore size (nm)	Pore volume (cm^3/g)	Si/Al ratio (a)	Si/Al ratio (b)	Na Content (mg/g)
Fresh	0.42	582	1.1	0.3	1.2	1.2	17.3
Spent	0.41	586	1.1	0.3	-	1.2	20.5

(a) Actual Si/Al ratio, (b) Observed Si/Al ratio
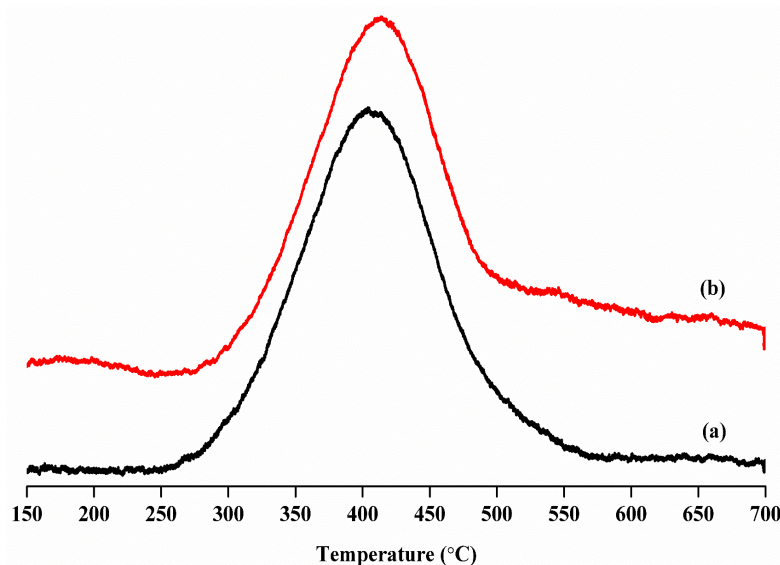
Figure 3.29. CO_2-TPD profile of (a) fresh and (b) spent NaX.

Early literature reports show that protonated zeolites have lower hydrothermal stability when heated at around 200 °C in water[4] during the conversion of hemicellulose. Later many detailed studies are done to show that acidic zeolites are unstable under reaction condiitions used in biomass conversions.[4, 36-38] It can also be noted that large volume of literature is available on the stability of zeolites under alkaline conditions used during their synthesis

and post-modifications.[39] It is claimed that based on the concentration of the charge-balancing counter cations (CBCC) stability of zeolites can be manipulated. Recent findings show that with an increase in CBCC, better resistance to alkaline conditions is possible. Also, it is mentioned that typically zeolites undergo hydrolysis of ≡Si-O-Si≡ bonds under acidic conditions or even under neutral conditions but when higher temperatures (due to change of ionic product, Kw) are used.[40] In basic media the stability of bonds typically follows =Al−O−Si≡ >> ≡Si−O−Si≡ order.[40] Since in this work basic zeolites are used with Si/Al ratio of 1-2.7, it appears that those are more stable than their acidic counterparts since under alkaline conditions, hydrolysis of =Al−O−Si≡ and ≡Si-O-Si≡ bonds is minimized. Nevertheless, it is reported that when highly alkaline solutions are used, base catalyzed hydrolysis of these bonds is also possible. Additionally, literature also reveals that stability of basic zeolites is dependent on size of cation.[41] For instance when Na is used as a cation, stability is better than Li exchanged zeolite. This is because with increase in cation size, diffusion of water or adsorption of water over catalyst is lowered. It is anticipated that in this work, since lower Si/Al ratio zeolites are used having basicity and Na as counter cation, those tend to stabilize the catalyst from hydrothermal degradation. It is postulated that because of presence of Na, even if water has higher Kw at elevated temperatures than at ambient temperature, acidity is neutralized.

3.4. Conclusion

In summary, depolymerization efficiencies of various solid base catalyst were evaluated and it was revealed that the solid base catalyst, NaX is capable of depolymerizing high molecular weight lignin (60,000 Da) into low molecular weight aromatic products (51% yield) in an ethanol: water (1: 2 v/v) ratio solvent system. The optimization of reaction conditions and detailed studies on catalyst properties reveal that pH 9.2 is optimum to catalyze depolymerization and catalyst having strong basicity are detrimental in yielding higher quantities of low molecular weight products. A unique product adsorption studies indicate that strong bases have more tendency to adsorb the products. Moreover, it is shown with the help of various

analytical tools that most of the functional groups present on lignin are retained in products thereby improving the atom efficiency.

3.5. References

1.   A. M. Ruppert, K. Weinberg and R. Palkovits, *Angew Chem Int Ed Engl*, 2012, 51, 2564-2601.

2.   M. R. Sturgeon, M. H. O'Brien, P. N. Ciesielski, R. Katahira, J. S. Kruger, S. C. Chmely, J. Hamlin, K. Lawrence, G. B. Hunsinger, T. D. Foust, R. M. Baldwin, M. J. Biddy and G. T. Beckham, *Green Chem.*, 2014, 16, 824-835.

3.   P. L. Dhepe and R. Sahu, *Green Chemistry*, 2010, 12, 2153.

4.   R. Sahu and P. L. Dhepe, *ChemSusChem*, 2012, 5, 751-761.

5.   B. M. Matsagar and P. L. Dhepe, *Catal. Sci. Technol.*, 2015, 5, 531-539.

6.   A. P. Tathod and P. L. Dhepe, *Bioresour Technol*, 2015, 178, 36-44.

7.   J. F. Stanzione, 3rd, J. M. Sadler, J. J. La Scala and R. P. Wool, *ChemSusChem*, 2012, 5, 1291-1297.

8.   E. Adler, *Wood Sci. Technol.*, 1977.

9.   F. S. Chakar and A. J. Ragauskas, *Industrial Crops and Products*, 2004, 20, 131-141.

10.   K. L. John Ralph, Gösta Brunow, Fachuang Lu, Hoon Kim, Paul F., J. M. M. Schatz, Ronald D. Hatfield, Sally A. Ralph, Jørgen Holst Christensen and W. Boerjan, *Phytochemistry Reviews*, 2004.

11.   J. P. John Ralph, Fachuang Lu,Ronald D. Hatfield,and Richard F. Helm, *J. Agric. Food Chem.*, 1999.

12.   A. K. Deepa and P. L. Dhepe, *RSC Advances*, 2014, 4, 12625.

13.   A. K. Deepa and P. L. Dhepe, *ACS Catalysis*, 2015, 5, 365-379.

14.   R. K. S. a. N. N. Bakhshi', *Energy & Fuels*, 1992.

15.   M. M. H. a. R. W. Thring, *J. Chem. Eng.*, 2000.

16.   J. A. Onwudili and P. T. Williams, *Green Chem.*, 2014, 16, 4740-4748.

17.   S. K. Singh and P. L. Dhepe, *Green Chem.*, 2016, DOI: 10.1039/c6gc00771f.

18.   K. Stark, N. Taccardi, A. Bosmann and P. Wasserscheid, *ChemSusChem*, 2010, 3, 719-723.

19.   N. Yan, C. Zhao, P. J. Dyson, C. Wang, L. T. Liu and Y. Kou, *ChemSusChem*, 2008, 1, 626-629.

20. W. Xu, S. J. Miller, P. K. Agrawal and C. W. Jones, *ChemSusChem*, 2012, 5, 667-675.

21. Q. Song, F. Wang, J. Cai, Y. Wang, J. Zhang, W. Yu and J. Xu, *Energy & Environmental Science*, 2013, 6, 994.

22. S. Van den Bosch, W. Schutyser, R. Vanholme, T. Driessen, S. F. Koelewijn, T. Renders, B. De Meester, W. J. J. Huijgen, W. Dehaen, C. M. Courtin, B. Lagrain, W. Boerjan and B. F. Sels, *Energy Environ. Sci.*, 2015, 8, 1748-1763.

23. Wahyudiono, T. Kanetake, M. Sasaki and M. Goto, *Chemical Engineering & Technology*, 2007, 30, 1113-1122.

24. T. Furusawa, T. Sato, M. Saito, Y. Ishiyama, M. Sato, N. Itoh and N. Suzuki, *Applied Catalysis A: General*, 2007, 327, 300-310.

25. Z. Yuan, S. Cheng, M. Leitch and C. C. Xu, *Bioresour Technol*, 2010, 101, 9308-9313.

26. J. Long, Q. Zhang, T. Wang, X. Zhang, Y. Xu and L. Ma, *Bioresour Technol*, 2014, 154, 10-17.

27. K. Barta, G. R. Warner, E. S. Beach and P. T. Anastas, *Green Chem.*, 2014, 16, 191-196.

28. http://www.tcichemicals.com/eshop/en/in/commodity/L0082/.

29. http://www.zeolyst.com/our-products/standard-zeolite-powders/zeolite-y.aspx.

30. R. Beauchet, F. Monteil-Rivera and J. M. Lavoie, *Bioresour Technol*, 2012, 121, 328-334.

31. W. Z. Joseph Shabtai, Esteban Chomet, and and D. K. Johnson, *Amer. Chemical Soc.*, 1999.

32. H. Hattori, *American Chemical Society*, 1995, 95, 537-558.

33. http://www.lime.org/documents/lime_basics/lime-physical-chemical.pdf.

34. D. E. Gardner and B. Walker, *Journal*, 2000, 99-131.

35. http://periodic-table-of-elements.org/SOLUBILITY.

36. F. S. b. Ryan M. Ravenelle, Andrew D'Amico, Nadiya Danilina, Jeroen A. van Bokhoven, Johannes A. Lercher, Christopher W. Jones, and Carsten Sievers, *J. Phys. Chem. C*, 2010, 114, 19582-19595.

37. H. Xiong, H. N. Pham and A. K. Datye, *Green Chem.*, 2014, 16, 4627-4643.

38. L. Zhang, K. Chen, B. Chen, J. L. White and D. E. Resasco, *J Am Chem Soc*, 2015, 137, 11810-11819.

39. J. V. A. Thijs Ennaert , Jan Dijkmans , Rik De Clercq , Wouter Schutyser , Michiel Dusselier , Danny Verboekend and Bert F. Sels *Chem. Soc. Rev.*, 2016, 45, 584-611.

40. D. Verboekend, M. Milina and J. Pérez-Ramírez, *Chemistry of Materials*, 2014, 26, 4552-4562.

41. J. P. B. J.C. Moise, A. Methivier, *Microporous and Mesoporous Materials*, 2001, 43, 91-101.

Chapter 4
Coconut Coir: Lignin Isolation, Characterization and Depolymerization of Isolated Lignin and Coir

4.1. Introduction

In Chapter 2 and 3, characterization and depolymerization of commercially procured lignin(s) is discussed. It was very clear from the characterizations that these samples possessed sodium contamination. As discussed in the chapter 1, lignocellulosic biomass is mainly composed of polysaccharides and lignin. So, it is also preferable to use abundant and inexpensive lignocellulose material (coconut coir) directly for the synthesis of value-added aromatic chemicals in order to develop a sustainable future technology. For the isolation of lignin, different methods are known in the literature e.g. Klason, Kraft, Soda, Lignosulfonate, Hydrolysis, Ionic liquids processes, Enzymatic, etc.[1-5] Most of these processes possess few of the drawbacks mentioned below like use of costly ionic liquid as solvent, contamination of metal, use of costly enzymes and longer time required for enzymatic process or harsh reaction conditions used etc. (Refer Chapter 1, Section 1.7, Figure 1.8). Out of the several known processes for the isolation of lignin four main industrial processes are currently used for producing high-purity lignin; the Sulfite (Lignosulfonate), Soda, Kraft, and Organosolv processes.[6] In this work, Klason, Organosolv and Soda processes were chosen for isolation of lignin. Klason method was chosen as it allows the complete isolation of lignin from the lignocellulosic material. The Organosolv process was selected since it uses milder reaction condition and isolated lignin is obtained in pure form. And to carry out a comparative study, Soda process was also used as is known to produce lignin at industrial scale.

Here, the waste coconut coir was used for the isolation of lignin, since coconut is one of the oldest crops grown in India and presently covers ca. 1.5 million hectares in our country.[7] The approximate quantity of coconut production per annum in world is shown in Table 4.1. Moreover, it is most readily available material that farmers and people in the community had access to. So, it was chosen as raw material and studied whether coconut waste (coconut coir) was a viable source for the lignin isolation and production of value-added chemicals, and what we could do more with it.

Table 4.1. Top worldwide coconut producers in 2013.[8]

Country	Annual Production (tonnes)
Indonesia	18.3×10^6
Philippines	15.3×10^6
India	11.9×10^6
Brazil	2.9×10^6
Sri Lanka	2.5×10^6
World	62.4×10^6

Coconut plays an important role in the economic, social and cultural activities of millions of people in our country. All parts of coconut tree are thus useful in one way or other and the crop profoundly influences the socio-economic security of millions of farming families. A typical cross section of coconut is shown in Figure 4.1.

According to official website of International Year for Natural Fibres 2009, approximately, 500 000 tonnes of coconut fibres (coir) are produced annually worldwide, mainly in India and Sri Lanka[9]. Its total value is estimated at $100 million. India and Sri Lanka are also the main exporters, followed by Thailand, Vietnam, Philippines and Indonesia. Around half of the coconut fibres produced is exported in the form of raw fibre.[10]
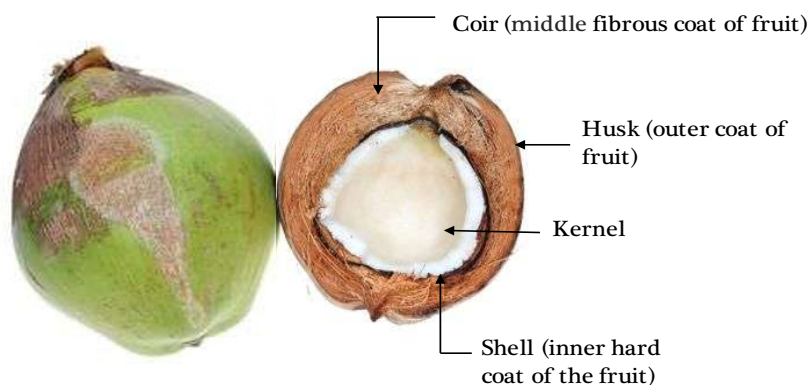
Figure 4.1. Cross Section of Coconut.

Coir is a biomass residue which is generated during the extraction of coir fibre from coconut husk and is a by-product of the coir manufacturing industry. The available literature for the chemical composition of coconut coir is presented in Table 4.2.

Table 4.2. Chemical composition of coconut coir.

S.No.	Water soluble (%)	Pectin & related compounds (%)	Hemi-cellulose (%)	Cellulose (%)	Lignin (%)	Ash (%)	Ref.
1.	5.25	3.30	0.25	43.44	45.84	2.22	[11]
2.	nd	nd	31.1	33.2	20.5	nd	[12]
3.	nd	nd	15-28	35-60	20-48	nd	[13]
4.	nd	nd	16.8	68.9	32.1	nd	[14]
5.	nd	nd	-	43.0	45.0	nd	[15]
6.	nd	nd	0.15-0.25	36-43	41-45	nd	[16]
7.	nd	3.0	0.25	43.44	45.84	5.6	[17]

The main content of coconut coir is cellulose, hemicellulose and lignin. Cellulose and hemicellulose is polysaccharide compound while lignin is a macromolecules polyphenolic compound.[18] Compared to other lignocellulosic materials (wheat straw, rice husk, bagasse, etc.) wherein lignin content is 10-35%, coir contains higher amount of lignin (20-48%). Available literature also focuses that lignin content in coconut coir is very high which are commercially valuable (20-48%).[18-20] Its accumulation on the ground during rainy seasons can pollute the soil and water through leaching of polyphenols which makes the coir pith unfit for the normal landfill practices. Therefore, suitable waste management strategies have to be employed to solve the pollution risks arising due to this particular lignocellulosic biomass. Recent research programs are focusing to convert waste coir pith in to useful products such as biomanure,[21] biochar[22] etc. The lignocellulosic composition

of the coconut coir can be explored for utilizing it as a substrate for bioenergy and for the production of value-added chemicals.

Traditionally, farmers harvested coconuts only to produce coconut milk and coconut oil while the husks and fibre/coir were not used significantly. Looking at the above concerns (high lignin content and reducing waste in an economical way), it was believed that coir can be converted into value-added chemicals. The initial phase of the research was to try to understand the lignin content in the coconut coir. Further, the isolation of lignin from the coconut coir was focused by three methods namely, Klason, Organosolv and Soda process followed by its complete characterization and depolymerization. Moreover, possibility of direct utilizing the coconut coir as a substrate for the production of value-added chemicals was also studied.

4.2. Experimental

4.2.1. Chemicals and Materials

After utilizing the edible part of coconut, the remaining non-edible part (raw biomass) is generally thrown away or used in non-economical way. So, coconut wastes were collected from the road side vendors of different places of Maharashtra. All the samples were first dried in sunlight for two days and further oven dried at 55 °C for 16 h. The dried coconut coir was crushed to powder form and kept in oven at 55 °C for 16 h followed by vacuum drying at 120 °C for 4 h and stored in air-tight lid container. Basic zeolite, NaX (Si/Al = 1.2) was procured from Zeolyst international. Various aromatic monomers like Guaiacol (99%), 2-methoxy-4-methylphenol (98%), pyrocatechol (99%), resorcinol (99%), 2,6-dimethoxyphenol (99%), 4-hydroxy benzyl alcohol (99%), Diethylterephthalate (99%), 2,4-ditert-butylphenol (99%), Acetoguaiacone (98%), 4-hydroxy-3-methoxybenzyl alcohol (98%), 1,2,4-trimethoxybenzene (97%), vanillin (99%), eugenol (99%), 3,4-dimethoxyphenol (99%) used for GC calibration were purchased from Sigma Aldrich, Alfa Aesar and TCI chemicals. All the chemicals were used as received. Solvents like ethanol (99%, Changshu Yangyuan Chemical Co., Ltd, China), diethyl ether (99.9%, LOBA Chemie) and ethyl acetate (99.9%, LOBA Chemie) were purchased and used as received. NaOH (98%, Loba Chemie), H_2SO_4 (98%, Loba Chemie), HCl (37%, Merck)

and HF (48%, Merck) were also purchased and used as received. Distilled water was used for all the experiments.

4.2.2. Lignin Isolation from Coconut Coir (CC)

For the value addition to lignin, the bio-refinery concept starts from the isolation of lignin from lignocellulosic materials. For that several methods are known in the literature such as, Kraft, Soda, Lignosulfonate, Hydrolysis, Milled Wood Lignin, Enzymatic, Ionic liquids process etc.[23, 24] Depending upon the isolation methods the structural and chemical properties of isolated lignin may vary. It is well known from the literature that linkages and functional groups present in lignin varies from plant to plant. Due to these reasons, determination of the exact structure, bonding and functional group present in lignin is still a big challenge for the researchers. Among various procedures known for the isolation of lignin, here three processes namely, Klason, Organosolv and Soda process for the delignification of coconut coir (CC) was used. The detailed analysis procedures are described below.

4.2.2.1. Klason method

Typically, 1 g biomass sample was taken in a 100 mL RB flask and digested it with 15 mL 72% H_2SO_4 (*wt./wt.*). Then the mixture was stirred vigorously at 30 °C for 2 h. Next, in another 1000 mL RB, 150 mL of water was taken and transferred the H_2SO_4 digested mass slowly as this step is an exothermic reaction. Subsequently, the leftover or sticked H_2SO_4 digested mass in 100 mL RB was washed thoroughly with 195 mL water and the total solution was transferred into 1000 mL same RB (current H_2SO_4 concentration = 3% *wt./wt.*). Then 1000 mL RB flask was kept in preheated oil bath at 100 °C for 4 h with continuous stirring. Later, the RB was kept at 30 °C for 16 h to settle down the solid. After settling down, the solid mass was filtered through G2 crucible and washed thoroughly with distilled water. The solid collected in crucible was dried at 55 °C for 16 h and then at 110 °C for 1 h under vacuum (10^{-4} MPa). This solid mass was called as 'uncorrected lignin'. Later, the uncorrected lignin mass was subjected for ash correction. The uncorrected lignin was heated at 620 °C for 2 h in presence of air. Final ash corrected lignin is termed as Klason Lignin (CC-KL).

$$\text{Ash Corrected Lignin} = \frac{(\text{Wt. of uncorrected lignin} - \text{Wt. of ash})}{\text{Oven dried (OD) wt. of coir}} \text{ x 100}$$

Below, the detailed process of Klason method is presented in diagram for better understanding (Figure 4.2).

Coir (1.0 g) in 100 mL RB + 72% H_2SO_4 (15 mL)

⬇ Stirred vigorously @ 30 ⁰C, 2 h

Another 1000 mL RB + 150 mL H_2O + Transferred H_2SO_4 digested mass slowly

⬇

Wash 100 mL RB with 195 mL H_2O & transfer it into 1000 mL RB

⬇

1000 mL RB placed in preheated oil bath @ 100 ⁰C, 4 h, stirring

⬇

Kept RB @ 30 ⁰C, 16 h

Filtered with G2 crucible & washed with H_2O

Liquid
(Acid soluble lignin, Polysaccharides)

Solid

⬇

Oven dried @ 55 ⁰C, 16 h

⬇

Vacuum Dried @ 110 ⁰C, 1 h

⬇

Uncorrected Lignin

⬇

Heat @ 620 ⁰C, 2 h for ash correction

⬇

Klason Lignin

Figure 4.2. Schematic representation of Klason method.

From Klason method 48% of the lignin yield was obtained. Since this procedure is known for the quantification of lignin present in the lignocellulosic biomass, it is estimated that the coir used in this study has 48% lignin content. The isolation experiments were performed at least three times to check the reproducibility of isolation processes. So, it is believed that 100% isolation of lignin from coconut coir is possible using Klason method.

4.2.2.2. Organosolv method

In a typical procedure, 8.0 g of coconut coir (CC) was dispersed in 1.024 mmol of H_2SO_4 solution. EtOH: H_2O (1: 1 *v/v*, 60 mL) was used as a reaction media. The reaction was done in Parr autoclave coated with Teflon liner. Initially stirring was kept to 100 rpm. After attaining the desired temperature (180 °C) stirring was increased to 1000 rpm. After completing the 1 h of reaction time autoclave was cooled to room temperature under flow of air and water flow. The mixture was filtered through whatmann filter paper (No. 110) in order to separate solid (pulp: solid containing cellulose, hemicellulose, ash etc.) and liquid (containing lignin and soluble sugar). Afterwards, the separated solid (pulp) was dried in an oven at 55 °C for 16 h. Later, this solid (pulp) was dried under vacuum (10^{-4} MPa) at 90 °C for 4 h. Liquid fraction was subjected for the addition of three volumes of distilled water of the initial volume of solvent taken (180 mL) in order to precipitate the hydrophobic lignin designated as organosolv lignin (CC-ORGL). During this course, soluble sugars would be separated out from the precipitated lignin. Lignin precipitation was possible from ethanol-water mixture because lignin is not soluble in water and addition of extra water acted as an antisolvent. Finally, precipitated lignin (CC-ORGL) was then filtered through whatmann filter paper (No. 110) thoroughly washed with 100 mL of water and then dried in an oven maintained at 55 °C for 16 h. Later it was dried under vacuum (10^{-4} MPa) at 90 °C for 4 h. All the isolation experiments were performed at least three times to check the reproducibility of isolation processes and in order to avoid any experimental error. The data presented here is the average of three experiments (Figure 4.3).

Coir (8.0 g) + H_2SO_4 (1.024 mmol) + EtOH:H_2O (60 mL, 1:1 v/v)

180 °C, 1 h

Cooled reaction mixture

Filter

Solid
(Pulp; Cellulose, Hemicellulose, Ash, etc)

Oven Dried @ 55 °C, 16 h

Vacuum Dried @ 90 °C, 4 h

Liquid
(Lignin & Soluble Sugars)

180 mL H_2O

Precipitate
(Hydrophobic lignin)

Liquid

Soluble Sugars

Wash with 100 mL H_2O

Oven Dried @ 55 °C, 16 h

Vacuum Dried @ 90 °C, 4 h
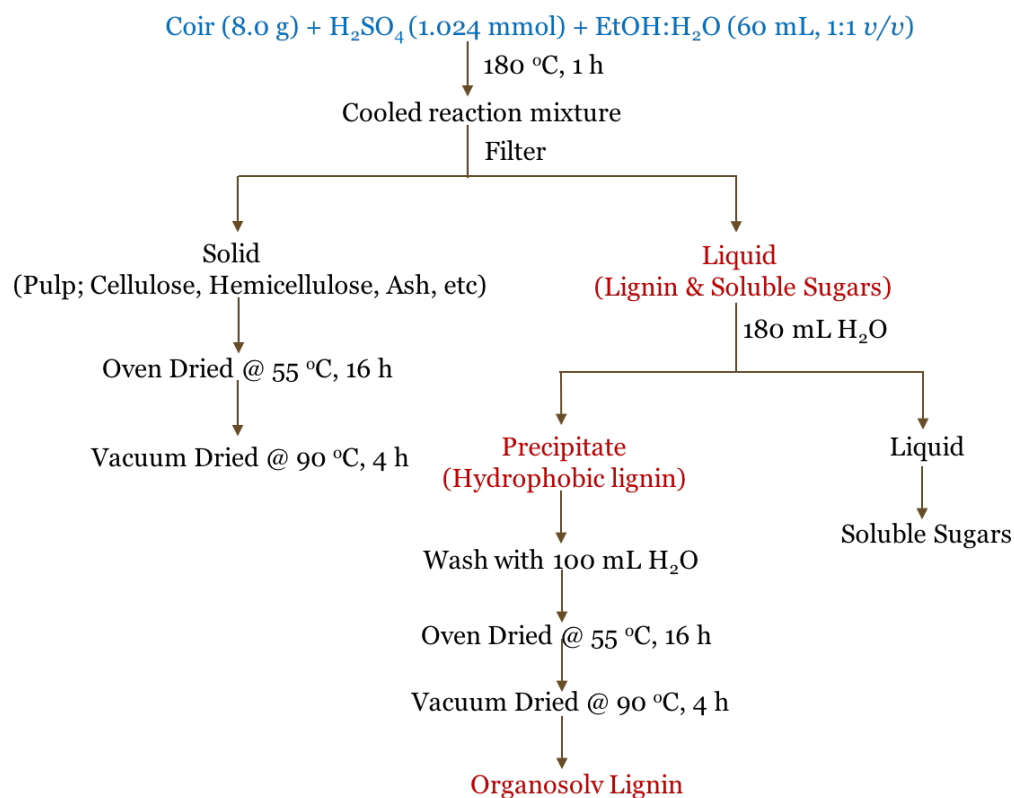
Organosolv Lignin

Figure 4.3. Schematic representation of Organosolv method.

The yield for the Organosolv lignin was calculate on the basis of total lignin present in coir (48%). Considering this 48% as 100%, the yield for organosolv lignin is 16%.

4.2.2.3. Soda method

To carry out the lignin isolation, the technique described by Lai and Sarkanen[25] was used. In a typical procedure, 3 g of coconut coir (CC) was subjected to a digestion process in a 60 mL of 2 *wt.%* NaOH solution. After cooling the reaction mixture, it was filtered and washed thoroughly with distilled water. The cellulosic residues were washed off with distilled water to separate out the solid cellulosic residue and liquid (soluble sugars and lignin). The aqueous solution (liquid) was acidified to pH 1 with the addition of concentrated H_2SO_4 and allowed to boil for one hour under reflux. The precipitate obtained in this operation was separated by filtration through coarse-porosity filter paper and washed with distilled water until a pH 7 was reached. The resulting lignin (CC-SL) was dried in an oven maintained at 55 °C for 16 h. Later it was dried under vacuum (10^{-4} MPa) at 100 °C for 4 h (Figure 4.4).

Coir (3.0 g) + 2 *wt.%* NaOH Solution (60 mL)

160 °C, 5 h

Cooled reaction mixture

Filtered & washed with H_2O

Solid
(Cellulosic residue)

Liquid

Acidified to pH 1
with conc. H_2SO_4

Oven Dried @ 55 °C, 16 h

Boiled, 1 h

Kept for 12 h

Vacuum Dried @ 90 °C, 4 h

Precipitate obtained

Filtered & washed with H_2O until pH comes 7

Oven Dried @ 55 °C, 16 h

Vacuum Dried @ 90 °C, 4 h

Soda Lignin
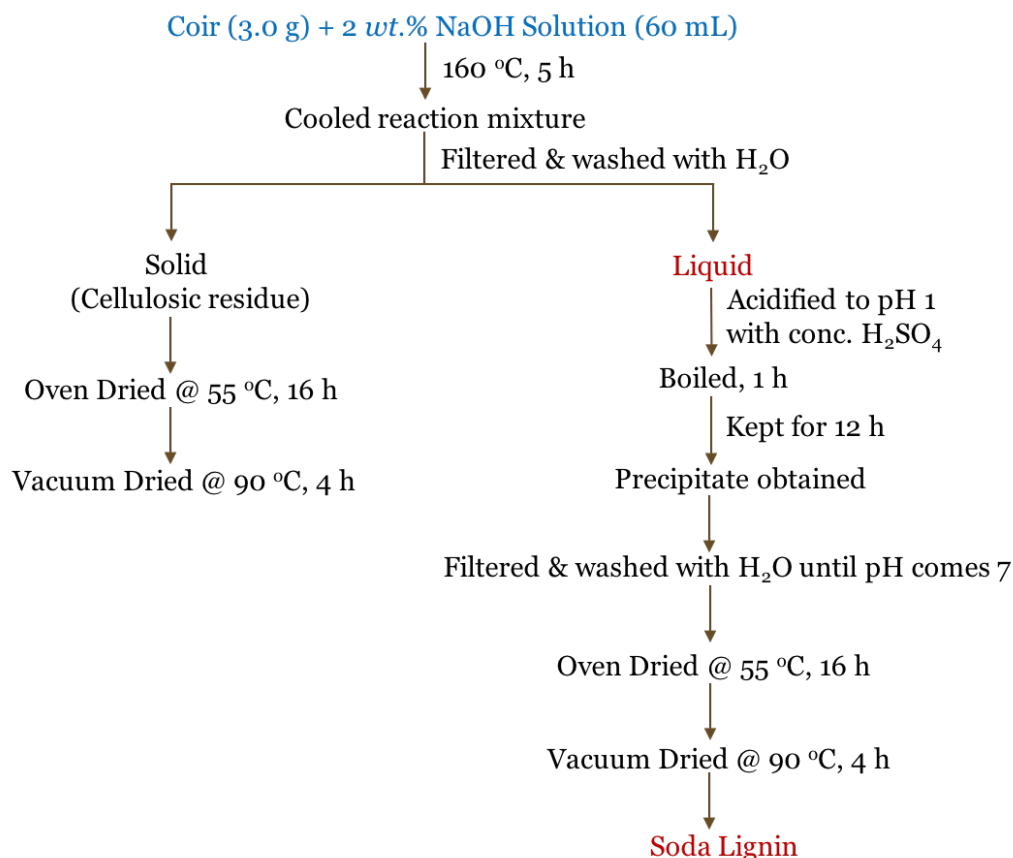
Figure 4.4. Schematic representation of Soda method.

Based on the lignin present in coconut coir, 20% isolation of lignin was possible using Soda process. Since in all the three processes (Klason, Organosolv, Soda) studied here for the isolation of lignin used different reaction conditions, it is possible to see the yield for isolated lignin (100%, 16 and 28%) is varying. The conditions used for all the process and yield obtained for isolated lignin is summarized in Table 4.3.

Table4.3. Summary on Lignin isolation processes.

Method	Conditions used	% Yield
Klason	72% H_2SO_4, 100 °C, 4 h	100
Organosolv	1.024 mmol H_2SO_4, 180 °C, 1h	16
Soda	2 *wt.%* NaOH sol., 160 °C, 5h	20

4.2.3. Catalytic runs of Coconut Coir and Isolated Lignin

In a typical reaction, the lignin: catalyst / coir: catalyst mass ratio was maintained at 1: 1 and lignin: solvent mass ratio was kept 1: 60. Initially, the reactor was flushed with nitrogen and the heating of reactor was started under slow stirring (100 rpm). After attaining the desired reaction temperature (200 °C/250 °C), the stirring rate was increased to 1000 rpm and this was considered as the starting time of the reaction. After the reaction, the reactor was cooled to room temperature. The catalyst was separated out from reaction mixture by centrifugation and washed thoroughly with EtOH: H_2O in order to remove any adsorbed lignin or products on the catalyst. After separation of catalyst from the reaction mixture, products were isolated in organic solvents DEE and EtOAc. Further the organic solvent (DEE and EtOAc) soluble products were analyzed by using GC and GC-MS. The methodology for the extraction of organic solvent soluble products are represented in Figure 4.5. A detailed procedure for the analysis of products was mentioned in Chapter 3.
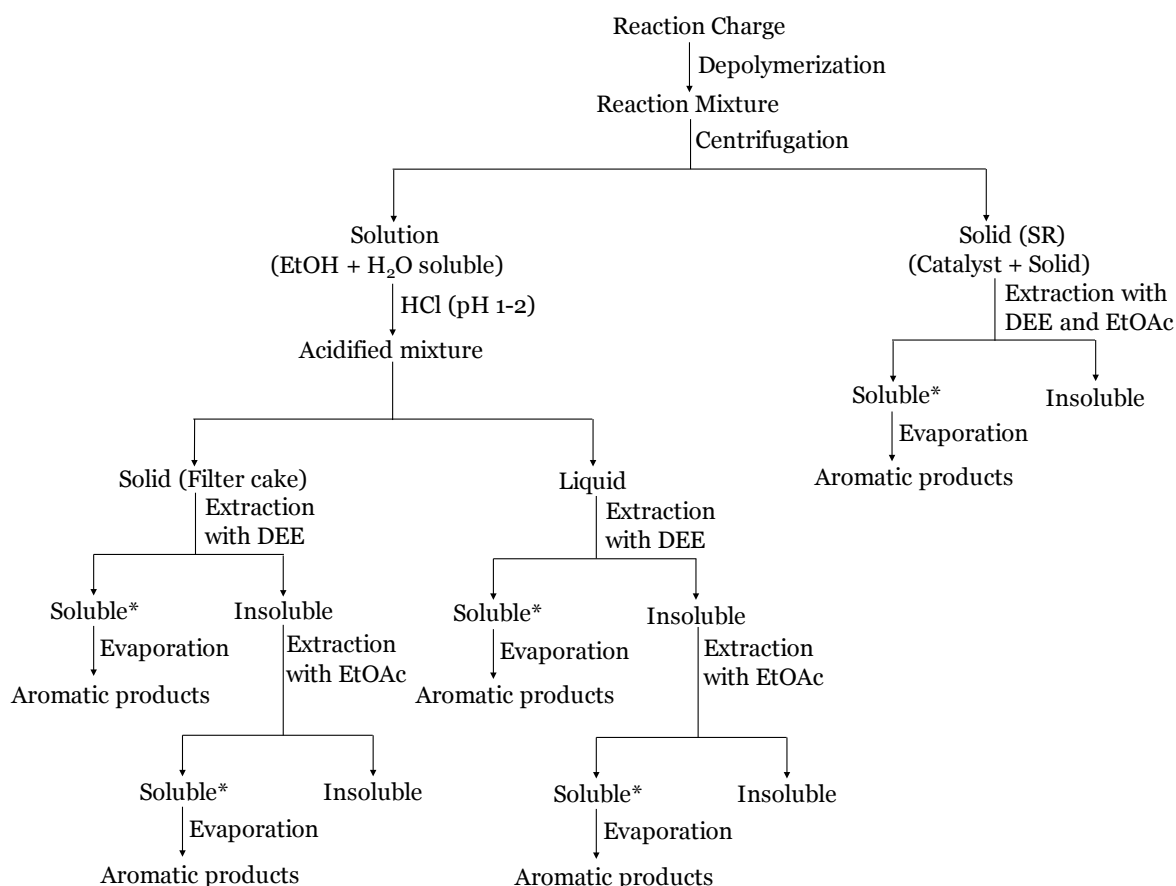
Figure 4.5. Methodology for the extraction of products (* Analyzed by using GC, GC-MS and HPLC).

4.3. Results and Discussions

4.3.1. Characterizations of Coconut Coir (CC) and Isolated Lignin (CC-KL, CC-ORGL, CC-SL)

Before subjecting the CC and isolated lignin for the depolymerization reactions, it was essential to do the complete characterization.

4.3.1.1. Dryness Analysis

Since coconut coir contains moisture in it, the quantification of the content is not possible without giving moisture correction Considering this, moisture content in the sample was calculated so that accurate quantification of products would be possible. For that 0.5 g of coconut coir (CC) was dried in an oven at 100 $^{\circ}$C for 12 h under vacuum (10^{-4} MPa). After that, the dried sample was immediately transfer into desiccator to avoid the moisture adsorption. After cooling the remaining weight of the leftover sample was taken (Table 4.4). Based on the dryness in sample, calculation of oven dried (OD) weight was done. Further, this oven dried (OD) weight was used for all the calculations.

$$\text{Dryness (\%) = 100 - } \frac{\text{(weight before drying - weight after drying)}}{\text{weight before drying}} \text{ x 100}$$

Table 4.4. Summary on dryness analysis of coconut coir.

S.No.	Sample weight before drying (g)	Sample weight after drying (g)	Dryness (%)
CC-1	0.5	0.472	94.44
CC-2	0.5	0.4812	96.32
CC-3	0.5	0.469	93.84
CC-4	0.5	0.470	94.00

4.3.1.2. Analysis of Ash

Apart from cellulose, hemicellulose and lignin, ash is also present in the coconut coir. The quantification of ash was done by taking 1 g of coconut coir (CC) in a quartz boat and kept in muffle furnace at 620 $^{\circ}$C with a ramp rate of 10 $^{\circ}$C/min for 2 h in presence of air. While cooling, when the temperature of furnace was reduced to 80 $^{\circ}$C, instantaneously the boat was transferred to a desiccator to prevent moisture adsorption in leftover mass. After cooling weight of boat with remaining residue (ash) was taken. OD weight of sample was calculated based on dryness analysis of coconut coir. The obtained ash contains minerals, silica and some of the metals. Ash content of four different coconut coir samples are represented in Table 4.5.

$$\text{Ash (\%)} = 100 - \frac{\text{final weight of (boat + ash) - weight of empty boat}}{\text{OD weight of sample}} \times 100$$

Table 4.5. Summary on ash analysis of coconut coir.

S.No.	Sample weight taken (g)	OD weight of sample (g)	Ash obtained (g)	Ash (%)
CC-1	1	0.9444	0.0290	2.90
CC-2	1	0.9632	0.0420	4.20
CC-3	1	0.9384	0.0319	3.19
CC-4	1	0.9400	0.0376	3.76

4.3.1.3. Nutrient Composition by ICP-OES

To determine the presence of metal components, present in the coconut coir, ICP-OES analysis was performed. For the preparation of the samples, 1 g of substrate was weighed in a crucible and then kept in the muffle furnace. Under air, sample was heated to 650 °C for 6 h with a ramp rate of 10 °C/min. It is suggested that during this process, C, H and O will burn off in the form of CO, CO_2, CH_4 etc. and some unburned residues will remain. This residue was first treated with HF, then leftover HF was evaporated by heating at 60 °C. Further, solid residue obtained after HF treatment was dissolved in freshly prepared aquaregia and diluted with deionized water and filtered before the analysis. The data is presented in Table 4.6. From the

data, it was clear that the metal concentrations in the coconut coir is very less and thereby it might be expected that poisoning of catalyst basic sites due to presence of metals in these substrates might be negligible. It was concluded from the obtained results that isolated Klason and Organosolv lignin (CC-KL, CC-ORGL) does not contain any impurity of metal while Soda lignin (CC-SL) contains 29 mg/g of sodium. In Soda method (Figure 4.4), NaOH was used during the isolation of lignin from coconut coir which may results the impurity of sodium.

Table 4.6. ICP-OES analysis of different Coconut Coir* and Isolated lignin*.

Element	CC-1	CC-2	CC-3	CC-4	CC-KL	CC-ORGL	CC-SL
Al	0.211	0.059	0.1	0.144	-	-	-
Ca	0.84	0.79	0.53	0.68	-	-	-
Fe	0.41	0.94	0.14	0.27	-	-	-
K	0.52	0.22	0.73	0.16	-	-	-
Mg	0.63	1.03	0.43	0.37	-	-	-
Mn	0.022	0.005	0.005	0.02	-	-	-
Na	3.3	9.14	6.82	6.22	-	-	29

*Data presented in mg/g.

It was observed from the results obtained from ICP-OES analysis that all the samples are for coconut coir but having variation in its elemental composition. Considering the variation in calcium, it is generally used for maintaining a desirable soil pH. Excess addition of calcium nitrate in the soil will give calcium ions. Likewise, when large quantities of sodium nitrate are added year after year, the nitrate ions are absorbed by crops and sodium ions accumulate and affect the structure of the soil. So, the concentration of nutrients in the soil can have a huge effect on the uptake of nutrients by varieties, Although, environmental conditions (temperature, water availability, etc.), climate, soil type, rainfall pattern, etc. are also major factors.

4.3.1.4. Microanalysis

To know the percentage of C, H and O in the coconut coir and isolated lignin, elemental analysis was performed. Results are summarized in Table 4.7 and Table 4.8. As it is well known that the composition of polysaccharides and lignin varies as the origin and type of plant varies. Even for the same species collected from different places shows the variation in its composition as it is affected by the type of soil, climate, etc. Here, four different coir samples were used and the results are compared with the isolated lignin samples. It was observed that coconut coir is having higher O/C ratio (1.10) compared to isolated lignin (0.48-0.56). This is very obvious as the oxygen content decreases after the removal of polysaccharides (C5 and C6 sugars) from the coconut coir. Higher heating value (HHV) calculated using Dulongs formula shows that coir having less HHV (15.9 MJ/kg) compare to isolated lignin (22.3-24.9) because of the presence of higher oxygen content and presence of polysaccharide in the coconut coir. This can be simply understood based on the molecular formula of polysaccharide (cellulose and hemicellulose) and lignin monomer like guaiacol. The molecular formula of cellulose (C6 sugar) and hemicellulose (C5 sugars) are $C_6H_{12}O_6$ and $C_5H_{10}O_5$ respectively. These will give the O/C ratio of 1 which is well resembles with the O/C ratio of coconut coir of approximate molecular formula $C_7H_{9-11}O_6$. Coniferyl alcohol, a lignin building block unit and guaiacol (lignin monomer) have the molecular formula $C_{10}H_{12}O_3$ and $C_7H_8O_2$ respectively, shows the less oxygen content with low O/C ratio. Similarly, H/C ratio was also calculated and observed to be ca. 0.1. The low H/C and O/C ratios are desirable for the use of coir for energy generation while in another case low O/C and high H/C ratio is suitable for using those as fuels. High HHV and lower O/C ratio of isolated lignin shows that it is a good source for the production of fuels and chemicals. Moreover, double bond equivalence (DBE) of all the samples (coir and isolated lignin) were also calculated and the data shows the DBE between 5.6-5.8 for all the lignin samples. This shows a good correlation with monomer molecular formula and building blocks of lignin i.e. sinapyl, coniferyl and coumaryl alcohol. DBE 4 is considered for one benzene ring and one for exo carbon-carbon double bond. Furthermore, higher value of DBE for CC-ORGL is observed which reflects that CC-ORGL has a highly condensed more aromatic structure. During organosolv

pulping treatment, condensation reactions besides from the fragmentation of lignin might also occur which gives rise to new carbon-carbon bonds in ORGL. According to a former study, these carbon-carbon inter-unit bonds were more easily formed by the guaiacyl (G) type lignin due to the presence of the free C-5 position.[26, 27] It can be stated that CC-ORGL is rich is 5-5 biphenyl type of linkages. Monomer molecular formula was also derived using elemental analysis and based on that it is suggested that lignin is rich in guaiacyl units which is very well matches with the literature also. [28]

Table 4.7. Microanalysis of different samples of Coconut Coir (CC).

Microanalysis	CC-1	CC-2	CC-3	CC-4
C (%)	45.35	45.70	42.51	46.03
H (%)	4.86	5.22	5.73	5.89
O (%)	49.79	49.08	51.76	48.08
O/C	1.09	1.07	1.22	1.04
H/C	0.11	0.11	0.13	0.13
HHV (MJ/kg)	13.4	13.9	13.8	15.4
DBE	2.18	1.85	1.6	1.3
MMF	$C_{7.6}H_{8.84}O_{6.22}$	$C_{7.6}H_{9.5}O_{6.22}$	$C_{7.08}H_{10.42}O_{6.46}$	$C_{7.66}H_{10.72}O_{6.02}$
pH	6.4	5.98	6.02	6.3

Table 4.8. Microanalysis of Coconut Coir and Isolated Lignin.

Microanalysis	Coconut Coir (CC-1)	Organosolv Lignin	Soda Lignin	Klason Lignin
C (%)	45.35	60.78	63.58	63.59
H (%)	4.86	5.41	6.08	6.12
O (%)	49.79	33.81	29.34	29.39
O/C	1.09	0.56	0.46	0.46

H/C	0.11	0.09	0.10	0.10
HHV (MJ/kg)^a	13.4	22.3	24.8	24.9
DBE^b	2.18	5.8	5.6	5.6
MMF^c	$C_{7.6}H_{8.84}O_{6.22}$	$C_{10.1}H_{10.7}O_{4.2}$	$C_{10.6}H_{12.1}O_{3.8}$	$C_{10.6}H_{12.1}O_{3.8}$
pH^d	6.4	6.3	5.9	2.95

[a] Higher heat value (HHV)= [0.3383 x C + 1.442 x [H-(O/8)] + 9.248 x S] where C, H, O and S are *wt.%* of carbon, hydrogen, oxygen and sulphur; [b] Double bond equivalence (DBE) = [C − (H/2) +(N/2) + 1] where C, H and N are number of carbon, hydrogen and nitrogen atoms found from monomer molecular formula [c] Monomer molecular formula (MMF) = 100 - ('C' *wt.%* + 'H' *wt.%* + 'O' *wt.%*). [d] pH was measured by dissolving 0.08 g sample in 5 mL water.

4.3.1.5. XRD

To understand the crystalline and amorphous nature of the coconut coir and isolated lignin (Klason, Organosolv, Soda) XRD analysis was done (Figure 4.6 and 4.7). A peak at 21.7 ° is observed for the crystalline phase of cellulose and 16.7 ° for the amorphous phase of cellulose.

Though, four different types of coconut coir was collected but in this study Coconut coir one (CC-1) was used for the lignin isolation. After the isolation of lignin (Klason, Organosolv, Soda) from the coconut coir (CC-1), no peaks are observed for the crystalline and amorphous phase of cellulose. This confirms that isolated samples do not contain cellulose impurities. A broad peak pattern for the isolated samples confirms the amorphous nature of lignin. Moreover, few peaks are also observed at 30.9 ° (CC-1) for sodium and 35 ° for $Na_2O_5S_2$ (common in all the samples of coconut coir). Furthermore, difference in the intensities of XRD peak pattern was also observed. This might be because of the variation in the quantity present of polysaccharides (celluloses) in coconut coir. As observed from the XRD pattern, CC-1 shows the high intense peak compared to others or CC-2 shows less intensity which confirms the presence of less amount of celluloses (because the polysaccharides are amorphous in nature which will results an amorphous peak pattern in XRD). On the basis of XRD peak pattern we can predict of order of polysaccharide present on the sample. The decreasing order of hemicellulose present in the coconut coir samples is:

CC-1 > CC-4 > CC-3 > CC-2. The obtained result is in a good correlation with the literature available which confirms the less hemicellulose present in coir (Table 4.2).
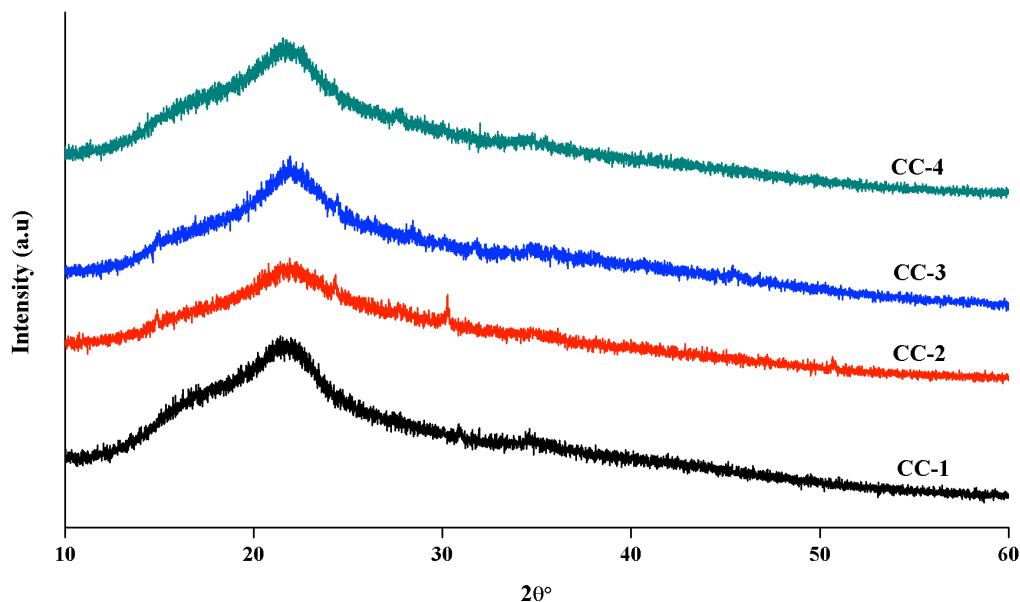
Figure 4.6. XRD patterns of different samples of Coconut Coir (CC-1-4).
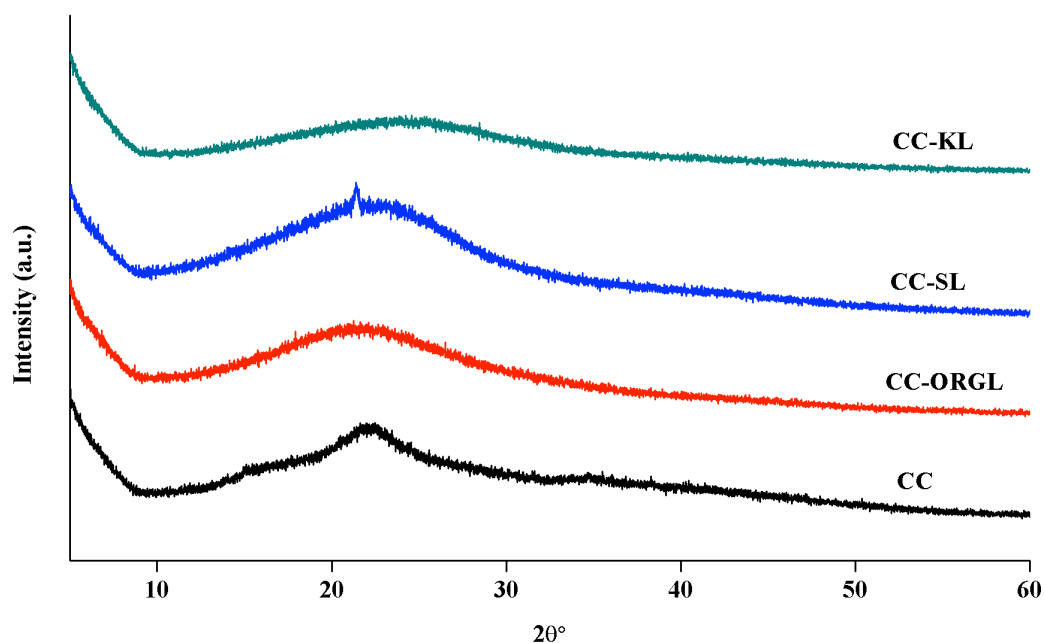
Figure 4.7. XRD patterns of Coconut Coir (CC-1) and Isolated Lignin [Organosolv (CC-ORGL), Soda (CC-SL) and Klason (CC-KL) lignin].

4.3.1.6. Attenuated Total Reflection (ATR) Spectroscopy

From the above analysis, it was observed that all the four samples of coir show similar behaviour with slight variation. Hence, among them CC-1 was chosen to determine the functional group present in it. The Attenuated Total Reflection (ATR) spectroscopic analysis of the coir and isolated lignin (from CC-1) (Figure 4.8) confirms the presence of various functional groups. In the ATR spectrum of the coir absorption band at the region near 1720 cm^{-1} which may be due to a carboxyl group of acetyl ester in cellulose and carboxyl aldehyde in lignin is observed.[29] Lignin present in the coir gives characteristics peak at 1220, 1608 and 1720 cm^{-1} for the aromatic skeletal vibrations and C=O stretching in ketone, carbonyl and ester groups. Isolation of lignin reduces hydrogen bonding due to the removal of the hydroxyl groups. This results in the decrease of –OH group concentration, as can be seen from the decreased intensity of the peak between 3650-3200 cm^{-1} compared to the coir. Absorption band present at 2900-2800 can be assigned for the asymmetric stretching and symmetric stretching of C-H bond in methyl and methylene groups. Significant functional groups in the range of 1700-1550 cm^{-1} present in all the isolated lignin samples. Peaks in the range of 1600-1400 cm^{-1} confirms the presence of aromaticity or benzene ring. Moreover, this band can be assigned for the presence of C=C attached to the aromatic rings. The ATR spectrum of isolated lignin clearly indicates the presence of the characteristic band of the C-O stretching of alkoxy groups or presence of ether linkages in the region of 1300-1000 cm^{-1}. Peaks in the range of 850-820 cm^{-1} corresponds to substituted phenolics and alkene groups. The observance of a peak at 780 cm^{-1} is due to deformation vibrations of C-H (oop) bonds associated to aromatic rings. All the absorption band observed are summarized in Table 4.9.
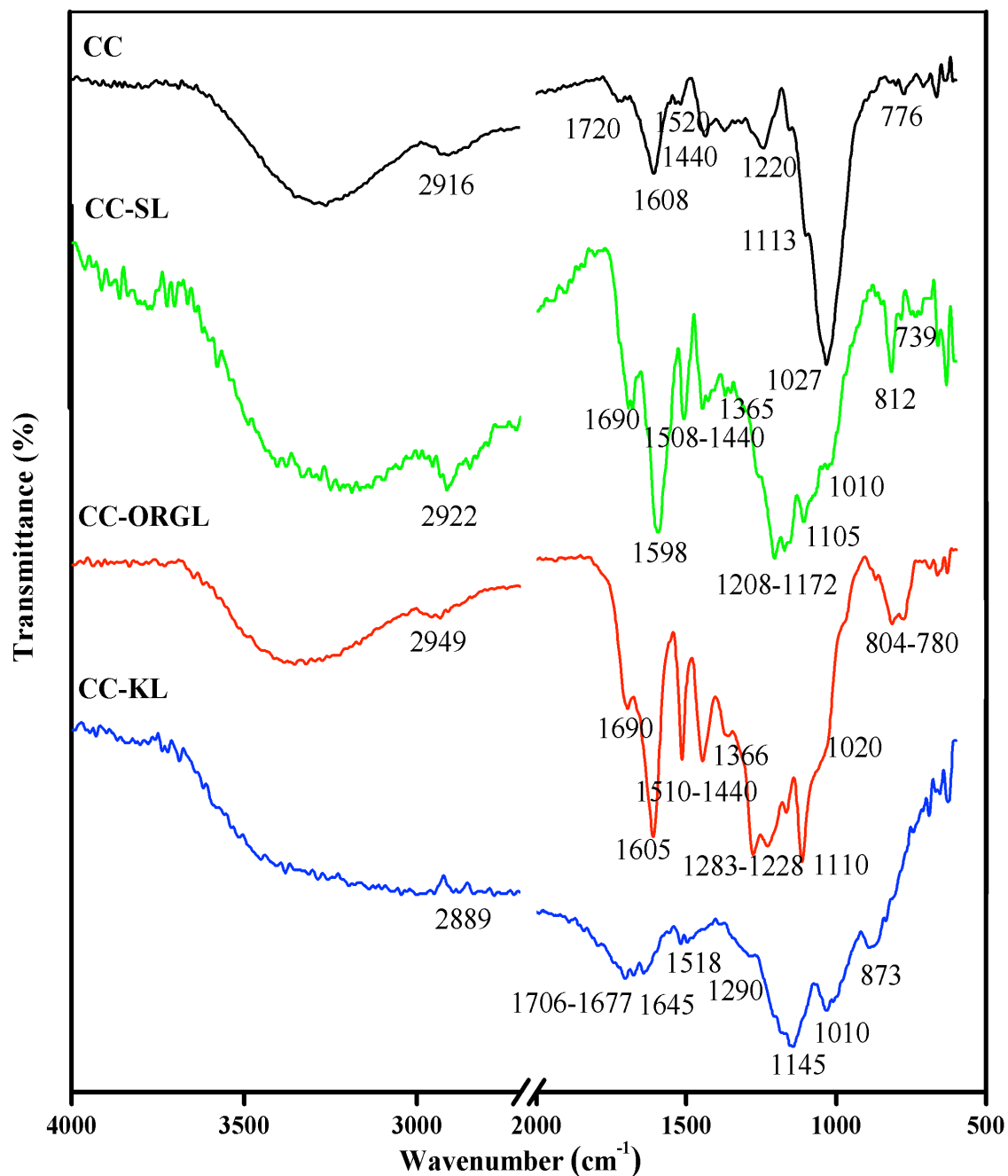
Figure 4.8. ATR analysis of Coir (CC-1) and Isolated lignin (CC-KL, CC-ORGL, CC-SL).

Table 4.9. Summary of ATR bands present in Coir (CC-1) and Isolated Lignin (CC-SL, CC-ORGL, CC-KL).

Absorption band (cm⁻¹)	Type of vibration	Wavenumber (cm⁻¹)			
		CC-1	CC-SL	CC-ORGL	CC-KL
3650-3200	Alcoholic & phenolic O-H stretching (free and involved in hydrogen bonding)	3298	3280	3378	3386
2960-2910	C-H asymmetric stretching in methyl and methylene group	2916	2922	2949	2889
1740-1680	C=O stretching in unconjugated ketone, carbonyl and ester groups	1720	1690	1690	1706
1670-1620	C=O stretching in conjugated substituted aryl group	-	-	-	1677 1645
1615-1595	C=O stretching with aromatic skeleton vibrations	1608	1598	1605	-
1520-1505	Aromatic skeleton vibrations	1520	1508	1510	1518
1470-1440	Deformation vibrations of C-H bond	1440	1450	1442	-
1370-1350	Aliphatic C-H stretching in methyl and phenolic OH		1355	1366	-
1300-1200	C-C, C-O, C=O stretching in guaiacyl units	1200	1208	1228 1283	1290
1120-1105	Deformation vibrations of C-H bonds in aromatic rings	1113	1105	1110	-
1195-1124	Deformation vibrations of C-H bonds in syringyl rings	-	1172	-	1145

1027-1010	C-O stretching in alcohol, ether/ in-plane deformation vibrations of C–H bonds in aromatic rings.	1027	1010	1020	1010
875-700	Substitution on aromatic ring or substituted phenolics	-	812 780	804	873

(-) Not assigned

4.3.1.7. Solid State ^{13}C NMR

^{13}C NMR characterizations of coir (CC-1) and isolated lignin was performed which reveals mainly the presence of monolignols and end group distributions. The ^{13}C NMR spectra of coir and isolated lignin are shown in Figure 4.9 (coir) and Figures 4.9-4.11 (Klason, Organosolv and Soda lignin). Peaks appearing in the range of 160-180 ppm represents the presence of ester group. High intense peak as observed in the range of 110-150 ppm which corresponds to the presence of sp^2 carbon in aromatics and alkenes, which again confirms the aromatic nature of the samples. The chemical shift for the aromatic regions for all the samples were recorded in the range of 90-140 ppm. Presence of sp^3 carbon attached to the oxygen atom is also observed in the range of 55-90 ppm. An intense peak at 55-56 ppm common in all the lignin samples shows the presence of methoxyl group attached to the aromatic ring. The appearance of methoxy groups in the range of 20-50 ppm was observed in all the samples. Detailed summary for the assigned peaks are tabulated in Table 4.10 Further on the basis of ^{13}C NMR analysis peaks were correlated to the structures present in isolated lignin samples (Figure 4.13)
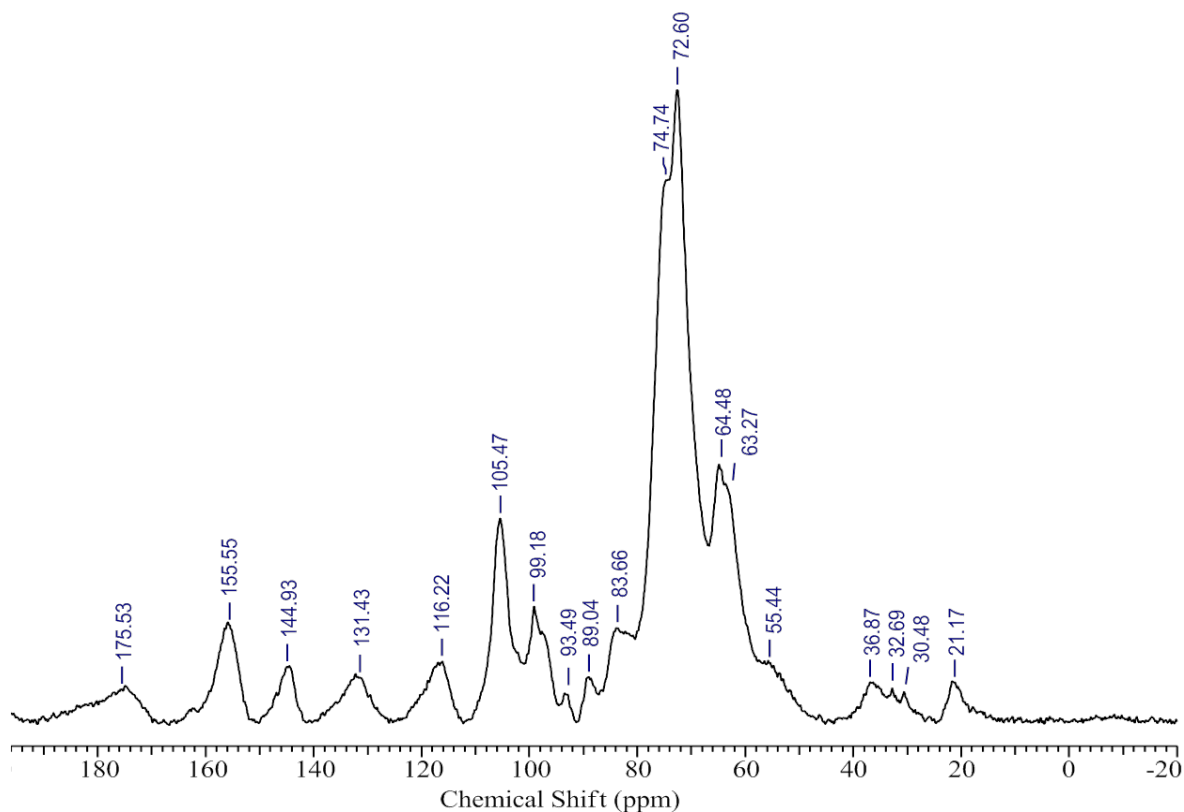
Figure 4.9. Solid state ^{13}C NMR of Coconut Coir (CC-1).
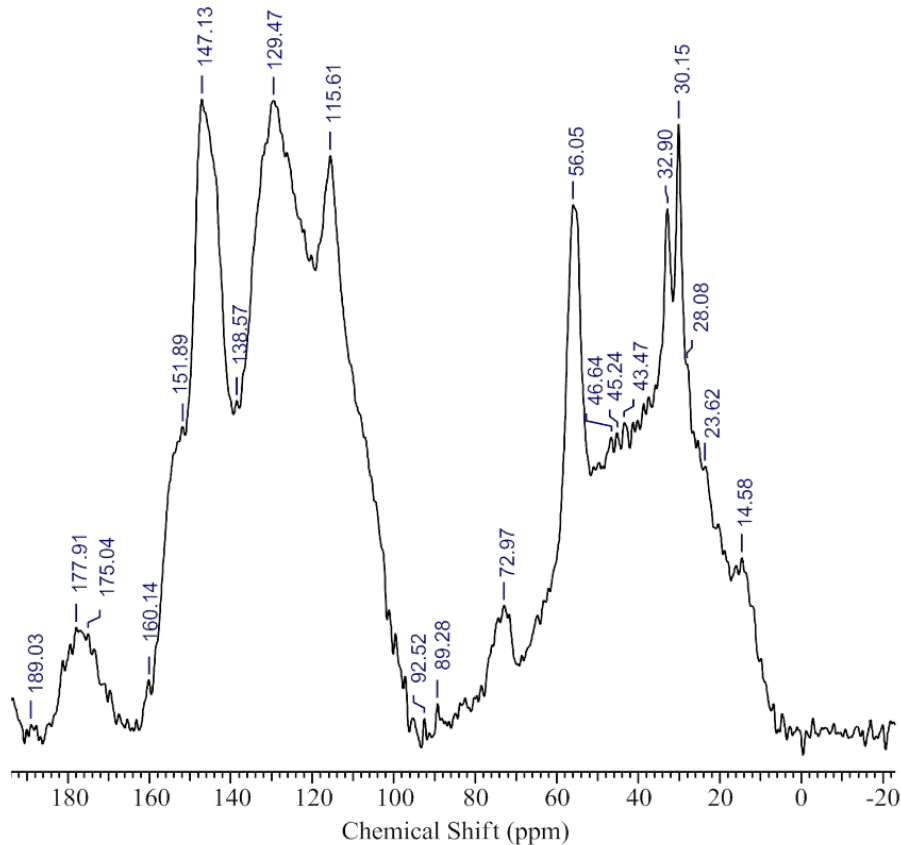
Figure 4.10. Solid state ^{13}C NMR of Klason lignin (CC-KL).
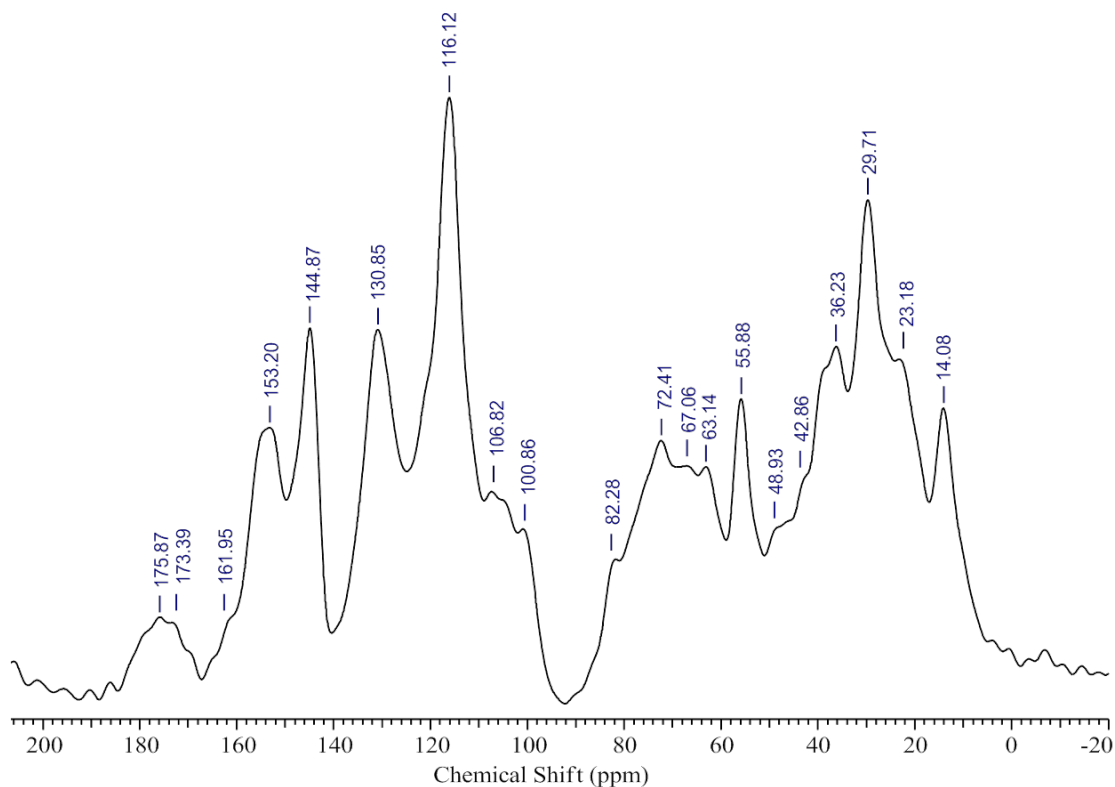
Figure 4.11. Solid state ^{13}C NMR of Organosolv lignin (CC-ORGL).
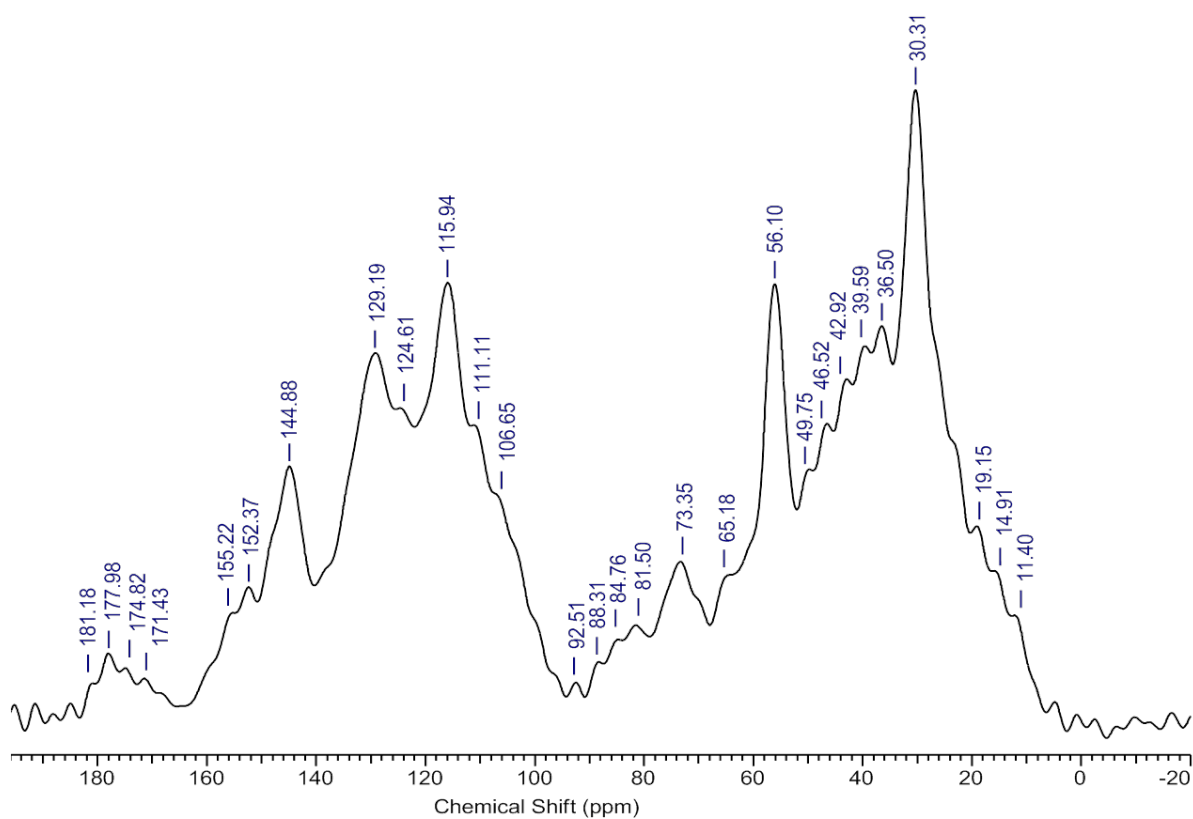
Figure 4.12. Solid state ^{13}C NMR of Soda lignin (CC-SL).

Table 4.10. Summary on ^{13}C NMR of Coconut Coir (CC-1) and Isolated Lignin (CC-KL, CC-ORGL, CC-SL).

Functional group	Chemical Shift (ppm)			
	CC-1	CC-KL	CC-ORGL	CC-SL
-	-	177.91	-	177.98
C=O group in Hibbert's ketone	175.53	175.04	175.87	-
-	-	-	173.39	174.82
C$_4$ in p-hydroxyphenyl unit	-	160.14	161.95	-
C in β-O-4 substructures linked with C=O	155.55	151.89	153.20	152.37
C$_3$ and C$_4$ in etherified guaiacyl unit	-	147.13	-	-
-	131.43	-	-	-
C$_{2,6}$ in *p*-hydroxyphenyl units	-	-	130.85	129.19
C$_{3,5}$ in *p*-hydroxyphenyl units	116.22	115.61	116.12	115.94
C$_2$ in guaiacyl units	-	-	-	111.11
C$_{2,6}$ in tricin	105.47	-	106.82	10.6.65
-	99.18	-	100.86	-
C$_8$ in tricin	93.49	92.52	-	92.51
-	89.04	89.28		88.31
C$_β$ in β-O-4 substructures	83.66	-	82.28	84.76
Cα in β-O-4 substructures	74.74 72.60	72.97	72.41	73.35
Cγ in β-O-4 substructures	-	-	67.06	
-	64.48	-	63.14	65.18
C-H in methoxyl group	55.44	56.05	55.88	56.10
-	-	-	48.93	49.75
-	-	46.64	-	46.52
α carbon CH$_2$ with aliphatic substituted group	-	43.47	42.86	42.92
-	43.47	-	-	39.59

α carbon in phenyl propanol group	36.87	-	36.23	36.50
	32.69	32.90	-	-
-CH$_2$ alkyl group	30.48	30.15	29.71	30.31
-	21.17	23.62	23.18	-
-	-	-	-	19.15
Terminal -CH$_3$ group	-	14.58	14.08	14.91
-	-	-	-	11.40

(-) Not assigned

β-O-4 linkages

Tricin

Guaiacyl

p-hydroxyphenyl

Syringyl
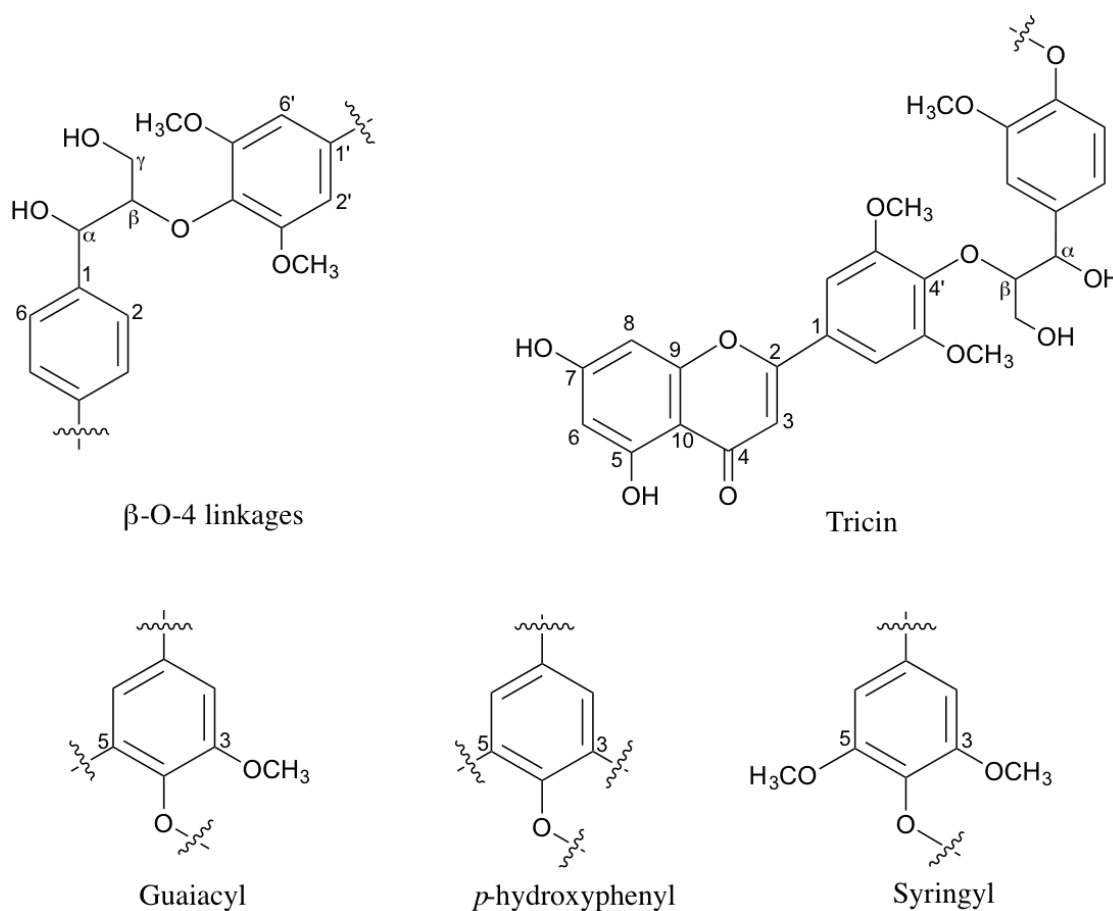
Figure 4.13. Structures present in isolated lignin samples based on ^{13} C NMR analysis.

4.3.1.8. Thermo Gravimetric Analysis - Differential Thermal Analysis (TGA - DTA)

Thermal analysis of coconut coir (CC-1) and isolated lignins was performed under nitrogen atmosphere upto 1000 °C. It was observed that coconut coir and lignin start losing weight at around 150 °C, may be due to the removal of moisture. Cleavage of α

and β-aryl-alkyl-ether linkages was observed in the range of 200-450 °C. Complete decomposition of organic moieties was observed at ~600 °C. Klason lignin shows ca. 35% of weight loss from 200-500 °C. It might be due to the cleavage of side chain or aryl alkyl ether linkages followed by the cleavage of C-C linkages present in lignin structural units. It can be stated from the TGA-DTA analysis of Klason lignin that it contains more number of aryl-alkyl-ether linkages as it takes long time to decompose at ~200-300 °C. It is well known from the literature that organosolv lignin is rich in carbon-carbon linkages between lignin subunits. It is well matched from the TGA-DTA analysis of organosolv lignin. Similar observation was made for the soda lignin also as it shows weight loss in the range of 200-360 °C for ether linkages and until 400 °C for the cleavage of C-C linkages. A careful observation suggests that for all the lignin samples having DTA peak maxima at different positions. This is because each lignin having different-different linkages with various functional groups (shown in ATR and ^{13}C NMR). Moreover, molecular weight and degree of polymerization also reflect in TGA-DTA graphs. Klason lignin shows peak maxima at 390 °C, having highest molecular weight and Soda lignin (low molecular weight compared to Klason lignin) shows at 375 °C, which indicates the complete cleavage of carbon-carbon linkages present in lignin structure. However, Organosolv lignin has least molecular weight among them, and it shows the peak maxima at 335 °C, which indicates the splitting off the aliphatic side chains and C-C bond.
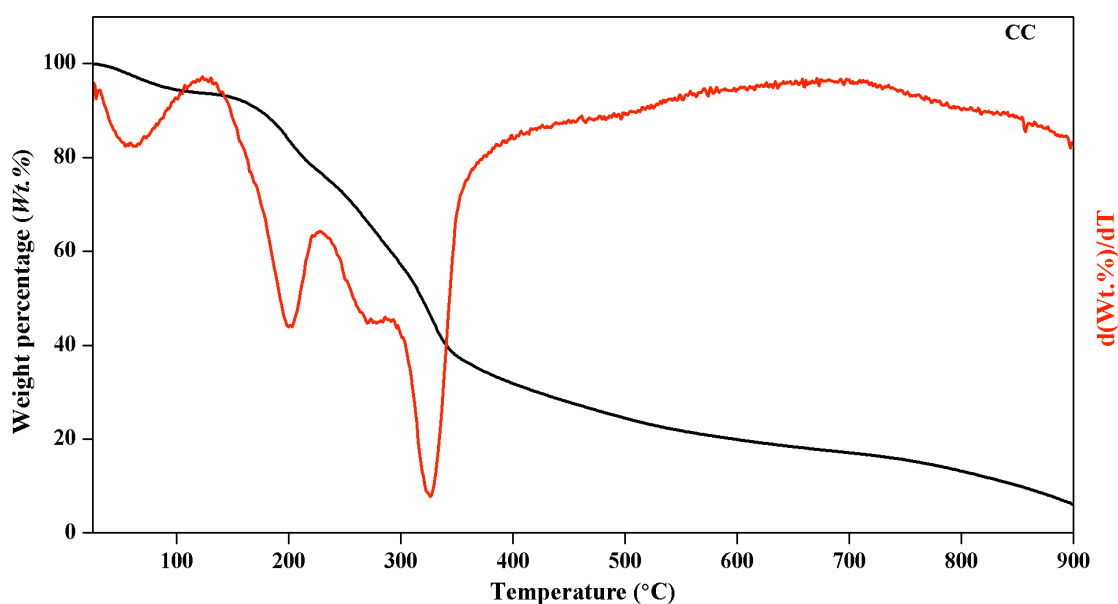
Figure 4.14. TGA-DTA analysis of Coconut Coir (CC-1).
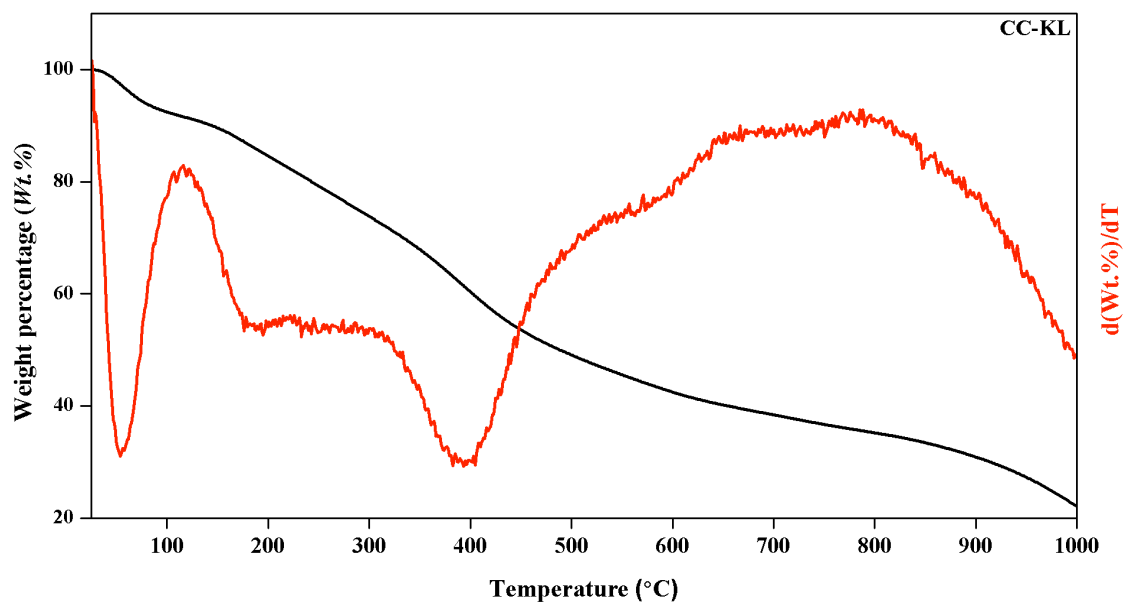
Figure 4.15. TGA-DTA analysis of Klason lignin (CC-KL).
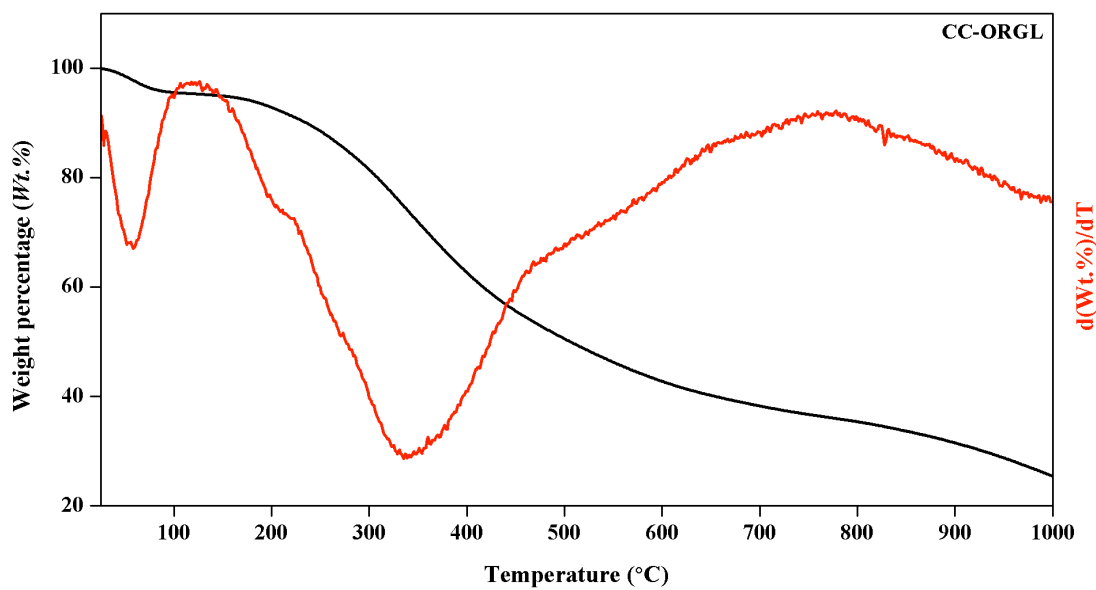
Figure 4.16. TGA-DTA analysis of Organosolv lignin (CC-ORGL).
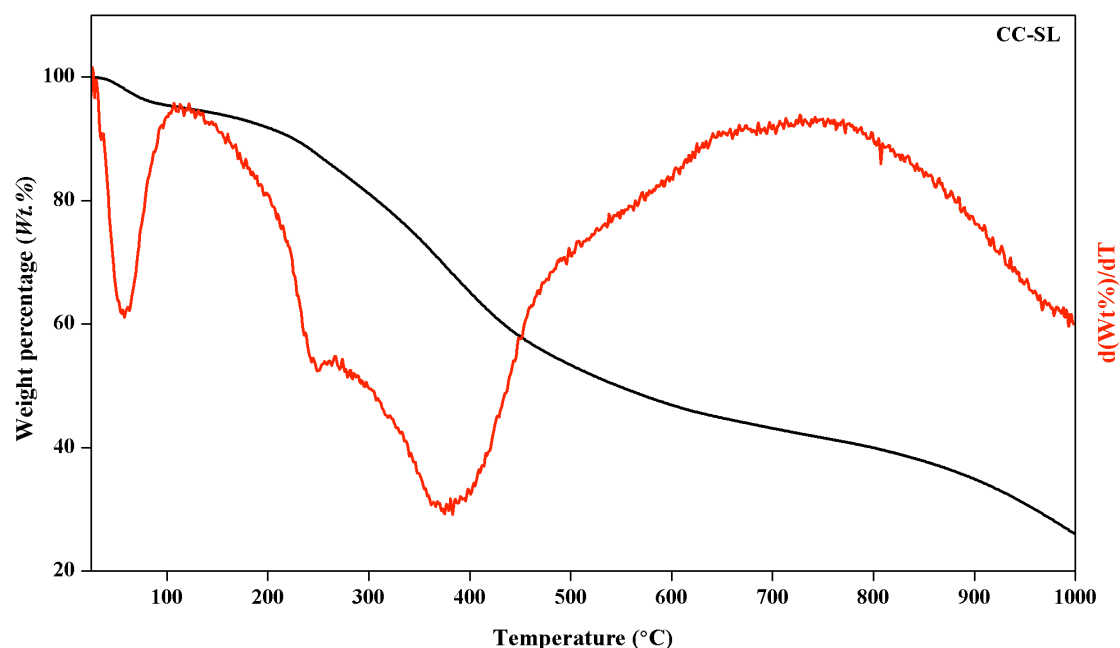
Figure 4.17. TGA-DTA analysis of Soda lignin (CC-SL).

Table 4.11. Summary of TGA-DTA analysis of Coconut Coir (CC-1) and Isolated Lignin in N_2 atmosphere.

Substrate	TGA Residue (%)	Moisture (%)
Coconut Coir (CC)	6	8
Klason lignin (CC-KL)	22	10
Organosolv lignin (CC-ORGL)	24	10
Soda lignin (CC-SL)	25	5

It was also observed that in extracted lignin, 22-25% of unburnt residue is obtained while in coir sample only 6 % residue is observed. These studies suggest that carbon in the sample will remain unburnt. This can be explained on the basis of monomer molecular formula derived from elemental analysis. Coir is having 7.6 'C' 8.8 'H' and 6 'O'. Considering this almost 95% of carbon is possible to burn in the form of CO and CH_4. It is possible that 6 'C' will be consumed in the form of 6 CO and another 1.2 carbon can be consumed as 1.2 CH_4 molecules. Still 0.4 'C' is remaining which will be remain as unburnt residue. A quick calculation discloses that this remaining 0.4 'C' out of 7.6 'C' gives rise to ca. 5 % of residue. This percentage of unburnt

residue matches well with the experimental data. Moreover, it is well correlation with the ash analysis which is also 3-4%. Similarly, for isolated lignin it contains 10 'C' 11 'H' and 4 'O'. After the complete use of 'H' and 'O' present in lignin in the form of 4 $CO + 3\ CH_4$, there will be remaining 3 'C' as unburnt residue. This will give ca. 30% of residue. Likewise, moisture present in the sample can be correlated with the dryness analysis. E.g. From dryness analysis, it was calculated that coir shows 93-94% dryness in the sample which shows the remaining % for moisture ca. 6-7%. This result also matches well with the experimental data (8% moisture) obtained from TGA-DTA.

4.3.1.9. UV-Visible Analysis

Contribution of colour in the lignin is identified by using UV-Vis spectroscopy. Samples were prepared in EtOH: H_2O (1: 2 *v/v*) and were analysed in the range of λ = 200-800 nm. UV-Vis spectra show an adsorption band at 280 nm and a shoulder at 230 nm with a gradual decrease in absorption extending towards visible region representing presence of several different chromophores. These bands are common in all the samples which corresponds to π-π* electronic transition in aromatic ring of unconjugated phenolic units. Peak appearing at 280 nm can be assigned for the presence of non-conjugated phenolic compounds which confirms the presence of hydroxyl groups. Moreover, occurrence of a shoulder band at 230 nm confirms the presence of mono and di-substituted aromatic rings.
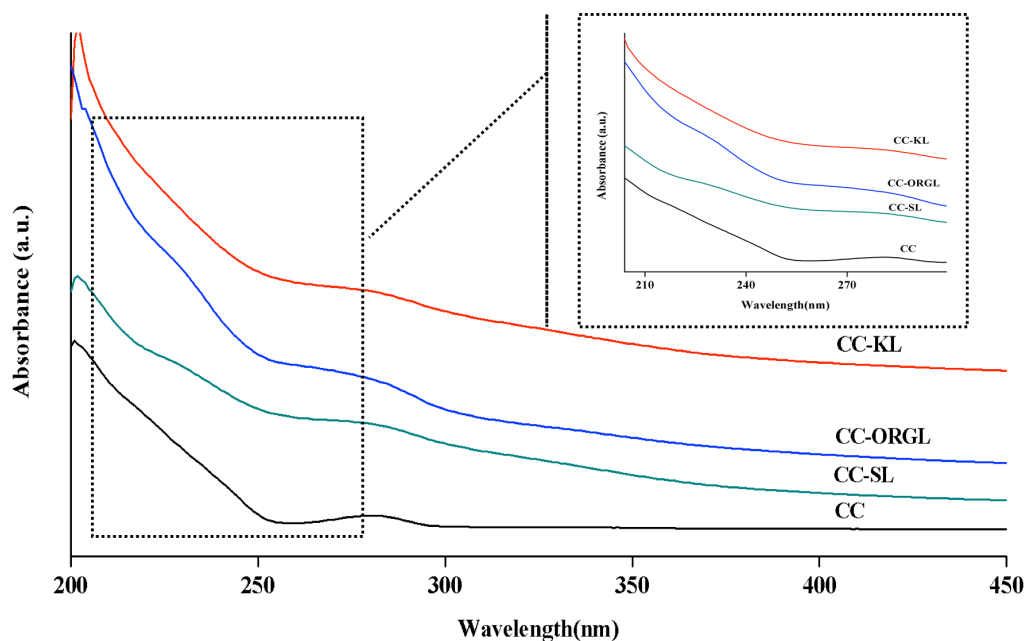
Figure 4.18. UV-Visible spectra of Coir (CC-1) and Isolated Lignin (Klason, Organosolv and Soda Lignin).

4.3.2. Depolymerization of Isolated Lignin (Klason, Organosolv and Soda) and Coconut Coir

In order to the complete value addition to coir and isolated lignin, it is important to depolymerize it into value-added chemicals. Since the depolymerization method is optimized and well established with commercial lignin (Chapter 3). Hence, further studies are proceeded with the best optimized reaction condition.

4.3.3. Depolymerization of isolated lignin using solid base catalyst (NaX)

Depolymerization studies were carried out for isolated Klason, Organosolv and Soda lignin and coir. All reactions were conducted in a batch mode autoclave (Parr, USA). EtOH: H2O (1: 2 *v/v*) was used as the solvent system in all the reactions. Variation in the product yield was observed from 5-28 %. Effect of various lignin substrate with different molecular weights was discussed in Chapter 3. The similar phenomenon is observed with isolated lignin samples and can be explained on the basis of lignin molecular weight and type of functional groups present. Order of molecular weight (Da) of isolated lignin: Klason lignin (CC-KL) > Soda lignin (CC-SL) > Organosolv lignin (CC-ORGL).[30, 31] As it is observed from the Figure 4.19 that Klason lignin shows a lowest product yield having highest molecular weight (18,000 Da)[31]. In case of organosolv and Soda lignin, yields are not observed in as expected (lowest

molecular weight lignin should give highest yield). The reason is that ORGL is known to be having more C-C linkages compare to C-O-C linkages and very few C-C linkages can be broken at milder reaction conditions governs less product yield. It can be seen from the ATR spectra of CC-ORGL and CC-SL, more intense peak at 1600-1400 cm^{-1} was observed which belongs to C=C groups attached to aromatic groups and 1300-1200 cm^{-1} for C-C stretching in guaiacyl units. Moreover, ^{13}C NMR also validate this fact as the intensity of the peak at 150-110 ppm for the presence of sp^2 carbon is more in CC-ORGL compare to CC-SL. Further the formation of aromatic products was confirmed using GC-MS (Figure 4.20-4.23). Similar type of product formation was observed with all the lignin. The identified products are tabulated in Table. 4.12.
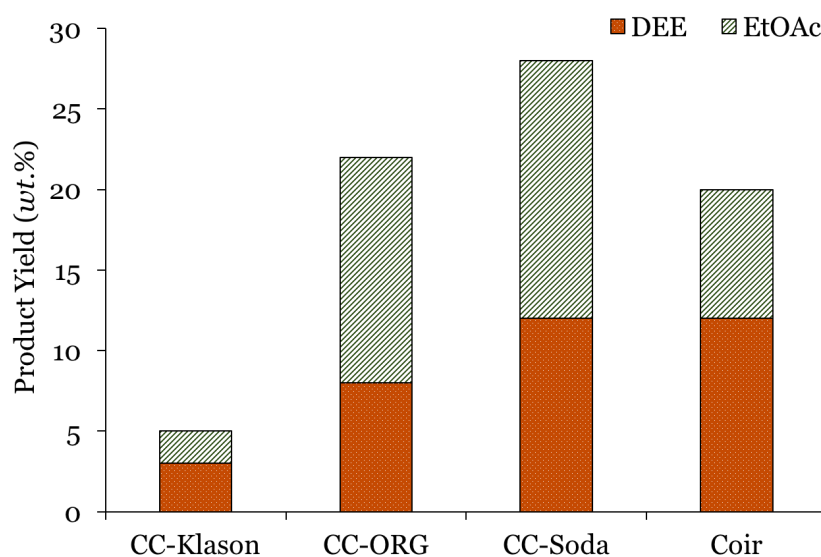
Figure 4.19. Depolymerization of isolated lignin and coir using NaX. Reaction Condition: Lignin/Coir (0.5 g), NaX (0.5 g), EtOH: H$_2$O (1: 2 v/v, 30 mL), 250 ^{o}C, 1 h.
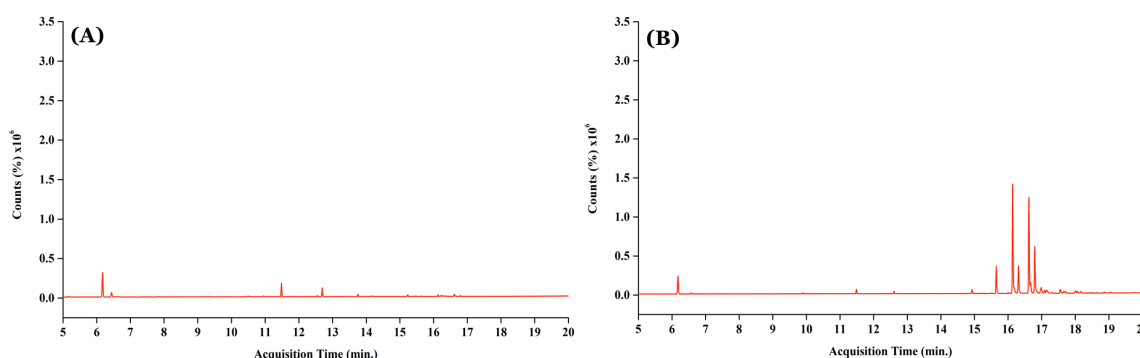
Figure 4.20. Klason Lignin: GC-MS chromatograph of products extracted in diethyl ether and ethyl acetate (A) DEE soluble products from liquid fraction, (B) EtOAc soluble products from liquid fraction. Reaction condition: Klason lignin: NaX = 1: 1 $wt./wt.$, EtOH: H$_2$O (1: 2 v/v, 30 mL), 250 ^{o}C, 1 h.
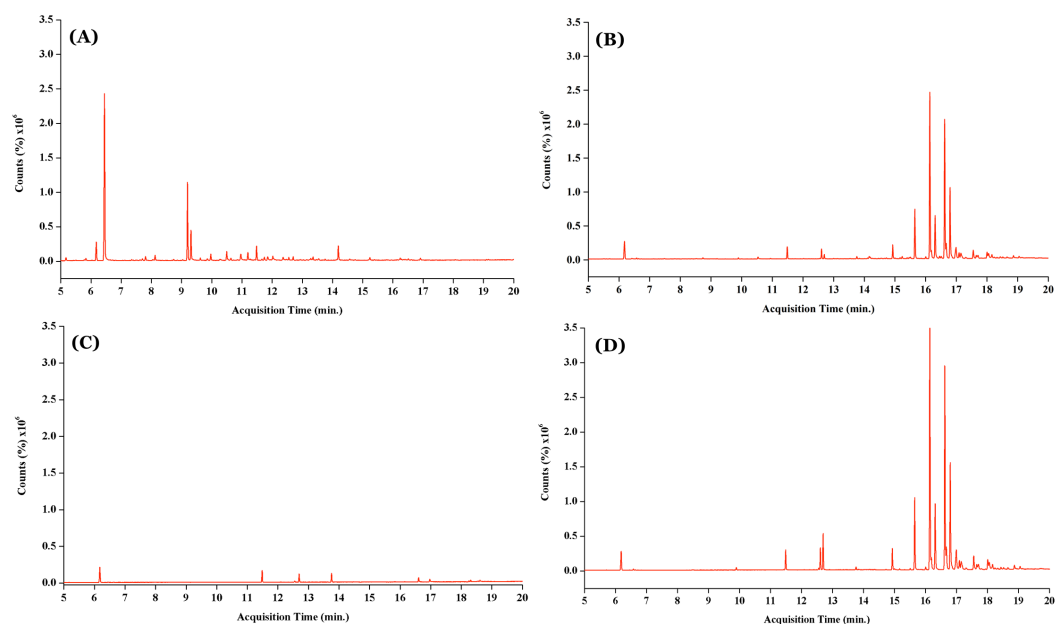
Figure 4.21. Organosolv lignin: GC-MS chromatograph of products extracted in diethyl ether and ethyl acetate (A) DEE soluble products from liquid fraction, (B) EtOAc soluble products from liquid fraction, (C) DEE soluble products from solid fraction, (D) EtOAc soluble products from solid fraction. Reaction condition: Organosolv lignin:NaX = 1:1 *wt./wt.*, EtOH:H_2O (1:2 *v/v*, 30 mL), 250 °C, 1 h.
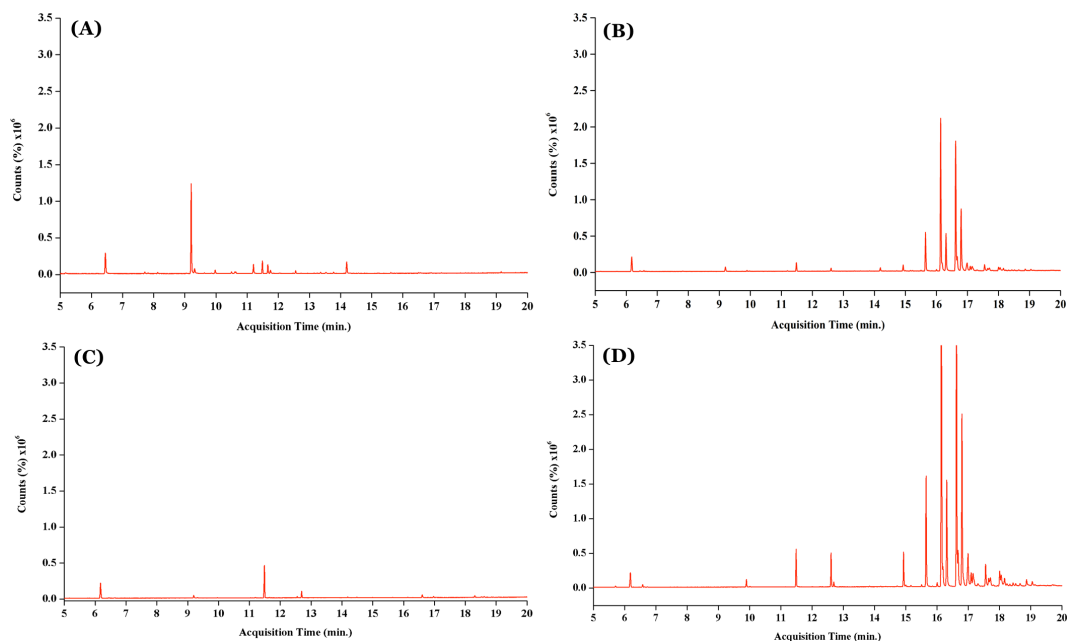
Figure 4.22. Soda lignin: GC-MS chromatograph of products extracted in diethyl ether and ethyl acetate (A) DEE soluble products from liquid fraction, (B) EtOAc soluble products from liquid fraction, (C) DEE soluble products from solid fraction, (D) EtOAc soluble products from solid fraction. Reaction condition: Soda lignin: NaX = 1: 1 *wt./wt.*, EtOH: H_2O (1: 2 *v/v*, 30 mL), 250 °C, 1 h.
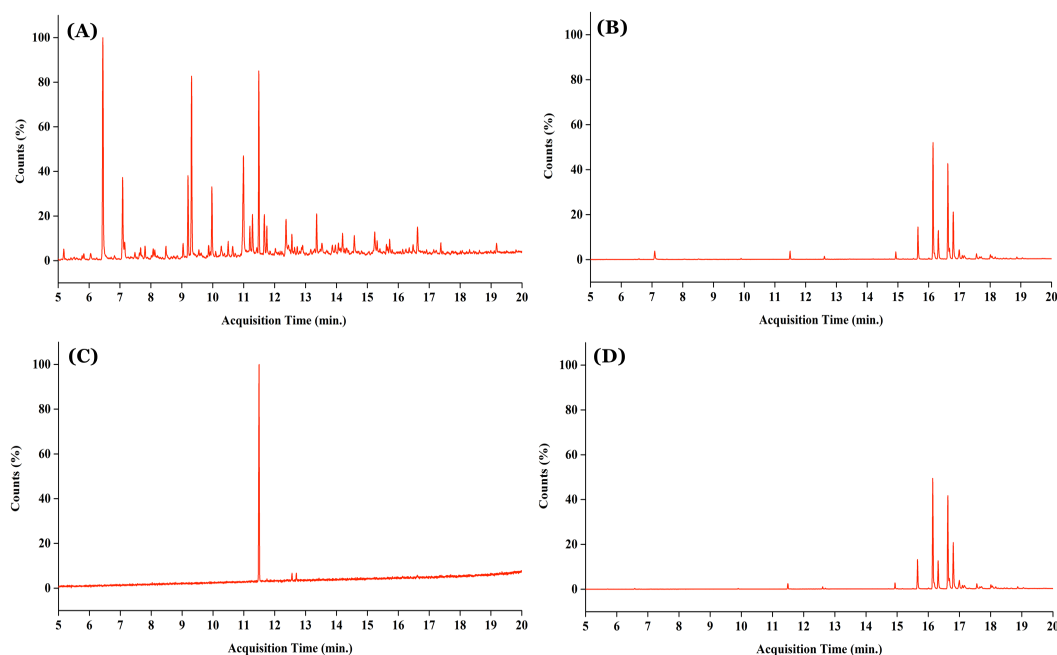
Figure 4.23. Coconut Coir: GC-MS chromatograph of products extracted in diethyl ether and ethyl acetate (A) DEE soluble products from liquid fraction, (B) EtOAc soluble products from liquid fraction, (C) DEE soluble products from solid fraction, (D) EtOAc soluble products from solid fraction. Reaction condition: Coconut Coir: NaX = 1: 1 *wt./wt.*, EtOH: H₂O (1: 2 *v/v*, 30 mL), 250 °C, 1 h.

Table 4.12. List of products identified from GC-MS.

S.No.	Compound
1	Catechol
2	*p*-hydroxyphenol
3	3-methyl catechol
4	2,6-dimethoxyphenol
5	4-hydroxy benzaldehyde
6	Vanillin
7	2-hydroxy acetophenone
8	3-hydroxy benzoic acid
9	Acetoguaiacone
10	Butylated hydroxytoluene
11	Acetosyringone

As it is always preferable to use abundant and inexpensive lignocellulose material (coconut coir) directly for the synthesis of value-added aromatic chemicals in order to develop a sustainable future technology. Hydrolysis of coir was also carried out using NaX as catalyst and it was compared with non-catalytic reaction (Figure 4.24.). EtOH: H_2O was used as the reaction media. Reaction was done at 200 ^{o}C for 1 h. It was observed that direct hydrolysis of coir shows a good product yield of 64% compared to non-catalytic reaction (27%). Further the formation of aromatic products was confirmed by using GC, GC-MS and HPLC techniques. The GC-MS chromatogram of the products confirms the formation of aromatic products (Figure 4.25). As cellulose and hemicellulose is also present in the coir, so in order to check the formation of any sugar products, HPLC analysis was also performed and very low intensity peak for glucose and HMF were observed (Figure 4.26).
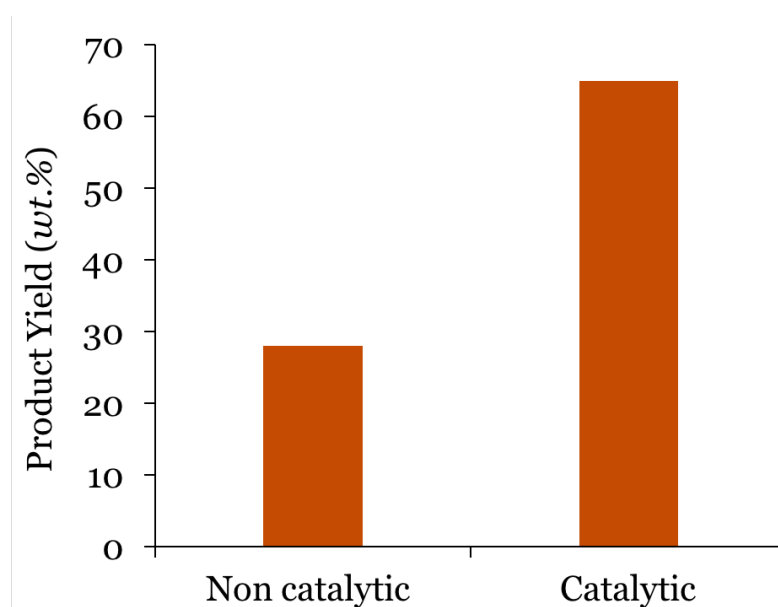
Figure 4.24. Direct hydrolysis of coir using NaX.

Reaction Condition: Coir (0.5 g), NaX (0.5 g), EtOH: H_2O (1: 2 v/v) 30 mL, 200 ^{o}C, 1 h.
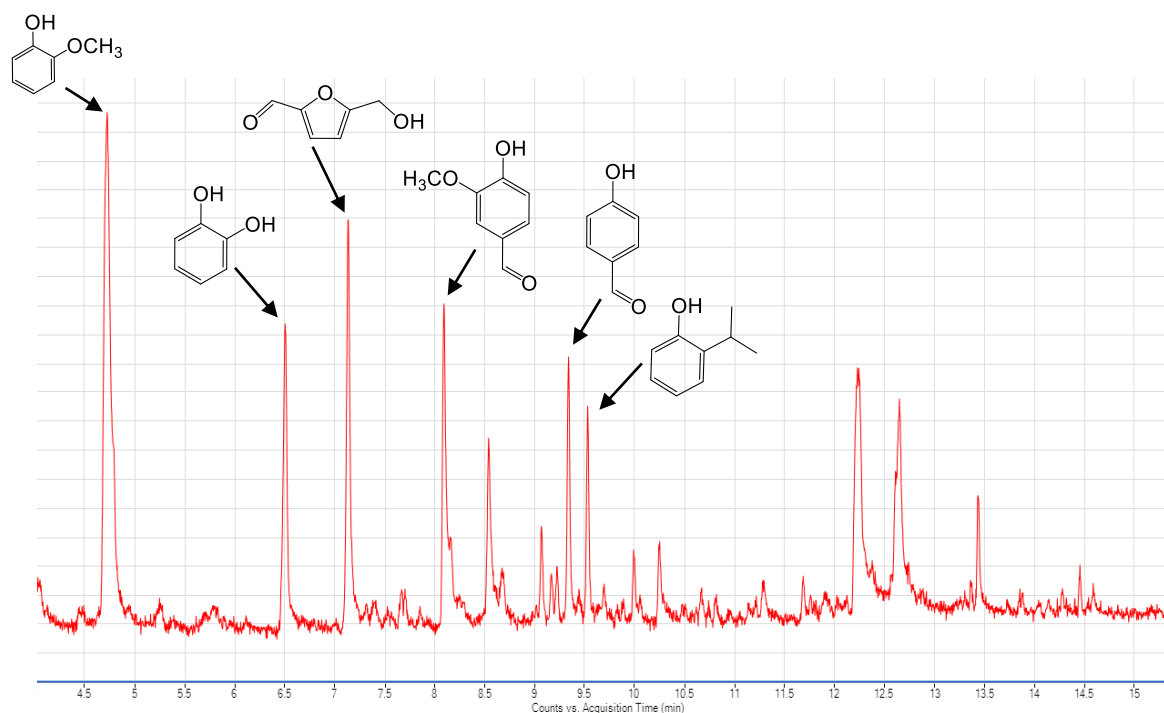
Figure 4.25. GC-MS chromatograph of obtained products.

Reaction Condition: Coir (0.5 g), NaX (0.5 g), EtOH: H_2O (1: 2 *v/v*, 30 mL), 200 ºC, 1 h.
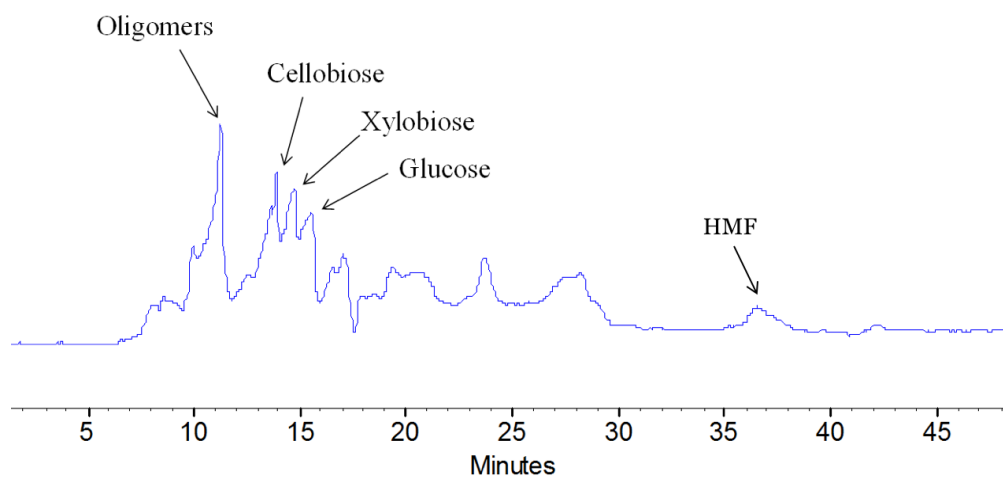
Figure 4.26. HPLC chromatograph of obtained products.

Reaction Condition: Coir (0.5 g), NaX (0.5 g), EtOH: H_2O (1: 2 *v/v*, 30 mL), 200 ºC, 1 h.

4.3.4. Coconut Coir and Isolated Lignin Correlation

In order to establish a correlation between the coconut coir and structure of the lignin with different functional groups is discussed. Presence of different functional in the isolated lignin was confirmed through ATR and ^{13}C NMR analysis. Monomer molecular formula was derived using CHNS analysis which shows the isolated lignin

is rich in guaiacyl units. It was understood that coir contains various characteristics functional groups like carbonyl, alkoxy groups, etc. Moreover, it is estimated that isolated lignin (CC-KL, CC-ORGL, CC-SL) having β-O-4 linkages along with tricin, guaiacyl, p-hydroxyphenyl and syringyl units.

4.4. Conclusions

It is anticipated in the literature that depending upon the isolation procedure lignin properties varies and upon its depolymerization obtained products will be having different functional groups. By keeping this into mind lignin was isolated from coconut coir using three different methods namely Klason, Organosolv and Soda method. It was possible to isolate maximum lignin (100%) from the coconut coir (based on the lignin present in coir) using Klason method. Coconut coir (CC) and isolated lignin (CC-KL, CC-ORGL, CC-SL) was characterized using various techniques like ICP-OES analysis. This analysis was performed in order to check the contamination present in coir and isolated lignin. Microanalysis reveals the coir is rich is guaiacyl type of units moreover monomer molecular formula, DBE, HHV, O/C and H/C ratio was also correlated. Various functional groups and linkages present in lignin were studied using ATR and ^{13}C NMR spectroscopy. TGA-DTA analysis was accomplished to check the thermal stability of coir and isolated lignin. Ash correction and dryness analysis was correlated with TGA-DTA results and nice coordination was observed. Furthermore, the best active alkali metal substituted zeolite (NaX) catalyst for the depolymerization of commercial lignin was explored for the conversion of coconut coir (CC) and isolated lignin (CC-KL, CC-ORGL, CC-SL) at milder reaction conditions ($\leq$ 250 °C, atmospheric pressure). Products obtained from the depolymerization of coconut coir and isolated lignin were confirmed using GC, GC-MS and HPLC analysis. Various physico-chemical characterizations for both fresh and spent catalysts were also performed to understand the morphologies of the catalysts. In summary, use of abundant and inexpensive lignocellulosic biomass i.e. coconut coir is shown to produce aromatic products using alkali metal substituted zeolite catalyst at milder reaction conditions.

4.5. References

1. F. S. Chakar and A. J. Ragauskas, *Ind. Crops prod.*, 2004, 20, 131-141.

2. X. L. J. Long, B. Guo, F. Wang, Y. Yu and L. Wang, Green Chem, 2012, 14, 1935-1941.

3. H. D. J. Zhang, L. Lin, Y. Sun, C. Pan and S. Liu, Biresour. Technol., 2010, 101, 2311-2316.

4. J.A. Perez Pimienta, M.G. Lopez Ortega, P.Varanasi, V. Stavila, G. Cheng, S. Singh and B.A.Simmons, 2013, 127.

5. A. W. R. Bhardwaj, B. Kinierim, S. Singh, B.M. Holmes, M. Auer, B.A. Simmons, P.D. Adams, and A.K. Singh, Biresour Technol, 2011, 102, 1329-1337.

6. Zea Strassberger, S. Tanase and G. Rothenberg, *RSC Advances*, 2014, 4, 25310-25318.

7. *NIIR Board of Consultants & Engineers, The Complete Book on Coconut & Coconut Products (Cultivation and Processing) Asia Pacific Business Press Inc.*, 2004.

8. *Food and Agriculture Organization of the United Nations: Statistical Division (FAOSTAT).* 2013. Retrieved 17 October 2015.

9. http://naturalfibres2009.org/en/fibres/coir.html.

10. http://www.naturalfibres2009.org/en/fibres/coir.html.

11. *Coir Board, Ministry of MSME, Govt. of India. ,* (http://coirboard.gov.in/?page_id=62).

12. G. Ramakrishna, and Sundararajan, , *T. Cement and Concrete Composites*, 2005a, 27, 575-582.

13. V. Agopyan, H. Savastano Jr, V. M. John and M. A. Cincotto, *Cement and Concrete Composites*, 2005, 2, 527-536. .

14. C. Asasutjarit, J. Hirunlabh, J. Khedari, S. Charoenvai, B. Zeghmati and U. C. Shin, *Construction and Building Materials*, 2007, 21, 277-288. .

15. K. G. Satyanarayana, K. Sukumaran, P. S. Mukherjee, C. Pavithran and S. G. K. Pillai, *Cement and Concrete Composites*, 1990, 12, 117-136.

16. E. Corradini, L. C. De Morais, M. F. De Rosa, S. E. Mazzetto, L. H. C. Mattoso and J. A. M. Agnelli, *Macromolecular Symposia*, 2006, 245-246, 558-564. .

17. S. R. Shukala and S. P. Roshan, *J. Hazard. Mater.*, 2005, 125, 147–153.

18. P. Muensri, T. Kunanopparat, S. Siriwattanayotin and e. al., *Composites*, 2011, 42, 173-179.

19. A. A. Waifielate and B. O. Abiola, *Master's Degree Thesis, Department of Mechanical Engineering, Blekinge Institute of Technology, Sweden*, 2008.

20. A. H. P. S. Khalil, M. S. Alwani, A. K. M. Omar and e. al., *Bioresources*, 2006, 1, 220-232.

21. P. S. S., U. C., J. R.M. and P. E., *J. Environ. Res. Develop.*, 2009, 3, 817-829.

22. R. G. and B. S. I.S., *Res. J. Recent Sci.*, 2012, 1, 270-274.

23. Heiko Lange, Silvia Decina and C. Crestini, *European Polymer Journal*, 2013, 49, 1151-1173.

24. Zakzeski J, Bruijnincx PCA, Jongerius AL and W. BM., *Chem Rev* 2010, 110, 3552-3599.

25. E. K. V. Sarkanen and C. H. Ludwig, *Wiley-Interscience,*, 1971, 165-240.

26. J. C. del Rio, A. Gutierrez, I. M. Rodriguez, D. Ibarra and A. T. Martinez, *J. Anal. Appl. Pyrolysis* 2007., 79, 39-46.

27. A. Guerra, J. P. Elissetche, M. Norambuena, J. Freer, S. Valenzuela, J. Rodríguez and C. Balocchi, *Ind. Eng. Chem. Res.*, 2008., 47, 8542-8549.

28. J. Rencoret, J. Ralph, G. Marques, A. Gutierrez, A. Martinez and J. C. del Rio, *J Agric Food Chem.*, 2013, 2434-2445.

29. H. Ismail, M. Edyhan and B. Wirjosentono, *Polym. Test.* , 2002, 21, 139-144.

30. Vishtal, Alexey Grigorievich and A. Kraslawski., *BioResources*, 2011, 3, 3547-3568.

31. T. Koshijima and T. Watanabe., *Springer Science & Business Media*, 2013., 131-140.

Chapter 5

Upgradation of Lignin Derived Monomers: Exploring the Effect of Basic Supported Metal Catalyst on Phenol, Guaiacol and Eugenol

5.1. Introduction

As discussed in previous chapters the depolymerization of lignin (commercial and isolated from coconut coir) into low molecular weight products/aromatic monomers was successfully performed using solid base catalysts at T ≤ 250 °C (Refer Chapter 3 and Chapter 4).[1] Generally, valorisation of lignin is a two-step process: 1) lignin is first converted into platform molecules mainly achieved via hydrogenolysis and pyrolysis reactions. 2) Upgradation of these platform molecules into fuels and chemicals via hydrogenation/deoxygenation to decrease the oxygen content or to decrease the O/C ratio. For the lignin depolymerisation, other methods like cracking, gasification, hydrolysis, etc. are also reported.[2-5] In all the aforementioned strategies, the controlled depolymerization of lignin is essential for producing intermediates with aromatic backbone for better processability.

To make the use of these platform molecules as octane enhancers or fuel additives, need further upgradation to yield biofuel or chemicals. The upgradation process involves deoxygenation and hydrogenation, which aims at reducing the O-functionalities and increase the energy density of the product upon saturation. It was observed from the lignin depolymerization using solid base catalysts that most of the products consist of several substitutions such as, alkyl, alkoxy, hydroxyl, olefinic double bonds etc. (Refer chapter 3, Table 3.3). Hence for the upgradation reactions, phenolic compounds with similar functionalities (obtained in lignin depolymerization reactions) such as phenol, guaiacol and eugenol were selected. In addition, basic supports are known to reduce the coke formation on the catalysts and thus increase the catalyst life[6,7-10] so, this study was performed with solid base catalyst along with metal. The reactions were performed under similar reaction conditions used for the depolymerization of lignin (250 °C) (Chapter 3 and Chapter 4). This study can be helpful for the development of one-pot method for the depolymerization of lignin followed by the upgradation of lignin derived products (Scheme 5.1).
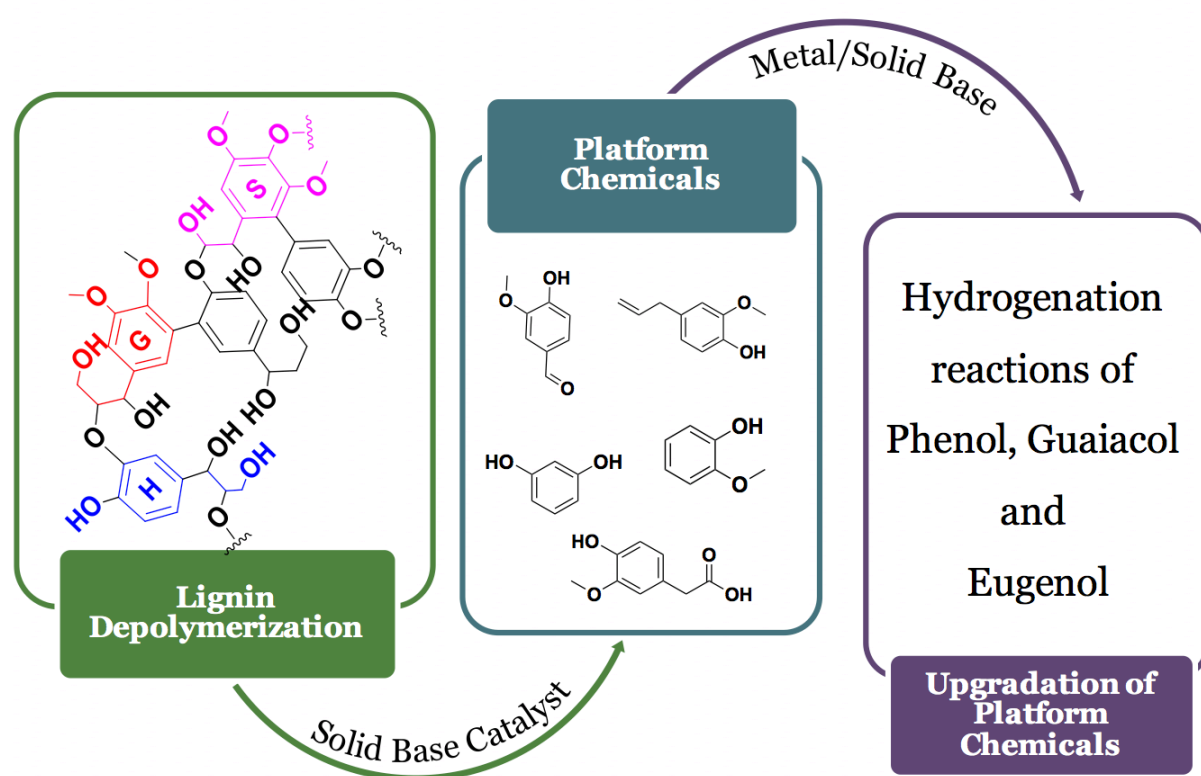
Scheme 5.1. Scheme for the upgradation of lignin derived platform chemicals.

With regard to the upgradation of lignin derived compounds to yield lower oxygen content products via hydrogenation or deoxygenation reactions, in the earlier studies researchers have focused on the utilization of conventional NiMo and CoMo sulfide and oxide catalytic systems. Partial conversion of phenol into benzene and cyclohexane at 325 °C was reported with alumina supported Co-Mo sulfide as a catalyst.[11] Upgradation reactions of guaiacol and syringol were studied at 450-500 °C with a MoO_3-NiO/Al_2O_3 catalyst to yield toluene and benzene as major products.[12] In the presence of a $CoMo/Al_2O_3$ catalyst, methyl phenols (methyl phenols, di- and tri-methyl phenols) were converted to arenes or cyclic alkanes over different active sites at 300 °C.[12] Generally, at low temperature (150 °C) the active sites are terminal sulphur vacancies on the Co-promoter atom while at temperature around 400 °C a second type of sites becomes active, which is believed to consist of bridging sulphur vacancies in between Co and Mo atoms on the MoS_2 edges.[13] Other lignin derived substrates are also studied for the upgradation via hydrogenation/ deoxygenation (HDO) reactions to yield low oxygen content products, including cresols (MoO_3-

NiO/Al_2O_3, 450 °C, 2.8 MPa H_2, 1h, xylene and dimethyl cyclohexane are major products),[12] anisole (Sulfided $CoMo/Al_2O_3$, 300 °C, phenol, benzene, cyclohexane, o-cresol are major products),[14] catechol (MoO_3-NiO/Al_2O_3, 500 °C, 2.8 MPa H_2, 1h, benzene, cyclohexane, methylcyclopentane are major products),[15] 4 methyl-acetophenone (sulfided CoMo/activated carbon, 280 °C, 7.0 MPa H_2, 2h, ethylmethylbenzene is the major product),[16] 4-methylguaiacol ($CoOMoO_3/Al_2O_3$, 325 °C, 6.9 MPa, 0.7 h, methylguaiacol isomer, methyl catechol, cresol, toluene are the major products),[17] eugenol ($CoOMoO_3/Al_2O_3$, 300 °C, 6.9 MPa, 0.7 h, propylguaiacol, propylcatechol, methylguaiacol are the major products),[17] benzofuran (Ni-Mo/Al_2O_3, 180 °C, 2.1 MPa, octahydro-1-benzofuran and ethylcyclohexane are major products).[18, 19] Though effective in giving HDO activity, Molybdenum (Mo) based catalysts were known to have several drawbacks like catalyst to be active requires very harsh conditions (300-500 °C), and are problematic due to the possible sulfur contamination of the products (like methanethiol and dimethyl sulfide). Looking at the drawbacks associated with Mo based catalysts, researchers have also used supported noble metal catalysts and were widely studied as alternative catalysts for the upgradation of lignin derived products. Guaiacol upgradation over Ru/C catalyst under 4.0 MPa of H_2 pressures was studied.[20] At 200 °C, guaiacol mainly underwent hydrogenation and demethoxylation to yield cyclic alcohols. The formation of cyclohexane was started to observe at 250 °C with selectivity of 20%. Rh, Pd, Pt, RhPd, RhPt and PdPt supported on ZrO_2 catalysts were used for guaiacol reactions at 300 °C under 8.0 MPa of H_2 (at the reaction temperature).[21] In these reactions, all the catalysts showed high selectivity for hydrogenated oxygen-containing compounds (1-methyl-1,2-cyclohexanediol and cyclohexanol). In addition, small amount of benzene was formed with cyclohexanol as by product. Pt/Al_2O_3 was used for the upgradation of phenolic compounds and the reforming of light oxygenates in bio-oil.[22] Liquid product, mostly arenes and alkanes with only 3% of oxygen was obtained. H_2 was generated in situ via the reforming of light oxygenates and the oxygen was removed as CO_2. Homogeneous acids (H_3PO_4) were also used in combination with supported metals (Pd/C and H_3PO_4) for the conversion of lignin derived aromatic monomers (phenols, guaiacols, and syringols) into hydrocarbons.[23] To avoid the drawbacks associated with the homogenous acids, those were replaced by solid acids (e.g. $Nafion/SiO_2$, H-ZSM-5).[24, 25] Guaiacol upgradation was reported

using Ru/C catalyst at 250 °C yielding methoxy cyclohexanol (60%) as the major product.[26] Moreover, guaiacol upgradation was studied with the addition of base (MgO) along with Ru/C catalyst, and it was observed that at relatively milder reaction condition (160 °C, 2 h) maximum yield for the cyclohexanol (80%) can be obtained.[27]

The catalytic activity of different noble metals (Pt, Pd, Ru) on supports like silica-alumina, alumina, etc. are studied on the lignin model compounds (phenol, guaiacol and eugenol). Reactions were done at 250 °C with 3.0 MPa of H_2 pressure.[28] It was proposed that the first step of ring hydrogenation is a metal-driven reaction however, further removal of oxygen is mostly governed by the supports (mainly on acidic supports such as alumina and silica-alumina). Overall, noble metals in the combination of acid catalysts are promising for upgradation of lignin derived chemicals as metals govern the hydrogenation reaction and acidic support is the driven force for the oxygen removal. However, the high price of precious noble metals is a limitation of these catalysts for the large-scale utilization. Several mono-, di- and tri-functional phenolic compounds were studied with a copper chromite catalyst. Formation of cyclic alkanes with a small amount of arenes were obtained at 200-275 °C under 5.0 MPa of H_2 pressure.[29] Iron supported on silica catalyst was also used for the gas phase hydrodeoxygenation of guaiacol to benzene and toluene at 350-450 °C.[1, 30]

It was understood from the literature, that noble metals are quite active for hydrogenation/ deoxygenation of phenolic compounds. Hence Pt, Pd and Ru metals were selected to study the upgradation of lignin derived monomers. In this chapter, upgradation studies on lignin derived aromatic monomers like phenol, guaiacol, eugenol and mixture of these compounds using supported metal catalysts is discussed. The catalysts used for this work were prepared by wet-impregnation method with 1-3 *wt.%* of metal loading (Refer chapter 2B, Section 2B.4.2.2 and Table 2B.4). As demonstrated in the last two chapters (Chapter 3 and 4), solid base catalyst NaX (Si/Al = 1.2) shows great potential in the depolymerization of lignin (commercial and isolated) and raw biomass (coconut coir). However, the obtained compounds still (Refer Chapter 3, Table 3.3) contain significant amount of oxygen. For the production of transportation fuels, current strategies focus on the upgradation of platform chemicals produced from lignin depolymerization. Ideally, it

would be very attractive to combine the upgradation step with the depolymerization step in a one-pot process, which could significantly reduce the operating costs.

For this purpose, intentionally basic supports (NaX, CaO, C-HT) were chosen to study the upgradation reactions of lignin derived monomers via hydrogenation. Additionally, those can possibly reduce the coke formation on the catalysts and may increase the catalyst life. To perform the upgradation reactions of phenol, guaiacol and eugenol compounds, purposefully selected the similar reaction condition as used for the lignin depolymerization (250 °C as the reaction temperature) (Refer chapter 3, Section 3.3.2).

5.2. Experimental

5.2.1. Catalyst Synthesis

All the supported metal catalysts were synthesized by wet-impregnation method. Pt (1-3 *wt.%*), Pd (*2* and *3 wt.%*) and Ru (2 and 3 *wt.%*) metals were impregnated on NaX (Si/Al = 1.2, Na: 17.3 mg/g), CaO and calcined-hydrotalcite (C-HT) supports. The details on the procured materials and synthesis procedure used for the preparation of different supported metal catalysts are given in chapter 2B (Refer chapter 2B; Section 2B.2, 2B.4).

5.2.2. Upgradation of Lignin Derived Monomers

Monomers used in this study, Phenol (99.5%, Sigma Aldrich), guaiacol (99%, Loba Chemie) and eugenol (99%, Sigma Aldrich), were purchased and used as received. Solvent, n-hexadecane (99%, Sigma Aldrich) was purchased and used as received. The possible products which are confirmed by GC-MS, cyclohexane (99%, Loba Chemie), cyclohexanol (99.5%, Loba Chemie), 2-methoxy cyclohexanol (99%, Alfa Aesar), 4-propyl phenol (99%, TCI chemicals) and 4-propyl cyclohexanol (> 98%, Loba Chemie) were purchased and used as calibration standards for GC analysis. All the reactions were carried out in a 100 mL batch mode Parr autoclave. For hydrodeoxygenation studies of phenol and eugenol the following reaction procedure was employed. Reactions of phenol and eugenol were done with 2 mmol of substrate with S/C mole ratio of 200 to 2000. Hexadecane (30 mL) were used as reaction medium for all the reactions. Guaiacol was studied by taking 12 mmol of it with, S/C = 214 mole ratio. Here also, hexadecane (30 mL) were used as solvent system. For

the reactions, substrate, catalyst and solvent were added to the autoclave. Later H_2 gas was charged with Initial pressure of 3 MPa (at RT). Reactions were performed at 250 °C for 1 h. Initially, the rpm was kept at 100 and after achieving the desired reaction temperature it was increased to 1000 and this time was considered as the starting time of the reaction. All the reactions were performed 2 times in order to check the reproducibility of results. After the reaction, reactor was cooled under water and air flow and the catalyst was recovered by centrifugation. Further, the recovered catalyst was washed with acetone, dried in oven at 55 °C for 12 h and followed by the vacuum dried at 150 °C for 2 h under (10^{-4} MPa). Prior to the use of recovered catalyst for the next reaction it was calcined (O_2, 20 mL/min) and reduced at 400 °C (H_2, 20 mL/min) for 2 h. Catalyst weight was taken to maintain the substrate/metal ratio of 200 is given in Table 5.1.

Table 5.1. Catalyst weight as per the S/M mole of 200 mol/mol.

Catalyst	Catalyst weight (g)
1 *wt.%* Pt/NaX	0.195
2 *wt.%* Pt/NaX	0.097
3 *wt.%* Pt/NaX	0.065
2 *wt.%* Pd/NaX	0.053
3 *wt.%* Pd/NaX	0.0353
2 *wt.%* Ru/NaX	0.0505
3 *wt.%* Ru/NaX	0.033
2 *wt.%* Pt/CaO	0.097
3 *wt.%* Pt/C-HT	0.065

5.2.3. Analysis

The reaction mixtures were injected on gas chromatograph (GC-FID), GC-mass spectroscopy (GC-MS), to draw a calibration curve with procured standard compound with a ± 2 % error.

5.2.3.1. GC-FID

For the identification of products obtained, reaction mixtures were analyzed using an Agilent 7890B model Gas Chromatograph (GC) equipped with a HP-5 capillary column (5 % phenyl 95 % dimethyl polysiloxane) (30 m x 0.25 mm) and flame ionization detector (FID). N_2 (30 mL/min) is used as a carrier gas with a flow rate of 0.6 mL/min. H2 (25 mL/min) is used for flame and air as oxidizer (300 mL/min). Injector and detector temperatures were maintained at 275 °C and 280 °C, respectively. Split mode injector (50:1) was used for sample delivery and the following column oven program used,

Temperature (°C)	Hold time (min)	Ramping rate (°C/min)	Total time (min)
50	10	10	10
150	2	2	2
250	20	10	42

5.2.3.2. GC-MS

The Agilent GC-MS (7890B GC and 5977A MSD) equipped with DB-5MS column (5% phenyl 95% dimethyl polysiloxane) (30 m x 0.25 mm) was used to determine the molecular weight of the products identified using GC-MS. Helium (0.6 mL/min) is used as a carrier gas; the column oven program used is same as that for GC analysis. From the mass spectrum, m/z value of the compounds and then corresponding molecular weight obtained was matched with the mass spectra in NIST library for compound identification.

5.2.4. Conversion, Selectivity and Yield Calculation

The conversion, selectivity and yields were calculated based on the calibration curve obtained from GC analysis (mol basis) using the following formulae:

$$\text{Conversion (\%)} = \frac{\text{No. of moles of Substrate charged} - \text{No. of moles of Substrate final}}{\text{No. of moles of Substrate charged}} \times 100$$

$$\text{Selectivity (\%)} = \frac{\text{No. of moles of product formed}}{\text{No. of moles of substrate converted}} \times 100$$

$$\text{Yield (\%)} = \frac{\text{Conversion (\%)} \times \text{Selectivity (\%)}}{100}$$

5.3. Results and Discussions

Phenol, guaiacol and eugenol were studied for upgradation using supported metal catalysts. Different supported metal catalysts were prepared by wet-impregnation method by varying metal loading from 1-3 *wt.%* of noble metals (Pt, Pd and Ru) on basic supports (NaX, CaO and C-HT) (Refer chapter 2B, Section 2B.4). Prior to the catalytic runs all these catalysts were characterized using various physico-chemical techniques. XRD analysis (Refer chapter 2B, Section 2B.5.2.1, Figure 2B.11-13) showed the characteristic peaks for all metals and supports. From ICP-OES analysis it was confirmed that metal loading on supports were similar to the theoretical loading of metal (1-3 *wt.%*) (Refer chapter 2B, Section 2B.5.2.6. Table 2B.6). From CO_2-TPD analysis it was observed that after metal impregnation basicity drops down due to the less availability of basic sites on the support. BET surface area of supported metal catalysts was determined using N_2 sorption analysis (Refer chapter 2B, Section 2B.5.2.3, Table 2B.7). Reactions were done at 250 °C in hexadecane solvent under 3.0 MPa of H_2 pressure.

5.3.1. Studies on Phenol Upgradation

Reactions of phenol upgradation were done in batch mode Parr autoclave. Reactions were performed with 2 mmol of phenol with substrate/metal (S/M) ratio of 2000 mole/mole and hexadecane as solvent. Reactions were done at 250 °C for 5 h under 3.0 MPa of H_2 pressure (5.0 MPa at 250 °C). Scheme 5.2 shows possible pathways for the upgradation of phenol into various products. First phenol upgradation reactions were performed using different loading of Pt metal (1, 2 and 3 *wt.%*) on NaX. In the

absence of metal under these conditions, phenol shows a conversion of only 13%. But when supported metal catalysts were used ca. 66 % phenol conversion with 39% of cyclohexanol yield was observed with 3 *wt.%* Pt/NaX (Figure 5.1). Moreover, it was observed that conversion and yield for cyclohexanol increases as the Pt loading increases. This could be because of the increase in the active metal sites with higher loading of metal (1 to 3 *wt.%* Pt/NaX). Particle size was calculated from TEM analysis and it was observed 4 nm, 8 nm and 3.5 nm for 1, 2 and 3 *wt.%* Pt/NaX, respectively. Contrary, decrease in the particle size for 3 *wt.%* Pt/NaX was observed. It might be due to the fine dispersion of metal particle over the support as can be clearly seen from TEM analysis (Chapter 2B, Figure 2B.14). Additionally, dispersion of the metal particles was also calculated and high dispersion of 32% was observed for 3 *wt.%* Pt/NaX compared to 1 and 2 *wt.%* Pt/NaX (28% and 14% dispersion), which could be another reason for the more activity of 3 *wt.%* Pt/NaX. Formation of cyclohexanol was confirmed using GC and GC-MS analysis. No coke and gas formation was observed under the reaction conditions used.
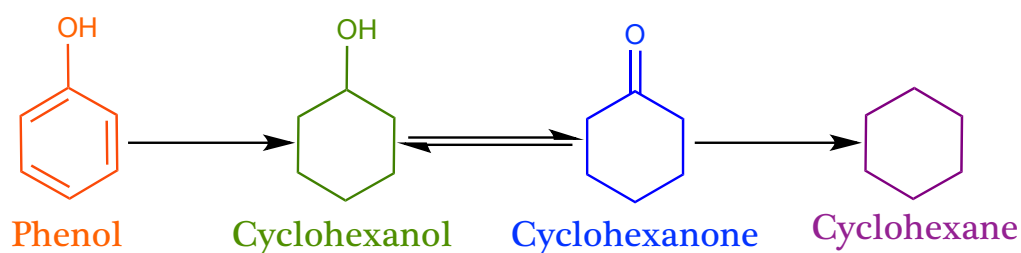
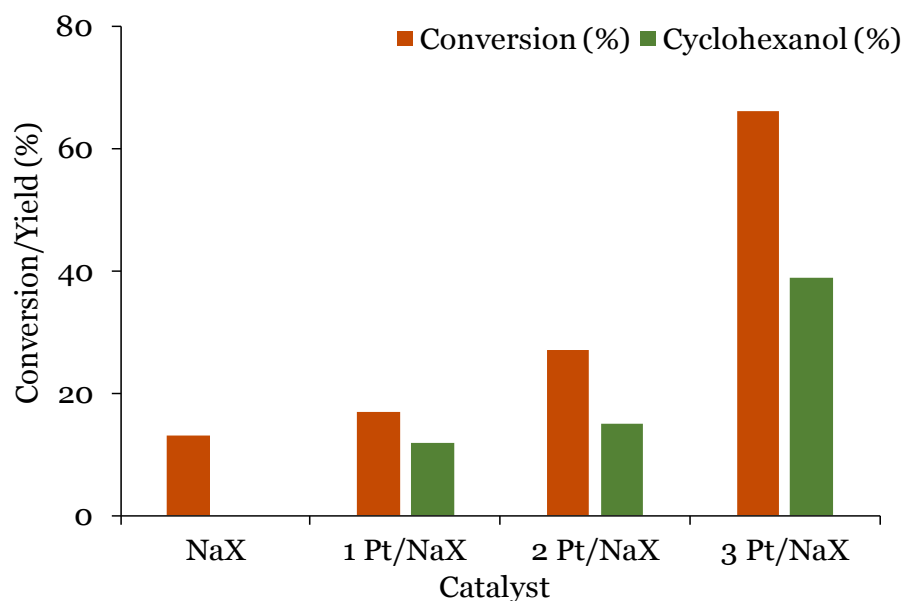**Scheme 5.2.** Phenol upgradation routes.

Figure 5.1. Effect of platinum (Pt) loading on phenol upgradation.

Reaction Condition: Phenol (2 mmol), Catalyst (S/M = 2000 mol/mol), Hexadecane (30 mL), 250 °C, 3.0 MPa H_2 at RT, 5 h.

Further, a series of catalysts by varying metal (Pt, Pd, Ru), metal loading (2, 3 *wt.%*) and support (NaX, CaO, C-HT) were studied (Figure 5.2). A conversion of 60% and 55% was observed with 2 *wt.%* and 3 *wt.%* loading of Pd on NaX with the formation of 2% and 3% cyclohexanol, respectively. While with 2 and 3 *wt.%* Ru/NaX catalyst, 15 and 23% conversions were observed along with 2% and 8% of cyclohexanol yield, respectively. The difference in the yields for Pt, Pd and Ru catalyst could be explained on the basis of dispersion of these metals on the support (Refer Chapter 2B, Figure 2B.14 and Table 2B.9). Percent dispersion for Pt/NaX was observed higher compare to Pd/NaX and Ru/NaX. For instance, dispersion of 3 *wt.%* Pt/NaX is 32% while for 3 *wt.%* Pd/NaX and 3 *wt.%* Ru/NaX is only 3%. Furthermore, variation of support from NaX to CaO and calcined HT (C-HT) was also studied. 3 *wt.%* Pt/C-HT shows 77% of conversion with the cyclohexanol yield of 7%. Additional temperature and time was also studied but not much improvement in the yields was observed (Figure 5.3). So, it was concluded that with such a low S/M ratio of 2000 mol/mol very less active sites of the catalyst are available for the conversion of phenol, because of that reactions were not going further.
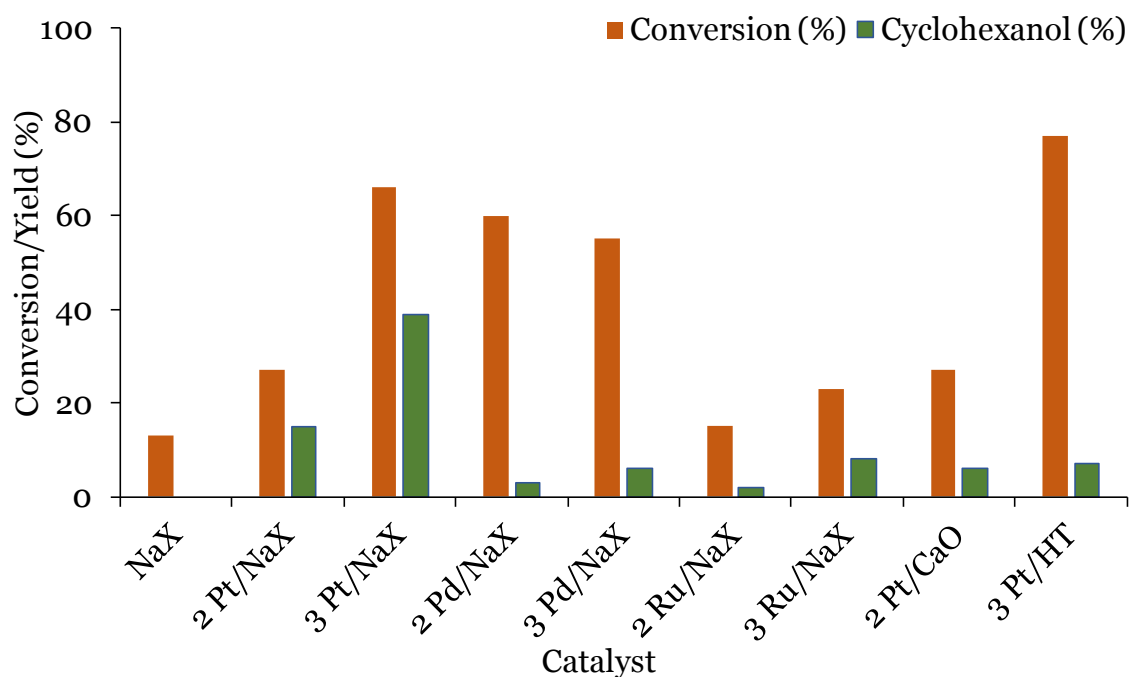
Figure 5.2. Effect of various supported metal catalysts on the phenol upgradation. Reaction condition: Phenol (2 mmol), Catalyst (S/M = 2000 mol/mol), Hexadecane (30 mL), 250 °C, 3.0 MPa H_2 at RT, 5 h.

Figure 5.3. Effect of (A) temperature and (B) time on the phenol upgradation. Reaction condition: (A) Phenol (2 mmol), Catalyst (S/M = 2000 mol/mol), Hexadecane (30 mL), 3.0 MPa H2 @ RT, 5 h, (B) Phenol (2 mmol), Catalyst (S/M = 2000 mol/mol), Hexadecane (30 mL), 250 °C, 3.0 MPa H_2 at RT.
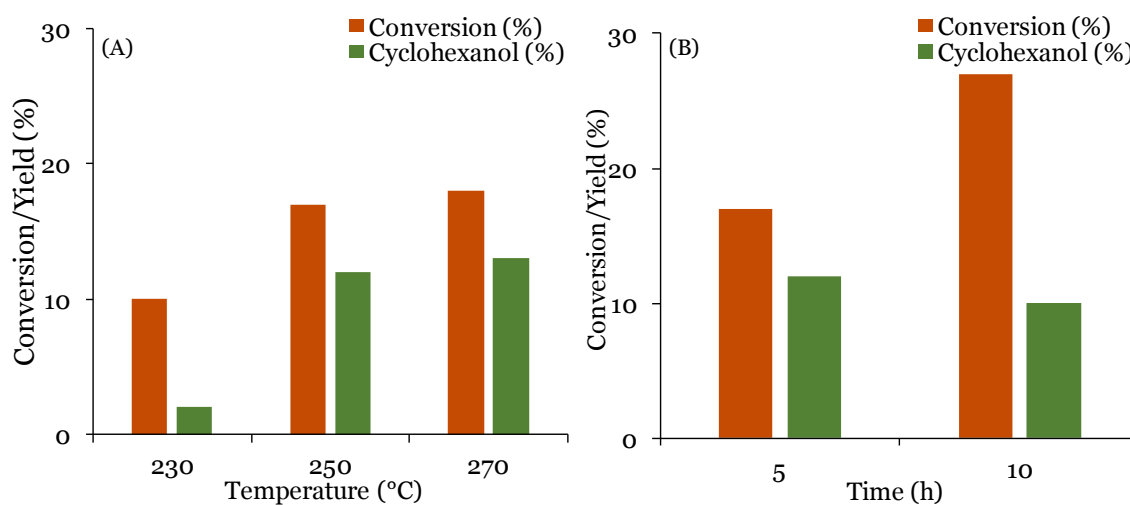
In order to improve the yields, S/M ratio was decreased from 2000 to 200 mol (Figure 5.4). Reactions were performed with 1 and 3 *wt.%* Pt/NaX at 250 °C for

1 h. With 1 *wt.%* Pt/NaX 55% conversion of phenol and 49% yield of cyclohexanol along with 0.8% of cyclohexanone formation was observed. When the reaction was carried out with high platinum loading of 3 *wt.%* Pt/NaX, 55% of phenol conversion with 31% of cyclohexanol and 1% of cyclohexanone was observed.
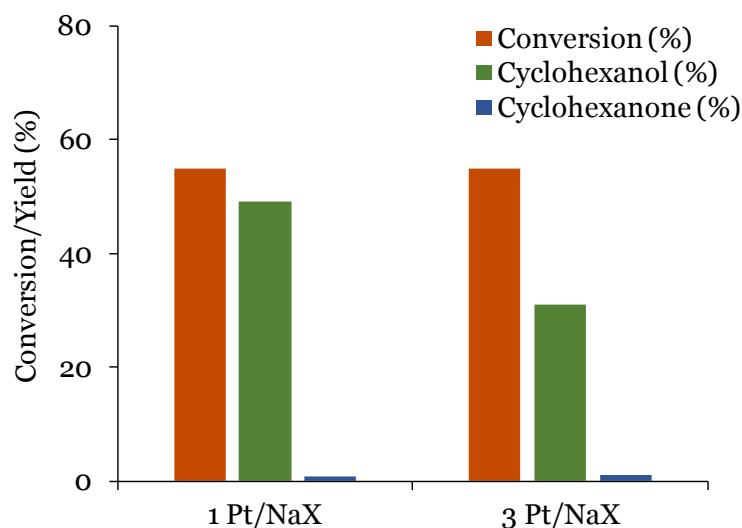

Figure 5.4. Upgradation of phenol using Pt/NaX (1 *wt.%* and 3 *wt.%*)
Reaction condition: Phenol (2 mmol), Catalyst (S/M = 200 mol/mol), Hexadecane (30 mL), 250 ºC, 1 h, 3.0 MPa H_2 at RT.

Results obtained with 3 *wt.%* Pt/NaX were compared with 3 *wt.%* Pt/C-HT. It is very clear from the Figure 5.5 that, as the NaX was replaced with a strong base such as calcined hydrotalcite (C-HT) yields for the cyclohexanol (55%) and cyclohexanone (11%) were increased. So, it can be concluded that not only Pt is playing a role in phenol upgradation but, reaction is also governed by the combination of Pt with C-HT. This selectivity difference for the cyclohexanol and cyclohexanone formation could be attributed to the acid-base interaction between the phenolic OH group of phenol and NaX/C-HT support, with Pt particles providing hydrogenation sites. Moreover, the basic sites of supports also play a role in governing the reaction. From the CO_2-TPD analysis, it was seen that in case of NaX, presence of moderate basic sites (0.42 mmol/g) were seen at 404 ºC while C-HT catalyst possess both weak and strong basic sites (0.40 mmol/g) at 294 ºC and 603 ºC. The interaction of basic sites of NaX and CaO with phenolic substrates was explored in Chapter 3, section 3.3.4. It was observed that due to the presence of moderate and strong basic sites in CaO (408 and 673 ºC: 1.96 mmol/g) strong

adsorption of phenolics substrates occurred. The same phenomenon is observed here also. Due to the presence of strong basic sites in C-HT, substrate (phenol, hydroxyl group) is interacting more and this results in the higher cyclohexanone formation. On the other hand, the diffusion of phenol towards the basic sites inside Pt/C-HT is expected to be easier than that inside Pt/NaX, because C-HT has a larger pore size (2.39 nm, Chapter 2, Table 2B.7) compare to 3 *wt.%* Pt/NaX (1.03 nm, Chapter 2, Table 2B.7) that is sufficient to allow phenol to pass inside and access the basic sites. The larger pore size of Pt/C-HT might be another reason for the better conversion of phenol.
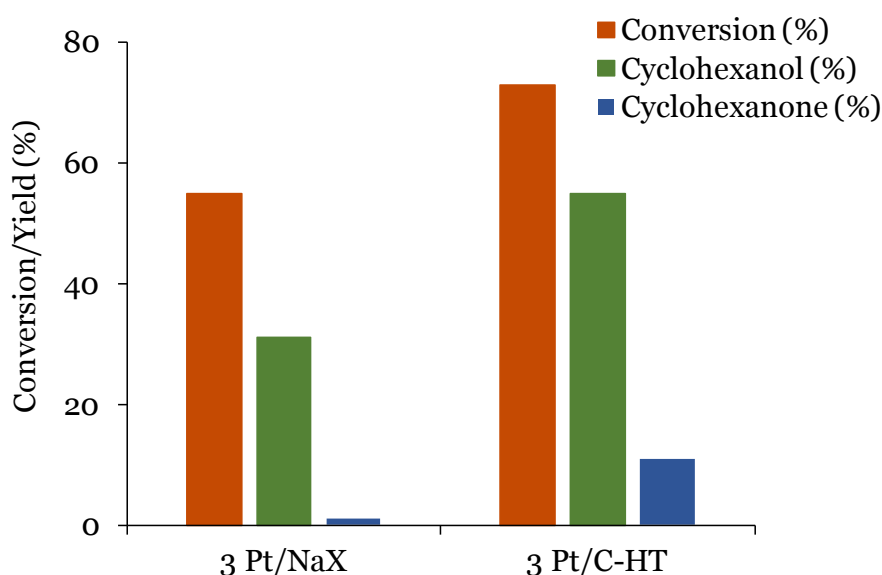
Figure 5.5. Effect of support on phenol upgradation

Reaction condition: Phenol (2 mmol), Catalyst (0.065 g) (S/M = 200 mol/mol), Hexadecane (30 mL), 250 $^{\circ}$C, 1 h, 3.0 MPa H_2 at RT.

Furthermore, the cyclohexanone formation is observed more (11%) with 3 *wt.%* Pt/C-HT. This might be possible due to the adsorption-desorption phenomenon. Adsorption of phenol on C-HT is strong compare to the desorption of cyclohexanol, and thus this results in the increase in cyclohexanone formation. The more adsorption on C-HT, CaO, MgO, HAP is also observed in the lignin depolymerization studies with various solid base catalysts. The same was explained in detail in Chapter 3, Section 3.3.4. It was observed from the upgradation of phenol over supported metal catalysts that the basic supports (NaX, CaO, C-HT) with Pt and

Ru catalysts gave cyclohexanol as a major product. Hence, the guaiacol upgradation reactions were carried out with optimum catalyst, 3 *wt.%* Pt/NaX, 3 *wt.%* Ru/NaX and 3 *wt.%* Pt/C-HT.

5.3.2. Studies on Guaiacol Upgradation

Guaiacol upgradation was performed using 3 *wt.%* Pt, Ru/NaX and 3 wt.% Pt/C-HT catalysts. Guaiacol substrate was chosen since it is also an example of lignin derived aromatic monomer and in my earlier work on depolymerisation of lignin (Chapter 3 and 4), this compound was identified as one of the products formed (Chapter 3: Section 3.3.2 and 3.3.3, Table 3.3, Figure 3.4 to Figure 3.7, Chapter 4: Section 4.3.3, Figure 4.24). Reactions were performed with 12 mmol of guaiacol with 0.2 g of catalyst at 250 °C for 1 h. Figure 5.6 represents the products obtained from guaiacol when it undergoes upgradation reaction.
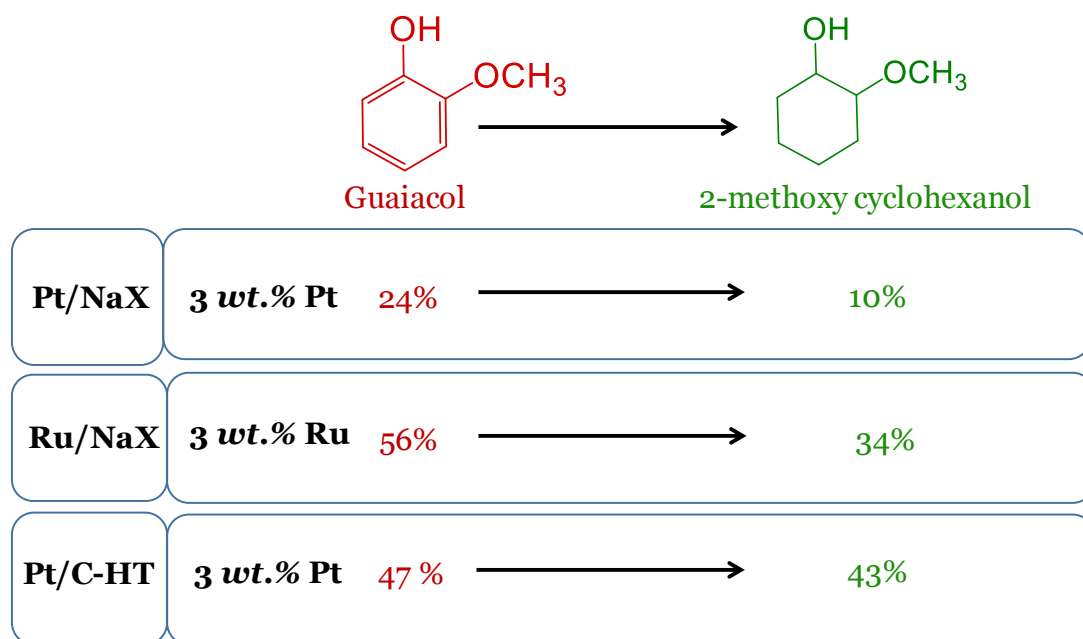
Figure 5.6. Upgradation of guaiacol

Reaction condition: Guaiacol (12 mmol), Catalyst (0.2 g), Hexadecane (30 mL), 250 °C, 1 h, 3.0 MPa H_2 at RT.

Guaiacol conversion of 24% and the formation of 10% 2-methoxy cyclohexanol was observed with 3 *wt.%* Pt/NaX catalyst. When the reaction was performed with 3 *wt.%* Ru/NaX, increase in the conversion and product yield was found (56% conversion, 34% 2-methoxy cyclohexanol). Further, guaiacol

upgradation was checked with 3 *wt.%* Pt/C-HT under the same reaction condition and 43% of 2-methoxy cyclohexanol with 47% conversion of guaiacol could be achieved. Methoxy cyclohexane, cyclohexanol, cyclohexanone, anisole, 1,2-dimethoxy cyclohexane were also found in trace amount (0.4-1 %). The increase in the conversion and product yield might be due the presence of strong basic support C-HT. Similar observation for the more conversion and product formation was observed with phenol upgradation studies also (Section 5.3.1). Moreover, it was discussed in the Chapter 3, that strong bases like CaO, C-HT, etc. shows the product adsorption phenomenon. This can be simply understood by adsorption-desorption phenomenon of substrate on the catalyst. Hence, it could be proposed that substrate is interacting with the catalyst through π-π bonding with benzene ring instead of hydroxyl and methoxy groups. Interaction of –OH and –OCH$_3$ could not be possible due the steric hindrance, which leads to the formation of 2-methoxy cyclohexanol.

5.3.3. Up-gradating Mixture of Aromatic Monomers

Since, better conversions and product yields were observed with 3 *wt.%* Pt/C-HT, the efficiency of this catalytic system was also checked in the eugenol upgradation. Due to the presence of different functional groups and resemblance with the lignin monomer unit coniferyl alcohol, eugenol was chosen for the study (Figure 5.7). Under this reaction condition it was possible to convert 100% of eugenol into 2-methoxy-4-propyl phenol (81%). Here, preferably hydrogenation of allylic double bond was observed. It could be attributed that allylic double bond is interacting with the catalyst through π-π bonding preferably. It is predicted that due to the steric hindrance, ring does not undergo hydrogenation. Moreover, the double bonds present in the aromatic ring are very stable, due to the resonance stabilization of the π-electrons in the aromatic ring.
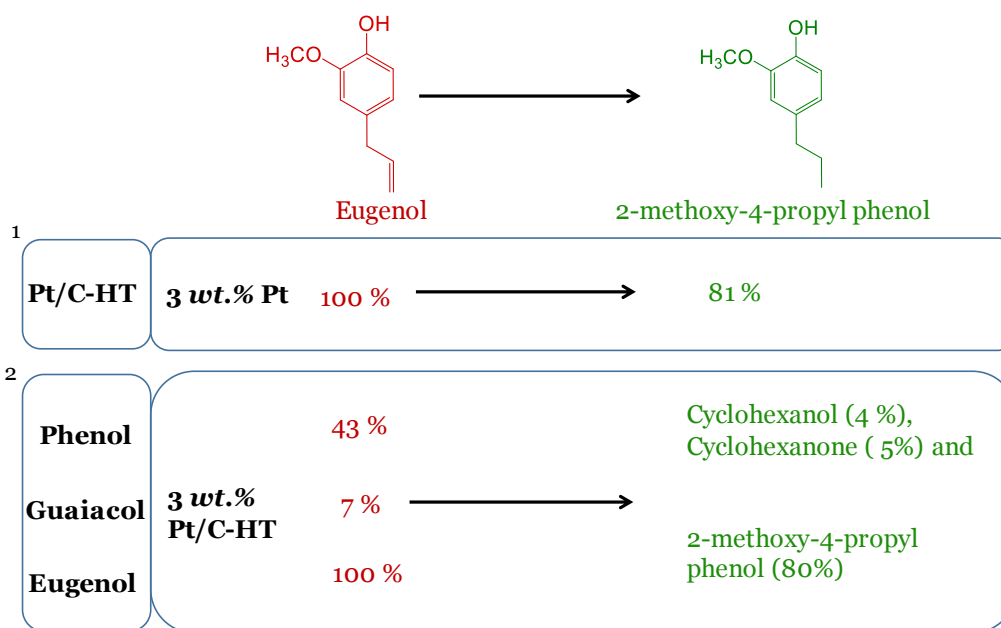
Figure 5.7. Upgradation of eugenol[1] and mixture of phenol, guaiacol and eugenol[2] Reaction condition: (1) Eugenol (2 mmol), Catalyst (S/M = 200 mol/mol), Hexadecane (30 mL), 250 °C, 1 h, 3.0 MPa H_2 @ RT, (2) Phenol, Guaiacol, Eugenol (2 mmol each), Catalyst = 0.056 g, Hexadecane (30 mL), 250 °C, 1 h, 3.0 MPa H_2 at RT.

Initially the catalytic system was studied for monomeric compounds (phenol, guaiacol and eugenol). Further, this catalytic system (3 *wt.%* Pt/C-HT) was explored with the physical mixture of aromatic compounds (like in the lignin depolymerization reaction, mixture of aromatic products was obtained). For this, reactions were performed with the mixture of phenol, guaiacol and eugenol with 3 *wt.%* Pt/C-HT at 250 °C for 1 h (same reaction condition used for lignin depolymerization). On the basis of individual calculations, 4% cyclohexanol, 5% cyclohexanone and 80% 2-methoxy-4-propyl phenol was observed with the conversion of 43%, 7% and 100% for phenol, guaiacol and eugenol, respectively. From the obtained results, it can be concluded that this catalytic system is active for the mixture of phenolic aromatic compounds. In my view, the studies performed here will be helpful in the developing/designing an active catalytic system for the upgradation of lignin derived aromatic monomers.

5.3.4. Catalyst Recyclability

The reusability of 1 *wt.%* Pt/NaX and 3 *wt.%* Pt/C-HT catalysts was studied for the upgradation reactions of phenol and the results are presented in Figures 5.8 and Figure 5.9. After reaction, catalyst was recovered by centrifugation and washed with acetone. Later, it was kept for drying in oven for 16 h. Prior to the next catalytic run it was subjected for calcination-reduction. Calcination was done in air flow of 20 mL/min and reduced under hydrogen flow of 20 mL/min at 400 °C for 2 h, each. It was observed that both the catalysts are stable under reaction condition. 1 *wt.%* Pt/NaX showed the slight decrease in the yield after each run with the selectivity of 43-45% yield of cyclohexanol. Moreover, *3wt.%* Pt/C-HT also showed good recyclability upto 3rd recycle run with slight decrease in the yield for cyclohexanol (1st run: 55%, 2nd run: 53%, 3rd run: 49%, 4th run: 44%) and cyclohexanone (1st run: 11%. 2nd run: 9%, 3rd run: 6%, 4th run 4%). Minor decrease in the yields after each run is because of probable loss of some catalyst quantity during separation.
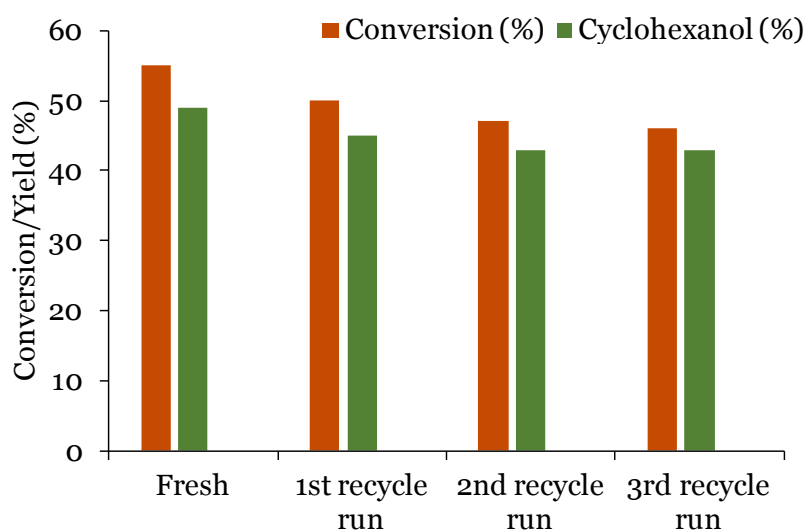
Figure 5.8. Recycle study with 1 *wt.%* Pt/NaX of phenol.

Reaction condition: Phenol (2 mmol), Catalyst (S/M = 200 mol/mol), Hexadecane (30 mL), 250 °C, 1 h, 3.0 MPa H_2 at RT.
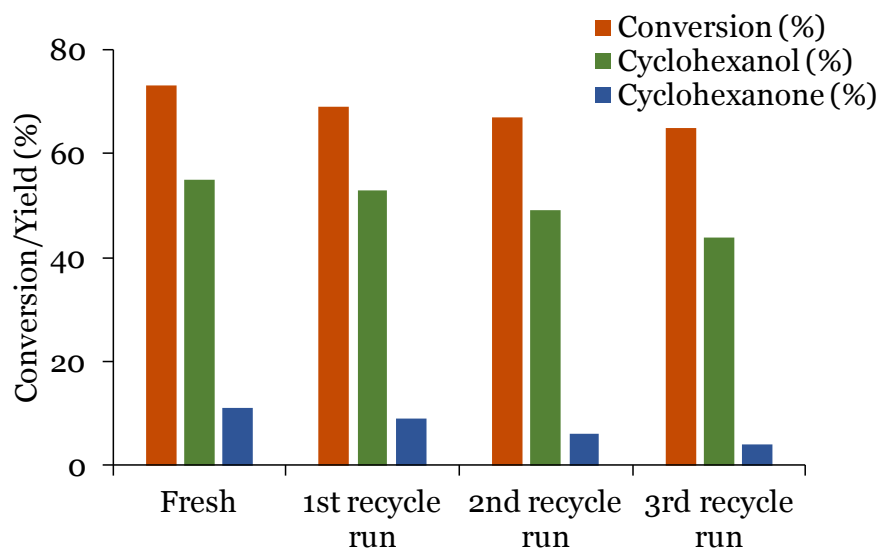
Figure 5.9. Recycle study with 3 *wt.%* Pt/C-HT of phenol

Reaction condition: Phenol (2 mmol), Catalyst (S/M = 200 mol/mol), Hexadecane (30 mL), 250 °C, 1 h, 3.0 MPa H2 at RT.

Characterizations of the fresh and spent catalysts were done by XRD, ICP-OES, N_2 sorption and TPD-CO_2 technique. XRD analysis shows similar peak pattern for the fresh and spent catalyst with the observance of metallic Pt peaks (Figure 5.10 and Figure 5.11). Furthermore, by ICP-OES technique it was found out that there was no leaching of the metal from the catalyst. From N_2 sorption analysis similar surface area, pore volume and pore size were observed. TPD-CO_2 shows that no change in the basicity for the catalyst. These all facts conclude that catalyst is stable under reaction condition and reusable.
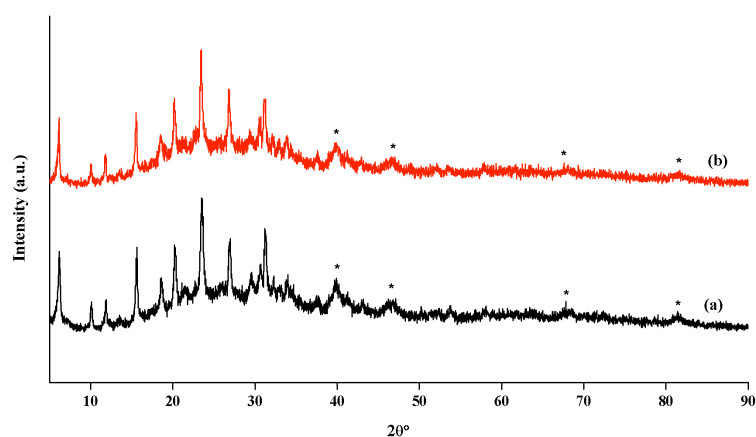
Figure 5.10. XRD analysis of (a) fresh and (b) spent 1 *wt. %* Pt/NaX (* indicates the presence of Pt peaks).
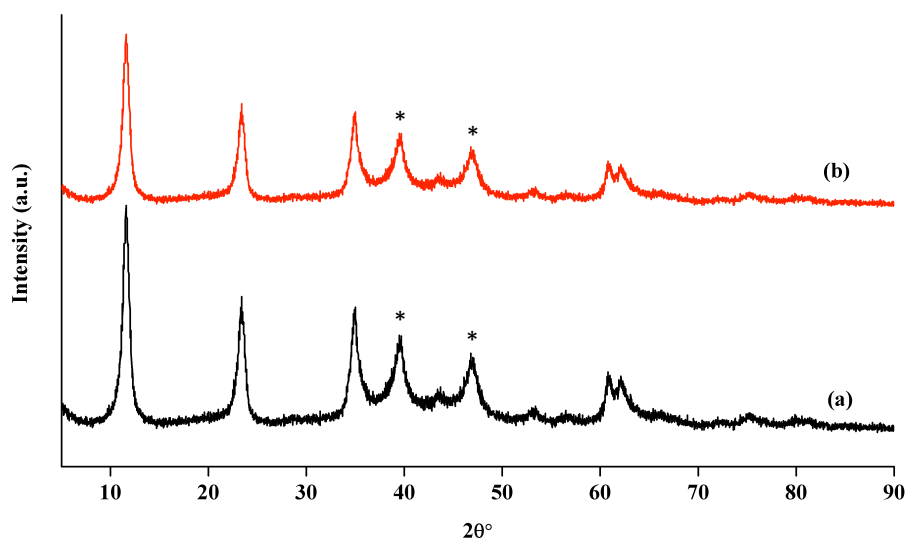
Figure 5.11. XRD analysis of (a) fresh and (b) spent 3 $wt.$ % Pt/NaX (* indicates the presence of Pt peaks).

Table 5.2. Summary of fresh and spent catalyst characterization.

Catalyst	ICP-OES (Metal loading observed)	N₂ Sorption			TPD-CO₂
		BET Surface area (m²/g)	Pore volume (cm³/g)	Pore size (nm)	Total Basicity (mmol/g)
1 $wt.$% Pt/NaX Fresh	0.90	528	0.09	1.35	0.38
1 $wt.$% Pt/NaX Spent	0.87	521	0.08	1.20	0.38
3 $wt.$% Pt/C-HT Fresh	2.80	168	0.2	2.39	0.31
3 $wt.$% Pt/C-HT Spent	2.74	160	0.18	2.01	0.29

5.4. Conclusions

Upgradation studies were performed with lignin derived monomers like phenol, guaiacol and eugenol using supported metal catalysts. Various metals (Pt, Pd, Ru) with different loadings (1, 2 and 3 *wt.%*) were impregnated on basic supports (NaX, CaO, C-HT). Catalysts were completely characterized using various physico-chemical techniques (Refer chapter 2B). Upgradation reactions of phenol, guaiacol and eugenol were performed at 250 °C with 3.0 MPa of H_2 pressure (at room temperature) in hexadecane solvent for 1-5 h. Foremost upgradation studies were performed on the simplest model compound, phenol. Effect of various supported metal catalyst were studied and it was observed that 1 *wt.%* Pt/NaX is a good catalyst for the conversion of phenol. 55% phenol conversion with 49% yield of cyclohexanol was achieved with low loading of Pt catalyst (1 *wt.%*).

Based on the catalytic system optimized for phenol upgradation reactions, studies were carried out with guaiacol and eugenol substrates. It was observed that selectively ring hydrogenated product was obtained due to the strong interaction of substrate with catalyst through π-π bonding. Similarly, the allylic double bond present in eugenol was more susceptible to hydrogenation reaction than the aromatic ring. This is due to the resonance stabilization of the π-electrons in the aromatic ring. From the studies, it was observed that noble metals impregnated on basic supports facilitates the hydrogenation of aromatic rings. Catalyst recyclability was performed with 1 *wt.%* Pt/NaX and 3 *wt.%* Pt/C-HT for the phenol upgradation reaction upto three runs. Fresh and spent catalyst were characterized using various techniques and it was found that catalyst is stable under reaction condition and can be reused.

5.5. References

1.   R. Chaudhary and P. L. Dhepe, *Green Chemistry*, 2017, 19, 778-788.
2.   B. P. Zakzeski J, Jongerius AL, Weckhuysen BM., *Chem Reviews* 2010, 110, 3552−3599.
3.   J. S. Z. Shabtai, W. W.; Chornet, E. , *5959167* 1999.
4.   R. K. B. Sharma, N. N., *Energy & Fuels*, 1993, 306-314.
5.   G. W. I. Huber, S.; Corma, A., *Chemical Reviews*, 2006, 4044-4098.
6.   H. Hattori, *Chemical Reviews*, 1995, 3, 537-558.

7. J. Oudar, *CRC Press*, 1985, 20, 160-170.

8. H. S. R. K.Y. Koo, Y.T. Seo, D.J. Seo, W.L. Yoon, S.B. Park, *Applied Catalysis A: General*, 2008, 340, 183-190.

9. N. Masiran, Dai-Viet N. Vo, Md Abdus Salam, and Bawadi Abdullah, *Procedia Engineering*, 2016, 148, 1289-1294.

10. K. Tanabe, Makoto Misono, H. Hattori, and Yoshio Ono, *Elsevier*, 1990, 51, 339-346.

11. J. H. Bredenberg, M.; Räty, J.; Korpio, M., *Journal of Catalysis*, 1982, 242-247.

12. R. K. M. R. Kallury, W. M.; Tidwell, T. T.; Boocock, D. G. B.; Crimi, and J. A.; Douglas, *Journal of Catalysis*, 1985, 535-543.

13. R. G. Leliveld, A. J. Van Dillen, J. W. Geus, and D. C. Koningsberger, *Journal of catalysis* 1998, 1, 108-116.

14. T. R. Viljava, R. S.; Krause, A. O. I., *Catalysis Today*, 2000, 83-92.

15. R. K. M. R. Kallury, W. M. Tidwell, T. T. Boocock, D. G. B. Crimi, A. Douglas, J., *Journal of Catalysis* 1985, 535-543.

16. G. G. de la Puente, A. Pis, J. J. Grange, P., *Langmuir* 1999 5800-5806.

17. F. P. K. Petrocelli, M. T., *Industrial & Engineering Chemistry Process Design and Development* 1985, 635-641.

18. A. Y. O. Bunch, U. S., *Journal of Catalysis Reviews*, 2002, 2, 177-187.

19. A. Y. W. Bunch, X. Ozkan, U. S., *Applied Catalysis A: General* 2008, , 1-2, 96-103.

20. D. C. H. Elliott, T. R., *Energy & Fuels* 2009, 631-637.

21. Gutierrez, R. K.; Honkela, M. L.; Slioor, R.; Krause, A. O. I., *Catalysis Today*, 2009, 3-4, 239-246.

22. C. A. M. Fisk, T.; Ji, Y.; Crocker, M.; Crofcheck, C.; Lewis, S. A., *Applied Catalysis A: General* 2009 2, 150-156.

23. C. K. Zhao, Y.; Lemonidou, A. A.; Li, X.; Lercher, J. A., *Angew. Chem., Int. Ed.*, 2009, 3987–3990.

24. C. L. Zhao, J. A., , *ChemCatChem*, 2012, 64–68.

25. C. K. Zhao, Y.; Lemonidou, A. A.; Li, X. B.; Lercher, J. A., *Chem. Commun.* , 2010, 412–414.

26. P. E. F. Ruiz, B. G.; De Sisto, W. J.; Austin, R. N.; Radovic, L. R.; Leiva, K.; García, R.; Escalona, N.; Wheeler, M. C., *Catal. Commun.*, 2012, 44-48.

27. Y. I. Nakagawa, M.; Tamura, M.; Tomishige, K., *Green Chem.*, 2014, 2197-2203.

28. A. K. Deepa, and Paresh L. Dhepe *ChemPlusChem* 2014, 11, 1573-1583.

29. K. L. S. Deutsch, B. H., *Applied Catalysis A: General* 2012, 447-448, 144-150.

30. R. N. B. Olcese, M.; Petitjean, D.; Malaman, B.; Giovanella, F.; Dufour, A., *Applied Catalysis B: Environmental* 2012, 115-116, 163-173.

Chapter 6
Summary and Conclusions

Lignocellulosic biomass has been identified as an important source for the production of biofuels and valuable chemicals. Lignin is one of the important constituent of lignocellulosic biomass and the most abundant naturally occurring phenolic polymer in the world. Homogeneous base catalyzed depolymerization of lignin is known for the production of fuels/chemicals. But there are several drawbacks associated with this method like corrosion of the reactor, needs an additional step for neutralization, etc. Considering these points, worked was carried out on the development of new catalytic systems for the depolymerization of lignin into value-added chemicals using heterogeneous base catalysts. The Ph.D. thesis is distributed into six chapters and the significant results and conclusions from each chapter are summarized in this Chapter.

Chapter 1

In the Chapter 1, an overview of the lignocellulosic biomass has been discussed along with its major constituents, cellulose, hemicellulose and lignin. Several processes are known for the isolation of lignin from lignocellulosic biomass. Out of those four process are known for the commercial lignin production (Sulfite, Soda, Kraft and Organosolv process) which are reviewed in this chapter. Based on the literature, several processes are known for the catalytic transformation of lignin (pyrolysis, gasification, hydrolysis, etc.) into value-added chemicals. But most of them possess few of the drawbacks, like use of high temperature, high pressure, precious metals, formation of char, tar and gas was also observed. Considering the drawbacks associated with the known methods, it is required to develop an efficient method for the depolymerization of lignin into value-added products.

In the current work, depolymerization of lignin into low-molecular weight products was accomplished using heterogeneous base catalysts. Further, isolation of lignin from coconut coir was performed using Klason, Organosolv and Soda process. Depolymerization of isolated lignin and the direct hydrolysis of coir was done using solid base catalyst. Moreover, studies on the upgradation of lignin derived monomers were carried out with basic supported metal catalysts.
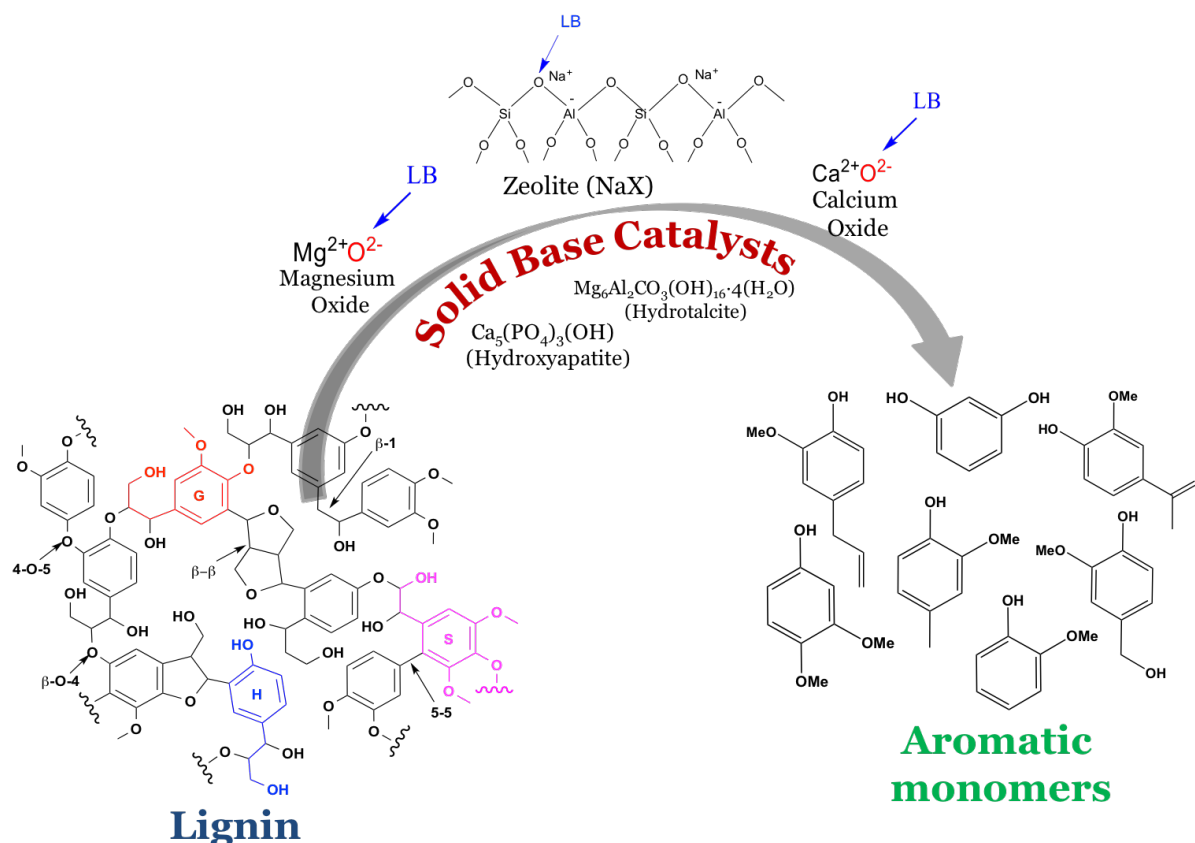
Figure 6.1. Lignin depolymerization into aromatic monomers using solid base catalysts.

Chapter 2

Section 2A

In the Section 2A, details on the various types of commercial lignin (alkaline, dealkaline, alkali, lignosulfonate sodium salt and lignosulfonate calcium salt) used for the Ph.D. work are given. All the procured lignin samples were characterized using various techniques. The key outcomes of this section are summarized below:

✓ CHNS elemental analysis was performed which revealed that lignin is composed of 39-63% C and 5-8% H along with sulphur contamination of 1-3.7%. Based on the elemental analysis general monomer molecular formula of all the lignin samples was calculated. Based on the sulphur contamination present in the lignin samples it was assumed that alkaline, dealkaline and alkali lignin isolation has been done using Kraft process as sulphur containing reagents are used (NaOH, Na_2S) in these processes while as the name suggests for lignosulfonate sodium and calcium salt lignin, possibly those might have been isolated using sulphite process (sulphite or bisulphite salts with counter cation such as Na, Mg or Ca are used).

- ✓ ICP-OES and SEM-EDAX analysis confirmed the presence of Na and S contamination in lignin which is possible from the isolation process used (Kraft or Sulphite pulping).

- ✓ ATR and ^{13}C NMR analyses were performed for the functional groups detection and confirmation of aromatic backbone of the lignin. The presence of various type of functional groups like hydroxyl, methoxy, carbonyl, etc. was also confirmed by these methods.

- ✓ TGA-DTA analysis revealed the thermal degradation behaviour of the lignin and it showed the presence of 18-44% of residue in nitrogen atmosphere.

- ✓ XRD analysis was accomplished to study the morphology of lignin and reveals that lignin is completely amorphous in nature while dealkaline lignin shows the presence of few crystalline peaks which corresponds to Na and S contamination which can be removed by water washing.

- ✓ Further, to confirm the aromatic nature of lignin UV-Vis analysis was performed.

- ✓ Solubility of lignin was checked in various solvents and correlated with polarity and Hansen solubility parameter (HSP). Based on the solubility results, ethanol:water in the ratio of 1:2 *v/v* was chosen as the solvent system for lignin depolymerization reactions. Moreover, diethyl ether (DEE) and ethyl acetate (EtOAc) were selected for the isolation of products as lignin is insoluble (least soluble) in these solvents.

Section 2B

In Chapter 2B, details on the synthesis and characterization of solid base catalysts along with the supported metal catalysts are discussed. The supported metal catalysts used for the upgradation of lignin derived monomers were synthesized by wet impregnation method.

- ✓ XRD analysis was performed and it confirmed the crystalline nature of zeolitic (NaX, NaP, NaP, KLTL) samples and metal oxides while amorphous peak pattern was observed for hydrotalcite. In case of supported metal catalysts, peaks for the Pt, Pd and Ru were clearly seen and matched with respective JCPDS files.

- ✓ To check the Si/Al ratio of zeolite and to compare the actual and theoretical loading of metal in the supported metal catalysts, ICP-OES analysis was accomplished. It was observed that Si/Al ratio (in catalysts) and actual and theoretical loading of metal is almost same for the procured/synthesized samples.

- ✓ CO₂-TPD analysis was performed to know the basic sites present in the solid base/supported metal catalysts. Various types of basic sites from weak to moderate and strong were observed. While for supported metal catalysts slight decrease in the basicity was observed compared to bare supports due to the surface coverage by the metal particles.

- ✓ Surface area, pore size and pore volume was studied using N_2 sorption analysis. Highest surface area was observed for NaX (586 m²/g). Moreover, the decrease in the surface area after metal impregnation was observed, which is obvious.

- ✓ The pH of various solid base catalysts was checked in water and reaction mixture which helped in understanding the effect of pH on the reaction.

- ✓ From the TEM analysis particle size and dispersion was calculated. Higher particle size was observed with increase in the metal loading. While for 3 *wt.%* Pt/NaX (3.5 nm) slight decrease in the particle size was observed compared to 1 *wt.%* Pt/NaX (4 nm)

Chapter 3

Chapter 3 deals with the results obtained for the lignin depolymerization reactions using various solid base catalysts. Moreover, the correlation of lignin with products and the adsorption of products on catalyst have also been discussed.

- ✓ Various type of solid base catalysts was evaluated for lignin depolymerization into low molecular weight products. Under the optimum reaction condition for the depolymerization of lignin (Lignin:Catalyst (1:1 *wt./wt.*), EtOH:H_2O (1:2 *v/v*) 30 mL, 250 °C, 1000 rpm, 1 h) upto 51% yield of the products was observed.

- ✓ Out of the several catalysts used, NaX is seen be capable to depolymerize lignin upto 51% of low molecular weight products while in case of strong bases like CaO, MgO, C-HT, HAP less yields were observed due to the adsorption of products on the catalyst.
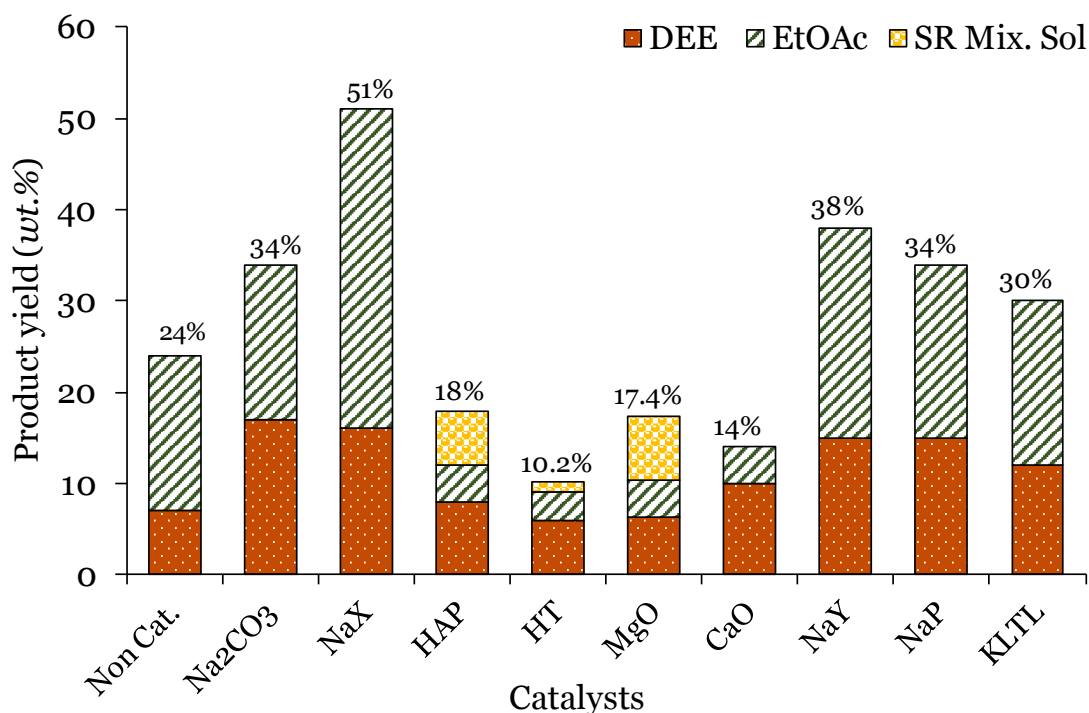
Figure 6.2. Depolymerization of lignin using solid base catalysts.

Reaction conditions: Alkaline lignin (0.5 g): Catalyst = 1: 1 *wt./wt.*, EtOH: H2O (1: 2 *v/v*) 30 mL, 250 °C, 1 h. DEE: diethyl ether, EtOAc: ethyl acetate, SR Mix. Sol.: products extracted from solid (catalyst + adsorbed products) using a mixture of DEE and EtOAc (1: 1 *v/v*) presented by yellow colour. Orange and green bar indicates the total products extracted using DEE and EtOAc (liquid + solid fraction). All the experiments were done 3 times and ±3% error in yields was observed. The results presented in this figure are the average of three runs.

✓ The product adsorption study was performed by taking the five lignin derived monomers (phenol, guaiacol, *p*-cresol, eugenol and vanillin) into account. It was concluded that these monomers are strongly adsorbing on the catalyst even at room temperature. It was also noticed that adsorption for vanillin and eugenol is more on these catalysts compared to others.

✓ Further this study was performed by considering the single compound vanillin and same phenomenon was observed. It might be possible that due to the presence of allylic double bond and carbonyl group in the eugenol and vanillin, respectively higher adsorption is observed.

✓ Identification and quantification of the depolymerized products was done using various techniques like GC, GC-MS, HPLC, etc.

- ✓ Effect of pH/basicity was studied on the lignin depolymerization and it is concluded that pH around 9.2 is the optimum pH for achieving maximum depolymerized products.
- ✓ At last the optimum reaction condition of the alkaline lignin was used for the depolymerization of various lignin substrate of different molecular weights and properties. And NaX is found to be capable for depolymerizing all the lignin substrates.
- ✓ Correlation of low molecular weight aromatic products with lignin was performed using FT-IR and NMR analysis which reveals that most of the functional groups present in lignin are retained in the products.
- ✓ Catalyst recyclability was performed upto 3rd run with NaX and it was observed that catalyst is recyclable with a decrease in the yield upto 33%.

Chapter 4

In the Chapter 4, isolation of lignin from coconut coir, its characterization followed by the depolymerization of isolated lignin and coir is discussed. It is well known from the literature that depending upon the isolation procedure, lignin properties vary and upon its depolymerization obtained products will have different functional groups. By keeping this into mind this study was accomplished.
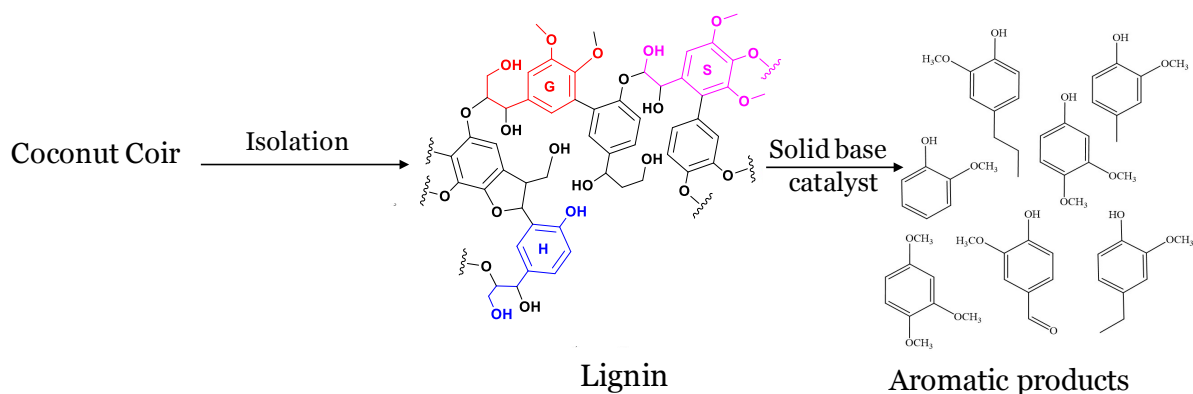

Figure 6.3. Lignin isolation and depolymerization from coconut coir.

- ✓ Lignin is isolated from coconut coir using three different methods namely Klason, Organosolv and Soda method. It was possible to isolate maximum lignin (100%) from the coconut coir (based on the lignin present in coir) using Klason method.
- ✓ Coconut coir (CC) and isolated lignin (CC-KL, CC-ORGL, CC-SL) were characterized using various techniques like XRD, ICP-OES, ATR, NMR, etc.

- ✓ ICP-OES analysis was performed in order to check the contamination present in coir and isolated lignin and the presence of few nutrients was observed in coir while in case of isolated lignin Na contamination was observed in Soda lignin.

- ✓ From microanalysis, monomer molecular formula, double bond equivalence, high heating value, O/C and H/C ratio were also calculated. It is revealed that the coir is rich is guaiacyl type of units.

- ✓ Various functional groups and linkages present in lignin were studied using ATR and ^{13}C NMR spectroscopy.

- ✓ TGA-DTA analysis was accomplished to check the thermal stability of coir and isolated lignin. Ash correction and dryness analysis was correlated with TGA-DTA results and nice coordination was observed.
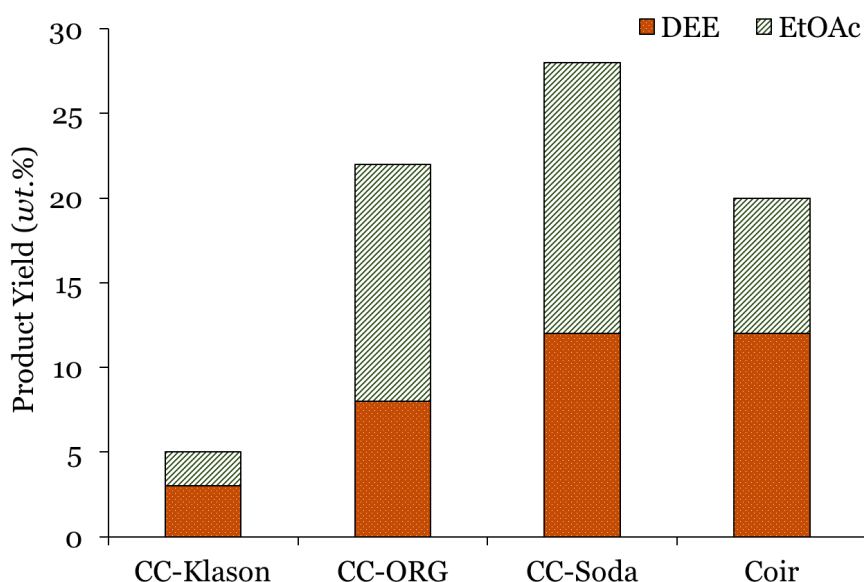

Figure 6.4. Depolymerization of isolated lignin and coir using NaX.
Reaction Condition: Lignin/Coir (0.5 g), NaX (0.5 g), EtOH: H2O (1: 2 *v/v*, 30 mL),
250 °C, 1 h

- ✓ Furthermore, the best active alkali metal substituted zeolite (NaX) catalyst for the depolymerization of commercial lignin was also explored for the conversion of coconut coir (CC) and isolated lignin (CC-KL, CC-ORGL, CC-SL) at milder reaction conditions (≤250 °C, atmospheric pressure).

- ✓ Products obtained from the depolymerization of coconut coir and isolated lignin were confirmed using GC, GC-MS and HPLC analysis.

- ✓ Various physico-chemical characterizations for both fresh and spent catalysts were also performed to understand the morphologies of the catalysts.

Chapter 5

Chapter 5 deals with the upgradation of lignin derived monomers via hydrogenation reactions. For that various supported metal catalysts were synthesized by wet impregnation method and employed for the study.

✓ Phenol, guaiacol and eugenol were used for the upgradation using supported metal catalysts.

✓ Various metals (Pt, Pd, Ru) with different loadings (1, 2 and 3 *wt.%*) were impregnated on basic supports (NaX, CaO, C-HT).

✓ Upgradation reactions of phenol, guaiacol and eugenol were performed at 250 °C with 3.0 MPa of H_2 pressure (at room temperature) in hexadecane solvent for 1-5 h.

✓ Foremost upgradation studies were performed on the simplest model compound, phenol. Effects of various supported metal catalyst were studied and it was observed that 1 *wt.%* Pt/NaX is a good catalyst for obtaining phenol conversion of 55% with 49% yield of cyclohexanol.
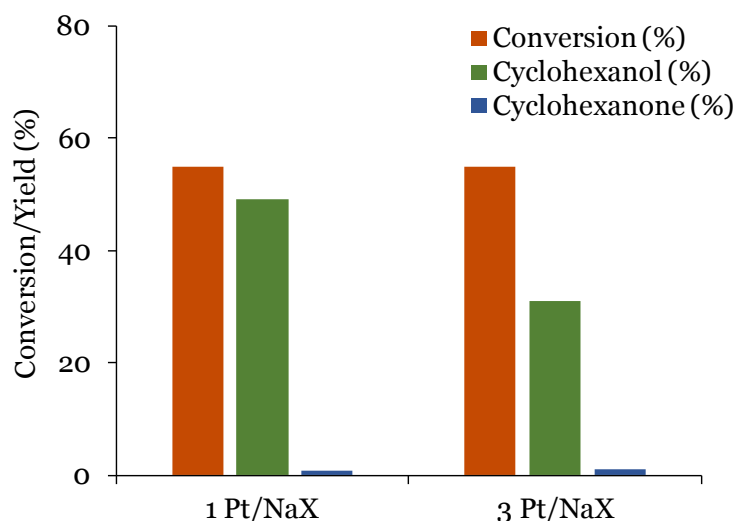

Figure 6.5. Upgradation of phenol using Pt/NaX (1 *wt.%* and 3 *wt.%*)
Reaction condition: Phenol (2 mmol), Catalyst (S/M = 200 mol/mol), Hexadecane (30 mL), 250 °C, 1 h, 3.0 MPa H_2 at RT.

✓ The optimized catalytic system for phenol upgradation was explored with guaiacol and eugenol substrates. It is observed that selectively ring hydrogenated product can be obtained due to the strong interaction of substrate with catalyst through π-π bonding. Similarly, the presence of allylic double bond in eugenol was more

susceptible to hydrogenation reaction than the aromatic ring hydrogenation. This is due to the resonance stabilization of the π-electrons in the aromatic ring.

✓ From the studies, it was observed that noble metals impregnated on basic supports facilitates the hydrogenation of aromatic rings.

✓ Catalyst recyclability was performed with 1 *wt.%* Pt/NaX and 3 *wt.%* Pt/C-HT for the phenol upgradation reaction upto three runs. Fresh and spent catalyst were characterized using various techniques and it was found that catalyst is stable under reaction condition and can be reused.

Chapter 6

All the major outcome of my work is summarized in this chapter. Moreover, the novelty of work is discussed below:

★ Use of actual lignin substrates of high molecular weight (60,000 Da).

★ Most of earlier studies are based on model substrates (dimers/ trimers).

★ Use of heterogeneous base catalysts at low temperature (T ≤ 250°C).

★ Higher yield of aromatic monomers was obtained (~50 %).

★ 100% isolation of lignin was achieved using Klason process (based on the lignin present in coir).

★ First time coconut coir was used for the depolymerization of isolated lignin (Organosolv, Klason and Soda) and coir.

★ Upgradation of lignin derived monomers were studied using basic supported metals.

Overall, In the present work, a detailed study on lignin chemistry was performed using heterogeneous bases which includes

✓ ***catalysis of lignin depolymerization***

✓ ***isolation of lignin from waste coconut coir followed by its complete characterization & depolymerization***

✓ ***upgradation of lignin derived aromatic monomers.***

List of Publications and Patents

- ❖ R. Chaudhary, P.L. Dhepe, Solid base catalyzed depolymerization of lignin into low molecular weight products, Green Chemistry, 19, 778-788 (2017).

- ❖ R. Chaudhary and P.L. Dhepe, Delignification of coconut coir followed by its characterization and depolymerization using heterogeneous base catalyst. (to be submitted)

- ❖ R. Chaudhary and P.L. Dhepe, Upgradation of lignin model compounds using supported metal catalyst. (to be submitted)

- ❖ R. Chaudhary and P.L. Dhepe, An improved heterogeneous base catalyzed process for depolymerization of lignin, Patent No 201611007650 (IN) (2016).

Contributions to Symposia and Conferences

- ❖ R. Chaudhary, P.L. Dhepe, A novel approach for the depolymerization of lignin, 4th International Symposium on Green Chemistry, La Rochelle France, 2017 (Oral presentation).

- ❖ R. Chaudhary, P.L. Dhepe, Effect of pH on the depolymerization of lignin over various solid base catalysts: A new and sustainable approach, National Science Day Celebration, CSIR-NCL, Pune, India, 2017 (Poster presentation).

- ❖ R. Chaudhary, P.L. Dhepe, Heterogeneous Base Catalyzed Depolymerization of Lignin into Aromatic Monomers, 7th Asia-Pacific Congress on Catalysis (APCAT-7), Mumbai, India, 2017 (Poster presentation).

- ❖ R. Chaudhary, P.L. Dhepe, Heterogeneous base catalyzed depolymerization of lignin into aromatic monomers, 3rd International Conference on Past and Present Research Systems of Green Chemistry, Las Vegas, USA, 2016 (Oral presentation).

- ❖ R. Chaudhary, P.L. Dhepe, Solid base catalyzed depolymerization of lignin into aromatic monomers, National Science Day Celebration, CSIR-NCL, Pune, India, 2016 (Poster presentation).

- ❖ Attended '22nd National Symposium on Catalysis for Better Tomorrow' held at CSIR-CSMCRI Bhavnagar, India during 7th to 9th Jan 2015.

- ❖ Attended a conference 'The International Conference on Structural and Inorganic Chemistry' held at CSIR-NCL Pune, India during 4th & 5th Dec 2014.

- ❖ Attended '21st National Symposium on Catalysis for Sustainable Development' held at CSIR-IICT Hyderabad, during 11th to 13th Feb 2013.

NOTES

NOTES